



THE UNIVERSITY *of* EDINBURGH

This thesis has been submitted in fulfilment of the requirements for a postgraduate degree (e.g. PhD, MPhil, DClinPsychol) at the University of Edinburgh. Please note the following terms and conditions of use:

This work is protected by copyright and other intellectual property rights, which are retained by the thesis author, unless otherwise stated.

A copy can be downloaded for personal non-commercial research or study, without prior permission or charge.

This thesis cannot be reproduced or quoted extensively from without first obtaining permission in writing from the author.

The content must not be changed in any way or sold commercially in any format or medium without the formal permission of the author.

When referring to this work, full bibliographic details including the author, title, awarding institution and date of the thesis must be given.

Synthesis and reactivity of low valent main-group compounds



Clément René Paul Millet

A Thesis Submitted in Fulfilment of Requirements for the

Degree of Doctor of Philosophy

School of Chemistry

Faculty of Science and Engineering

The University of Edinburgh

The work described in this thesis was carried out in the M. Cowley group in the School of Chemistry in **The University of Edinburgh** between September 2015 and October 2018.

This thesis was submitted on the 22-07-2019.

External Examiner: Doctor Stephen Mansell

Assistant Professor

School of Engineering & Physical Sciences, Heriot-Watt
University, UK

Internal Examiner: Professor Simon Parsons

Professor of Crystallography

Department of Chemistry, University of Edinburgh, UK

Declaration of originality

I declare that this thesis and the research described in this thesis are my own work. Where others have contributed, their contribution is clearly indicated in the text. The work of other researchers is appropriately referenced where discussed in the thesis. Previously published journal articles resulting from research carried out during my studies are listed below. I attest that no part of this work has been previously submitted to obtain a qualification or degree at this or any other institution.

Publication

'Preparation and Characterization of P₂BCh Ring Systems (Ch=S, Se) and Their Reactivity with N-Heterocyclic Carbenes', C. Graham, C. Millet, A. Price, M. Cowley, H. Tuononen, P. Ragogna, *Chem. Eur. J.*, **2018**, 24, 672-680.

Abstract

Low-valent, low-coordinate or multiply bonded main group compounds are of interest for their reactivity. Properties usually observed for transition metals, such as small molecule activation, are possible for these classes of main group compounds. The development of the coordination chemistry of main group elements allows the synthesis of new types of species, which could not be achieved before, by providing electronic and kinetic stabilisation. In the following sections are presented reactivity studies of silylenes, low-valent silicon species, and phosphaborenes ($RP=BR'$), multiply bonded phosphorus-boron compounds.

Chapter I gives an overview of low-valent and low-coordinate silicon chemistry. Two main types of silicon species can be distinguished in this area: silylenes and base-stabilised silicon compounds. Silylenes ($:SiR_2$) are heavier analogue of carbenes ($:CR_2$) and have simultaneously similar and different properties compared to carbenes. Although less studied than carbenes, silylenes also have interesting potential for coordination chemistry to transition metals or main group elements. Base-stabilised silicon compounds have been known for more than a century, however, only the recent use of N-heterocyclic carbene (NHC) ligands has allowed isolation of new low coordinate silicon species, such as the carbene-stabilised diatomic and triatomic silicon(0) clusters, which respectively feature two and three silicon atoms in the formal oxidation state of zero.

Chapter II is a study of oxidative addition to an N-heterocyclic silylene 1,3-bis(diisopropylphenyl)-1,3-diaza-2-silacyclopent-4-en-2-ylidene, a heavier analogue of N-heterocyclic carbene. An N-heterocyclic silylene was reacted with several main group halides (SiI_4 , PCl_3 and BBr_3). Oxidative addition was observed in each case, however, stability studies of the oxidative addition products show that only the product

from the reaction with SiI_4 is isolable. The reactivity of this product was studied toward reduction with alkali metals, reaction with bases, such as carbenes, organolithium reagents and phosphines. The addition of an excess of the N-heterocyclic silylene allows double oxidative addition from SiI_4 to two N-heterocyclic silylenes. Finally, the addition of an excess of N-heterocyclic silylenes to BBr_3 allows the observation of a relatively stable silylene-coordinated silylborane.

Chapter III covers the attempted synthesis of a new type of N-heterocyclic silylene, which involves a bridgehead nitrogen atom, providing enhanced reactivity to this N-heterocyclic silylene compared to classical examples. This chapter includes the full synthesis and characterisation of the diamine ligand precursor *N*-1,3-diisopropylphenyl-3-piperidinemethanamine. The study of its reactivity was then carried out in order to insert silicon halide species into the structure, to reach the targeted N-heterocyclic silylene by reduction. The different conditions, which were tried on the ligand, did not successfully afford the targeted silane. The N-heterocyclic silylene could not be achieved.

Chapter IV introduces the chemistry of mixed group III-V (13-15) compounds, which are widely used in electronic devices. Their synthesis involves harsh conditions such as chemical vapor deposition (CVD), metal-organic chemical vapor deposition (MOCVD) or molecular beam epitaxy (MBE). Solution phase synthesis is a possible route to these mixed group III-V compounds, which will allow the use of milder conditions. Already achieved for some of them (GaAs, GaP, GaSb, InP, InSb), the solution phase synthesis of lighter mixed group III-V compounds, such as boron-phosphide (PB), is still elusive. The recent development of the chemistry of base-stabilised phosphaborenes $\text{RP}=\text{BR}'(\text{L})$, mixed compounds involving a phosphorus-boron double bond, highlighted a possible way to make boron-phosphide through

solution phase preparation. The use of N-heterocyclic carbenes (L) could also allow stabilisation of new allotropes of boron-phosphide PB(L).

Chapter V explores the chemistry of minimally substituted base-stabilised phosphinoboranes $[(\text{Me}_3\text{Si})_2\text{PBBr}_2(\text{L})]$ (L = NHC) and phosphaborenes $[\text{Me}_3\text{SiP}=\text{BBr}(\text{L})]$ achieved by base-promoted abstraction of trimethylsilyl halide from a phosphorus-borane adduct precursor $[(\text{Me}_3\text{Si})_3\text{P}\rightarrow\text{BBr}_3]$. The functionalisation of $[(\text{Me}_3\text{Si})_2\text{PBBr}_2(\text{L})]$ affords the $[\text{H}_2\text{PBBr}_2(\text{L})]$ and similar base-promoted dehydrohalogenation allows the synthesis of the phosphaborene $[\text{HP}=\text{BBr}(\text{L})]$. An unsaturated NHC used in this chemistry showed limited stability to the conditions used in the attempt to form base-stabilised boron-phosphide. The chemistry has been reexplored using a new NHC, which is expected to be more stable and enable the synthesis of base-stabilised boron-phosphide PB(L). The reactivity of phosphaborenes has been explored and hydrogenation of $[\text{HP}=\text{BBr}(\text{L})]$ or $[(\text{Me}_3\text{Si})\text{P}=\text{BBr}(\text{L})]$ successfully gives the phosphinoboranes $[\text{H}_2\text{PBHBr}(\text{L})]$ and $[(\text{Me}_3\text{Si})\text{HPBHBr}(\text{L})]$. Base-promoted dehydrohalogenation from $[\text{H}_2\text{PBHBr}(\text{L})]$ allows the observation of the base-stabilised parent diphosphadiboretane, $[(\text{HPBH})_2(\text{L})_2]$.

Lay summary

Molecules are built up from atoms. Each atom in a molecule can be described according to its environment. The number of connections (bonds) shared with neighbouring atoms (valency) or the capacity of an atom to lose their electrons (oxidation state) depend on the nature of the atoms which are involved in the observed system. In nature atoms tend to have valencies and oxidation states that they adopt more favourably over others. Similarly, some elements will happily form multiple bonds to another atom, like carbon, whilst other elements, like silicon or boron, will not favour it. By using the right structure or the adequate supporting molecule (ligand), it is, however, possible to synthesise molecules which involve atoms with a valence or an oxidation state which is normally considered as unfavourable for these atoms. The characteristics of these molecules, which involve atoms in an uncommon state, allow new properties and reactivity usually not observed for these elements.

In the following sections, the reactivity of low valent silicon with main group halide species is first studied. The development of a new low valent silicon compound is then presented. Finally, the synthesis of multiply bonded phosphorus-boron containing molecules is studied.

“By nature, I’m curious

Science is serious

I wanna learn and study, ‘Cause life is too mysterious”

Pupajim

My Research, 2017

Dedicated to

Paul Spehner

Acknowledgements

I would like to thank my supervisor, **Dr. Michael Cowley**, for offering me the opportunity to carry out my PhD on low valent/coordinate main group chemistry, his constant support, feedback and availability over those three years. I would like also to thank the members of the Cowley group: **Dr. Amy Price**, **Dr. Stephanie Urwin**, **Dr. Alessandro Bismuto**, **Martin Stanford**, **Daniel De Rosa**, **Dr. Lena Albers**, **Abigail Levy**, **Dr. Rosalyn Falconer**, **Dr. Andryj Borys** and **Ella Rice** for being amazing work partners and nice friends.

I would like to thank all the technical staff from the School of Chemistry, especially **Dr. Gary S. Nichol** for the resolution of my X-ray crystal structures, **Juraj Bella** and **Dr. Lorna Murray** for their great support with NMR, and to **Alan Taylor** for doing the mass spectrometry analysis.

I finally would like to thank my family, my mother and my sister in particular, **Viviane** and **Alice**, for the support during the last few months.

Table of Contents

Abstract	2
Lay summary	5
Acknowledgements	11
Table of Contents	13
List of abbreviations	18
Chapter I – Introduction to low coordinate/valent silicon chemistry	23
Disilenes	25
Disilynes	27
Carbenes and N-Heterocyclic Carbenes	29
Silylenes	31
Dicoordinate N-Heterocyclic Silylenes	33
Tricoordinate N-Heterocyclic Silylenes	37
Acyclic Dicoordinate Silylenes	40
Base coordinated silicon species	42
Hypervalent Base-Silicon adducts	42
Base-Silicon(II) adducts	45
Base-Silicon(0) adducts	50
Silylone	50
Base-stabilised disilicon(0)	52
Base-stabilised trisilicon(0)	54
Conclusion	55
References	56
Chapter II – Oxidative addition of main group halides to an N-Heterocyclic Silylene	65
Introduction - Cyclic dialkylsilylene	65
Oxidative addition of silicon halides to an N-heterocyclic Silylene	68
Reduction of the disilane 2.1	73
Generation and reactivity study of the trisilane 2.5	76
Reduction of 2.5 with KC_8	77
Reduction of 2.5 with an organosilicon reagent	77
Reactions of the disilane 2.1 with coordinating-bases	79

Reaction of 2.1 with Organolithium reagents	83
Oxidative addition of boron and phosphorus halide on N-Heterocyclic Silylene	84
Conclusion and perspectives	90
References	92
Chapter III – Synthesis of an anti-Bredt Silylene	99
Introduction	99
An anti-Bredt N-Heterocyclic Carbene	99
Cyclic (Alkyl)(Amino) Silylene	103
Synthesis of an anti-Bredt N-Heterocyclic Silylene	105
Synthetic strategy towards an anti-Bredt N-Heterocyclic Silylene	105
Boc protection: synthesis of III.15	107
Alcohol oxidation: synthesis of 3.1	108
Swern-oxidation	108
Dess-Martin oxidation	109
One-pot synthesis of 3.3 from 3.1	109
Imine condensation: synthesis of the imine 3.2	112
Imine reduction: synthesis of the amine 3.3	114
Boc deprotection: synthesis of the ligand 3.4	115
Synthesis of the dichlorosilane 3.5	117
Triethylamine (NEt ₃) and silicon tetrachloride (SiCl ₄)	117
Lithiation of 3.4 and SiCl ₄ addition	119
Conclusion and perspectives	125
References	127
Chapter IV – Introduction to mixed group III-V compounds	131
Route to group III-V (13-15) semiconductors	131
Mixed group III-V compounds of heavier elements	131
Mixed group III-V compounds of lighter elements	132
Base-stabilised low-coordinate main-group (E=E) compounds	134
Aminoboranes and Phosphinoboranes	138
Iminoboranes	140
Phosphaborenes	142
References	149
Chapter V – Functionalised Phosphaborenes	155
Introduction	155
Minimally substituted phosphinoboranes	155

Minimally substituted phosphaborenes	160
Attempted synthesis of molecular boron-phosphide	161
Synthesis of the SIPr coordinated 1-di(trimethylsilyl)-2-dibromo-phosphinoborane 5.1	163
Synthesis of the SIPr coordinated 1-trimethylsilyl-2-bromo-phosphaborene 5.2	166
Attempted synthesis of NHC stabilised boron-phosphide	169
Attempt from the SIPr phosphinoborane adduct 5.1	170
Attempt from the SIPr phosphaborene adduct 5.2	175
Attempt of coordination from 5.2 to Lewis acid	177
Functionalization of the phosphinoborane 5.1	178
Synthesis of the 1-dihydro-2-dibromo-phosphinoborane 5.6	178
Synthesis of the 1-hydro-2-bromo-phosphaborene 5.7	181
Synthesis of the 1-dihydro-2-bromohydro-phosphinoboranes 5.8 and 5.9	187
Attempted synthesis of the parent phosphaborene: synthesis of the parent diphosphadiboretane 5.10	193
Synthesis of the 1-hydrotrimethylsilyl-2-bromohydro-phosphinoboranes 5.11 and 5.12	199
Attempted synthesis of a phosphinoborane with an extremely bulky NHC202	
Conclusion and perspectives	203
References	208
<i>Summary and Outlook</i>	213
<i>Experimental Methods</i>	219
General Information	219
Experimental Details for Chapter II	220
Reaction between silylene 1.26 and SiCl ₄	220
Preparation of the disilane 2.1	220
Monitoring of the stability of 2.1 in solution	221
Preparation of the diiodosilane 2.2	222
Reduction of the disilane 2.1	223
Preparation of the trisilane 2.5	226
Reduction of 2.5 using KC ₈	226
Reduction of 2.5 using organosilicon reagent	227
Reactions of the disilane 2.1 with coordinating-bases	227
Generation of 2.6	229
Reaction with organo-lithium reagents	230

Oxidative addition of boron and phosphorus halide compounds on the N-heterocyclic silylene I.26	231
Reaction between I.26 and PCl_3	231
Reaction between I.26 and BBr_3	232
Experimental Details for Chapter III	233
Preparation of the alcohol III.15	233
Swern oxidation of the alcohol III.15	234
Preparation of the aldehyde 3.1	234
Attempt of one-pot synthesis of 3.3 from 3.1	235
Preparation of the imine 3.2	236
Preparation of the amine 3.3	236
Preparation of diamine 3.4	237
Synthesis of the dichlorosilane 3.5	238
Triethylamine (NEt_3) and silicon tetrachloride (SiCl_4)	238
Lithiation of 3.4 and SiCl_4 addition	240
Experimental Details for Chapter V	242
Preparation of the $(\text{Me}_3\text{Si})_3\text{PBBR}_3$ adduct IV.4	242
Preparation of the SIPr coordinated 1-di(trimethylsilyl)-2-dibromophosphinoborane 5.1	242
Preparation of the SIPr coordinated 1-trimethylsilyl-2-bromophosphaborene 5.2	243
Attempted synthesis of NHC boron-phosphide adduct	244
Attempt from the SIPr coordinated phosphinoborane 5.1	244
Attempt from the SIPr coordinated phosphaborene 5.2	245
Attempted coordination of 5.2 to Lewis acid	245
Functionalization of the SIPr coordinated phosphinoborane 5.1	246
Preparation of the SIPr coordinated 1-dihydro-2-dibromo-phosphinoborane 5.6	246
Preparation of the SIPr coordinated 1-hydro-2-bromo-phosphaborene 5.7	246
Generation of the SIPr coordinated 1-dihydro-2-bromohydro-phosphinoborane 5.8	247
Preparation of the IPr coordinated 1-dihydro-2-bromohydro-phosphinoborane 5.9	248
Generation of the parent diphosphadiboretane 5.10	249
Generation of the SIPr coordinated 1-hydrotrimethylsilyl-2-bromohydro-phosphinoborane 5.11	250
Generation of the IPr coordinated 1-hydrotrimethylsilyl-2-bromohydro-phosphinoborane 5.12	250
Reaction between IV.4 and ITr	251
X-Ray Crystallography Details	251
NMR and UV-Vis Data	251

DFT-Calculations	251
Origin Calculation	252
References	253

List of abbreviations

Ar	aryl
Ar*	2,6-bis-(2,4,6-trimethylphenyl)-phenyl
Ar'	2,6-bis-(2,6-diisopropylphenyl)-phenyl
Ar''	2,6-bis-(2,4,6-triisopropylphenyl)-phenyl
BAr ^F ₃	tris[3,5-bis(trifluoromethyl)phenyl]borane
cAAC	cyclic alkylaminocarbene
coe	cyclooctene
Cp	cyclopentadienyl
Cp*	pentamethylcyclopentadienyl
CVD	chemical vapor deposition
Cy	cyclohexyl
DCE	dichloroethane
DCM	dichloromethane
DFT	density functional theory
Dipp	2,6-diisopropylphenyl
DMAP	4-dimethylaminopyridine
Dur	2,3,5,6-tetramethylphenyl
EPR	electron paramagnetic resonance
Et	ethyl
HMBC	heteronuclear multiple bond correlation
HMQC	heteronuclear multiple-quantum correlation
HOMO	highest occupied molecular orbital
HSQC	heteronuclear single-quantum correlation
IPr	1,3-bis(2,6-diisopropylphenyl)imidazol-2-ylidene
ⁱ Pr	isopropyl
IR	infra-red
ITr	1,3-bis(trityl)imidazol-2-ylidene
KO ^t Bu	potassium <i>tert</i> -butoxide
LB	Lewis base
LDA	lithium diisopropylamide
LiHMDS	lithium bis(trimethylsilyl)amide
LiNap	lithium naphthalenide
LUMO	lowest unoccupied molecular orbital
MBE	molecular beam epitaxy
Me methyl	methyl
Me ⁱ Pr	1,3-diisopropyl-4,5-dimethyl-imidazol-2-ylidene
Me ⁱ Me	tetramethylimidazol-2-ylidene
Mes	2,4,6-trimethylphenyl
Mes*	2,4,6-tri- <i>tert</i> -butylphenyl
MOCVD	metal-organic chemical vapor deposition
NaNap	sodium naphthalenide
nBuLi	<i>n</i> -butyllithium
NHC	N-heterocyclic carbene
NICS	nucleus-independent chemical shift
NMR	nuclear magnetic resonance
NOESY	nuclear overhauser effect spectroscopy
NR ₂	2,2,6,6-tetramethylpiperidine

OTf	triflate
Ph	phenyl
rt	room temperature
SIPr	1,3-bis(2,6-diisopropylphenyl)-4,5-dihydroimidazol-2-ylidene
^t Bu	<i>tert</i> -butyl
TEP	Tolman electronic parameter
Boc	<i>tert</i> -butyloxycarbonyl
TFA	trifluoroacetic acid
THF	tetrahydrofuran
Tip	2,4,6-triisopropylphenyl
UV/Vis	ultraviolet-visible
Xyl	2,6-dimethylphenyl

Chapter I

Introduction to low coordinate/valent

silicon chemistry

Chapter I – Introduction to low coordinate/valent silicon chemistry

Silicon is one of the most abundant elements on the earth (around 28% by weight). Elemental silicon is not naturally present, but silicon commonly exists at the oxidation state of +IV, combined with oxygen to form a wide variety of silicates. Discovered in 1824 by Jöns Jacob Berzelius, elemental silicon was obtained by reduction of potassium fluorosilicate with potassium.

Elemental silicon is now widely used as a semiconductor in many electronic devices or solar panels. Industrially, elemental silicon is primarily produced by two methods: through reduction of quartz (SiO_2) with carbon at high temperature or through thermal decomposition of silane (SiH_4). The use of silicon has recently reached new domains such as batteries, electrodes or nanoparticles.

Silicon belongs to the group 14 elements, which includes carbon (C), germanium (Ge), tin (Sn), lead (Pb) and flerovium (Fl). However, silicon, germanium, tin and lead are usually described as heavier group 14 elements, in comparison to carbon. Silicon has a similar electronic configuration to carbon (ns^2, np^2). However, carbon does not have a filled p orbital in its inner shell. With the increase of principal quantum number, n , from 2 to 3, silicon has occupied 2p orbitals in its inner shell. The presence of these 2p orbitals causes repulsion of the 3p orbitals, resulting in more diffuse 3p orbitals than the 3s (*Figure 1*). Whilst carbon exhibits a difference of radii of the maximal electron density between its valence p and s orbital of $\Delta r = -0.2 \text{ pm}$ ($\Delta r = r_p - r_s$), silicon shows a difference significantly bigger of $\Delta r = 20.3 \text{ pm}$.^[1]

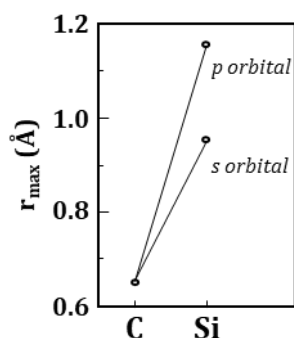


Figure 1: Size of the valence s and p orbitals of carbon and silicon.

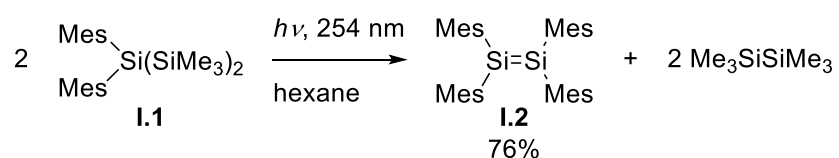
This difference in radii between the s and p valence orbitals leads to different structural behaviour. Hybridization becomes harder down the group since promoting an electron between the different orbitals requires more energy. Pitzer postulated that the inner shell repulsive effect from the core electrons, which becomes a lot greater below the first row, makes multiple bonds weaker for all atoms outside the first row.^[2] As an example, a typical silicon-silicon double bond has a low π -bond energy (60-100 kJ mol^{-1}), much smaller than those of alkenes ($>200 \text{ kJ mol}^{-1}$) and a smaller π - π^* gap ($\sim 3 \text{ eV}$) compared to the alkenes ($\sim 6 \text{ eV}$).^[3] These differences are illustrated by a higher reactivity of the silicon-silicon double bond. In nature, this is highlighted by the ability of carbon to form stable multiple bonds, whilst the heavier group 14 analogues oligomerise.

Multiple bonds for heavier carbon analogues were elusive for a long time. The unsuccessful attempts to synthesise multiply bonded heavier compounds led chemists to consider multiply bonded main-group elements as unstable, with the statement of the “double-bond rule” based on this assumption.^[4] Considered as unstable or transient species, it was only 20 years before the twenty-first century that low coordinate silicon compounds were isolated for the very first time.^[5]

Although widely used in organic synthesis as protecting groups, Lewis acidic catalysts or hydroxyl group precursors, the chemistry of low coordinate and low valent silicon has only been extensively developed over the last four decades, allowing the discovery of new and unexpected reactivity of this element.

Disilenes

Disilenes are compounds involving a Si=Si double bond. Analogous to alkenes, which are ubiquitous in nature, disilenes are much rarer and more reactive. In 1981, the challenge of forming a Si=Si double bond was overcome, with the synthesis of the first disilene **I.2** reported by West and Fink.^[5] The tetramesityldisilene **I.2** was synthesised by photolysis of 2,2-bis(mesityl)hexamethyltrisilane **I.1** in hexane (*Scheme 1*). In a similar way to alkenes, the disilene **I.2** can undergo addition across the Si=Si double bond. However, **I.2** is more reactive than alkenes and is not stable to air and moisture, reacting with O₂ at room temperature. Bulky substituents are necessary to stabilise **I.2**, West and Fink reported that polymerisation occurred if the steric protection was reduced.



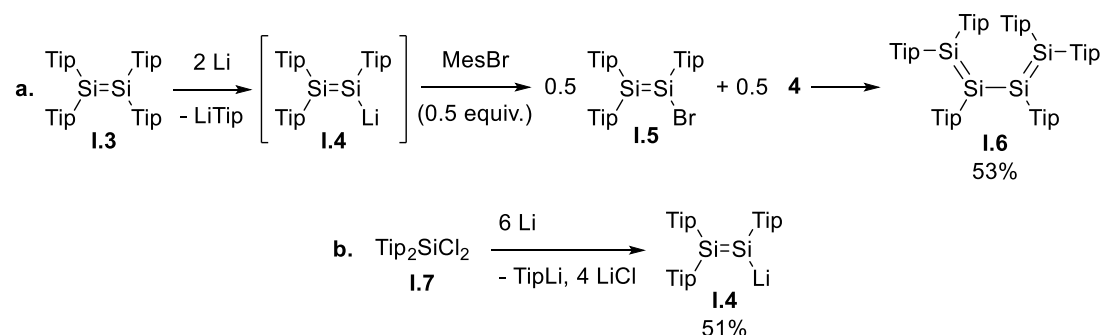
Scheme 1: Synthesis of the first disilene **I.2** by photolysis of **I.1**. Mes = 2,4,6-trimethylphenyl.

Several disilenes were reported in the following decade, including an air stable compound with four 2,4,6-triisopropylphenyl groups (Tip) **I.3**.^[6–13] The average Si=Si bond length, 2.14 Å for disilenes, is 8.5% shorter than the typical Si–Si single bond (2.34 Å).^[14] This shortening is comparable to the difference of 13% observed between

alkanes (C–C around 1.54 Å) and alkenes (C=C around 1.34 Å). The crystal structure from **I.1** revealed a not entirely planar geometry around the Si=Si double bond.^[15] This results from a very small pyramidalization at each silicon atom and a slight twist around the Si=Si double bond (5°). The solid-state structure of the disilene is in accordance with the calculated structure of the parent disilene H₂Si=SiH₂, which was predicted to have a doubly bonded structure with a *trans*-bent geometry.^[16]

The primary reactivity of disilenes is cycloadditions with multiply bonded compounds (eg. alkenes, nitrile), or addition of small molecules (eg. H₂O, O₂) across the double bond.^[17–19] However, reduction of the disilene **I.3** followed by addition of MesBr was reported by Weidenbruch *et al.* to form the product **I.6** (Scheme 2.a).^[20] They proposed the disilenide intermediate **I.4**, which gave the product **I.5** when treated with half an equivalent of mesitylene bromide (MesBr). Disilene **I.5** reacted slowly with the excess of the proposed intermediate **I.4**, giving the conjugated disilene **I.6**. Both of the observed products **I.5** and **I.6** provided evidences for the postulated intermediate **I.4**.

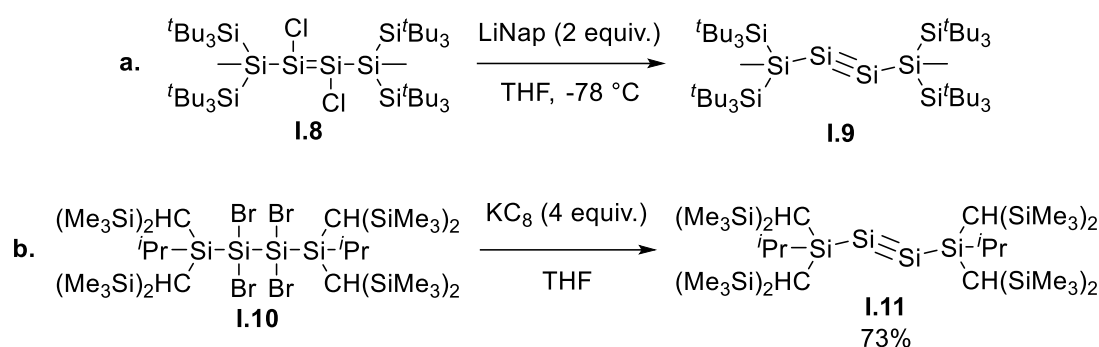
The disilenide **I.4** was isolated, in 2004 by Scheschkewitz, by reduction of the silicon halide **I.7** (Scheme 2.b).^[21] The isolation of **I.4** allows reaction of a nucleophilic disilene fragment with electrophiles similarly to organosilyl anions.



Scheme 2: a. Reduction of the disilene **I.3** and formation of the hexaaryltetrasilabut-1,3-diene **I.6**. **b.** Synthesis allowing isolation of the disilenide **I.4**. Tip = 2,4,6-triisopropylphenyl. Mes = 2,4,6-trimethylphenyl.

Disilynes

Disilynes, heavier alkyne analogues, are compounds which feature a silicon-silicon triple bond. In 2002, Wiberg *et al.* reported the reduction of the disilene **I.8** using lithium naphthalenide (LiNap).^[22] They latter characterised the product as the disilyne **I.9** (*Scheme 3.a*),^[23] which could initially not be isolated, due to its instability leading to isomerisation. In 2004, Sekiguchi reported the first stable disilyne **I.11**,^[24] by the reduction of the tetrabromodisilane precursor **I.10** using potassium graphite (KC₈), protected with two very bulky silyl substituents (*Scheme 3.b*). Disilyne **I.11** is rapidly formed and stable under inert atmosphere, no isomerization or dissociation was observed in solution, which evidenced a strong Si≡Si triple bond. The solid-state structure of **I.11** confirmed the triply bonded silicon atoms, with a Si≡Si triple bond of 2.06 Å, which is 3.8% shorter than the Si=Si double bond. The bond-distance change is noticeably smaller than the one for the carbon equivalents, with a C≡C triple bond (1.20 Å) about 10.4% shorter than the C=C double bond. The X-ray analysis also confirmed the predicted *trans*-bent structure of the disilyne^[25–27] with an R-Si≡Si angle of 137.4°. This angle was slightly larger than the calculated angle for the parent disilyne H-Si≡Si-H (124.9°), which is due to substitution by electropositive silyl groups, leading to a less *trans*-bent structure. The dibridged structure (*Figure 2*), which is calculated to be the lowest in energy for the parent disilyne, was never observed. This was in accordance with calculations, which predicted the instability of this structure with larger substituents.^[26] The disilyne **I.11** is highly reactive and reaction with two equivalents of bromine at room temperature forms **I.10** almost quantitatively.



Scheme 3: a. Reduction of disilene **1.8**, synthesis of the disilyne **1.9**, isolated in 2004.

b. Reduction of the disilane **1.10**, synthesis of the first stable disilyne **1.11**.

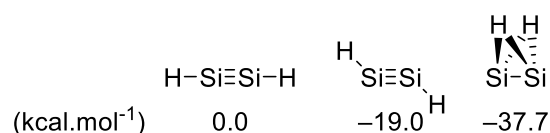
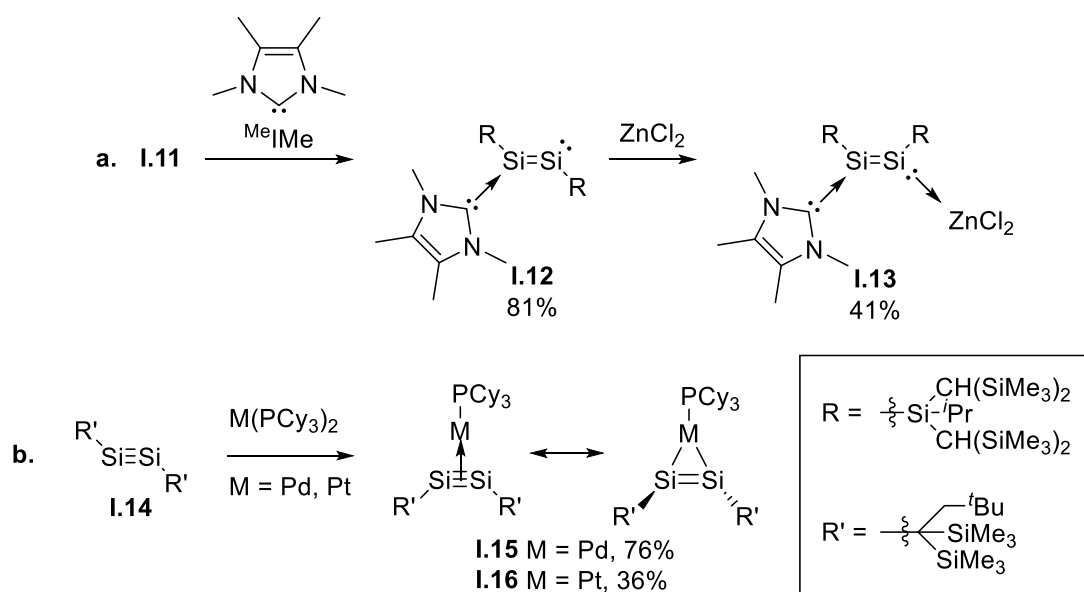


Figure 2: The calculated potential energy surface of Si_2H_2 .^[26]

Due to the complexity of their synthesis, very few examples of disilynes have been reported.^[28–30] Reported reactivities for disilynes include classic cycloadditions and additions across the triple bond.^[31,32] The coordination chemistry of disilynes has also been explored. Treating **1.11** with the N-heterocyclic carbene (NHC) tetramethylimidazol-2-ylidene (^{Me}Ime) produced the complex disilyne-NHC **1.12**, which can react with a Lewis acid ZnCl_2 to form the push-pull complex **1.13**.^[33] The reaction between the disilyne **1.14** and the $\text{M}(\text{PCy}_3)_2$ ($\text{M} = \text{Pd}$ or Pt) gave a ligand-exchange product, mono(phosphine)palladium or platinum η^2 -disilyne complexes **1.15** and **1.16**, which can be drawn as a π -complex or a metallacycle (Scheme 4.b).^[30] Multiply-bonded silicon species showed new reactivity compared to the usual chemistry of silicon, including coordination to transition metals.



Scheme 4: a. Reaction of the disilyne **I.11** and $\text{Me}|\text{Me}$ and coordination from the formed complex **I.12** to ZnCl_2 . b. Reaction of the disilyne **I.14** and $\text{M}(\text{PCy}_3)_2$ ($\text{M} = \text{Pd}, \text{Pt}$), synthesis of the mono(phosphine)palladium or platinum η^2 -disilyne complexes **I.15** and **I.16**.

Carbenes and N-Heterocyclic Carbenes

Carbenes are neutral compounds with a divalent carbon atom with six valence electrons. The bent geometry of carbenes breaks the degeneracy and the carbon atom adopts a sp^2 hybridization with the p_y orbital almost unchanged, whilst the p_x is stabilised, acquiring some s character. Therefore, p_y and p_x orbitals are called p_π and σ orbitals respectively. Carbenes have two possible electronic configurations (Figure 3). The two nonbonding electrons can be in paired in the σ orbital, as the σ^2 configuration or singlet state. Alternatively, the two nonbonding electrons can be in the two orbitals p_π and σ , as the $\sigma^1 p_\pi^1$ configuration or triplet state. Singlet carbenes have a filled orbital (σ -donating character) as well as a vacant orbital (π -accepting character), they have ambiphilic character. Triplet carbenes have two half-filled orbitals and can be considered as diradicals. The ground-states of carbenes depend

on the relative energy of the p_{π} and σ orbitals. For this reason, the substituents of carbenes determine their ground state and their reactivity.

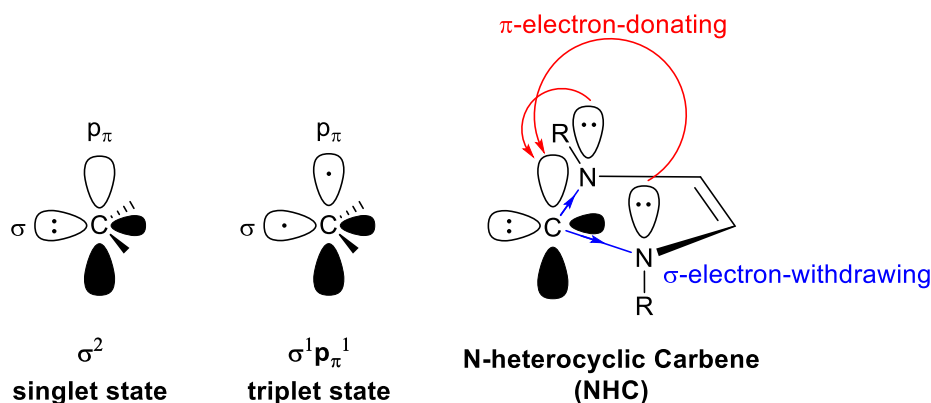
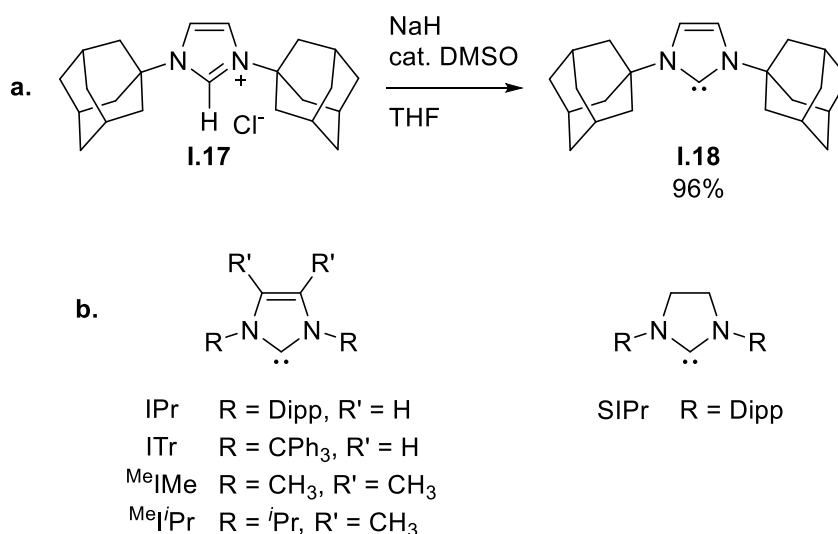


Figure 3: Carbene possible electronic configurations, singlet (left) and triplet state (centre). N-heterocyclic carbene electronic properties (right).

N-heterocyclic carbenes (NHCs) have the adequate structure to be stable singlet carbenes (Figure 3). The σ -electron withdrawing character of the nitrogen atoms stabilise the σ nonbonding orbital by increasing its s character. The nitrogen atoms have π -electrons that donate into the vacant p_{π} orbital of the carbene. This interaction with the nitrogen lone pairs increases the energy of the p_{π} orbital. The overall effect favours the singlet state by increasing the σ - p_{π} gap. The ring constraint also favours the bent singlet ground state and the N-substituents can provide kinetic stabilisation via steric bulk.

Wanzlick *et al.* showed that deprotonation of imidazolium salts was possible using potassium *tert*-butoxide ($t\text{BuOK}$), forming the corresponding NHC, which was trapped but not isolated.^[34] More than 20 years later, Arduengo *et al.* isolated the first NHC **I.18**, by deprotonation of 1,3-di-1-adamantatylimidazolium chloride **I.17** with sodium or potassium hydride and a catalytic amount of $t\text{BuOK}$ or DMSO (Scheme 5.a).^[35]

Since Arduengo's NHC, a wide variety of NHCs have been synthesised, featuring different structures (substituents or ring size and saturation) (*Scheme 5.b*). NHCs are now one of the most common ligands used in chemistry for coordination to transition metals or *p*-block elements and for organocatalysis purpose.^[36]



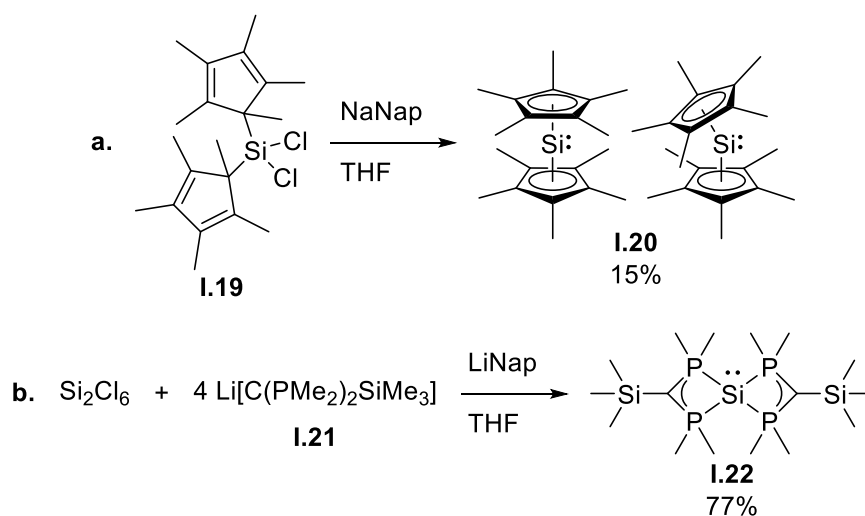
Scheme 5: **a.** Synthesis of the first isolated NHC **1.18**. **b.** Examples of NHCs. Dipp = 2,6-diisopropylphenyl.

Silylenes

Silylenes belong to the metallylene family, which are heavier group 14 analogues of carbenes, R_2M : ($\text{M} = \text{Si}, \text{Ge}, \text{Sn}, \text{Pb}$). The valency of metallylenes is two, as for carbenes, and their stability increases down the group. Heavier group 14 elements are less likely to form hybrid orbitals due to the size difference between the valence orbitals, and promotion of an electron from the s orbital to the p orbital becomes harder (*See Chap. 1, Introduction*). Therefore, the electronic configuration of silylenes will stay preferentially as a $3s^23p^2$. Calculations have shown that the difference in energy between the singlet and triplet state ΔE_{ST} ($\Delta E_{\text{ST}} = E(\text{triplet}) - E(\text{singlet})$) was 16.7 and $-14.0 \text{ kcal mol}^{-1}$ for $:\text{SiH}_2$ and $:\text{CH}_2$ respectively.^[16] Moreover, disilenes have been

theoretically and experimentally observed as *trans*-bent double-bond species (See *Chap. I, Disilenes*), whose dissociation product is a pair of singlet $:\text{SiR}_2$ species.^[16] Therefore, silylenes are expected to have a singlet ground state, with an empty p-orbital and a lone pair. The lone pair should be less reactive than in the case of carbenes due to a higher s-character, however the larger p-orbital will be highly reactive. In summary, silylenes are more π -accepting but less σ -donating compared to their carbene homologues.

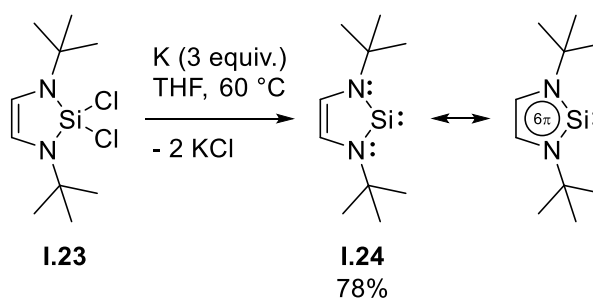
Firstly observed as transient species during reactions, the first stable silylene, decamethylsilicocene **I.20** was synthesised in 1986 by Jutzi *et al.* by reduction of the bis(pentamethylcyclopentadienyl)silicon dichloride **I.19** with sodium naphthalenide (NaNap) (*Scheme 6.a*).^[37,38] A few years later, a tetracoordinated silylene **I.22** was isolated by reduction of hexachlorodisilane (Si_2Cl_6) with lithium naphthalenide (LiNap) in the presence of lithiated diphosphine **I.21** (*Scheme 6.b*).^[39] Similarly to carbenes, the isolation of stable silylenes required kinetic and electronic stabilisation. For instance, in the case of **I.22** the two phosphorus atoms covalently bound to the silylene are slightly σ -electron-withdrawing and also π -electron-donating providing electronic stabilisation. Moreover, the presence of the two phosphorus coordinated to the p-orbital of the silylene also provides kinetic and electronic stabilisation.



Scheme 6: a. Synthesis of the first stable silylene **I.20**, by reduction with sodium naphthalenide. b. Synthesis of the tetracoordinated silylene **I.22**, by reduction with lithium naphthalenide.

Dicoordinate N-Heterocyclic Silylenes

N-heterocyclic silylenes are cyclic dicoordinate silylene compounds, analogous to NHCs. As in the case of NHCs, the kinetic and electronic stabilisation is provided by the cyclic structure and the substituents. The first dicoordinate silylene was achieved with the synthesis of the N-heterocyclic silylene **I.24** by West *et al.* in 1994, by reduction with potassium of the N-heterocyclic dichlorosilane **I.23** (Scheme 7).^[40] The silylene **I.24** showed a remarkable stability resulting from an aromatic stabilisation, which was confirmed by X-ray analysis with a shortening of the C–N and C–C bonds from the N-heterocycle between **I.23** and **I.24**. The Si–N of **I.24** are slightly longer (increased by 5.6 pm). This elongation is surprising, considering that the silicon centre becomes divalent and the ring becomes aromatic. The silylene **I.24** also showed a lower reactivity compared with transient silylenes, but **I.24** was able to coordinate to metal carbonyl $[\text{Ni}(\text{CO})_4]$ to give the complex $\text{Ni}(\text{I.24})_2(\text{CO})_2$.



Scheme 7: Reduction of **I.23** in the synthesis of the N-heterocyclic silylene **I.24**.

There now exists a large family of dicoordinate N-heterocyclic silylenes with tuned properties by the use of different substituents (*Figure 4*). The nitrogen atoms stabilise the silicon p_π orbital in a similar way for the NHCs (See *Chap. 1, Carbenes and N-Heterocyclic Carbenes*).

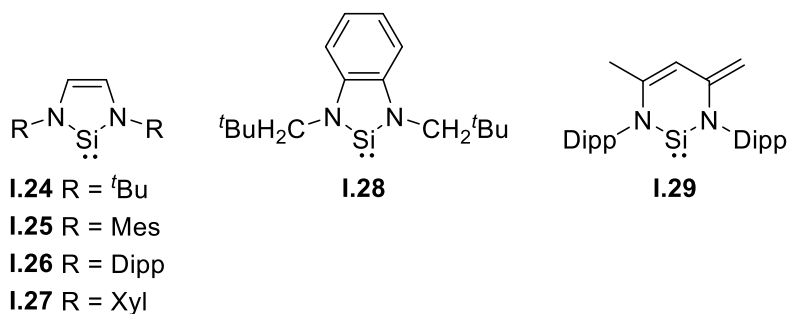
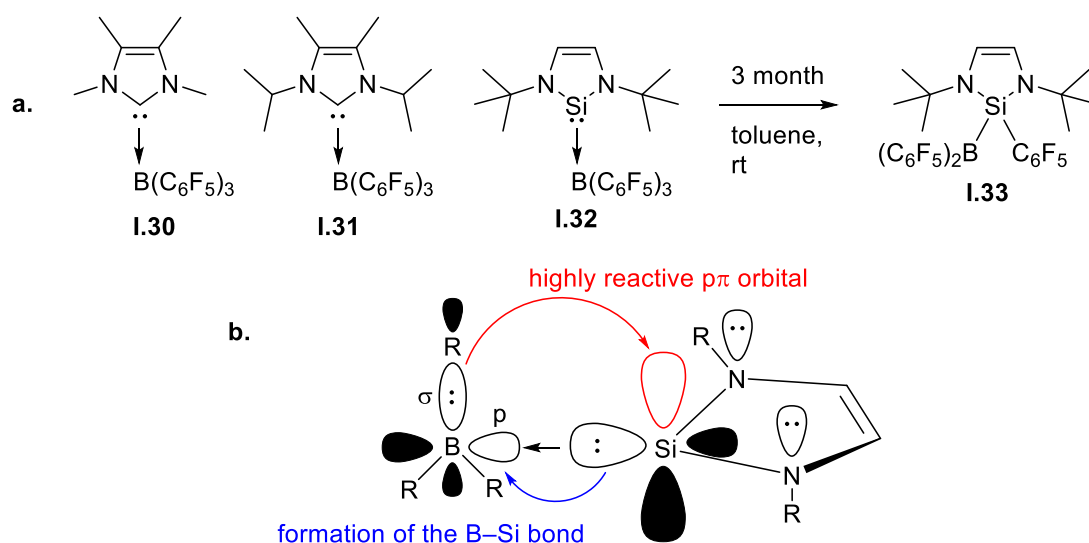


Figure 4: Examples of reported dicoordinate N-heterocyclic silylenes. Mes = 2,4,6-trimethylphenyl. Dipp = 2,6-diisopropylphenyl. Xyl = 2,6-dimethylphenyl.

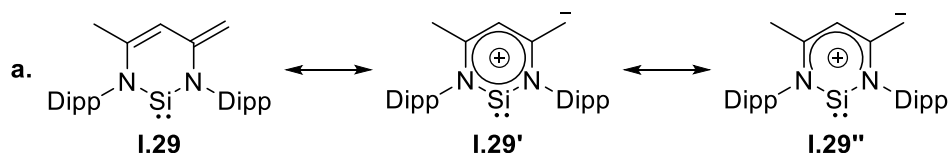
The reactivity of N-heterocyclic silylenes **I.24-28** has been investigated through oxidative additions (alcohol, haloalkane, halosilane) or coordination to both transition and main-group metals.^[41-48] While NHCs form the stable NHC-borane adducts **I.30** and **I.31** with $\text{B}(\text{C}_6\text{F}_5)_3$ (*Scheme 8.a*),^[49] the N-heterocyclic silylene-borane adduct **I.32** rearranges over time to the silylborane **I.33** by oxidative addition. This degradation is attributed to the higher reactivity of the p_π orbital of the N-heterocyclic silylene compared to NHCs, which allows nucleophilic attack from one of the B–C σ -orbital

into the vacant p_{π} orbital of the silicon(II) centre. This is followed by the formation of the B–Si bond between the lone pair from the σ orbital of the silylene and the empty p orbital from the boron (Scheme 8.b). This is an example of the general tendency of N-heterocyclic silylenes to form oxidative addition products rather than Lewis acid-base adducts.^[41–48]



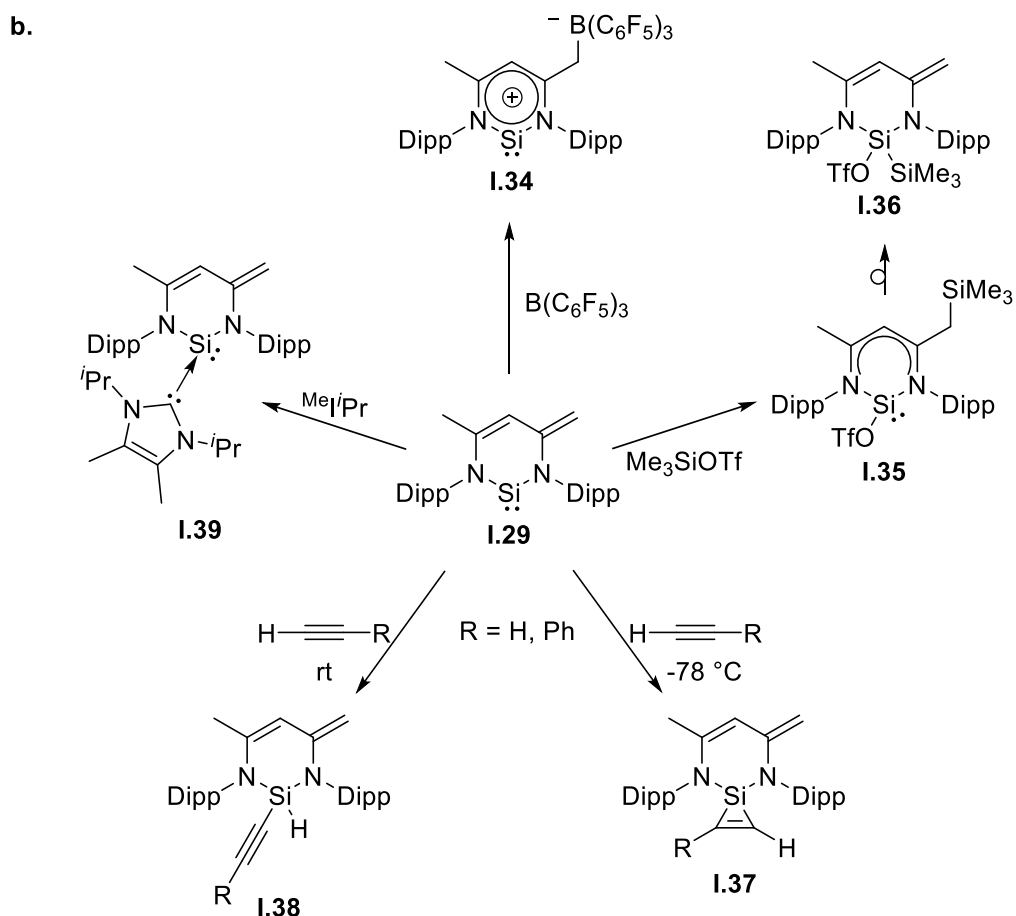
Scheme 8: a. The stable NHC-borane adducts **I.30** and **I.31** and the N-Heterocyclic Silylene-borane adduct **I.32** slowly forming the silylborane **I.33**. b. Overview of the orbital interaction leading to the disproportion of the adduct **I.32** to the silylborane **I.33**.

The six-membered ring N-heterocyclic silylene **I.29**, reported by Driess *et al.* in 2006,^[50] has a unique zwitterionic nature and calculations showed that **I.29** preferentially adopts the anti-aromatic configuration **I.29''** over **I.29'** (Scheme 9.a), with positive Nucleus-independent chemical shift (NICS(0) = 3.6, NICS(1) = 1.4 ppm) confirming the anti-aromaticity of **I.29**.^[51]



Scheme 9: a. Resonance forms for the N-Heterocyclic Silylene **I.29**.

The configuration of **I.29** is also confirmed by its reactivity; the reaction with the Lewis acid $B(C_6F_5)_3$ gives an N-heterocyclic silylene-borane adduct **I.34**^[52] and the reaction with Me_3SiOTf gives the kinetic product **I.35** which isomerises over days to the thermodynamic product **I.36** (*Scheme 9.b*). In silylene **I.29**, the π -electron-donating effect from the nitrogen atoms is decreased, therefore the p_π orbital from the silicon centre is not stabilised and is more reactive compared to the other N-heterocyclic silylenes (**I.24-28**).^[53,54] Indeed, in addition to the coordination chemistry and the compounds activated by the usual N-heterocyclic silylenes, **I.29** is able to activate a bigger range of small molecules like CO_2 or the group 15 compounds NH_3 , PH_3 and AsH_3 . The zwitterionic silylene also showed its capacity to carry out C–H and C–F activations. The silylene **I.29** was able to activate alkynes to give, surprisingly, two different products depending on the reaction conditions. At low temperature the reaction between **I.29** and alkynes gives the [2+1] cycloaddition product **I.37**, while the reaction at room temperature gives **I.38**, the oxidative addition product by C–H activation (*Scheme 9.b*). The enhanced reactivity of its vacant p_π orbital allowed coordination of NHC to **I.29**, giving the NHC-silylene adduct **I.39** (*Scheme 9.b*), which can activate N_2O .



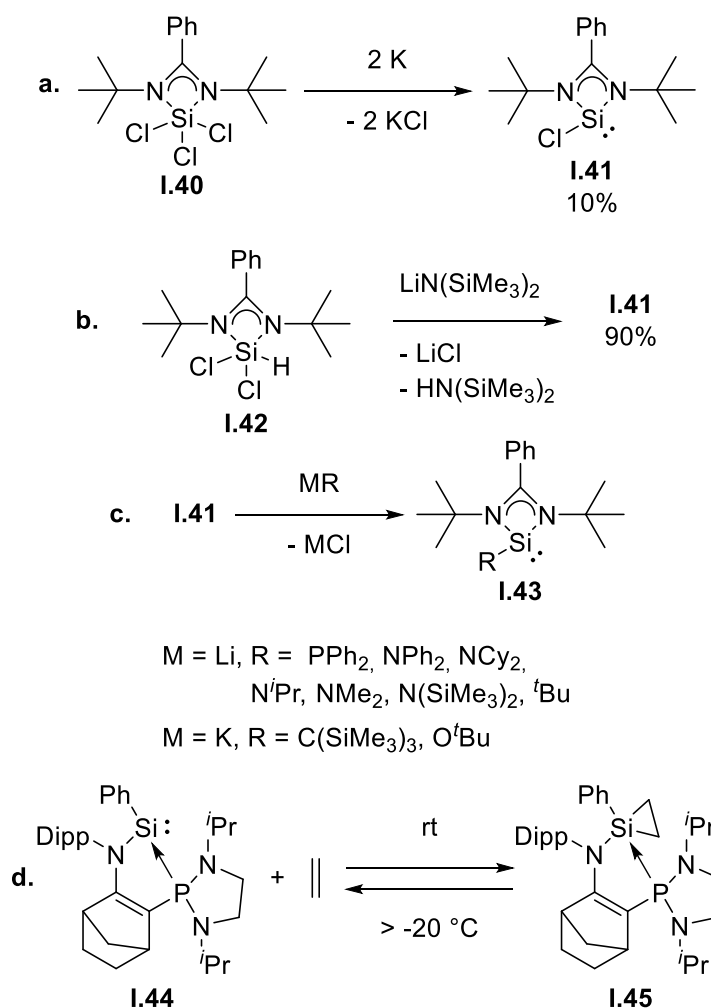
Scheme 9: b. Reaction of **1.29** with $\text{B}(\text{C}_6\text{F}_5)_3$ and Me_3SiOTf , alkyne and Me^iPr . $\text{OTf} = \text{OSO}_2\text{CF}_3$.

Tricoordinate N-Heterocyclic Silylenes

Amidinato silylenes are tricoordinate silylenes, with a silylene silicon atom bound to two substituents and coordinated by a third chelating substituent. The first amidinato silylene **1.41** was prepared in 2006 by Roesky *et al.*, the X-ray crystal structure confirmed the presence of a lone pair showing a pyramidal geometry at the silicon atom (*Scheme 10.a*).^[55] However, the reduction of trichlorosilane precursor **1.40** with potassium only afforded the silylene **1.41** in 10% yield. Access to **1.41** was improved by dehydrochlorination of **1.42** using lithium bis(trimethylsilyl)amide (LiHMDS) with 90% yield (*Scheme 10.b*). Substitution on the silicon(II) centre is possible without changing its oxidation state. A series of silylenes **1.43** were synthesised substituted

with a large variety of groups including phosphinyl, alkyl and amine (*Scheme 10.c*).^[56,57] The reactivity of tricoordinate silylenes differs from dicoordinate N-heterocyclic silylenes, which do not react with organolithium reagents. [1+2] Cycloaddition reactions were reported between **I.41** and ketones, giving monosilicon epoxides.^[58]

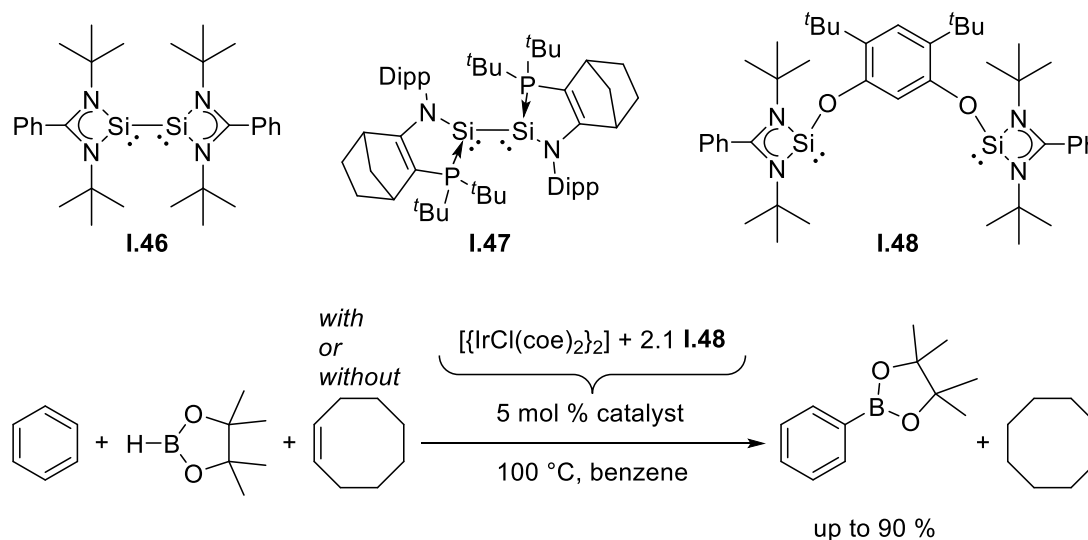
Reversible coordination of ethene to the tricoordinated-silylene was also reported, with the reaction of the phosphine-silylene complex **I.44** with ethylene at room temperature giving the silirane **I.45**, which features a pentacoordinated silicon atom. The regeneration of the silylene **I.44** was observed by decreasing the pressure of ethylene (*Scheme 10.d*).^[59] The value of Gibbs free energy for the addition reaction of **I.44** to ethylene was determined ($\Delta G_{20^\circ\text{C}} = -0.717 \pm 0.452 \text{ kcal mol}^{-1}$). Its low value shows the neutrality of the reaction, which is in contrast with the cycloaddition reactions of typical N-heterocyclic silylene with olefins. This particular reactivity of **I.44** depends on the nucleophilic character of the phosphine ligand, changing the substituent on the phosphorus for PPh_2 makes the reaction irreversible. Catalysis, in the form of the Kumada cross-coupling, was also performed using a metal complexed with **I.41** as a ligand.^[60]



Scheme 10: a. Synthesis of the silylene **I.41** by potassium reduction of **I.40**. b. Improved synthesis of **I.41** by dehydrochlorination of **I.42** with LiHMDS. c. Series of silylene derived from **I.41**. d. Reversible coordination of ethylene to the phosphine-silylene **I.44**.

In 2009, the bis-silylene **I.46** with two silicon(I) atoms was reported by Roesky *et al.* by reducing **I.40** with an excess of potassium (Scheme 11).^[61] Diverse cycloaddition with alkynes, phosphalkynes, ketones as well as reaction with Br₂ and N₂O were reported with **I.46**.^[62] Another bis-silylene (**I.47**) was reported few years later, which successfully activates CO₂ (Scheme 11).^[63] Pincer bis-silylene ligand **I.48** was also

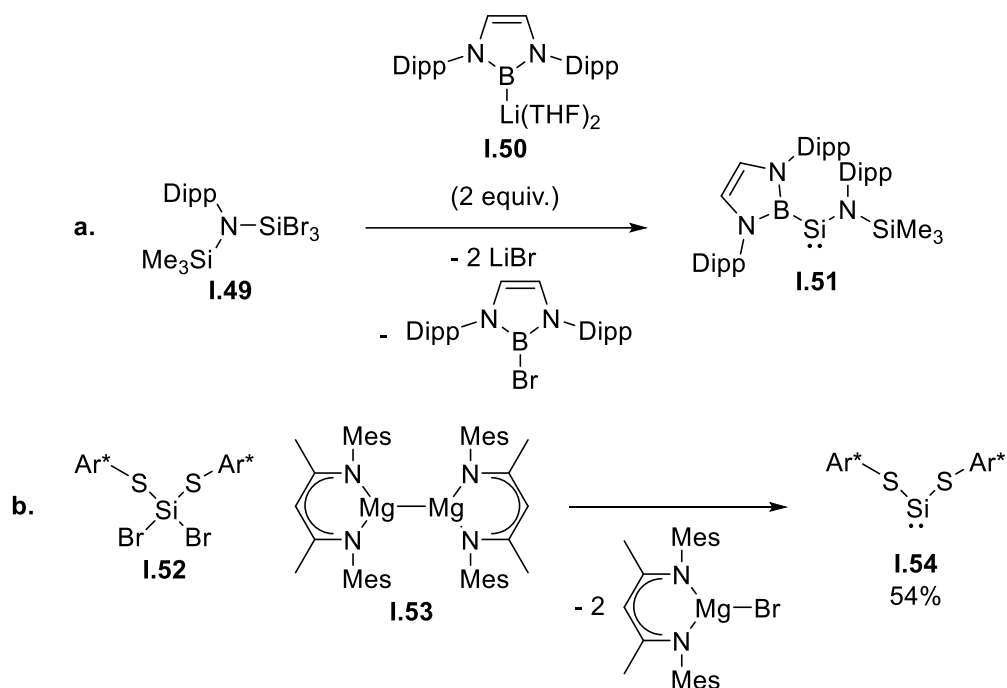
synthesised^[64] and reported to act as a pre-catalyst for C–H borylation of aryl (Scheme 11).^[65]



Scheme 11: Reported bis-silylenes **I.46**, **I.47** and **I.48**. Example a catalytic C–H borylation using the **I.48** as pre-catalyst. *coe* = cyclooctene.

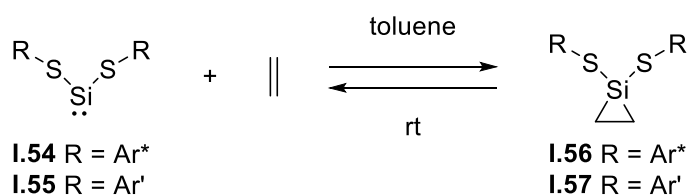
Acyclic Dicoordinate Silylenes

Acyclic dicoordinated-silylenes were for a long time limited to transient intermediates only observed spectroscopically. In 2003, the bis(*tri-tert*-butylsilyl) silylene was observed by Sekiguchi *et al.* as a triplet state silylene through EPR analysis.^[66] Silylenes usually have singlet ground states, and the observation of this triplet ground state suggested that acyclic dicoordinate silylenes should be more reactive with an accessible triplet ground state, but this also made the synthesis of acyclic dicoordinate silylenes challenging. It was only in 2012 that Power and Aldridge reported simultaneously the acyclic silylenes **I.51** and **I.54** (Scheme 12).^[67,68] **I.51** was obtained by reacting the trihalosilane **I.49** with two equivalents of the boryllithium **I.50** which both reduced **I.49** and acted as a nucleophilic boryl source. The silylene **I.54** was synthesised by reduction of the dihalosilane **I.52** with a mild magnesium(I) reducing agent **I.53**.^[69]



Scheme 12: Synthesis of the acyclic silylenes **1.51** and **1.54**. $Ar^* = C_6H_3-2,6(C_6H_2-2,4,6-Me_3)_2$.

Acyclic dicoordinated-silylenes are highly reactive, activating small inherently inert species such as H_2 .^[67,70] Cycloaddition with alkynes and dienes,^[71] and the activation of ethylene, has also been achieved,^[72] including an example with reversible coordination of ethylene under ambient conditions.^[73] Treatment of the silylene **1.54** and **1.55** with ethylene results in the rapid formation of the siliranes **1.56** and **1.57** (Scheme 13). 1H NMR spectroscopic analysis of the products **1.56** and **1.57** revealed signals from free ethylene and silylene precursors **1.54** and **1.55** respectively showing an equilibrium between the coordinated and free form, which happens under ambient conditions.



Scheme 13: Reversible coordination of ethylene to acyclic silylenes **I.54** and **I.55** under ambient conditions. Ar* = C₆H₃-2,6(C₆H₂-2,4,6-Me₃)₂. Ar' = C₆H₃-2,6(C₆H₃-2,6-ⁱPr₂)₂.

Base coordinated silicon species

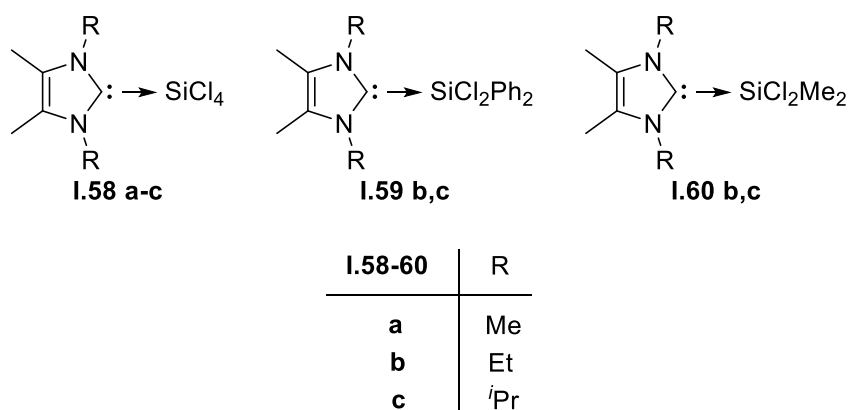
Hypervalent Base-Silicon adducts

Hypervalent silicon species were first reported at the beginning of the 19th century by Gay-Lussac and Davy, who synthesised ammonia adducts of SiF₄. In 1887, A. Harden also reported that the treatment of SiCl₄ with pyridine was accompanied by heat generation as a white amorphous solid formed.^[74] Analysis of the SiCl₄:pyridine ratio allowed the identification of the product as a “double compound” [SiCl₄(pyridine)₂]. These “double compounds” have been extensively studied and are now known as Lewis adducts. The majority of these compounds are silicon complexes involving anionic bi- or poly dentate N- or O-donor ligands.^[75] Lewis base adducts of silicon(IV) with neutral N- or O-donor ligands are also very common.^[76]

In contrast, there are only a limited number of examples of silicon(IV) adducts with phosphines. [SiX₄(PMe₃)₂] (X = Cl or Br) species were reported by Beattie *et al.* in 1969^[77] and characterised the following year by IR spectroscopy and X-ray diffraction.^[78,79] The next examples were achieved^[78,79] more than 40 years later by Levason *et al.* who reported several SiX₄ (X = F, Cl or Br) and SiHCl₃ adducts with phosphine or diphosphine ligands.^[80] Attempts to reduce these silicon(IV) complexes were unsuccessful. Levason reported that [SiCl₄(diphosphine)] was unreactive to potassium graphite or sodium naphthalenide and decomposed when treated with

potassium mirror or Jones' magnesium(I) reducing agent **I.53**,^[69] resulting in the formation of the free phosphine ligand and an unidentified pyrophoric solid.

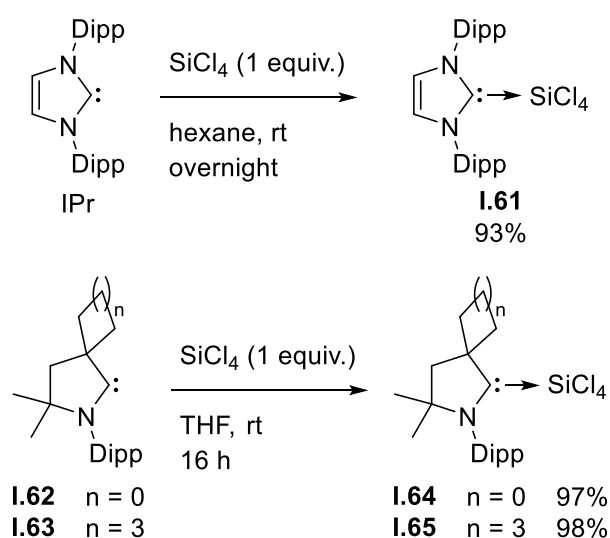
More recently silicon-base adducts were discovered by Kuhn *et al.* in 1995 with the synthesis of several SiR_4 adducts featuring an NHC **I.58-60**, simply by treating NHCs with different silicon(IV) species.^[81] Computational studies have showed that the NHC adducts were more stable than their corresponding ammonia, trimethylamine, pyridine and trimethylphosphine complexes (-8.5 , -8.2 , -7.5 and -2.4 kcal mol⁻¹ respectively) (Scheme 14).^[82]



Scheme 14: Neutral silicon(IV)-NHC adducts.

More sterically encumbered NHCs and cyclic alkylaminocarbenes (cAACs) have also been reported to form stable adducts (**I.61**, **I.64**, **I.65**) with SiCl_4 in high yields, by simple addition of SiCl_4 to the respective heterocyclic carbenes (Scheme 15).^[83,84] Further calculations showed as well that these SiCl_4 adducts with NHC were more stable than their phosphine equivalent.^[85] The free energy (ΔG) of the following reaction $\text{SiCl}_4 + \text{L} \rightarrow \text{L-SiCl}_4$ ($\text{L} = \text{NHC}$ {1,3-R-imidazole-2-ylidene} or R_3P , with $\text{R} = \text{H}$, Me , Ph) was calculated. In each case the formation of the adducts was unfavoured for the phosphine ligand with positive ΔG values (41.4 and 87.5 kJ mol⁻¹ respectively

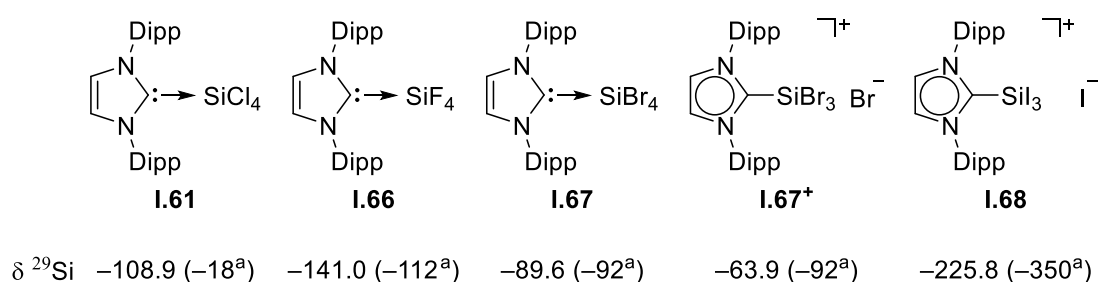
for PMe_3 and PPh_3 , no minima were located for PH_3). The NHC- SiCl_4 adducts were contrariwise favoured ($\Delta G = -43.6, -35.3, -56.2 \text{ kJ mol}^{-1}$ for the NHC {1,3-R-imidazole-2-ylidene} with R = H, Me, Ph respectively). The bulkier NHC was found to be the most stable, which is in accordance with the adducts which have been isolated with aryl substituents.



Scheme 15: IPr- SiCl_4 adduct **1.61** and cAAC- SiCl_4 adduct **1.64** and **1.65** synthesis.

Analogues of **1.61** have also been reported with all the different halogens. Roesky *et al.* reported the IPr- SiF_4 **1.66** and IPr- SiBr_4 **1.67** (Scheme 16),^[86] whilst Filippou and co-workers reported the analogue made from SiI_4 . In the latter case, the product was observed as the cation $[\text{IPr-SiI}_3]^+$ **1.68** with a dissociated iodide as counter ion by X-ray analysis.^[87] The ionic nature of **1.68** was also confirmed by ^{29}Si NMR spectroscopy with a signal considerably lower field ($\delta -225.8$) compared to SiI_4 ($\delta -350$).^[88] In the case of **1.61** and **1.66** the ^{29}Si NMR signal were considerably high field ($\delta -108.9$ and -141.0 respectively) compared to SiCl_4 ($\delta -18$) and SiF_4 ($\delta -112$), resulting from the higher silicon coordination number.^[89] The difference between **1.61**, **1.66**, **1.67** and **1.68** can easily be explained by the weakening of the silicon-halogen bond ($\Delta H_{\text{diss}} =$

540(13), 456(42), 343(50), 339(84) kJ mol⁻¹ for Si–F, Si–Cl, Si–Br, Si–I respectively), which favours the formation of an ionic product rather than an adduct.^[90] The adduct **I.67** has also been isolated in its cationic form **I.67⁺** by Filippou's group, confirming this tendency to dissociate for the heavier halogens.^[91]



Scheme 16: IPr-Silicon halide adducts and cations and their respective ²⁹Si NMR chemical shifts. [a] Signal from their respective non-coordinated tetrahalosilanes SiX₄ (X = Cl, F, Br or I).

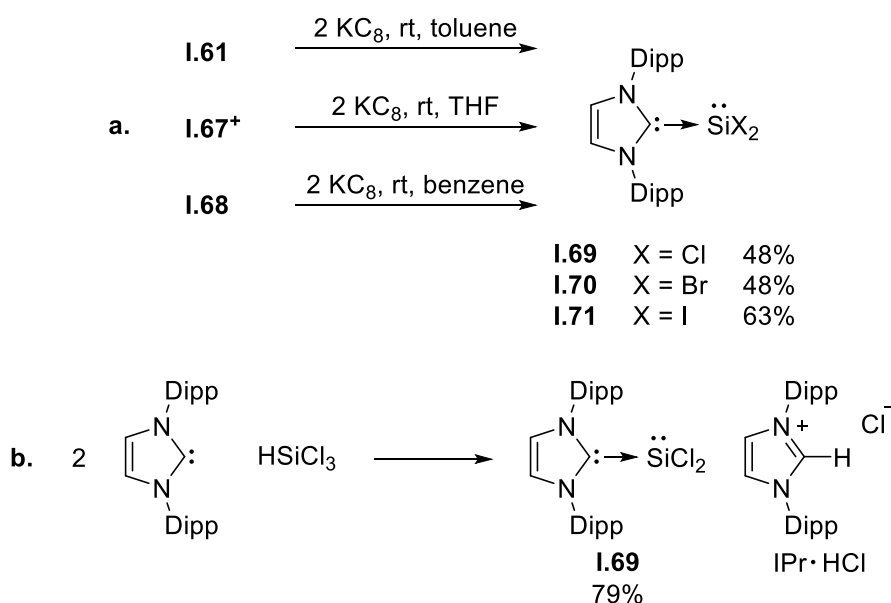
There are few examples of base-stabilised low valent and oxidation state silicon species. Their challenging synthesis has mostly been achieved through reduction of NHC-SiX₄ or cAAC-SiX₄ (X = Cl, Br or I) precursors. Dutton *et al.* stated in their computational studies that the stability of the adducts was crucial for accessing lower oxidation state silicon species,^[85] which was in accordance with their theoretical study and the already reported experimental results (*Described in the following section*). The stability of the NHC-SiX₄ and cAAC-SiX₄ adducts allowed the synthesis of low oxidation state silicon species.

Base-Silicon(II) adducts

The base-stabilised silylenes described in this section are minimally-substituted dihalosilylenes stabilised with NHCs. Unlike the previously described tricoordinate silylenes (*See Chap. I, Tricoordinate N-Heterocyclic Silylenes*), NHC-stabilised

silylenes have small substituents bound to the silicon centre, evidencing the strong ability of the coordinated NHC to stabilise low valent species.

In 2009, the groups from Roesky and Filippou reported respectively dichloro- and dibromosilylene stabilised with IPr.^[91,92] Filippou and co-workers also achieved the diiodosilylene supported by IPr a few years later.^[87] The dihalosilylenes **1.69-71** were obtained by reduction of the NHC adduct precursors **1.61**, **1.67⁺** and **1.68** with KC_8 (Scheme 17.a). The dichlorosilylene **1.69** was also obtainable under mild conditions by treating trichlorosilane $HSiCl_3$ with two equivalents of IPr. The product **1.69** was recovered along with the imidazolium chloride salt IPr \cdot HCl (Scheme 17.b).

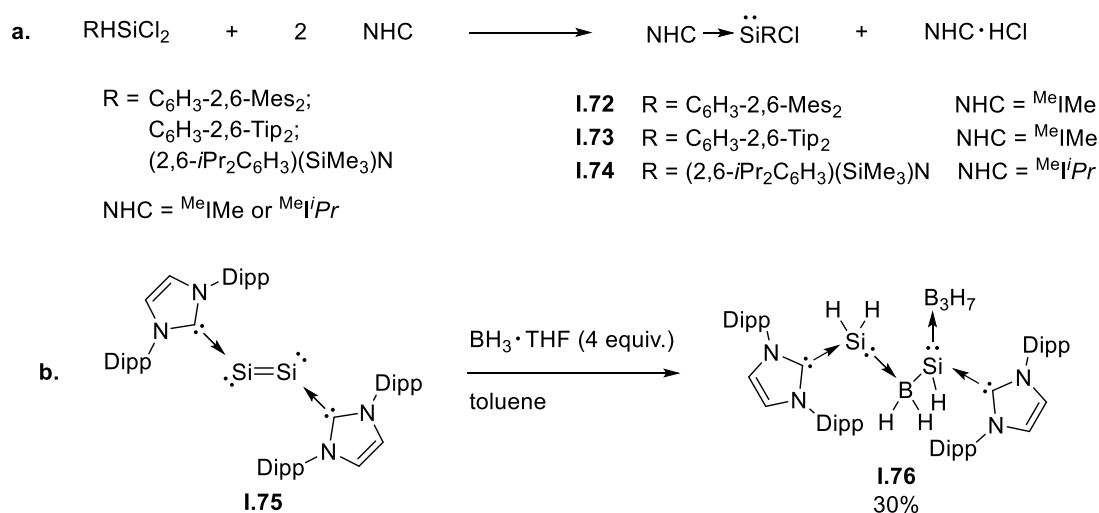


Scheme 17: a. Synthesis of the dihalosilylene via KC_8 reduction. b. Synthesis of the dichlorosilylene via mild reaction conditions.

^{29}Si NMR spectroscopy of the three dihalosilylenes **1.69**, **1.70** and **1.71** revealed signals in a similar region (δ 19.1, 10.9, -9.7 respectively). The deshielding observed on the ^{29}Si nucleus follows the same trend as the Si(IV) halides ($\chi_I < \chi_{Br} < \chi_{Cl}$). The very

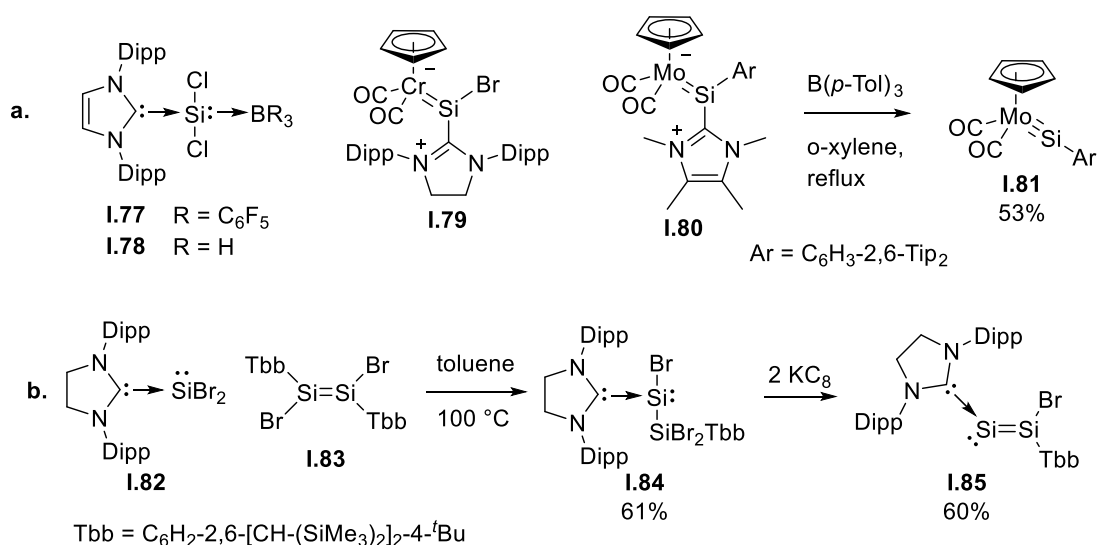
deshielded silicon signals of the dihalosilylenes compared to their Si(IV) adduct precursors is in accordance with the formation of silicon(II) centres. The tricoordinate silicon centres feature a trigonal pyramidal geometry in each case, which indicates the presence of a lone pair of electrons at the silicon atom.

Other examples of NHC-stabilised silylenes have been isolated. The silylenes **1.72-74** were obtained using a similar procedure used for the dichlorosilylene **1.69**.^[93,94] An excess of NHC was added to the silane, promoting the reductive elimination of HCl to give the products **1.72-74** along with the corresponding imidazolium salt NHC·HCl (*Scheme 18.a*). The last method to achieve an NHC stabilised silylene was the cleavage of a disilicon(0) specie **1.75** (*See Chap. I, Base-stabilised disilicon(0)*) using BH₃, forming the product **1.76** which features the first donor-acceptor complex of SiH₂, the parent silylene (*Scheme 18.b*).^[95]



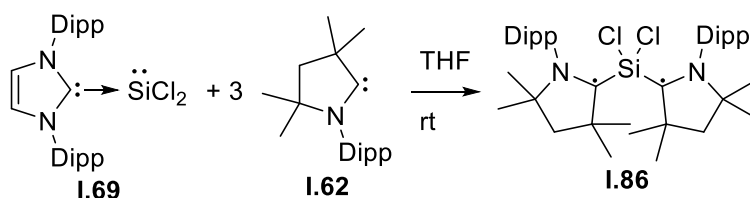
Scheme 18: a. Synthesis of silylenes **1.72-74** by reductive elimination of HCl using NHC. b. Synthesis of the complex **1.76** featuring a silylene SiH₂.

The complex **I.76** shows that the lone pair of the silylene centre has a σ -donor capacity, forming an acceptor-donor product. The ambiphilicity of the silylene has been explored toward several reactions. By reacting the dichlorosilylene **I.69** with the Lewis acids $B(C_6F_5)_3$ and BH_3 , two acceptor-donor complexes were obtained **I.77** and **I.78** respectively (Scheme 19.a).^[96,97] Treatment of the different dihalosilylenes with $Li[CpM(CO)_3]$ (M = Cr or Mo) in hot toluene allowed the synthesis of metal-silicon multiply bonded compounds **I.79**, **I.80** and **I.81** (Scheme 19.a).^[98,99] The analogous dibromosilylene **I.82** (Scheme 19.b) was also reported by Filippou *et al.* using a similar preparation with SIPr instead of IPr.^[98] Their group also reported that the reaction between the silylene **I.82** and the disilene **I.83** followed by reduction with KC_8 allowed the synthesis of the disilavinylidene **I.85** (Scheme 19.b).^[100]



Scheme 19: **a.** The acceptor-donor complex and the metal-silicon multiply bonded compounds obtained from the silylenes **I.69**, **I.73** and **I.82**. **b.** Synthesis of the disilavinylidene **I.85** from the silylene **I.82**.

The last interesting example of reactivity is the reaction between the dichlorosilylene **I.69** and an excess of cAAC **I.62** which gave the biradical product **I.86** (Scheme 20).^[101] Firstly, a ligand exchange reaction occurs between the NHC and the stronger donor carbene, cAAC. Two bonds are formed between a triplet state SiCl_2 fragment and the cAACs, the unpaired electrons from the singly occupied σ -orbitals of the carbene couple with the unpaired electrons of the SiCl_2 . Each carbene has an unpaired electron which couples with the lone-pair orbital of the nitrogen atom. The structure of the product was confirmed by the short C–Si bonds (1.8455(16), 1.8482(17) Å) compared to the donor-acceptor complex (**I.69**: C–Si = 1.985(4) Å) and the Cl–Si–Cl angle which is larger in the case of **I.86** (105.51(3)°, **I.69**: Cl–Si–Cl = 97.25(6)°). This is due to the absence of lone pair on the triplet state silicon centre of **I.86**, which normally repels the chlorine atoms.



Scheme 20: Synthesis of the biradical **I.86**.

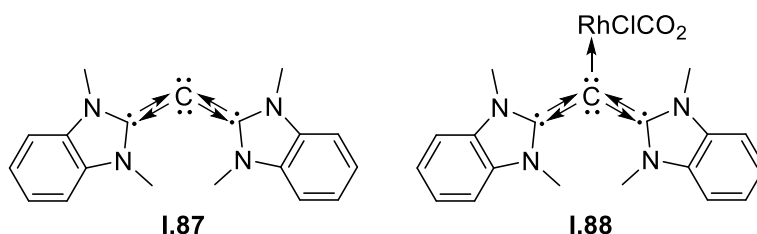
The formation of the product **I.86** required the excitation of SiCl_2 and the two cAAC ligands from the singlet state to the triplet state, followed by the formation of two C–Si bonds (113.6 kcal mol⁻¹ per bond) which is higher in energy than the coordination from the cAAC to the silylene (42.5 kcal mol⁻¹). However, the bond dissociation energy of **I.86** (227.2 kcal mol⁻¹) compensates the energy required for the singlet-triplet state excitation of the different fragments (159.9 kcal mol⁻¹). The gain in energy with the formation of **I.86** (67.3 kcal mol⁻¹) is higher than the bond dissociation of the

cAAC:SiCl₂ donor-acceptor product (42.5 kcal mol⁻¹). The product **I.86** is thermodynamically more stable compared to the singlet complex. Theoretical studies, however, stated that there is a small preference for the singlet biradical state (3-5 kcal mol⁻¹) compared to the triplet state.

Base-Silicon(0) adducts

Silylone

Silylones are compounds which feature one atom of silicon in the formal oxidation state of zero, coordinated by two carbene carbon atoms. Silylones were introduced by Frenking *et al.* through theoretical studies,^[102,103] which followed the synthesis of the carbon analogue **I.87** (Scheme 21).^[104] The carbodicarbene **I.87** features a bent geometry with a C_{carbene}-C-C_{carbene} angle of 134.8(2)°, and substituents on the carbene ligands which are not orthogonal to each other. The carbodicarbene **I.87** formed a η¹-coordinated complex **I.88** instead of a η²-coordination involving a C=C π bond typically observed for allene-metal complexes (Scheme 21).^[105] Different to the allenes, the structure and reactivity of **I.87** confirmed the presence of the lone pairs on the carbon(0) centre and the coordination from the carbenes. The structure of the silylone was predicted to be similar to the carbodicarbene.

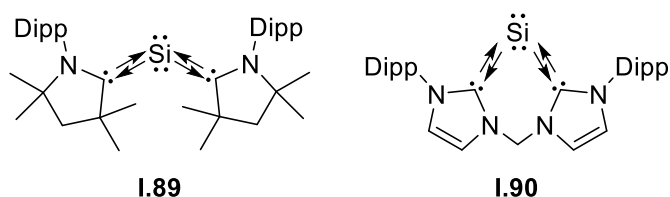


Scheme 21: The carbodicarbene **I.87** and its Rhodium complex **I.88**.

The first silylone **I.89** was isolated by Roesky and co-workers by reduction of the biradical **I.86** (See Chap. I, Base-Silicon(II) adducts) using two equivalent of KC_8 (Scheme 22).^[106] ^{29}Si NMR spectroscopic studies of **I.89** showed a downfield silicon signal (δ 66.71) compared to the precursor **I.86** (δ 4.13).^[101] The silylone **I.89** has a bent geometry with a C-Si-C angle of $117.70(8)^\circ$, which follows the predicted geometry (95.0°).^[102] The Si-C bonds in **I.89** ($1.8411(18)$ and $1.8417(17)$ Å) are slightly shorter than the calculated values (1.869 Å),^[102] but are longer than Si=C double bonds (1.702 - 1.775 Å),^[107] which confirms the coordination of the carbene ligands to the silicon atom. Calculations revealed that **I.89** was in the singlet state, with the triplet state higher in energy (17.2 - 18.5 kcal mol $^{-1}$). The HOMO-1 is a σ lone-pair at the silicon atom and the HOMO is a π -type orbital which shows Si-C π bonding. This is consistent with the presence of a silicon(0) centre and with the π -accepting character from the cAAC ligand.

A few other silylones have been reported with different cAACs,^[108] as well as the cyclic silylone **I.90** which features a bis-NHC ligand (Scheme 22).^[109] ^{29}Si NMR spectroscopy shows a very highfield signal (δ -80.1) compared to **I.89** (δ 66.71). The strong σ -donor and weak π -acceptor ability from the bis-NHC ligand compared to the cAACs is responsible for this important shielding.

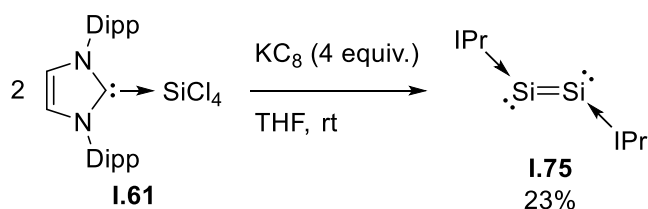
The heavier analogue trisilaallene, which involves silylene ligands instead of carbenes, was reported by Kira *et al.* in 2003 and will be discussed in the following section.^[110]



Scheme 22: The silylone **1.89** stabilised with two cAACs and the cyclic silylone **1.90**.

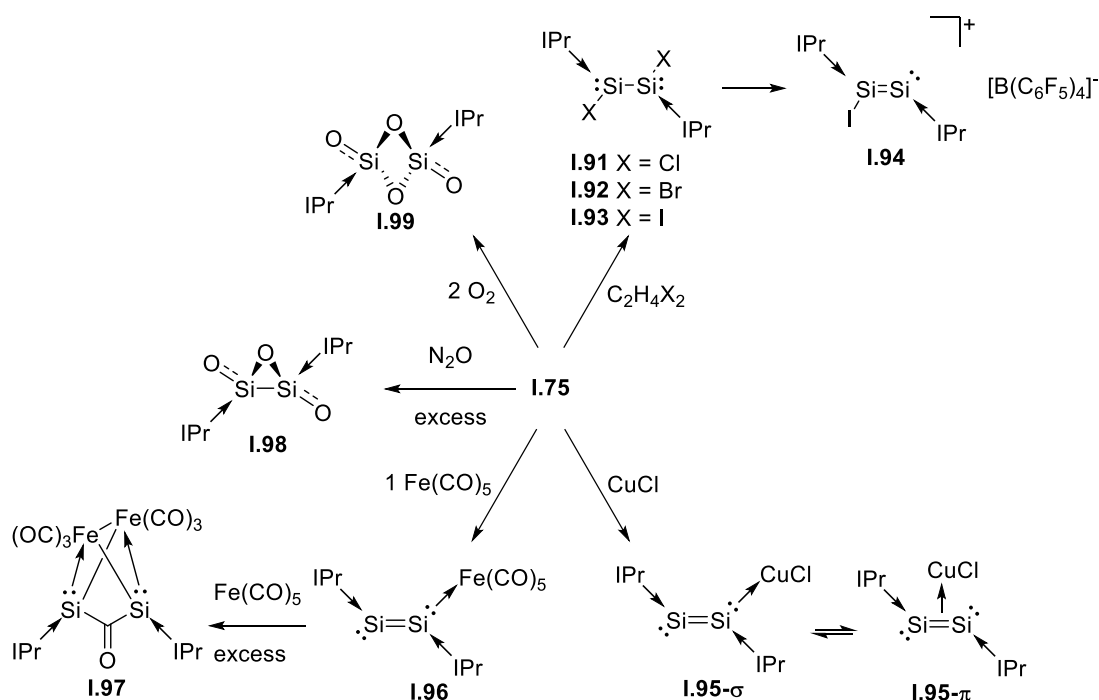
Base-stabilised disilicon(0)

In 2008, Robinson *et al.* reported that reduction of the silicon adduct **1.61** with KC_8 afforded the product **1.75** with two silicon atoms in the formal oxidation state of zero stabilised by two NHCs (IPr) (Scheme 23).^[83] The disilicon(0) species **1.75** shows a very deshielded silicon signal in the ^{29}Si NMR at δ 224.5, this value is much higher than the precursor (δ –108.9) or other low valent species like silylones, N-heterocyclic silylenes. The two central silicon atoms feature a double bond with a Si–Si bond length of 2.2294(11) Å in the region of disilenes (2.14–2.29 Å).^[14] The disilicon(0) species **1.75** adopts a noticeably more *trans*-bent geometry than disilenes, the two NHCs are parallel and almost perpendicular to the Si=Si double bond (C–Si–Si angle = 93.37(5)°). This configuration is in accordance with the presence of a lone-pair on each silicon atom. The HOMO corresponds to the Si–Si π orbital and the HOMO–1 and HOMO–2 correspond to the two-nonbonding lone-pairs on the silicon atoms.



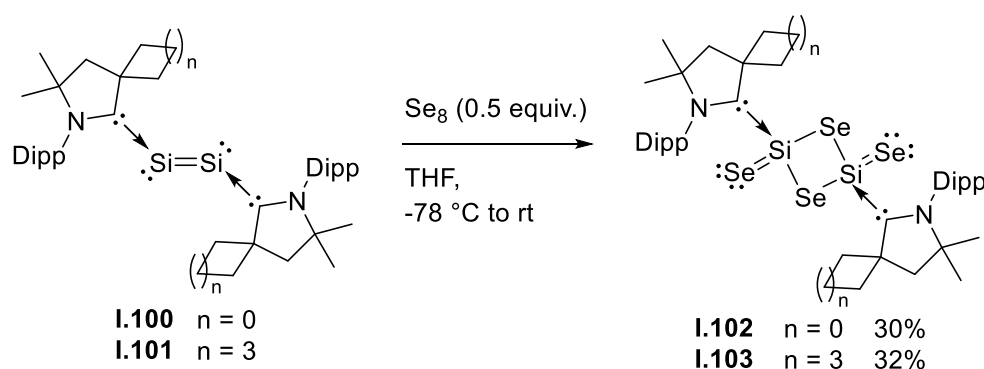
Scheme 23: Synthesis of the disilicon(0) species **1.75**.

Few examples of its reactivity have been reported. Cleavage of the Si=Si double bond using BH_3 gives the product **I.76** (See Chap. I, Base-Silicon(II) adducts).^[95] Filippou and co-workers reported halogenation of the double bond using 1,2- $\text{C}_2\text{H}_4\text{X}_2$ (X = Cl, Br, I) which gave the product **I.91-93** as well as the synthesis of the cation **I.94** by abstraction of an iodide using $[\text{Li}(\text{Et}_2\text{O})_{2.5}][\text{B}(\text{C}_6\text{F}_5)_4]$ (Scheme 24).^[111] Reactions with transition metals have also been explored: the treatment of **I.75** with copper(I) chloride gives a metal complex which is in an equilibrium between the σ and the π complex **I.95- σ** and **I.95- π** (Scheme 24).^[112] The reaction of the disilicon(0) **I.75** with one equivalent of $\text{Fe}(\text{CO})_5$ initially gives the donor-acceptor complex **I.96**, whilst cleavage of the Si=Si double bond and CO insertion is observed when excess $\text{Fe}(\text{CO})_5$ is used, giving the complex **I.97**.^[113] Finally, oxidation of **I.75** with N_2O or O_2 give respectively the NHC stabilised silicon-oxides **I.98** and **I.99** (Scheme 24).^[114]



Scheme 24: Diverse reactivities of the disilicon(0) **I.75**.

Similar compounds to disilicon(0) **I.100-101** have been prepared using cAACs by reduction of silicon(IV) halide cAAC-adduct precursors **I.64-65** with KC_8 at -78°C .^[115] **I.100** shows a single signal by ^{29}Si NMR spectroscopy (δ 254.6) in a region which is similar to the disilicon(0) **I.75**. Surprisingly, **I.101** shows two signals at two very different resonances (δ 190.1 and 318.3), which was attributed to the two inequivalent silicon atoms, but no precise explanation was found for this large difference. The Si=Si bond lengths (**I.100**: 2.254(2) Å, **I.101**: 2.255(4) Å) were similar in each case to the Si=Si double bond from **I.75**. Treatment with selenium afforded the Se-bridged and Si=Se species **I.102-103** (Scheme 25).

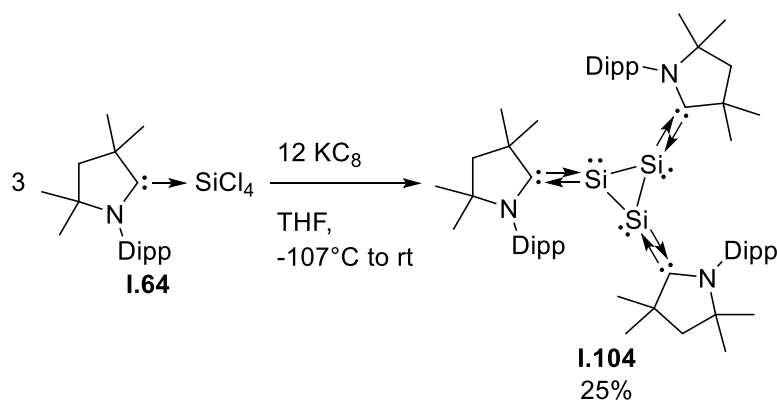


Scheme 25: The cAAC-stabilised disilicon(0) and its reaction with selenium.

Base-stabilised trisilicon(0)

In 2016, Roesky *et al.* synthesised a triatomic silicon(0) cluster stabilised with three cAACs (**I.104**).^[116] Using a similar protocol as was used to prepare **I.100** and **I.101**, but at a lower temperatures, the reduction of **I.64** with KC_8 at -107°C afforded the trisilicon(0) species **I.104** (Scheme 26). The ^{29}Si NMR spectrum of **I.104** showed a surprisingly upfield signal (δ 7.20) compared to the disilicon(0) **I.100** (δ 254.6) and **I.101** (δ 190.1 and 318.3). The Si–Si bond lengths of **I.104** (2.399(8), 2.369(8) and 2.398(8) Å) are close to the typical Si–Si single bond (2.34 Å).^[14] Each silicon atom

has a trigonal pyramidal structure, which is due to the presence of a lone pair on each silicon. Computational studies showed that the cAAC ligands were strongly σ -donating to the silicon atoms but there was a strong π -back-donation from the silicon lone-pair orbitals. They explained that this strong back-donation was most likely due to the repulsion of the lone pair of the three silicon atoms. They concluded that the high π -accepting character from the cAAC ligands compared to NHCs was essential to stabilise this low valent species.



Scheme 26: Synthesis of the cAAC-stabilised trisilicon(0) **I.104**.

Conclusion

Since their discovery, the reactivity of silylenes has been intensively investigated. Recently, the use of carbene ligands allowed the stabilisation of low valent silicon species, providing kinetic and thermodynamic stabilisation. The use of silylenes to stabilise low valent species is rarer. Only a few examples have been reported using a cyclic silylene and will be discussed in the following section. The similar properties, shared between NHCs and N-heterocyclic silylenes, make the latter interesting candidates to stabilise low valent species in the same fashion observed for NHCs.

References

- [1] Y. Apeloig, *The Chemistry of Organic Silicon Compounds*, **2001**.
- [2] K. S. Pitzer, *J. Am. Chem. Soc.* **1948**, *70*, 2140–2145.
- [3] D. Scheschkewitz, *Functional Molecular Silicon Compounds II*, **2013**.
- [4] L. E. Gusel’Nikov, N. S. Nametkin, *Chem. Rev.* **1979**, *79*, 529–577.
- [5] R. West, M. J. Fink, J. Michl, *Science* **1981**, *214*, 1343–1344.
- [6] S. Masamune, Y. Hanzawa, S. Murakami, T. Bally, J. F. Blount, *J. Am. Chem. Soc.* **1982**, *104*, 1150–1153.
- [7] M. J. Fink, D. J. DeYoung, R. West, J. Michl, *J. Am. Chem. Soc.* **1983**, *105*, 1070–1071.
- [8] S. Murakami, S. Collins, S. Masamune, *Tetrahedron Lett.* **1984**, *25*, 2131–2134.
- [9] R. West, *J. Am. Chem. Soc.* **1984**, *106*, 821–822.
- [10] R. West, D. J. De Young, K. J. Haller, *J. Am. Chem. Soc.* **1985**, *107*, 4942–4946.
- [11] H. Watanabe, *Chem. Lett.* **1987**, 1341–1344.
- [12] H. B. Yokelson, A. J. Millevolte, B. R. Adams, R. West, *J. Am. Chem. Soc.* **1987**, *109*, 4116–4118.
- [13] M. Driess, A. Funta, D. D. Powell, R. West, A. D. Fanta, *Angew. Chem.* **1989**, *101*, 1087–1088.
- [14] Y. Apeloig, *The Chemistry of Organic Silicon Compounds*, Vol. 3, Chap. 5, **2001**.
- [15] M. J. Fink, M. J. Michalczyk, K. J. Haller, R. West, J. Michl, *J. Chem. Soc., Chem. Commun.* **1983**, 1010–1011.
- [16] G. Trinquier, *J. Am. Chem. Soc.* **1990**, *112*, 2130–2137.
- [17] R. West, *Polyhedron* **2002**, *21*, 467–472.
- [18] M. Weidenbruch, *J. Organomet. Chem.* **2002**, *646*, 39–52.
- [19] M. Weidenbruch, *Organometallics* **2003**, *22*, 4348–4360.
- [20] M. Weidenbruch, S. Willms, W. Saak, G. Henkel, *Angew. Chem. Int. Ed.* **1997**, *36*, 2503–2504.
- [21] D. Scheschkewitz, *Angew. Chem. Int. Ed.* **2004**, *43*, 2965–2967.
- [22] N. Wiberg, W. Niedermayer, G. Fischer, H. Nöth, M. Suter, *Eur. J. Inorg. Chem* **2002**, 1066–1070.
- [23] N. Wiberg, S. K. Vasisht, G. Fischer, P. Mayer, *Zeitschrift für Anorg. und Allg. Chemie* **2004**, *630*, 1823–1828.
- [24] A. Sekiguchi, R. Kinjo, M. Ichinohe, *Science* **2004**, *305*, 1755–1757.

- [25] B. T. Colegrove, H. F. Schaefer, *J. Phys. Chem.* **1990**, *94*, 5593–5602.
- [26] S. Nagase, K. Kobayashi, N. Takagi, *J. Organomet. Chem.* **2000**, *611*, 264–271.
- [27] P. P. Power, *Chem. Commun.* **2003**, *3*, 2091–2101.
- [28] T. Sasamori, K. Hironaka, Y. Sugiyama, N. Takagi, S. Nagase, Y. Hosoi, Y. Furukawa, N. Tokitoh, *J. Am. Chem. Soc.* **2008**, *130*, 13856–13857.
- [29] Y. Murata, M. Ichinohe, A. Sekiguchi, *J. Am. Chem. Soc.* **2010**, *132*, 16768–16770.
- [30] S. Ishida, R. Sugawara, Y. Misawa, T. Iwamoto, *Angew. Chem. Int. Ed.* **2013**, *52*, 12869–12873.
- [31] M. Asay, A. Sekiguchi, *Bull. Chem. Soc. Jpn.* **2012**, *85*, 1245–1261.
- [32] T. Sasamori, N. Tokitoh, *Bull. Chem. Soc. Jpn.* **2013**, *86*, 1005–1021.
- [33] T. Yamaguchi, A. Sekiguchi, M. Driess, *J. Am. Chem. Soc.* **2010**, *132*, 14061–14063.
- [34] V. H.-J. Schonherr, H.- Werner, *Liebigs Ann. Chem.* **1970**, *731*, 176–179.
- [35] A. J. Arduengo, M. Kline, *J. Am. Chem. Soc.* **1991**, *113*, 361–363.
- [36] M. N. Hopkinson, C. Richter, M. Schedler, F. Glorius, *Nature* **2014**, *510*, 485–496.
- [37] P. Jutzi, D. Kanne, C. Krüger, *Angew. Chem. Int. Ed.* **1986**, *25*, 164–164.
- [38] P. Jutzi, U. Holtmann, D. Kanne, C. Kruger, R. Blom, R. Gleiter, I. Hylakryspind, *Chem. Ber.* **1989**, *122*, 1629–1639.
- [39] C. D. R. J. Gillespie, J. J. Park, J. P. I. Chem, J. P. Sawyer, A. Crystollogr, M. J. C. R. J. Gillespie, *Angew. Chem. Int. Ed.* **1990**, *29*, 295–296.
- [40] M. Denk, R. Lennon, R. Hayashi, R. West, A. V. Belyakov, H. P. Verne, A. Haaland, M. Wagner, N. Metzler, *J. Am. Chem. Soc.* **1994**, *116*, 2691–2692.
- [41] B. Gehrhus, P. B. Hitchcock, M. F. Lappert, J. Heinicke, R. Boese, D. Bläser, *J. Organomet. Chem.* **1996**, *521*, 211–220.
- [42] N. Metzler, M. Denk, *Chem. Commun.* **1996**, 2657–2658.
- [43] M. Haaf, A. Schmiedl, T. A. Schmedake, D. R. Powell, A. J. Millevolte, M. Denk, R. West, *J. Am. Chem. Soc.* **1998**, *120*, 12714–12719.
- [44] D. F. Moser, T. Bosse, J. Olson, J. L. Moser, I. A. Guzei, R. West, *J. Am. Chem. Soc.* **2002**, *124*, 4186–4187.
- [45] D. F. Moser, A. Naka, I. A. Guzei, T. Müller, R. West, *J. Am. Chem. Soc.* **2005**, *127*, 14730–14738.
- [46] B. Gehrhus, P. B. Hitchcock, H. Jansen, *J. Organomet. Chem.* **2006**, *691*, 811–816.
- [47] L. Kong, J. Zhang, H. Song, C. Cui, *Dalt. Trans.* **2009**, 5444–5446.

- [48] P. Zark, A. Schafer, A. Mitra, D. Haase, W. Saak, R. West, T. Muller, *J. Organomet. Chem.* **2010**, 695, 398–408.
- [49] J. Chen, E. Y. Chen, *Isr. J. Chem.* **2015**, 55, 216–225.
- [50] M. Driess, S. Yao, M. Brym, C. Van Wüllen, D. Lentz, *J. Am. Chem. Soc.* **2006**, 128, 9628–9629.
- [51] † Zhongfang Chen *, † Chaitanya S. Wannere, † Clémence Corminboeuf, ‡ Ralph Puchta, † and Paul von Ragué Schleyer*, *Chem. Rev.* **2005**, 105, 3842–3888.
- [52] M. Driess, S. Yao, M. Brym, C. Van Wüllen, *Angew. Chem. Int. Ed.* **2006**, 45, 6730–6733.
- [53] D. Scheschkewitz, *Functional Molecular Silicon Compounds II*, **2013**.
- [54] S. Yao, Y. Xiong, M. Driess, *Organometallics* **2011**, 30, 1748–1767.
- [55] C. So, H. W. Roesky, J. Magull, R. B. Oswald, *Angew. Chem. Int. Ed.* **2006**, 45, 3948–3950.
- [56] M. Scheer, *Chem. Commun.* **2012**, 48, 4561–4563.
- [57] R. Azhakar, R. S. Ghadwal, H. W. Roesky, H. Wolf, D. Stalke, *Organometallics* **2012**, 31, 4588–4592.
- [58] R. S. Ghadwal, S. S. Sen, H. W. Roesky, M. Granitzka, D. Kratzert, S. Merkel, D. Stalke, *Angew. Chem. Int. Ed.* **2010**, 49, 3952–3955.
- [59] R. Rodriguez, D. Gau, T. Kato, N. Saffon-Merceron, A. De Cózar, F. P. Cossío, A. Baceiredo, *Angew. Chem. Int. Ed.* **2011**, 50, 10414–10416.
- [60] X. Qi, H. Sun, X. Li, O. Fuhr, D. Fenske, *Dalt. Trans.* **2018**, 47, 2581–2588.
- [61] S. S. Sen, A. Jana, H. W. Roesky, C. Schulzke, *Angew. Chem. Int. Ed.* **2009**, 48, 8536–8538.
- [62] S. S. Sen, S. Khan, S. Nagendran, H. W. Roesky, *Acc. Chem. Res.* **2012**, 45, 578–587.
- [63] D. Gau, R. Rodriguez, T. Kato, N. Saffon-Merceron, A. De Cózar, F. P. Cossío, A. Baceiredo, *Angew. Chem. Int. Ed.* **2011**, 50, 1092–1096.
- [64] W. Wang, S. Inoue, E. Irran, M. Driess, *Angew. Chem. Int. Ed.* **2012**, 51, 3691–3694.
- [65] A. Brück, D. Gallego, W. Wang, E. Irran, M. Driess, J. F. Hartwig, *Angew. Chem. Int. Ed.* **2012**, 51, 11478–11482.
- [66] A. Sekiguchi, T. Tanaka, M. Ichinohe, K. Akiyama, S. Tero-kubota, *J. Am. Chem. Soc.* **2003**, 125, 4962–4963.
- [67] A. V. Protchenko, K. H. Birj Kumar, D. Dange, A. D. Schwarz, D. Vidovic, C. Jones, N. Kaltsoyannis, P. Mountford, S. Aldridge, *J. Am. Chem. Soc.* **2012**, 134, 6500–6503.
- [68] B. D. Reken, T. M. Brown, J. C. Fettinger, H. M. Tuononen, P. P. Power, *J. Am. Chem. Soc.* **2012**, 134, 6504–6507.

- [69] S. P. Green, C. Jones, A. Stasch, *Science* **2007**, *318*, 1754–1757.
- [70] A. V. Protchenko, A. D. Schwarz, M. P. Blake, C. Jones, N. Kaltsoyannis, P. Mountford, S. Aldridge, *Angew. Chem. Int. Ed.* **2013**, *52*, 568–571.
- [71] F. Lips, A. Mansikkamäki, J. C. Fettinger, H. M. Tuononen, P. P. Power, *Organometallics* **2014**, *33*, 6253–6258.
- [72] D. Wendel, D. Reiter, A. Porzelt, P. J. Altmann, S. Inoue, B. Rieger, *J. Am. Chem. Soc.* **2017**, *139*, 17193–17198.
- [73] F. Lips, J. C. Fettinger, A. Mansikkamäki, H. M. Tuononen, P. P. Power, *J. Am. Chem. Soc.* **2014**, *136*, 634–637.
- [74] A. Harden, *J. Chem. Soc., Trans.*, **1887**, *51*, 40–47.
- [75] C. Chuit, R. J. P. Corriu, C. Reye, J. C. Young, *Chem. Rev.* **1993**, *93*, 1371–1448.
- [76] W. Levason, G. Reid, W. Zhang, *Coord. Chem. Rev.* **2011**, *255*, 1319–1341.
- [77] I. R. Beattie, G. A. Ozin, *J. Chem. Soc. A* **1969**, 2267.
- [78] I. R. Beattie, G. A. Ozin, *J. Chem. Soc. A* **1970**, 370–377.
- [79] H. E. Blayden, M. Webster, *Inorg. Nucl. Chem. Lett.* **1970**, *6*, 703–705.
- [80] W. Levason, D. Pugh, G. Reid, *Inorg. Chem.* **2013**, *52*, 5185–5193.
- [81] N. Kuhn, T. Kratza, D. Blaserb, *Chem. Ber.* **1995**, *128*, 245–250.
- [82] O. Hollóczki, L. Nyulászi, *Organometallics* **2009**, *28*, 4159–4164.
- [83] Y. Wang, Y. Xie, P. Wei, R. B. King, H. F. Schaefer, P. V. R. Schleyer, G. H. Robinson, *Science* **2008**, *321*, 1069–1071.
- [84] K. C. Mondal, H. W. Roesky, A. C. Stückl, F. Ehret, W. Kaim, B. Dittrich, B. Maity, D. Koley, *Angew. Chem. Int. Ed.* **2013**, *52*, 11804–11807.
- [85] D. J. D. Wilson, S. A. Couchman, J. L. Dutton, *Inorg. Chem.* **2012**, *51*, 7657–7668.
- [86] R. S. Ghadwal, S. S. Sen, H. W. Roesky, G. Tavcar, S. Merkel, D. Stalke, *Organometallics* **2009**, *28*, 6374–6377.
- [87] A. C. Filippou, Y. N. Lebedev, O. Chernov, M. Straßmann, G. Schnakenburg, *Angew. Chem. Int. Ed.* **2013**, *52*, 6974–6978.
- [88] L. Gil, *Front. Chem.* **2014**, *2*, 208–222.
- [89] E. A. Williams, *Recent Advances in Silicon-29 NMR Spectroscopy*, **1984**.
- [90] J. A. Dean, *Lange's Handbook of Chemistry*, **1999**.
- [91] A. C. Filippou, O. Chernov, G. Schnakenburg, *Angew. Chem. Int. Ed.* **2009**, *48*, 5687–5690.
- [92] R. S. Ghadwal, H. W. Roesky, S. Merkel, J. Henn, D. Stalke, *Angew. Chem. Int. Ed.* **2009**, *48*, 5683–5686.
- [93] A. C. Filippou, O. Chernov, B. Blom, K. W. Stumpf, G. Schnakenburg, *Chem.*

- *A Eur. J.* **2010**, *16*, 2866–2872.
- [94] H. Cui, C. Cui, *Dalt. Trans.* **2011**, *40*, 11937–11940.
- [95] M. Y. Abraham, Y. Wang, Y. Xie, P. Wei, H. F. Schaefer, P. V. R. Schleyer, G. H. Robinson, *J. Am. Chem. Soc.* **2011**, *133*, 8874–8876.
- [96] R. S. Ghadwal, H. W. Roesky, S. Merkel, D. Stalke, *Chem. - A Eur. J.* **2010**, *16*, 85–88.
- [97] R. Azhakar, G. Tavčar, H. W. Roesky, J. Hey, D. Stalke, *Eur. J. Inorg. Chem.* **2011**, 475–477.
- [98] A. C. Filippou, O. Chernov, G. Schnakenburg, *Chem. - A Eur. J.* **2011**, *17*, 13574–13583.
- [99] A. C. Filippou, O. Chernov, K. W. Stumpf, G. Schnakenburg, *Angew. Chem. Int. Ed.* **2010**, *49*, 3296–3300.
- [100] P. Ghana, M. I. Arz, U. Das, G. Schnakenburg, A. C. Filippou, *Angew. Chem. Int. Ed.* **2015**, *54*, 9980–9985.
- [101] K. C. Mondal, H. W. Roesky, M. C. Schwarzer, G. Frenking, I. Tkach, H. Wolf, D. Kratzert, R. Herbst-Irmer, B. Niepötter, D. Stalke, *Angew. Chem. Int. Ed.* **2013**, *52*, 1801–1805.
- [102] N. Takagi, T. Shimizu, G. Frenking, *Chem. - A Eur. J.* **2009**, *15*, 3448–3456.
- [103] N. Takagi, T. Shimizu, G. Frenking, *Chem. - A Eur. J.* **2009**, *15*, 8593–8604.
- [104] C. A. Dyker, V. Lavallo, B. Donnadiu, G. Bertrand, *Angew. Chem. Int. Ed.* **2008**, *47*, 3206–3209.
- [105] B. L. Shaw, A. J. Stringer, *Inorganica Chim. Acta Rev.* **1973**, *7*, 1–10.
- [106] K. C. Mondal, H. W. Roesky, M. C. Schwarzer, G. Frenking, B. Niepötter, H. Wolf, R. Herbst-Irmer, D. Stalke, *Angew. Chem. Int. Ed.* **2013**, *52*, 2963–2967.
- [107] A. Sekiguchi, Y. V. Lee, *Organometallic Compounds of Low-Coordinate Si, Ge, Sn and Pb*, **2010**.
- [108] K. C. Mondal, P. P. Samuel, M. Tretiakov, A. P. Singh, H. W. Roesky, A. C. Stückl, B. Niepötter, E. Carl, H. Wolf, R. Herbst-Irmer, et al., *Inorg. Chem.* **2013**, *52*, 4736–4743.
- [109] Y. Xiong, S. Yao, S. Inoue, J. D. Epping, M. Driess, *Angew. Chem. Int. Ed.* **2013**, *52*, 7147–7150.
- [110] S. Ishida, T. Iwamoto, C. Kabuto, M. Kira, *Nature* **2003**, *421*, 725–727.
- [111] M. I. Arz, D. Geiß, M. Straßmann, G. Schnakenburg, A. C. Filippou, *Chem. Sci.* **2015**, *6*, 6515–6524.
- [112] M. Chen, Y. Wang, Y. Xie, P. Wei, R. J. Gilliard, N. A. Schwartz, H. F. Schaefer, P. V. R. Schleyer, G. H. Robinson, *Chem. - A Eur. J.* **2014**, *20*, 9208–9211.
- [113] H. P. Hickox, Y. Wang, Y. Xie, M. Chen, P. Wei, H. F. Schaefer, G. H. Robinson, *Angew. Chem. Int. Ed.* **2015**, *54*, 10267–10270.

- [114] Y. Wang, M. Chen, Y. Xie, P. Wei, H. F. Schaefer, G. H. Robinson, *Nat. Chem.* **2015**, 7, 509.
- [115] K. Chandra Mondal, S. Roy, B. Dittrich, B. Maity, S. Dutta, D. Koley, S. K. Vasa, R. Linser, S. Dechert, H. W. Roesky, *Chem. Sci.* **2015**, 6, 5230–5234.
- [116] K. C. Mondal, S. Roy, B. Dittrich, D. M. Andrada, G. Frenking, H. W. Roesky, *Angew. Chem. Int. Ed.* **2016**, 55, 3158–3161.

Chapter II

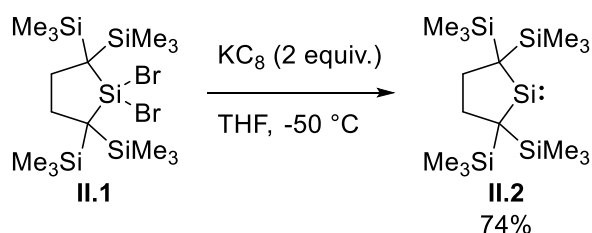
*Oxidative addition of main group
halides to an
N-Heterocyclic Silylene*

Chapter II – Oxidative addition of main group halides to an N-Heterocyclic Silylene

Introduction - Cyclic dialkylsilylene

The electronic properties of silylenes strongly depend on their substituents (See *Chap. I, Silylenes*). The classical N-heterocyclic silylenes are known for being less electron donating than their NHC homologues, due to the poor nucleophilic and high electrophilic character of the silicon atom, which comes from the polarisation of the N–Si bond due to a large difference in electronegativity between N and Si.

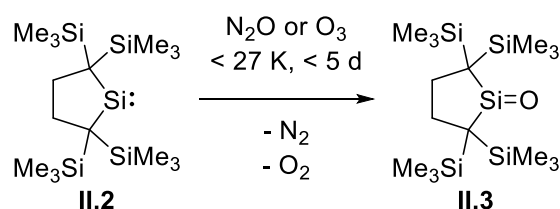
In 1999, the cyclic dialkylsilylene **II.2** was synthesised by Kira *et al.* by reduction of the dibromosilane **II.1** with potassium graphite (KC_8) (*Scheme 1*).^[1] The obtained silylene **II.2** features a remarkably low-field ^{29}Si resonance at δ 567.4. The absence of nitrogen substituents furthermore increases the electron density on the silicon atom and therefore its σ -donating character. The absence of π -donation from the lone-pair of the nitrogen atoms into the empty π -orbital from the silylene also increases the π -accepting character of **II.2**.



Scheme 1: Synthesis of the cyclic dialkylsilylene **II.2**.

The reactivity of **II.2** is enhanced compared to the classical dicoordinate N-heterocyclic silylenes (See *Chap. I, Dicoordinate N-heterocyclic Silylenes*). In addition to the usual reactivity of cyclic silylenes such as oxidative additions of haloalkanes and halosilanes^[2–4] or reaction with chalcogens (S, Se, Te),^[5] the higher reactivity of

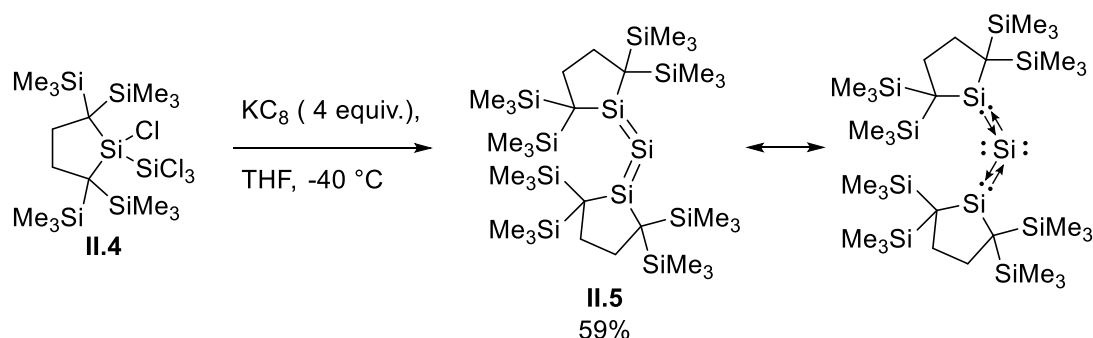
II.2 allowed C–H bond activation of alkanes and C–C bond activation of aryls, which is possible through an excited singlet state in photoreactions.^[6,7] The dialkylsilylene **II.2** is also capable of cycloaddition with ketones,^[8] imines,^[9] nitriles^[10] and diazocarbonyl compounds.^[11] Coordination to transition metals is reported,^[12,13] including an example of a complex capable of H₂ activation.^[14] Several small molecule activations have been reported such as CO₂,^[15] alkenes^[16] or N₂O which allowed the observation of a cyclic uncomplexed silanone **II.3** at low temperature by IR spectroscopy (*Scheme 2*).^[17]



Scheme 2: Reaction of **II.2** with N₂O and O₃.

In 2003, Kira and co-workers reported that reduction with KC₈ at low temperature of the oxidative addition product **II.4** (from reaction of SiCl₄ with the dialkylsilylene **II.2**), afforded the trisilaallene **II.5** (*Scheme 3*).^[18] Unlike the carbon allenes, the silicon analogue has a bent geometry with an Si-Si-Si angle of 136.49(6)°, which indicates that the central silicon could not be described simply as *sp*-hybridised. The Si=Si bonds length (2.177(1), 2.188(1) Å) are in the range of typical Si=Si double bond in disilenes (2.14-2.29 Å).^[19] The geometry of the two terminal silicon atoms is not trigonal planar but slightly pyramidal (sum of bond angles around Si = 354.1° and 354.9°). The ²⁹Si NMR spectrum reveals, in addition to the Me₃Si signal (δ 1.6), two very deshielded signals at δ 157.0 and 196.9 (for the central and terminal silicon atoms respectively), which are different from the usual disilene ²⁹Si NMR signals (δ 56.2-154.5).^[20] Despite the noticeably different characteristics compared to the

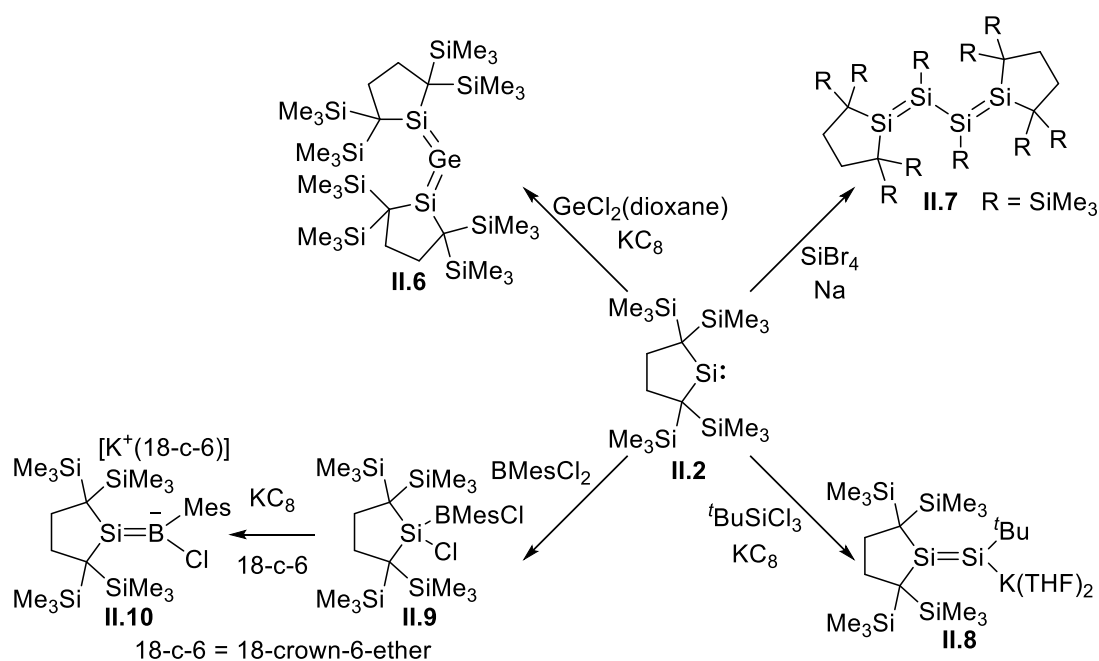
allenes, **II.5** was reported as a trisilaallene, an analogue reasonably close to the carbon allenes. A few years later, Frenking *et al.* published computational studies of divalent silicon(0) compounds.^[21] They optimised the geometry from **II.5** and obtained theoretical values (Si–Si 2.230 Å and Si–Si–Si 135.7°), close to the experimental values. The HOMO and HOMO–1 are respectively the silicon π -lone pair and σ -lone pair orbitals. They concluded that the trisilaallene was better described as a divalent silicon(0) compound with Si–Si bonds formed from donor-acceptor interactions between a naked silicon atom in a singlet state and two silylenes. The similar geometry later found for the silylone (See Chap. I, Silylone) supports the structure proposed by Frenking.^[22]



Scheme 3: Synthesis of the trisilaallene **II.5**.

The cyclic dialkylsilylene **II.2** showed a very good ability to stabilise several unsaturated main group compounds. The reduction of GeCl_2 (dioxane) with KC_8 in presence of the silylene **II.2** afforded a germanium analogue of the trisilaallene, **II.6** (Scheme 4).^[23] The reduction of the oxidative addition product of SiBr_4 on the dialkylsilylene did not give the trisilaallene **II.5**, but instead the tetrasila-1,3-diene **II.7** was obtained (Scheme 4).^[24] Treatment of **II.2** with $t\text{BuSiCl}_3$ followed by reduction with KC_8 in THF afforded a stable disilenide without any aryl substituents **II.8** (Scheme 4).^[3] Other disilenides have also been reported with different substituents.^[25] Lastly,

Iwamoto *et al.* reported the borasilene-chloride adduct **II.10** obtained by the attempt to synthesise the first base-free Si=B double bonds, by reduction of a silylborane precursor **II.9** (Scheme 4).^[26]



Scheme 4: Synthesis of unsaturated main group compounds using the dialkylsilylene **II.2**.

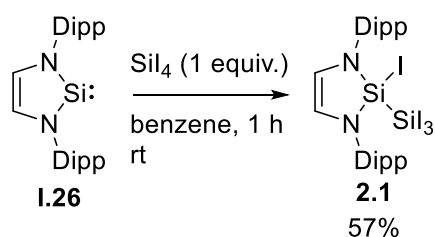
Oxidative addition of silicon halides to an N-heterocyclic Silylene

Stable low valent species have been reported with the dialkylsilylene **II.2**, however, no examples have been achieved using an N-heterocyclic silylene. 1,3-Bis(2,6-diisopropylphenyl)imidazol-2-ylidene (IPr) is a commonly used NHC to stabilise low valent silicon species (See Chap. I, Base-Silicon(II) adducts and Base-Silicon(0) adducts). For this reason, the silylene analogue to IPr, the N-heterocyclic silylene **I.26** was chosen. The silylene **I.26** was obtained in a good yield (61%), through a simple synthesis reported by Müller *et al.*, by reduction of the dichlorosilane precursor with lithium naphthalenide in tetrahydrofuran.^[27] Treatment of **I.26** with SiCl_4 in hexane or

benzene did not show any reactivity. After more than 24 hours only starting material was observed by ^1H NMR spectroscopy.

SiI_4 is a more reactive halosilane than SiCl_4 , with a weaker Si–I bond (339(84) kJ mol^{-1}) relative to Si–Cl (456(42) kJ mol^{-1}).^[28] For that reason, SiI_4 was selected as a reagent for oxidative addition.

The silylene **1.26** was treated with SiI_4 in benzene, which resulted in a spontaneous colour change to an intense orange/red colour (*Scheme 5*). Removal of the volatiles, followed by washing with hexane to remove the remaining starting material, afforded the oxidative addition product **2.1** as a bright orange solid in 57% yield. The solid-state structure of **2.1** was determined by single crystal X-ray diffraction (*Figure 1*). Both silicon atoms show tetrahedral geometry and the Si–Si bond (2.3648(12) Å) is in the range of Si–Si single bonds (2.31–2.38 Å).^[19] Both nitrogen atoms have a slight pyramidal configuration (sum of angle: 357.5(4)°, 358.0(4)° for N1 and N2), while the nitrogen atoms from **1.26** have trigonal planar geometries.^[29] Surprisingly, the Si1–N1 (1.721(3) Å) and Si1–N2 (1.719(3) Å) bonds are shorter for **2.1** than for the N-heterocyclic silylene **1.26** (Si–N 1.76–1.77 Å),^[29] despite the increase in valency of Si1. Unlike the silylene **1.26**, **2.1** does not have an empty π -orbital on Si1, therefore the π -donation from the nitrogen lone pair is expected to decrease from **1.26** to **2.1**, making the Si–N bond longer. This contradictory observation can be explained by the electron deficient nature of the substituents on Si1 (iodine and SiI_3). This decreases the electron density on Si1 and polarises the nitrogen-silicon bonds, making Si1–N1 and Si1–N2 shorter. This shortening of the Si–N bonds from the divalent to tetravalent silicon species is also observed for other N-heterocyclic silylene (*See Chap. I, Dicoordinate N-Heterocyclic Silylenes*).



Scheme 5: Synthesis of the disilane **2.1** via oxidative addition of **1.26**.

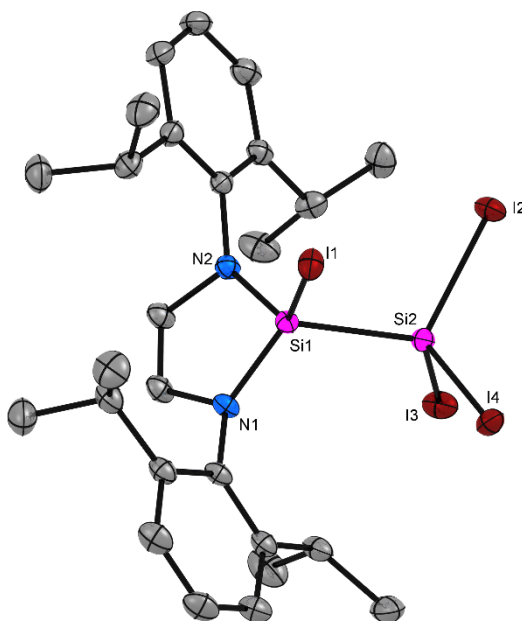


Figure 1: Molecular structure of **2.1** in the solid state. Ellipsoids are drawn at 50% probability; hydrogen atoms are omitted for clarity. Selected bond distances [Å] and angles [°] for **2.1**: Si1–Si2 2.3648(12), Si1–N1 1.721(3), Si1–N2 1.719(3); Si2–Si1–I1 97.92(4), N1–Si1–I1 115.43(10), N1–Si1–Si2 117.07(11), N2–Si1–I1 117.17(11), N2–Si1–Si2 116.51(11), N2–Si1–N1 94.20(14), I2–Si2–I3 108.98(3), I2–Si2–I4 107.36(4), I4–Si2–I3 108.24(3), Si1–Si2–I2 109.37(4), Si1–Si2–I3 113.86(4), Si1–Si2–I4 108.83(4).

The NMR data also supports the structure of **2.1**. ^{29}Si NMR spectroscopy shows two resonances at δ –74.5 and –123.2 that couple to each other ($^1J_{\text{SiSi}} = 201.3$ Hz), which confirms the presence of an Si–Si bond. The ^{29}Si chemical shifts are more shielded than that for silylene **1.26** (δ 75.9), which is consistent with oxidative addition to the silylene. Both ^1H and ^{13}C NMR spectra are in accordance with the structure of **2.1**. The backbone hydrogens from the heterocycle of **2.1** resonate at δ 5.74 in the ^1H

NMR spectrum (Figure 2) and show coupling to silicon ($^3J_{\text{HSi}} = 8.6$ Hz). The 2,6-diisopropylphenyl (Dipp) groups are desymmetrised by restricted rotation, as evidenced by the observation of four resonances for the methyl groups in the ^1H and ^{13}C NMR.

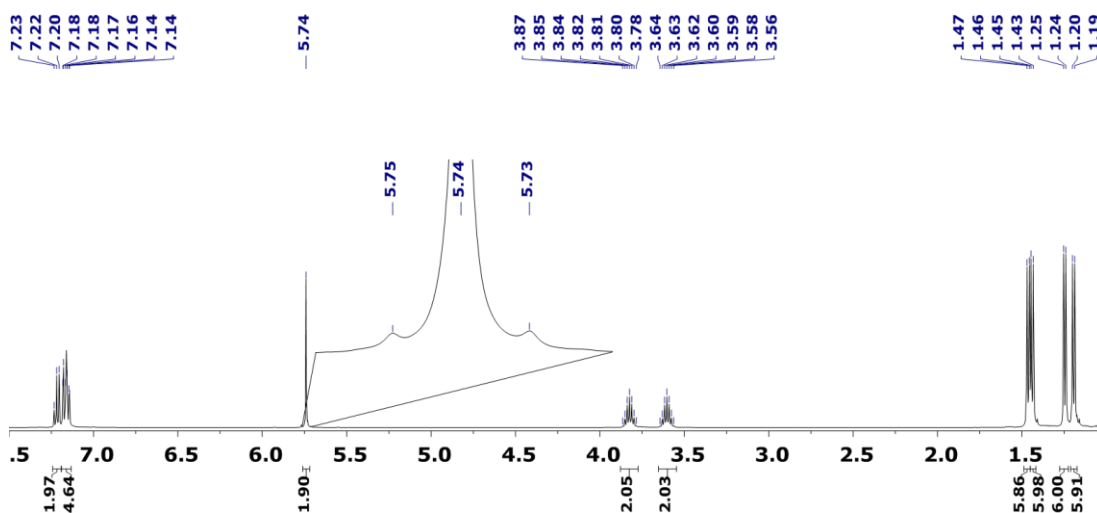


Figure 2: ^1H NMR spectrum (500 MHz, C_6D_6) of 2.1.

^{29}Si - ^1H HMBC experiment reveals coupling between the silicon at $\delta -74.5$ and the backbone hydrogen atoms from the N-heterocycle at $\delta 5.74$ (Figure 3). This allows assignment of Si1 to the peak at $\delta -74.5$ and Si2 to the peak at $\delta -123.2$.

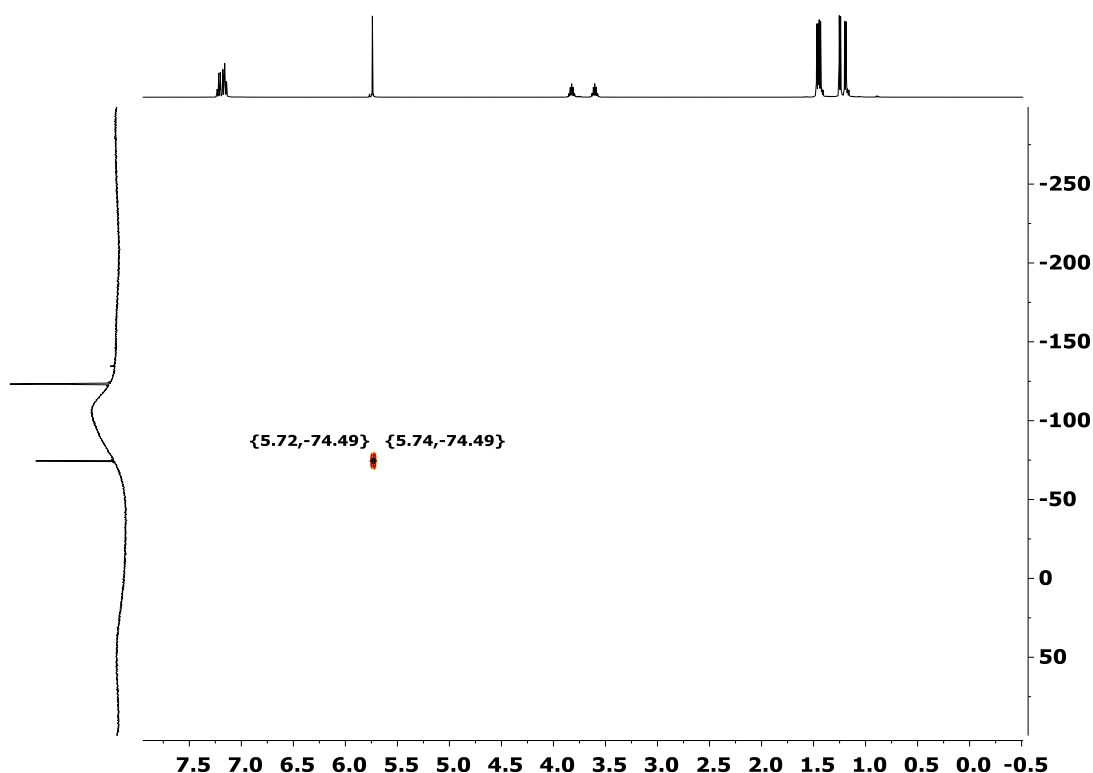
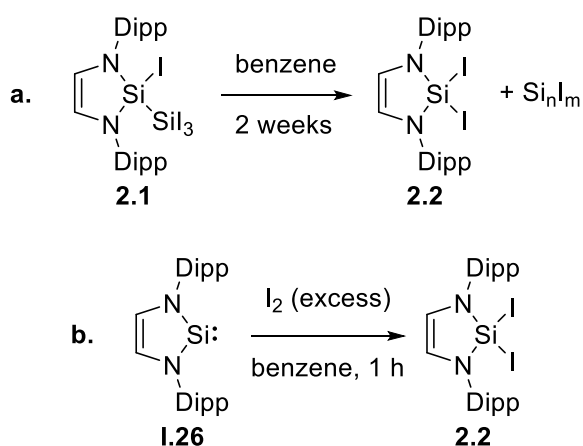


Figure 3: ^{29}Si - ^1H HMBC NMR spectrum (99 MHz - 500 MHz, C_6D_6) of **2.1**.

Although oxidative addition to N-heterocyclic silylenes is known (See *Chap. I, Dicoordinate N-Heterocyclic Silylenes*),^[30–36] **2.1** is the first isolated example of an oxidative addition of a tetrahalosilane (SiX_4 , X = Br, Cl, I) to an N-heterocyclic silylene. Previous examples of tetrahalosilane addition to N-heterocyclic silylenes were reported, but attempts to synthesise them gave a mixture of products and they were never isolated.^[35] Despite being indefinitely stable under argon in the solid state, **2.1** slowly decomposes in benzene over two weeks to a new product which gives a signal in the ^{29}Si NMR spectrum at δ -134.5 . The decomposition is faster in polar solvent (less than 12 hours in THF). The presence of a single signal in the ^{29}Si NMR spectrum suggests the cleavage of the Si–Si bond in the decomposition product. A possible explanation would be the decomposition of **2.1** into the diiodosilane **2.2** and silicon halide aggregates (Si_nI_m) (*Scheme 6.a*).

To confirm this possibility, silylene **1.26** was treated with an excess of iodine (*Scheme*

6.b). The reaction results in the formation of the same product to the one from the decomposition of **2.1**, with identical ^1H , ^{13}C and ^{29}Si NMR spectra. This shows that **2.1** is decomposing to **2.2**. The solid-state structure of **2.2** was determined by X-ray crystallography (See *Experimental Methods*), confirming the decomposition pathway of **2.1**.

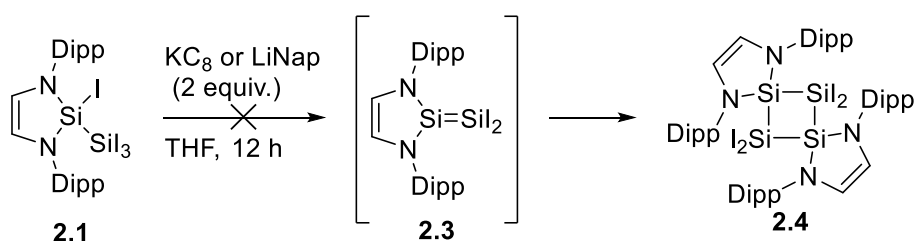


Scheme 6.a: Overtime decomposition of the disilane **2.1** in benzene. **b.** Reaction of silylene **1.26** with iodine.

Reduction of the disilane **2.1**

In order to form low valent silicon species, the reduction of **2.1** was carried out under a range of conditions. Treatment of **2.1** with four equivalents of KC_8 in THF led to decomposition or reduction back to the silylene **1.26**. Reduction using two equivalents of KC_8 showed no consistent results in the ^1H NMR spectrum. The ^{29}Si NMR spectrum showed a main signal at $\delta -63.2$ along with two small signals at $\delta -85.5$ and -88.1 , the unique main silicon environment suggests that the main product had no remaining Si–Si bond. At this time, the small signals ($\delta -85.5$ and $\delta -88.1$) could not be assigned. The heterogeneous nature of the KC_8 reagent slows down the reaction. Considering the instability of **2.1** in THF (complete degradation in less than 12 hours) and the usual

time of reaction of KC_8 reduction (12 to 24 hours), **2.1** is decomposing to **2.2** faster than it reacts with KC_8 . Changing the reducing agent or the solvent was necessary. Lithium naphthalenide (LiNap) is a more soluble reducing agent. A solution of lithium naphthalenide in THF (0.3 M) was synthesised following a reported procedure.^[37] Disilane **2.1** was treated with 2 equivalents of LiNap in order to reach the intermediate disilene **2.3**, which is expected to dimerise to form the four-membered ring **2.4** (Scheme 7). However, the reduction of **2.1** with LiNap gave similar results to the reduction with KC_8 . ^1H NMR spectroscopy did not reveal clean formation of a new product. The ^{29}Si NMR spectrum shows a mixture of silicon containing species, with one main signal at $\delta -63.2$. In both cases, the Si–Si bond from **2.1** is cleaved during the reduction as no Si–Si coupling was observed. It is possible that the reduction with KC_8 and LiNap gave a silylenoid product, with the metal (K or Li) as counter ion with coordinated-THF.^[38–40] However, the products could not be isolated or identified.



Scheme 7: Reduction of **2.1** with KC_8 or LiNap (2 equiv.).

Using non-polar solvents should avoid the rapid decomposition of **2.1** and formation of side products. Reduction of **2.1** with KC_8 was carried out in benzene, as it was known that decomposition occurs over 2 weeks. After one day of monitoring the reaction by ^1H NMR spectroscopy, only starting material was observed. After five days, one main product was formed according to ^1H NMR spectroscopy. The ^{29}Si NMR spectrum showed two signals at $\delta -88.1$ and -85.5 . The solid-state structure revealed the unexpected trisilane **2.5** (Figure 4). Considering the instability of **2.1** in

solution, the following mechanism was proposed to explain the formation of **2.5** (Scheme 8). The disilane **2.1** does not react with KC_8 in non-polar solvents, but it slowly decomposed overtime in solution to **2.2** (Scheme 6.a). The formed diiodosilane **2.2** is then reduced back to the silylene **1.26** by KC_8 . Finally, a second oxidative addition occurs between the remaining disilane **2.1** and **1.26** forming the trisilane **2.5**. The formation of the trisilane **2.5** suggested that it may be possible to synthesise it using an excess of **1.26** with SiI_4 .

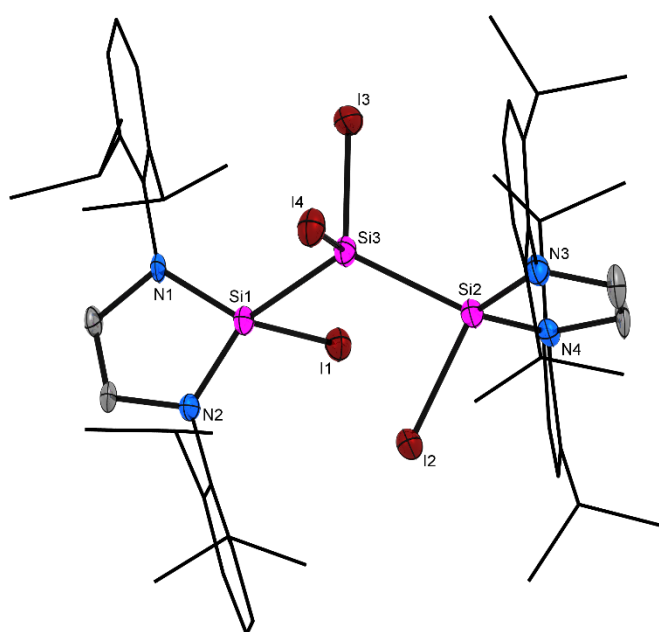
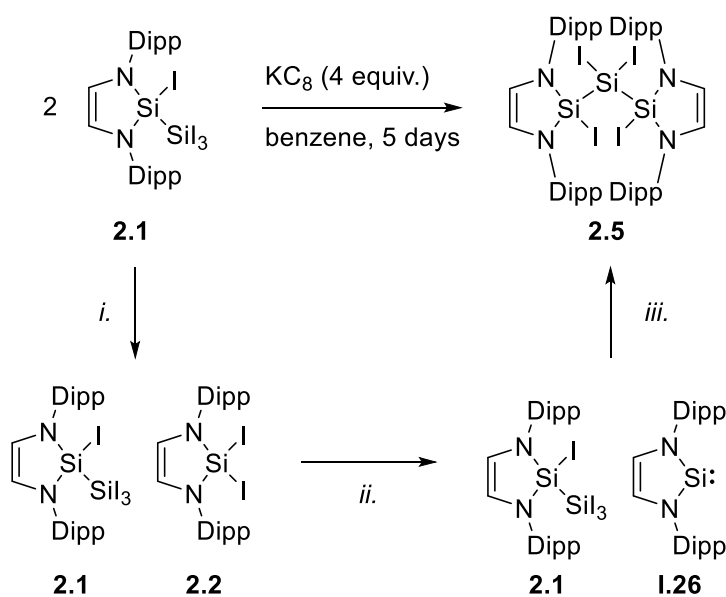


Figure 4: Molecular structure of **2.5** in the solid state. Ellipsoids are drawn at 50% probability; hydrogen atoms are omitted for clarity. Selected bond distances [\AA] and angles [$^\circ$] for **2.5**: Si1–Si3 2.374(6), Si2–Si3 2.362(6), Si1–N1 1.719(12), Si1–N2 1.738(13), Si2–N3 1.725(13), Si2–N4 1.729(13); Si1–Si3–Si2 118.18(17).

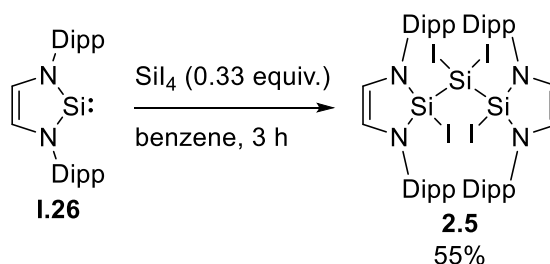


Scheme 8: Proposed mechanism for the formation of **2.5** through KC_8 reduction. *i.* Slow decomposition of **2.1** to **2.2**. *ii.* Reduction of the diiodosilane **2.2** by KC_8 . *iii.* Oxidation addition of remaining **2.1** on **1.26**.

Generation and reactivity study of the trisilane **2.5**

In an attempt to synthesise **2.5** from **1.26**, three equivalents of **1.26** were added to SiI_4 in benzene (Scheme 9). After three hours, the solvent was removed *in vacuo*. Fractional crystallisation from cold pentane afforded **2.5** as a yellow solid in 55% yield. The ^{29}Si NMR spectroscopy showed the two expected signals at δ -88.1 and -85.5 . The two silicon signals are very close in the case of **2.5**, which is in accordance with the similar environments of the silicon atoms in the trisilane **2.5**. The 1H NMR spectrum showed four septets at δ 3.97, 3.89, 3.79, 3.49 from the Dipp groups and two doublets at δ 5.55, 5.49 from the backbone protons. The high number of signals, despite the symmetry of the structure, implies a very restricted rotation. The ^{13}C NMR spectrum was in accordance with the product. The solid-state structure of **2.5** (Figure 4) has an Si1-Si3-Si2 angle of $118.18(17)^\circ$, which is in the range of the trisilanes reported by Kira (117 - 136°).^[41] The Si1-Si3 and Si2-Si3 bond lengths (2.374(6) and 2.362(6) Å) are typical of Si-Si single bonds. The Si-N bonds of **2.5** (1.719(12),

1.738(13), 1.725(13), 1.729(13) Å) are shorter than the N-heterocyclic silylene **1.26** (1.76 and 1.77 Å). As for **2.1**, the electron withdrawing nature of the substituents increases the electron deficiency at Si1 and Si2, polarises the nitrogen-silicon bonds, and decreases the Si1–N1/2 and Si2–N3/4 distances. Unlike the disilane **2.1**, the trisilane **2.5** is stable in the solid and solution state under argon atmosphere.



Scheme 9: Synthesis of the trisilane **2.5** by two successive oxidative additions of SiI_4 .

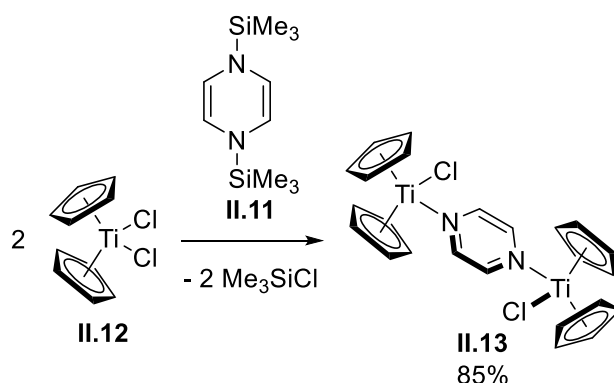
Reduction of **2.5** with KC_8

Trisilane **2.5** was a good candidate to afford a homologue of the trisilaallene **11.5** (See *Chap. II, Cyclic dialkylsilylene*).^[18] However, when treated with KC_8 at low temperature (-78°C), the reduction of **2.5** showed the formation of the silylene **1.26** by ^1H NMR spectroscopy. A less strongly reducing agent was used as an alternative.

Reduction of **2.5** with an organosilicon reagent

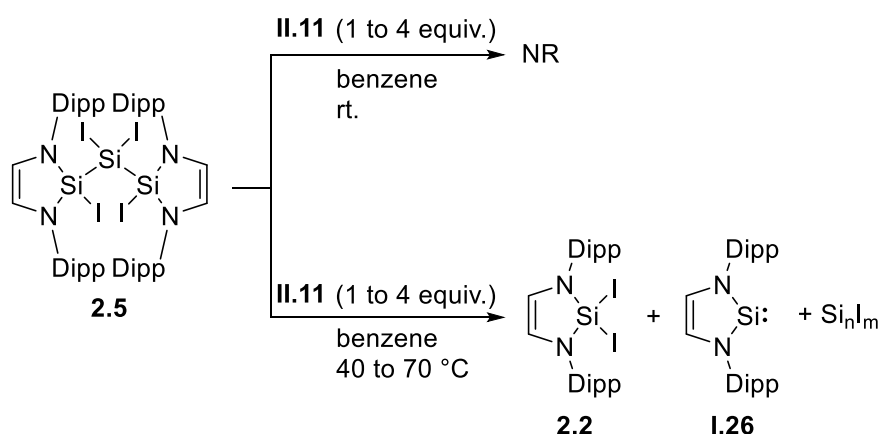
Despite being reported in the 1970's,^[42] the reducing properties of the 1,4-bis(trimethylsilyl)-1,4-diaza-2,5-cyclohexadiene **11.11** has only been explored recently. In 2014, Mashima and co-workers reported the reduction of early transition metal using **11.11** (*Scheme 10*).^[43] The Ti(IV) chloride complex **11.12** is reduced to a pyrazine-bridged dimeric Ti(III) complex **11.13**, by treatment with **11.11**. The advantages of using an organic reducing agent rather than alkali and alkaline-earth metal amalgams are to avoid over-reduced species or reductant-derived salts and simplify the purification

of the products. In the case of **II.11**, the by-products are Me_3SiCl and pyrazine which can be easily removed *in vacuo*. Moreover, the pyrazine can play the role of a ligand as in the complex **II.13**.



Scheme 10: Reduction of Cp_2TiCl_2 **II.12** by **II.11** forming a pyrazine-bridged dimeric $\text{Ti}(\text{III})$ complex **II.13**.

Treating **2.5** with **II.11** at room temperature resulted in no reaction (*Scheme 11*), even when adding a large excess of **II.11** (four equivalents) only the starting material was observed by ^1H NMR spectroscopy. When the reaction was performed at 40 to 70 °C, formation of the silylene **I.26** along with the diiodosilane **2.2** were observed by NMR spectroscopy. Heating is most likely degrading **2.5** to the **2.2** (and silicon aggregate Si_nI_m), which is then reduced by **II.11** to the silylene **I.26** (*Scheme 11*).



Scheme 11: Reduction of the trisilane **2.5** by **II.11**.

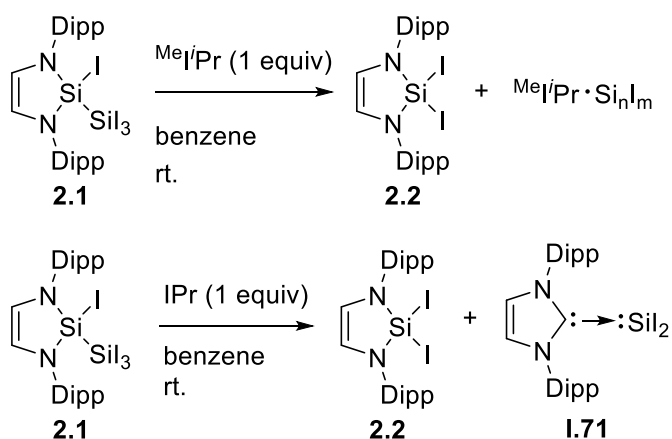
No evidence of a trisilaallene was observed by NMR in the above reactions using **II.11**. However, these reactions show that reduction of main group halide using **II.11** is possible as the silylene **I.26** was obtained from the reduction of the diiodosilane **2.2**. The only reactivity between **II.11** and main group halides previously reported were transmetalation or substitution reactions.^[44–46] The reported reactions suggest that 1,4-bis(trimethylsilyl)-1,4-diaza-2,5-cyclohexadiene **II.11** could be used as an organic reducing agent for main group halide compounds.

Reactions of the disilane **2.1** with coordinating-bases

Reduction of **2.1** and **2.5** with LiNap or KC_8 does not afford a clean product. The addition of a coordinating base could stabilise the compound and allow reduction, by avoiding side reactions or aggregation. For steric reasons, the coordination of a base to **2.5** was unlikely to happen, so the study was carried out using **2.1** only. The disilane **2.1** was reacted with two different NHCs, IPr and 1,3-diisopropyl-4,5-dimethylimidazol-2-ylidene ($^{\text{Me}}\text{IPr}$) (Scheme 12). These NHCs were selected as they have been already used for coordination chemistry with silicon halides, forming base-silicon adducts.^[47–49] The reaction was monitored by ^1H NMR spectroscopy, no

evidence of NHC coordination was observed. In each reaction an insoluble yellow solid formed rapidly, but the main species which were observed by ^1H NMR spectroscopy were the starting material **2.1** and the diiodosilane **2.2**. In the case of $^{\text{Me}}\text{IPr}$, absence of any remaining signal from the NHC in each reaction suggests that the yellow insoluble solid formed contains a mixture of imidazolium salt and silicon aggregate.

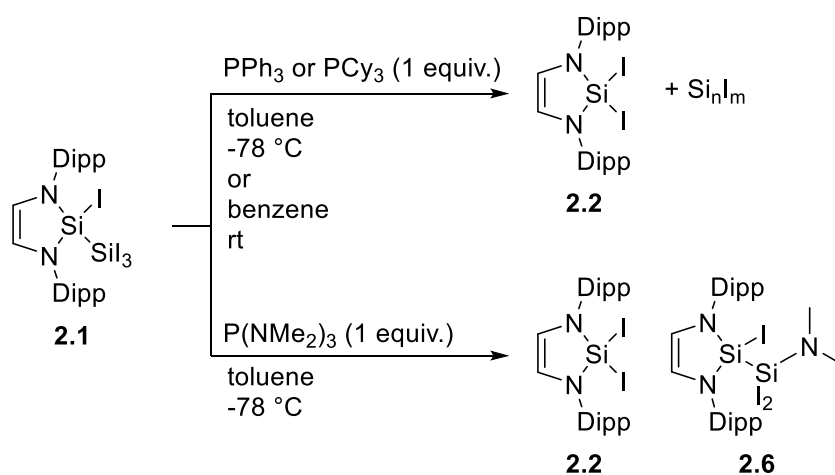
Interestingly the reaction with IPr sometimes showed the NHC-silylene adduct **1.71** by ^1H NMR spectroscopy, however, no stable preparation could be achieved. No further investigation was carried out as the NHCs were promoting the cleavage of the Si–Si bond from **2.1** giving **2.2**.



Scheme 12: Reaction of **2.1** with NHCs IPr or $^{\text{Me}}\text{IPr}$ leading to decomposition.

NHCs are strong bases, with pK_a values of around 20-25.^[50] The use of a weaker base could promote coordination and prevent cleavage of the Si–Si bond in **2.1**. Phosphines are weaker bases and commonly have pK_a values below 10.^[51] They are primarily used in coordination to transition metals but examples of coordination to main group compounds have been reported, including silicon(IV) halide adducts (See *Chap. I, Hypervalent Base-Silicon adducts*). Compound **2.1** was treated with

triphenylphosphine (PPh_3), tricyclohexylphosphine (PCy_3) and tris(dimethylamino)phosphine ($\text{P}(\text{NMe}_2)_3$). In the reaction with PPh_3 and PCy_3 , ^1H NMR spectroscopy showed decomposition of **2.1** to **2.2** along with unreacted phosphines. This suggests that the phosphines are promoting the degradation of **2.1**. ^1H and ^{29}Si NMR spectra from the reaction with $\text{P}(\text{NMe}_2)_3$ showed the formation of a new product **2.6** along with the degradation product **2.2**.



Scheme 13: Reactions of **2.1** with PPh_3 and PCy_3 leading to decomposition, and with $\text{P}(\text{NMe}_2)_3$ forming a mixture of N-substituted product **2.6** and diiodosilane **2.2**.

Analysis of the integration from the ^1H NMR spectrum of the dimethylamino resonance (δ 2.33) with respect to the enamine protons (δ 5.75) allowed the identification of **2.6** (Figure 5). The aromatic region and the region around δ 3.7-3.8 showed overlapping signals corresponding to both **2.6** and **2.2**. In addition to the signals of **2.2**, the ^{29}Si NMR showed two signals at δ -56.9 and -76.7 which indicate the presence of two silicon environments in **2.6**. A ^{29}Si - ^1H HMBC experiment confirmed the coupling between the ^{29}Si signal at δ -76.7 and the ^1H signal at δ 2.33 corresponding to the dimethylamino protons, and between the ^{29}Si resonance at δ -56.9 and the ^1H signal at δ 5.75 corresponding to the backbone of the N-heterocycle. This allowed the assignment of the ^{29}Si signal at δ -76.7 to Si2 and δ -56.9 to Si1 (Figure 6).

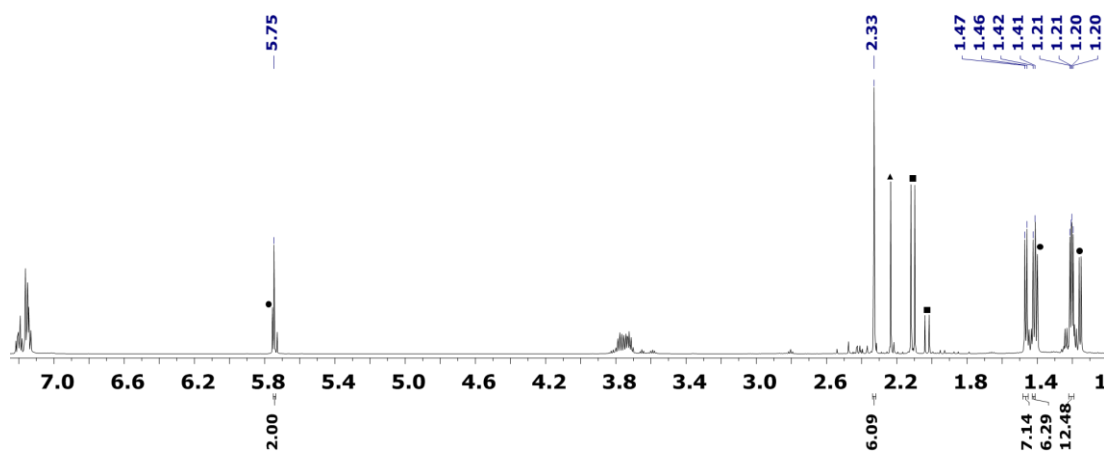


Figure 5: ^1H NMR spectrum (600 MHz, C_6D_6) of the reaction of **2.1** with $\text{P}(\text{NMe}_2)_3$. ● Signals from **2.2**. ■ Signal from $\text{PI}(\text{NMe}_2)_2$ and PI_2NMe_2 . ▲ Signal from $\text{SiI}_2(\text{NMe}_2)_2$ or SiI_3NMe_2 .

Along with the product **2.6**, by-products were observed by ^1H (Figure 5.■) and ^{31}P NMR spectroscopy. The ^{31}P NMR signals at δ 169.9 and 195.8 are comparable to $\text{PCI}(\text{NMe}_2)_2$ (δ 158.9)^[52] and PCI_2NMe_2 (δ 164.0).^[53] These signals are most likely $\text{PI}(\text{NMe}_2)_2$ and PI_2NMe_2 , respectively, evidenced by P-H couplings observed by a ^{31}P - ^1H HMBC experiment. Another amino-silane (Figure 5.▲) species was observed, which does not contain any signals from the N-heterocycle or the Dipp group, which is consistent with $\text{SiI}_2(\text{NMe}_2)_2$ or SiI_3NMe_2 . These two silicon species are by-products from the decomposition which forms **2.2**. The solid-state structure of **2.6** was confirmed by single crystal X-ray diffraction (Figure 6). **2.6** has a slightly shorter Si-Si bond (2.355(3) Å) than **2.1** (2.3648(12) Å).

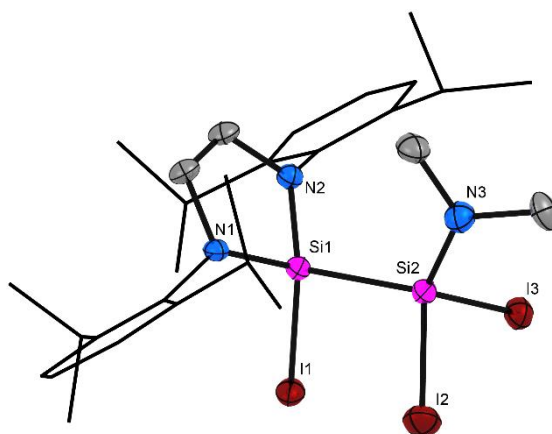


Figure 6: Molecular structure of **2.6** in the solid state. Ellipsoids are drawn at 50% probability; hydrogen atoms are omitted for clarity. Selected bond distances [Å] and angles [°] for **2.6**: Si1–Si2 2.355(3), Si1–N1 1.727(6), Si1–N2 1.731(6), Si2–N3 1.669(12); I1–Si1–Si2 98.49(8), Si1–Si2–N3 108.8(3).

The amine substitution of the silicon iodide atom was unexpected as P–N bonds are reported to form from the reaction of halophosphines and aminosilanes. For example, $\text{PCl}(\text{NMe}_2)_2$ is synthesised from the reaction of PCl_3 with $\text{Me}_2\text{NSiMe}_3$.^[52] In the reaction to give **2.6**, the reactivity is reversed. Attempts to isolate **2.6** were unsuccessful, due to slow decomposition, **2.6** was always contaminated with side-products after purification attempts.

In summary, no coordination by the phosphines was observed and **2.1** decomposes when reacted with PPh_3 and PCy_3 . However, the reaction with $\text{P}(\text{NMe}_2)_3$ allowed substitution on the silane with an amino group. This suggests that it was possible to modify the substituent on **2.1**. A bigger amino or aryl group on the silicon Si2 (Figure 6) may stabilise the Si–Si bond.

Reaction of **2.1** with Organolithium reagents

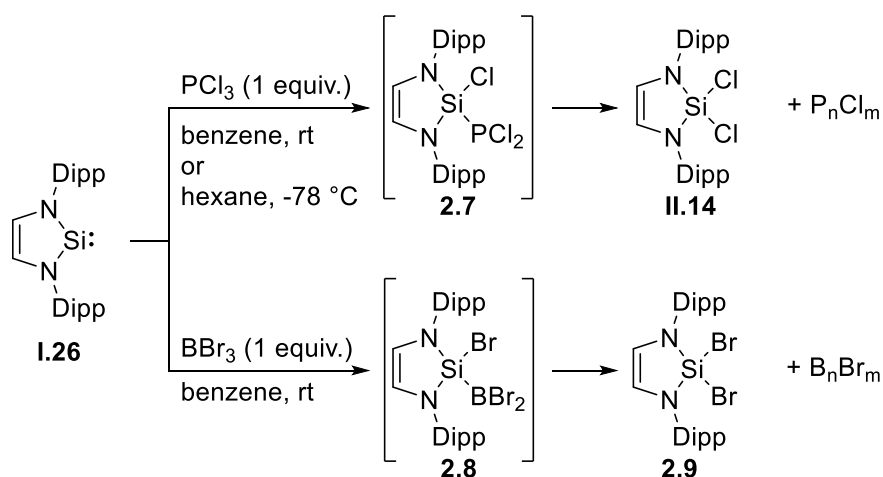
Tetraiodo disilane **2.1** was treated with organolithium reagents mesityllithium (MesLi) and lithium diisopropylamide (LDA) but showed no reactivity in either case. ^1H NMR

spectroscopy showed starting material **2.1** with a small amount of **2.2** formed due to decomposition.

The absence of reaction between **2.1** and the different organolithium reagents showed that nucleophilic substitutions using strong nucleophiles are not possible on **2.1**. The lack of reaction with LDA also showed that the formation of **2.6** from **2.1** and $\text{P}(\text{NMe}_2)_3$ was not due to a simple nucleophilic attack from the nitrogen on the silicon centre.

Oxidative addition of boron and phosphorus halide on N-Heterocyclic Silylene

Following the successful oxidative addition of SiI_4 , other main group halides were reacted with **I.26** (*Scheme 14*). The reaction with PCl_3 rapidly formed a new product which gave a comparable ^1H NMR signal to **2.1**. The ^{31}P NMR spectrum showed a mixture of products with two main signals at δ 131.6, 131.5 and a minor signal at δ – 9.37. ^1H NMR spectroscopy showed that the new product turned quickly into the reported dichlorosilane **II.14**.



Scheme 14: Oxidative addition product of PCl_3 on **1.26**, **11.14** and its proposed intermediate **2.7**; proposed oxidative addition product of BBr_3 on **1.26**, **2.8** and its proposed intermediate **2.9**.

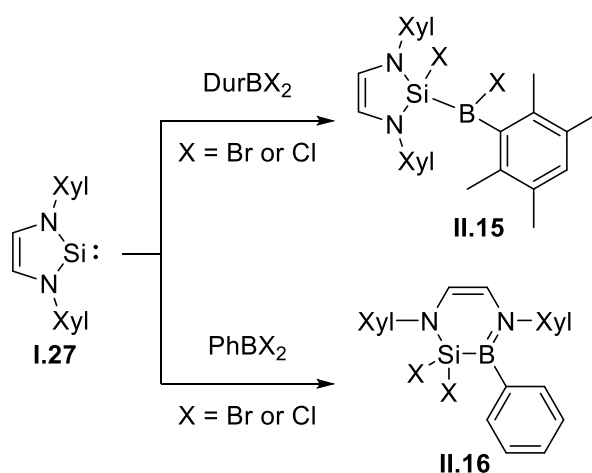
The reaction between the silylene **1.26** and PCl_3 was repeated and monitored by ^1H NMR spectroscopy and showed that 100% of the starting material was converted after only five minutes into the proposed intermediate **2.7**, however, this product was already decomposing in this time into the dichlorosilane **11.14**.

The reaction was reproduced in hexane at low temperature, in order to precipitate the unstable intermediate **2.7** from the solution as a stable solid, but only the dichlorosilane **11.14** was obtained, according to ^1H NMR spectroscopy. The similarity between the ^1H NMR signals of the intermediate **2.7** and the disilane **2.1**, along with the observation of the dichlorosilane **11.14** analogue from the diiodosilane **2.2** obtained from the decomposition from **2.1** evidenced that the unidentified and unstable product is most likely the oxidative addition product **2.7** (Scheme 14). Unfortunately, attempts to isolate **2.7** were unsuccessful and no confirmation of its structure was possible.

Silylene **1.26** was also treated with BBr_3 (Scheme 14). The reaction gave one main product according to the ^1H NMR spectroscopy. The signals showed asymmetry in the compound with a restrained geometry, which was similar for **2.1**. This suggests

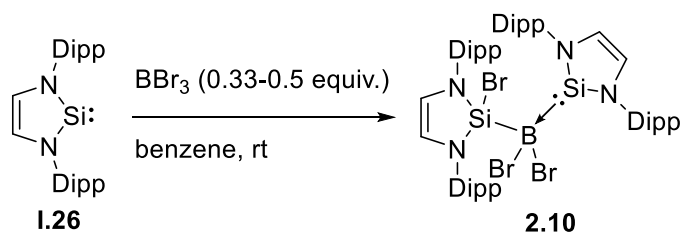
again that oxidative addition may occur during the reaction, giving the product **2.8**. The ^{11}B NMR spectroscopy revealed a mixture of products, with one broad main signal at δ 36.0 confirming the tricoordinate nature of the boron containing species. The new product from the reaction slowly decomposed into another unidentified compound. The most likely hypothesis was that, as previously, the oxidative addition product **2.8** was obtained, which then decomposed into the dibromosilane **2.9** following the same pathway of the formation and slow decomposition of the disilane **2.1**. The treatment of **I.26** with an excess of BBr_3 was monitored by NMR and showed that the intermediate product formed faster, but also decomposed quicker into the second product. These observations are in accordance with the proposed products **2.8** and **2.9**. The first oxidative addition giving **2.8** will be favoured by an excess of BBr_3 , as well as the decomposition by reaction between **2.8** and the excess of BBr_3 , which would give **2.9** and B_2Br_4 (trace observed by ^{11}B NMR spectroscopy δ 67.7) or bigger boron aggregate. Attempts to isolate the products were unsuccessful.

Although some evidence suggests that oxidative addition occurred, the products assigned to it are unstable. In 2016, during the course of this work, Braunschweig *et al.* published boron halide oxidative addition to a similar silylene **I.27**.^[36] They reported the stable addition products **II.15** using DurBX_2 precursors (Dur = 2,3,5,6-tetramethylphenyl, X = Br or Cl) (*Scheme 15*). A smaller aryl substituent on the boron leads to ring expansion of the silylene **I.27** and the formation of the product **II.16**. The size of the aryl substituent on the boron is essential for the stability of the compound **II.15**. They did not report any reaction with a boron trihalide. This is consistent with the instability of **2.7** and **2.8**, which may have required a bigger substituent to increase their stability.



Scheme 15: Oxidative addition of DurBX_2 and PhBX_2 on the *N*-heterocyclic silylene **1.27**. Dur = 2,3,5,6-tetramethylphenyl, Xyl = 2,6-dimethylphenyl.

Given the stability of trisilane **2.5** compared to that of disilane **2.1**, silylene **1.26** was treated with half an equivalent of BBr_3 in order to target **2.10**, the boron analogue of **2.5** (Scheme 16).



Scheme 16: Reaction of **1.26** with BBr_3 (0.33 to 0.5 equiv.) forming the silylene-silylborane adduct **2.10**.

However, in contrast to the reaction with SiI_4 , ^1H NMR spectroscopy showed the formation of **2.8** along with the new product **2.10**. It was found that the formation of **2.10** could be promoted by carrying out the reaction with an excess of silylene **1.26** with respect to BBr_3 (3:1). Surprisingly this new product had a single signal for the Dipp groups and the backbone protons (Figure 7), unlike the trisilane **2.5** which showed a more restrained rotation with different ^1H NMR signals for each fragment of

the molecule. The ^{11}B NMR spectrum showed a signal at $\delta -10.9$, which is indicative of a tetracoordinated boron species. A long ^{29}Si NMR experiment was carried out but only a signal at $\delta 76.2$, which can be assigned to **1.26** ($\delta 75.9$) was observed. The simplicity of the ^1H NMR signal and the tetracoordinated boron signal suggest a silylene-boron adduct.

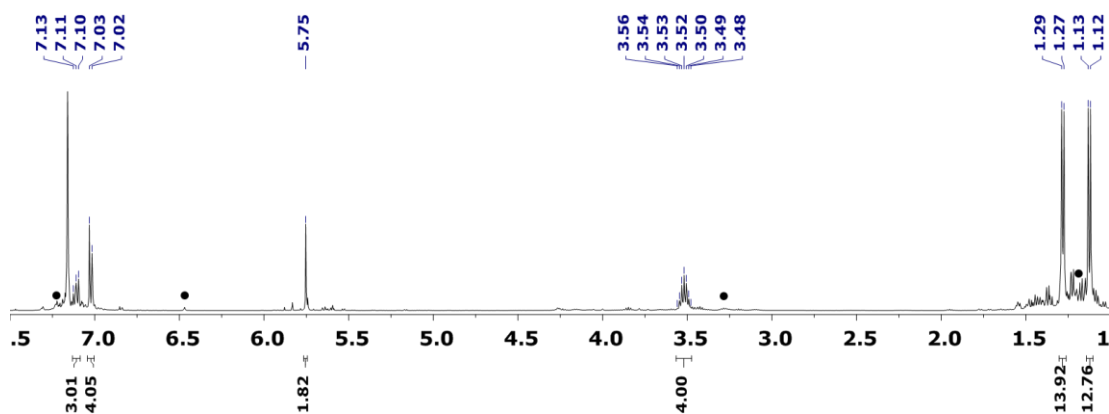


Figure 7: ^1H NMR spectrum (500 MHz, C_6D_6) of **2.10**. ● Signal from **1.26**.

Single crystals for X-ray diffraction were obtained from cold hexane (Figure 8). The solid-state structure revealed the unexpected product **2.10** as a silylborane with a silylene coordinated to the boron centre. The solid-state structure of **2.10** shows two different silicon environments: one for the silylene-borane and one for the silylborane fragments.

However, the ^1H NMR spectrum shows a single set of signals for the ligand (no significant ^{29}Si observed). It implies that the two silicon atoms are in a similar environment, suggesting that, in solution, the bromine is undergoing a rapid 1,3-shift between both silicon atoms, making them equivalent by ^1H NMR spectroscopy.

Analysis of the bond distances and angles evidences as well that the bromine is undergoing a rapid 1,3-shift, in solution, between both silicon atoms. The similar bond lengths Si1–B1 and Si2–B1 (2.023(2) and 2.015(2) Å respectively) support that the silicon atoms are in a similar environment. The very bent geometry of **2.10**, with the

B1-Si1-Br1 95.27(7)° and Si1-B1-Si2 112.81(11)° angles, and the small torsion angle Br1-Si1-B1-Si2 of 21.50° also support a possible shifting of the bromine atom between the two silicon centres. Few silylene-borane adducts have been reported for BR₃ (R = H, alkyl, aryl), and most of them feature a tetra- or pentacoordinate silicon centre.^[35,55, 56–64] Previous reactions between boron halides and dicoordinate silylenes have only shown oxidative addition.^[36,64]

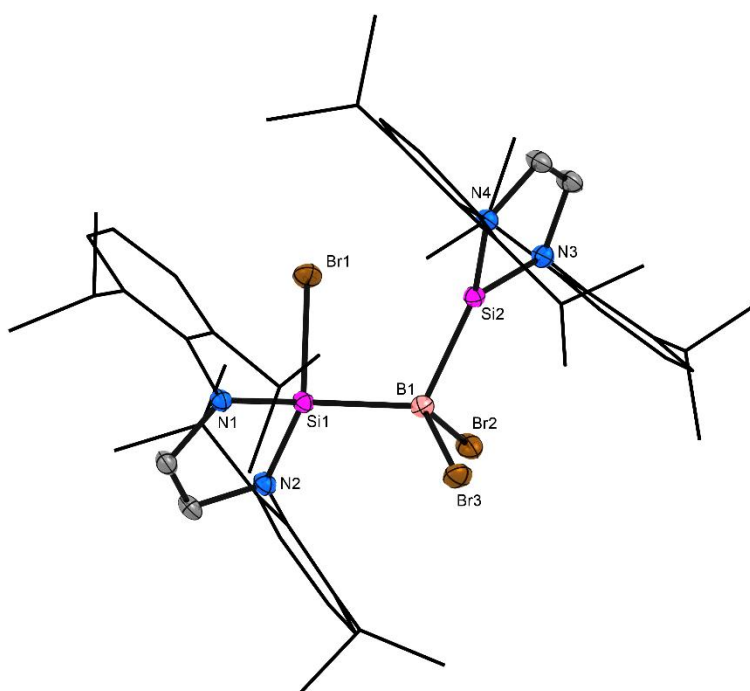


Figure 8: Molecular structure of **2.10** in the solid state. Ellipsoids are drawn at 50% probability; hydrogen atoms are omitted for clarity. Selected bond distances [Å] and angles [°] for **2.10**: Si1–B1 2.032(2), Si2–B2 2.015(2), Si1–N1 1.7367(18), Si1–N2 1.7365(18), Si2–N3 1.7096(18), Si2–N4 1.7094(18), B1–Si1–Br1 95.27(7), Si1–B1–Si2 112.81(11).

Dissolved in solution, ¹H NMR spectroscopy shows that **2.10** releases free silylene overtime leading to decomposition. Crystals of **2.10** are obtained in solution containing a large excess of silylene **1.26**, which does not exist anymore when pure crystals are dissolved in solution.

The decomposition of **2.10** occurs most likely through an equilibrium between coordinated and free silylene in solution, during which the unstable non-coordinate silylborane will decompose. Attempts to isolate **2.10** on a larger scale were unsuccessful.

Conclusion and perspectives

The silylene **I.26** was treated with numerous main group halides resulting in oxidative addition reactions. The disilane **2.1** and trisilane **2.5** were isolated and showed a relatively good stability compared to the products resulting from reactions of boron or phosphorus halides with the silylene. Indeed, the proposed product **2.7** and **2.8** were only observed by NMR spectroscopy and cannot be isolated. The unexpected **2.10** isolated as crystals suitable for X-ray crystallography could never be isolated on preparative scale due to its instability in solution. This difference in stability is in accordance with the relative stability of the bonds Si–Si ($\Delta H_{\text{diss}} = 327 \text{ kJ mol}^{-1}$), Si–B ($\Delta H_{\text{diss}} = 289 \text{ kJ mol}^{-1}$) and Si–P ($\Delta H_{\text{diss}} = 70\text{-}90 \text{ kcal mol}^{-1}$).^[28,65] The reactivity of disilane **2.1** and trisilane **2.5** was explored. The Si–Si bonds are not stable to reduction and lower valence silicon species are not accessible. Attempts to stabilise **2.1** using NHC or phosphine ligands do not show any coordination.

The electronic properties from silylenes or NHC are crucial for the formation donor-acceptor complexes and stabilisation of reduced main group species. Unlike the dialkylsilylene **II.2**, the silylene **I.26** appears to have not strong enough σ -donating and π -accepting character to reach stable reduced species.

Two ways to increase the stability of the Si–E (E = Si, B, P) bond can be considered. The first way would involve increasing the steric protection from the main group halide species. As reactions between **I.26** and pure halide main group compounds have shown limited stability, the use of reagents which also have a bulky substituent, REX_2

(R = aryl; E = Si, B, P; X = Cl, Br, I) could stabilise the Si–E bond. The reaction of bulkier boron halides or silicon halides with silylene have been recently reported to form stable silylboranes^[36] and disilanes and allowed their reduction in some examples.^[25,64] The second way would be to change the properties of the silylene, and to use a N-heterocyclic silylene with electronic properties closer to the dialkylsilylene

II.2.

References

- [1] M. Kira, S. Ishida, T. Iwamoto, C. Kabuto, *J. Am. Chem. Soc.* **1999**, *121*, 9722–9723.
- [2] S. Ishida, T. Iwamoto, C. Kabuto, M. Kira, *Chem. Lett.* **2001**, *11*, 1102–1103.
- [3] T. Iwamoto, M. Kobayashi, K. Uchiyama, S. Sasaki, S. Nagendran, H. Isobe, M. Kira, *J. Am. Chem. Soc.* **2009**, *131*, 3156–3157.
- [4] X. Q. Xiao, X. Liu, Q. Lu, Z. Li, G. Lai, M. Kira, *Molecules* **2016**, *21*, 1–10.
- [5] T. Iwamoto, K. Sato, S. Ishida, C. Kabuto, M. Kira, *J. Am. Chem. Soc.* **2006**, *128*, 16914–16920.
- [6] M. Kira, S. Ishida, T. Iwamoto, C. Kabuto, *J. Am. Chem. Soc.* **2002**, *124*, 3830–3831.
- [7] M. Kira, S. Ishida, T. Iwamoto, A. De Meijere, M. Fujitsuka, O. Ito, *Angew. Chemie - Int. Ed.* **2004**, *43*, 4510–4512.
- [8] S. Ishida, T. Iwamoto, M. Kira, *Organometallics* **2010**, *29*, 5526–5534.
- [9] W. Chen, L. Wang, Z. Li, A. Lin, G. Lai, X. Xiao, Y. Deng, M. Kira, *Dalt. Trans.* **2013**, *42*, 1872–1878.
- [10] L. Wang, W. Chen, Z. Li, X. Q. Xiao, G. Lai, X. Liu, Z. Xu, M. Kira, *Chem. Commun.* **2013**, *49*, 9776–9778.
- [11] Z. Dong, X. Q. Xiao, Z. Li, Q. Lu, G. Lai, M. Kira, *Org. Biomol. Chem.* **2015**, *13*, 9471–9476.
- [12] H. F. T. Klare, M. Oestreich, *Dalt. Trans.* **2010**, *39*, 9176–9184.
- [13] T. Iimura, N. Akasaka, T. Iwamoto, *Organometallics* **2016**, *35*, 4071–4076.
- [14] C. Watanabe, T. Iwamoto, C. Kabuto, M. Kira, *Angew. Chemie - Int. Ed.* **2008**, *47*, 5386–5389.
- [15] X. Liu, X. Xiao, Z. Xu, X. Yang, Z. Li, Z. Dong, C. Yan, *Organometallics* **2014**, *33*, 5434–5439.
- [16] S. Ishida, T. Iwamoto, M. Kira, *Heteroat. Chem.* **2011**, *22*, 432–437.
- [17] M. M. Linden, H. P. Reisenauer, D. Gerbig, M. Karni, A. Schäfer, T. Müller, Y. Apeloig, P. R. Schreiner, *Angew. Chemie - Int. Ed.* **2015**, *54*, 12404–12409.
- [18] S. Ishida, T. Iwamoto, C. Kabuto, M. Kira, *Nature* **2003**, *421*, 725–727.
- [19] Y. Apeloig, *The Chemistry of Organic Silicon Compounds, Vol. 3, Chap. 5*, **2001**.
- [20] D. Auer, C. Strohmam, A. V Arbuznikov, M. Kaupp, *Organometallics* **2003**, *22*, 2442–2449.

- [21] N. Takagi, T. Shimizu, G. Frenking, *Chem. - A Eur. J.* **2009**, *15*, 3448–3456.
- [22] K. C. Mondal, H. W. Roesky, M. C. Schwarzer, G. Frenking, B. Niepötter, H. Wolf, R. Herbst-Irmer, D. Stalke, *Angew. Chemie - Int. Ed.* **2013**, *52*, 2963–2967.
- [23] T. Iwamoto, T. Abe, C. Kabuto, M. Kira, *Chem. Commun.* **2005**, 5190–5192.
- [24] K. Uchiyama, S. Nagendran, S. Ishida, T. Iwamoto, M. Kira, *J. Am. Chem. Soc.* **2007**, *129*, 10638–10639.
- [25] S. Si, D. Bond, *J. Am. Chem. Soc.* **2017**, *139*, 18146–18149.
- [26] Y. Suzuki, S. Ishida, S. Sato, H. Isobe, T. Iwamoto, *Angew. Chemie - Int. Ed.* **2017**, *56*, 4593–4597.
- [27] P. Zark, A. Schafer, A. Mitra, D. Haase, W. Saak, R. West, T. Muller, *J. Organomet. Chem.* **2010**, *695*, 398–408.
- [28] J. A. Dean, *Lange's Handbook of Chemistry*, **1999**.
- [29] L. Kong, J. Zhang, H. Song, C. Cui, *Dalt. Trans.* **2009**, 5444–5446.
- [30] *J. Organomet. Chem.* **1996**, *521*, 211–220.
- [31] N. Metzler, M. Denk, *Chem. Commun.* **1996**, 2657–2658.
- [32] M. Haaf, A. Schmiedl, T. A. Schmedake, D. R. Powell, A. J. Millevolte, M. Denk, R. West, *J. Am. Chem. Soc.* **1998**, *120*, 12714–12719.
- [33] D. F. Moser, T. Bosse, J. Olson, J. L. Moser, I. A. Guzei, R. West, *J. Am. Chem. Soc.* **2002**, *124*, 4186–4187.
- [34] D. F. Moser, A. Naka, I. A. Guzei, T. Müller, R. West, *J. Am. Chem. Soc.* **2005**, *127*, 14730–14738.
- [35] B. Gehrhus, P. B. Hitchcock, H. Jansen, *J. Organomet. Chem.* **2006**, *691*, 811–816.
- [36] A. Gackstatter, H. Braunschweig, T. Kupfer, C. Voigt, N. Arnold, *Chem. - A Eur. J.* **2016**, *22*, 16415–16419.
- [37] D. J. Ager, *J. Organomet. Chem.* **1983**, *241*, 139–141.
- [38] J. Xie, D. Feng, M. He, S. Feng, *J. Phys. Chem. A* **2005**, *109*, 10563–10570.
- [39] G. Molev, D. Bravo-Zhivotovskii, M. Karni, B. Tumanskii, M. Botoshansky, Y. Apeloig, *J. Am. Chem. Soc.* **2006**, *128*, 2784–2785.
- [40] H. M. Cho, Y. M. Lim, B. W. Lee, S. J. Park, M. E. Lee, *J. Organomet. Chem.* **2011**, *696*, 2665–2668.
- [41] T. Iwamoto, T. Abe, S. Ishida, C. Kabuto, M. Kira, *J. Organomet. Chem.* **2007**, *692*, 263–270.
- [42] *Angew. Chem. Int. Ed.* **1971**, *10*, 127.

- [43] T. Saito, H. Nishiyama, H. Tanahashi, K. Kawakita, H. Tsurugi, K. Mashima, *J. Am. Chem. Soc.* **2014**, *136*, 5161–5170.
- [44] A. Lichtblau, H. D. Hausen, W. Schwarz, W. Kaim, *Inorg. Chem.* **1993**, *32*, 73–78.
- [45] A. Lichtblau, A. Ehrend, H. -D Hausen, W. Kaim, *Chem. Ber.* **1995**, *128*, 745–750.
- [46] M. Noguchi, K. Suzuki, J. Kobayashi, T. Yurino, H. Tsurugi, K. Mashima, M. Yamashita, *Organometallics* **2018**, *37*, 1833–1836.
- [47] Y. Wang, Y. Xie, P. Wei, R. B. King, H. F. Schaefer, P. von R Schleyer, G. H. Robinson, *Science* **2008**, *321*, 1069–1071.
- [48] N. Kuhn, T. Kratz, D. Bläser, R. Boese, *Chem. Ber.* **1995**, *128*, 245–250.
- [49] A. C. Filippou, Y. N. Lebedev, O. Chernov, M. Straßmann, G. Schnakenburg, *Angew. Chemie - Int. Ed.* **2013**, *52*, 6974–6978.
- [50] T. L. Amyes, S. T. Diver, J. P. Richard, F. M. Rivas, K. Toth, *J. Am. Chem. Soc.* **2004**, *126*, 4366–4374.
- [51] K. Haav, J. Saame, A. Kütt, I. Leito, *European J. Org. Chem.* **2012**, 2167–2172.
- [52] D. J. Dellinger, D. M. Sheehan, N. K. Christensen, J. G. Lindberg, M. H. Caruthers, *J. Am. Chem. Soc.* **2003**, *125*, 940–950.
- [53] G. Mourgas, M. Nieger, D. Fo, D. Gudat, *Inorg. Chem.* **2013**, *52*, 4104–4112.
- [54] R. S. Ghadwal, H. W. Roesky, S. Merkel, D. Stalke, *Chem. - A Eur. J.* **2010**, *16*, 85–88.
- [55] S. Kaufmann, S. Schäfer, M. T. Gamer, P. W. Roesky, *Dalt. Trans.* **2017**, *46*, 8861–8867.
- [56] R. Azhakar, G. Tavčar, H. W. Roesky, J. Hey, D. Stalke, *Eur. J. Inorg. Chem.* **2011**, 475–477.
- [57] A. Jana, R. Azhakar, S. P. Sarish, P. P. Samuel, H. W. Roesky, C. Schulzke, D. Koley, *Eur. J. Inorg. Chem.* **2011**, 5006–5013.
- [58] A. Jana, D. Leusser, I. Objartel, H. W. Roesky, D. Stalke, *Dalt. Trans.* **2011**, *40*, 5458–5463.
- [59] R. Rodriguez, T. Troadec, T. Kato, N. Saffon-Merceron, J. M. Sotiropoulos, A. Baceiredo, *Angew. Chemie - Int. Ed.* **2012**, *51*, 7158–7161.
- [60] S. M. I. Al-Rafia, A. C. Malcolm, R. McDonald, M. J. Ferguson, E. Rivard, *Chem. Commun.* **2012**, *48*, 1308–1310.
- [61] S. Inoue, K. Leszczyńska, *Angew. Chemie - Int. Ed.* **2012**, *51*, 8589–8593.

- [62] K. Junold, J. A. Baus, C. Burschka, C. Fonseca Guerra, F. M. Bickelhaupt, R. Tacke, *Chem. - A Eur. J.* **2014**, *20*, 12411–12415.
- [63] F. M. Mück, J. A. Baus, R. Bertermann, C. Burschka, R. Tacke, *Organometallics* **2016**, *35*, 2583–2588.
- [64] Y. Suzuki, S. Ishida, S. Sato, H. Isobe, T. Iwamoto, *Angew. Chem. Int. Ed.* **2017**, *56*, 4593–4597.
- [65] A. G. Baboul, H. B. Schlegel, *J. Am. Chem. Soc.* **1996**, *118*, 8444–8451.

Chapter III

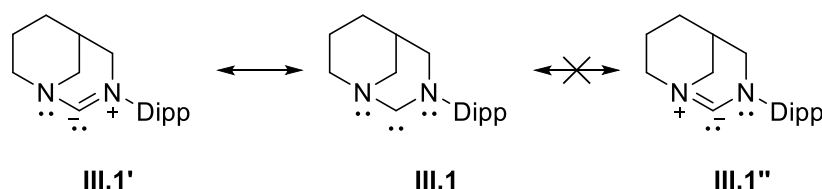
Synthesis of an anti-Bredt Silylene

Chapter III – Synthesis of an anti-Bredt Silylene

Introduction

An anti-Bredt N-Heterocyclic Carbene

In 2012, Bertrand and co-workers reported the synthesis of an N-heterocyclic carbene (NHC), **III.1**, which involved an N-bridgehead next to the carbene carbon.^[1] This nitrogen has a pyramidalized geometry with a sum of the bond angles of 339°, a value in the range of sp³-hybridized nitrogen atoms. In addition, the carbene-nitrogen bond had a dihedral angle of 34° between the p-orbital of the carbene and the lone pair of the N-bridgehead. The conformation of this nitrogen prevents the π-donation into the vacant p-orbital of the carbene, in accordance with Bredt's rule, which states that a double bond cannot be located at the bridgehead of a bridged compound, unless the size of the ring is large enough.^[2] Therefore between the three possible resonance structures **III.1**, **III.1'** and **III.1''**, the form **III.1''** is irrelevant (*Scheme 1*). This characteristic makes the NHC slightly more σ-donating but also significantly more π-accepting and induces a higher reactivity than the classical NHCs, evidenced by its smaller singlet-triplet gap of 43 kcal mol⁻¹ (classical NHCs: 62 kcal mol⁻¹).



Scheme 1: Lewis structure of the anti-Bredt NHC **III.1**, its resonance structure **III.1'**, and its disallowed structure **III.1''**.

The electronic properties from **III.1** have been studied by the determination of the Tolman electronic parameter (TEP). The TEP gives a measure of the donating ability

of a ligand to a transition metal. The TEP is determined by measurement of the CO bond stretching frequency of ligand-metal complexes such as $[\text{RhCl}(\text{CO})_2(\text{L})]$, $[\text{Ni}(\text{CO})_3(\text{L})]$ or *cis*- $[\text{IrCl}(\text{CO})_2(\text{L})]$ (L = carbene ligand). G. Bertrand *et al.* synthesized the *cis*-chlorodicarbonyliridium complex of **III.1** and analysis by IR spectroscopy allowed them to calculate the TEP value of 2047 cm^{-1} . This TEP value is intermediate between that of a classical NHC and cyclic (alkyl)(amino)carbene (cAAC), which are known to be more reactive (Table 1).

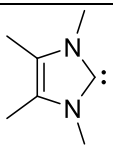
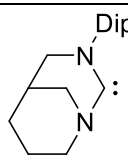
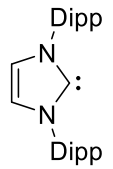
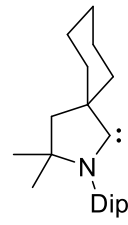
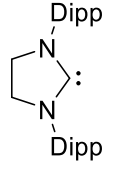
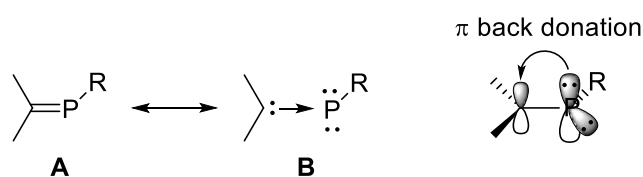
	Carbene	TEP (cm^{-1})		Carbene	TEP (cm^{-1})
MeIme		2051.7 ^[a]	III.1		2047 ^[c]
IPr		2051.5 ^[b]	I.63		2046 ^[d]
SIPr		2052.2 ^[b]			

Table 1: [a] Calculated value for $\text{Ni}(\text{CO})_3(\text{NHC})$ complex.^[3] [b] Determined experimentally from $\text{Ni}(\text{CO})_3(\text{NHC})$ complexes in DCM.^[4] [c] Calculated by linear regression from the experimentally measured ν_{CO} of the $\text{IrCl}(\text{CO})_2(\text{NHC})$ complex in DCM.^[1,5] [d] Calculated by linear regression from the experimentally measured ν_{CO} of $\text{Ni}(\text{CO})_3(\text{cAAC})$ in DCM.^[6]

TEP values allow for the evaluation of the overall donor properties of carbenes but it does not consider both σ -donating and π -accepting characters distinctly. Moreover, IR frequencies for NHC complexes come in a narrow region which makes this characterisation method less informative.

G. Bertrand and co-workers developed a different method using carbene-phosphinidene adducts as indicators of the π -accepting properties of carbenes.^[7] These carbene-phosphorus adduct can be drawn as a standard phosphalkene **A** (Scheme 2) with a formal P=C double bond, or as carbene-phosphinidene adduct **B** with a P–C dative bond with two lone pairs located on the phosphorus.



Scheme 2: The possible resonance structures of the carbene-phosphorus adduct: phosphalkene **A** and carbene-phosphinidene **B**.

By measuring the ^{31}P NMR chemical shift of the carbene-phosphinidene adducts, the π -accepting character of the different carbenes could be quantified (Table 2). The more π -accepting the carbene is the more resonance form **A** will be favoured. Therefore, the more π -accepting the carbene is the more down-field the ^{31}P NMR signal will. Conversely, the less π -accepting the carbene is, the resonance form **B** will be favoured, resulting in high-field ^{31}P NMR signals.

	Carbene- phosphinidene adduct	$\delta^{31}\text{P}$ (ppm)	Carbene- phosphinidene adduct	$\delta^{31}\text{P}$ (ppm)	
III.2		-53.5 ^[a]	III.5		34.9
III.3		-18.9	III.6		68.9
III.4		-10.2 ^[b]			

Table 2: Carbene-phosphinidene adduct (drawn in their phosphalkene form) and corresponding ^{31}P NMR chemical shift (measured in C_6D_6). [a] NMR spectrum recorded in THF-d_8 . [b] NMR spectrum recorded in CDCl_3 .

The ^{31}P NMR chemical shift for **III.3** ($\delta -18.9$) is observed at a significantly higher field than its saturated analogue **III.4** ($\delta -10.2$). The corresponding free carbenes IPr and SIPr have identical substituents, but SIPr has a saturated N-heterocycle. In this case, the π -donation from the nitrogen is lowered and therefore the π -accepting character of the carbene is higher. The adduct **III.6** ($\delta 68.9$) is considerably shifted down-field compared to the NHC adducts, which is in accordance with the high π -accepting character of the cAAC, due to the alkyl substituent instead of a nitrogen. The carbene-phosphinidene **III.5** ($\delta 34.9$), with its enhanced π -accepting character due to the geometry of its related carbene **III.1**, is intermediate between the classical NHC (**III.2-III.4**) and the cAAC (**III.6**).

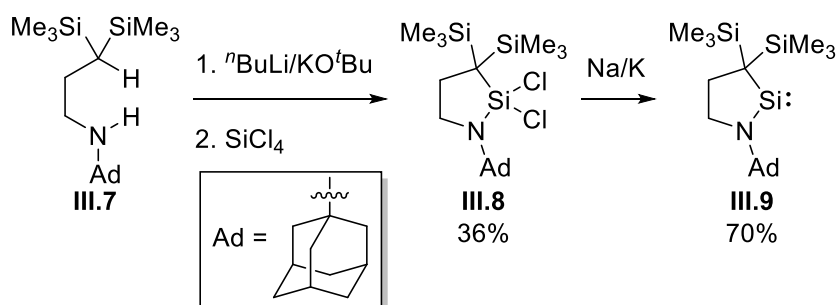
Other properties will make an NHC a good ligand for low coordinate chemistry, such as steric bulk and stability to reduction. However, the electronic properties of the selected carbene play a very important role. For instance, the synthesis of the

trisilicon(0) **I.104** cluster (See Chap. I, *Base-stabilised trisilicon(0)*) was achieved using coordinated cAACs.^[8] The high π -accepting character of the cAAC is essential for the stability of **I.104** and it cannot be made using classical NHCs.

Cyclic (Alkyl)(Amino) Silylene

In a similar way to NHCs, cAACs and anti-Bredt NHC, the σ -donating and π -accepting properties of N-heterocyclic silylenes are modulated by their structure (See Chap. I, *Dicordinate N-Heterocyclic Silylenes*). The cyclic dialkylsilylene **II.2** has shown higher reactivity than classical N-heterocyclic silylenes, since it has both stronger σ -donating and π -accepting character. No classification of the electronic properties of the heterocyclic silylenes has been made, such as the one achieved for NHCs. However, heterocyclic silylenes have been developed at the same time and some N-heterocyclic silylenes have been designed to approach the electronic properties of the dialkylsilylene **II.2**.

The cyclic (alkyl)(amino)silylene is a new class of heterocyclic silylene analogous to cAACs. Reported by Iwamoto and co-workers, the synthesis of the silylene **III.9** required harsh reaction conditions.^[9] In the ring closing step, the use of Schlosser's base was necessary for deprotonation of **III.7** to form **III.8** by addition of SiCl_4 . Treatment with other bases ($^n\text{BuLi}$, $^t\text{BuLi}$ and $^n\text{BuLi/TMEDA}$) did not form the desired dianion. The reduction of **III.8** was carried out with a sodium-potassium alloy, affording the cyclic (alkyl)(amino)silylene **III.9** (Scheme 3).



Scheme 3: Synthesis of cyclic (alkyl)(amino)silylene **III.9**.

The TEP of **III.9** has not yet been determined but the characteristics of **III.9** suggest that its electronic properties are intermediate between N-heterocyclic silylenes and the dialkylsilylene **II.2** (Figure 1). The ^{29}Si NMR resonance of **III.9** (δ 274.7) comes in between the dialkylsilylene **II.2** (δ 567.4)^[10] and the most deshielded N-heterocyclic silylene **III.10** (δ 118.9).^[11] The UV/Vis spectrum showed an absorption band corresponding to the HOMO–LOMO transition at $\lambda = 351$ nm, which is also intermediate between the values found for the dialkylsilylene **II.2** ($\lambda = 440$ nm) and the silylene **III.10** ($\lambda = 292$ nm). The high thermal stability (above 150 °C) of **III.9** allows reactivity comparable to the dialkylsilylene **II.2**, with C–C bond activation of aryl, C–H bond activation of alkyl and [1+2] or [1+4] cycloadditions.^[9]

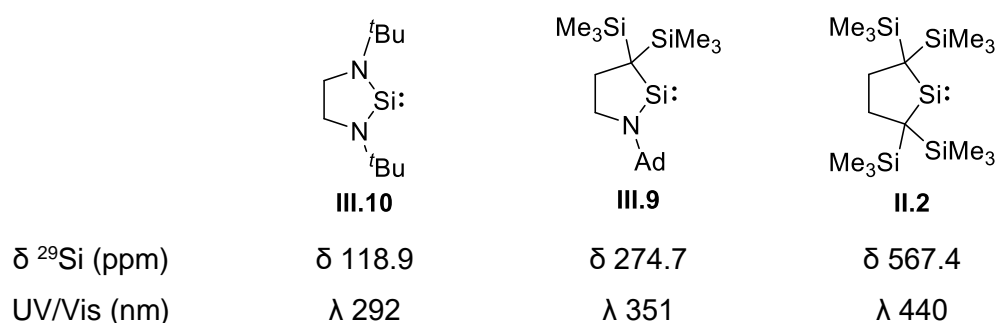


Figure 1: Comparison of N-heterocyclic silylene, cyclic (alkyl)(amino)silylene and dialkylsilylene.

Synthesis of an anti-Bredt N-Heterocyclic Silylene

In families of both cyclic dicoordinate carbenes and silylenes, some members have still not been achieved. Indeed, the dialkylsilylene **II.2** does not have a stable carbene equivalent and the anti-Bredt NHC **III.1** does not have a silylene equivalent (Figure 2).

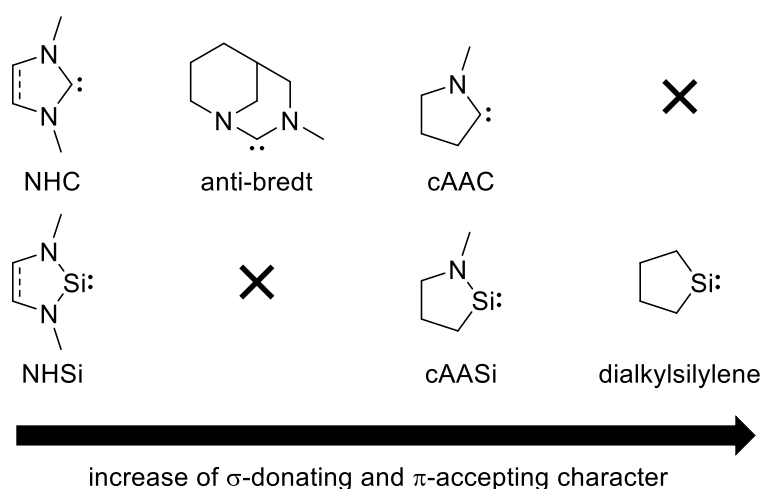
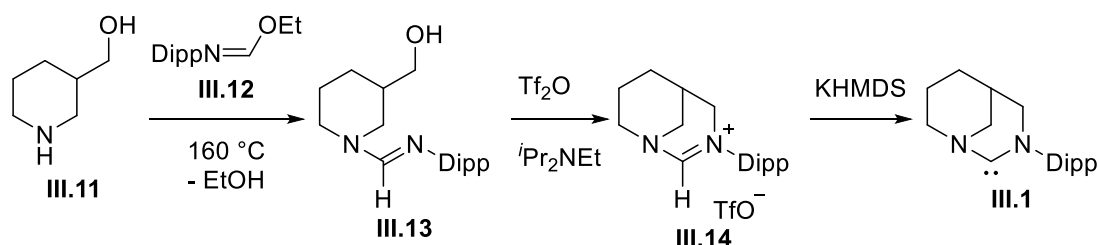


Figure 2: Schematic classification of the different classes of cyclic dicoordinate carbenes and silylenes.

Synthetic strategy towards an anti-Bredt N-Heterocyclic Silylene

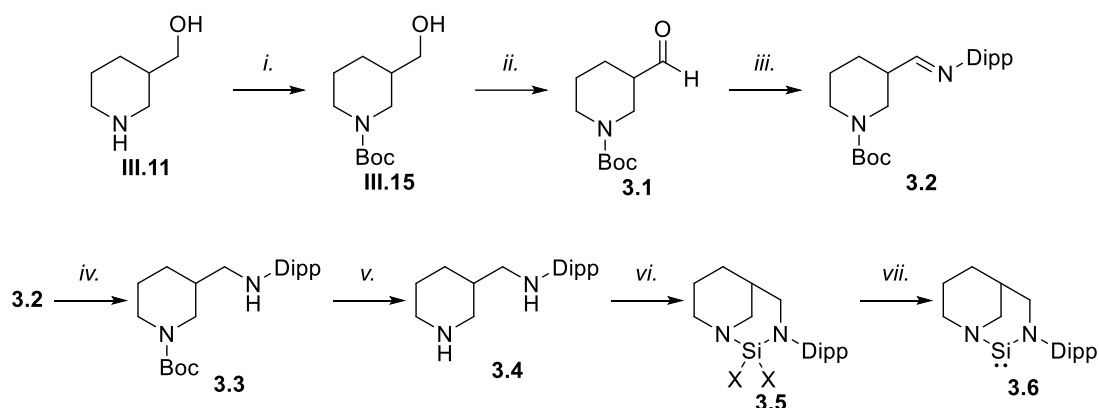
The synthesis of a silylene analogue to the anti-Bredt NHC **III.1** is anticipated to provide a more reactive silylene, with electronic properties intermediate to the classical N-heterocyclic silylene and the cyclic (alkyl)(amino)silylene **II.2**.^[9] The geometry of the targeted anti-Bredt silylene **3.6** should enhance the π -accepting character of the silylene in a similar way observed for **III.1**. The synthetic route used for **III.1** (Scheme 4) cannot be used for the silicon analogue. Silaimines $\text{RN}=\text{SiR}_2$ are highly reactive compounds, stable examples of which have only previously been synthesised using bulky substituents or coordinating bases.^[12,13] The analogous

silimine of the *N*-2,6-diisopropylphenylformamidinate **III.12** will not be stable enough to undergo the first or the second step of the synthesis.



Scheme 4: The multistep synthesis of the anti-Bredt NHC **III.1**.

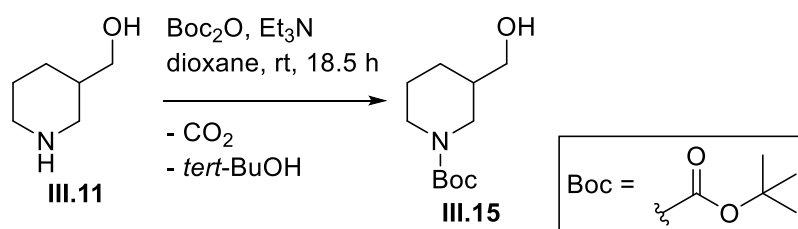
A new synthesis was designed to reach the silylene **3.6** (Scheme 5). The 3-(hydroxymethyl)piperidine **III.11** is protected with a *tert*-butyloxycarbonyl protecting group (Boc) to prevent side reactions during the further steps (Scheme 5.i).^[14] The Boc-protected 3-(hydroxymethyl)piperidine **III.15** is oxidised to the aldehyde **3.1** (Scheme 5.ii). Imine condensation reaction from **3.1** and 2,6-diisopropylaniline forms **3.2** (Scheme 5.iii). Reduction of the imine **3.2** gives the amine **3.3** (Scheme 5.iv). Boc-deprotection affords the diamine ligand **3.4** (Scheme 5.v). Double deprotonation of the two amine moieties from **3.4** followed by addition of SiX_4 forms the dihalosilane **3.5** (Scheme 5.vi). Finally, reduction of **3.5** affords the desired anti-Bredt silylene **3.6** (Scheme 5.vii).



Scheme 5: Proposed synthetic route for **3.6**. *i.* Boc-protection of **III.11**. *ii.* Alcohol oxidation of **III.15**. *iii.* Imine condensation from **3.1**. *iv.* Reductive amination of **3.2**. *v.* Boc-deprotection of **3.3**. *vi.* Double deprotonation followed by SiCl_4 addition to **3.4**. *vii.* Reduction of **3.5**.

Boc protection: synthesis of **III.15**

The synthesis starts from the commercially available 3-(hydroxymethyl)piperidine **III.11**. Following the reported preparation, **III.11** was treated with an equivalent of di-*tert*-butyl dicarbonate (Boc_2O) in a presence of a base, triethylamine (Et_3N) (Scheme 6),^[14] affording the protected amine **III.15**. The purification procedure, which involved removing volatiles *in vacuo*, did not afford **III.15** as a pure product. The ^1H NMR spectrum showed trace of starting material, which was removed by recrystallisation overnight from dioxane at low temperature ($-20\text{ }^\circ\text{C}$), yielding **III.15** as a pure product after filtration and washing with cold pentane. The protected-amine **III.15** was obtained in 78% yield, with ^1H NMR analysis in accordance with the reported literature.



Scheme 6: Boc-protection reaction of **III.11**, synthesis of **III.15**.

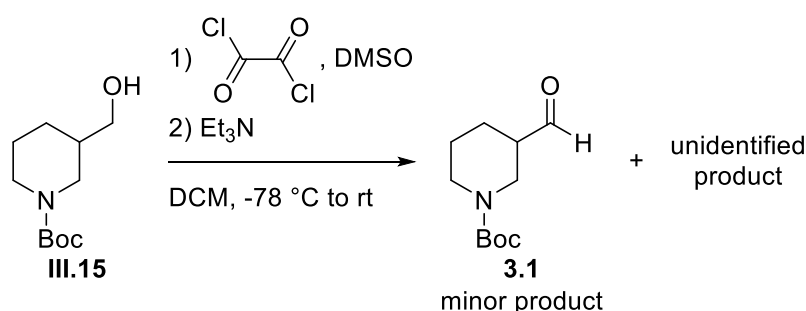
Alcohol oxidation: synthesis of 3.1

The Boc-protecting group is sensitive to acidic conditions, so the preparation used for the following step had to avoid the use of acids. Common oxidation methods were tried to synthesise **3.1**.

Swern-oxidation

Swern-oxidation was carried out on **III.15** (Scheme 7). After work-up, ^1H NMR analysis of the isolated oil showed no more starting material **III.15**. Unfortunately, the desired compound **3.1** was only observed as a minor product.

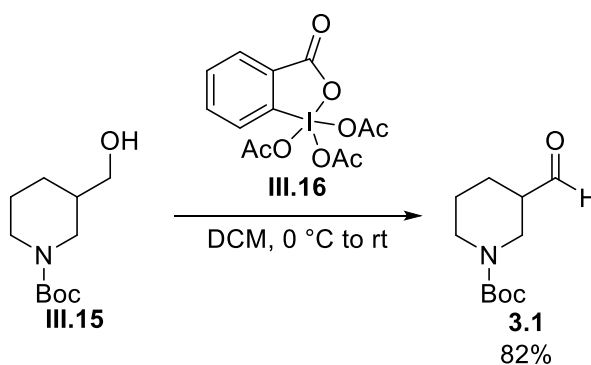
Analysis of the integration from the ^1H NMR spectrum of the aldehyde proton resonance (δ 9.68) with respect to the Boc-group protons (δ 1.46) confirmed the presence of the aldehyde **3.1**. However, another signal from the Boc group (δ 1.45) was observed as the major product, with no relative integration to any aldehyde signal and differs from the starting material. This implied that the Boc group has been cleaved during the reaction or an undesired product is formed by a side-reaction. As the aldehyde **3.1** could not be synthesised by Swern-oxidation, a different preparation was used.



Scheme 7: Swern-oxidation of **III.15**.

Dess-Martin oxidation

The alcohol **III.15** was treated with 1.1 equivalent of Dess-Martin periodinane **III.16** in DCM at 0 °C (*Scheme 8*). The ^1H NMR spectrum showed the formation of the aldehyde **3.1** as the major product. Carrying out the reaction using distilled DCM, under an argon atmosphere was found to give cleaner product. After work-up and removing the volatiles *in vacuo*, the pure product **3.1** was obtained as a colourless oil in 82% yield. The ^1H NMR spectrum has all the expected signals from the product: the aldehyde resonance (δ 9.68) integrates to 1 relative to the Boc group (δ 1.44, 9H) and the heterocycle (δ 3.91-1.48, 9H). Due to the success of this step, the Dess-Martin oxidation was kept as the oxidation procedure. It was also shown that the aldehyde **3.1** could easily be synthesised on larger scale (up to 5 grams).



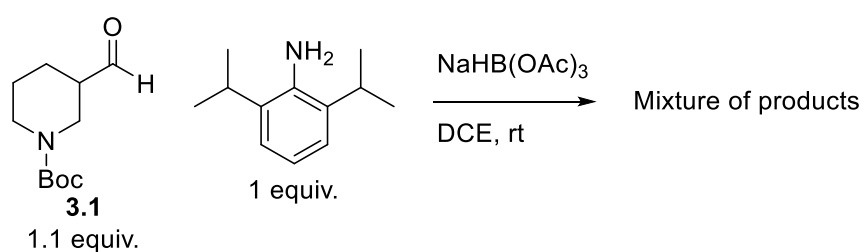
Scheme 8: Synthesis of the aldehyde **3.1** by Dess-Martin oxidation of **III.15**.

One-pot synthesis of 3.3 from 3.1

Reductive amination was attempted. A reported procedure of reductive amination between cyclohexanecarboxaldehyde and aniline was carried out on **3.1** in order to make **3.3**.^[15] Aldehyde **3.1** and 2,6-diisopropylaniline in dichloroethane (DCE) were treated with sodium triacetoxyborohydride ($\text{NaHB}(\text{OAc})_3$), a milder reducing agent than sodium borohydride (NaBH_4). After 24 hours, a mixture of aniline, alcohol **III.15**, the imine **3.2** and the amine **3.3** were observed by ^1H NMR spectroscopy. As

reduction of the aldehyde **3.1** to the alcohol **III.15** was observed, it implied that the imine condensation reaction was very slow. The slow rate of the imine condensation is a problem as the aldehyde **3.1** can also be reduced by the NaHB(OAc)_3 , forming **III.15** instead of desired product **3.3**.

The reaction was reproduced with a small excess of aldehyde **3.1** (Scheme 9) and monitored by ^1H NMR spectroscopy (Figure 3.a-3.b).



Scheme 9: Reductive amination reaction of **3.1** and 2,6-diisopropylaniline, with excess of **3.1**.

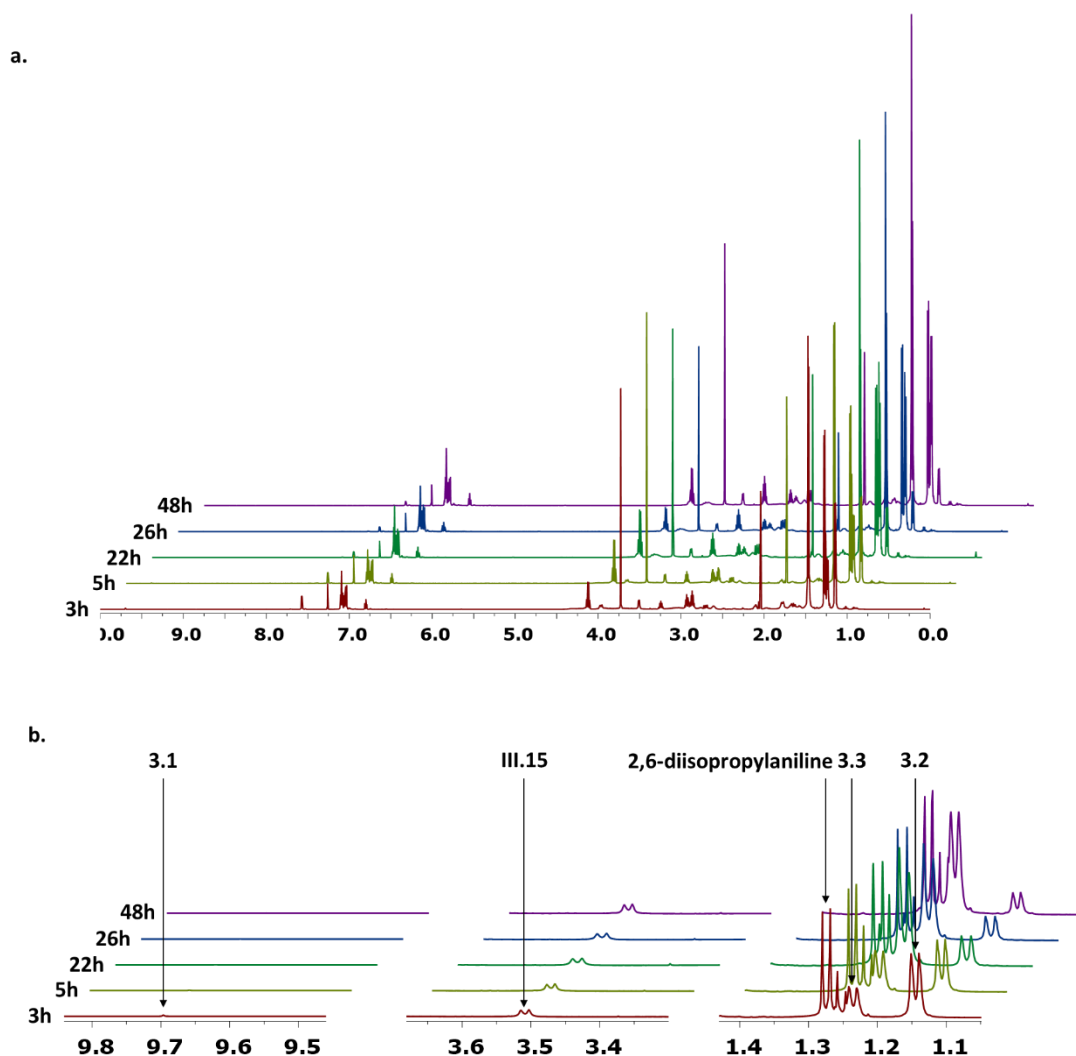


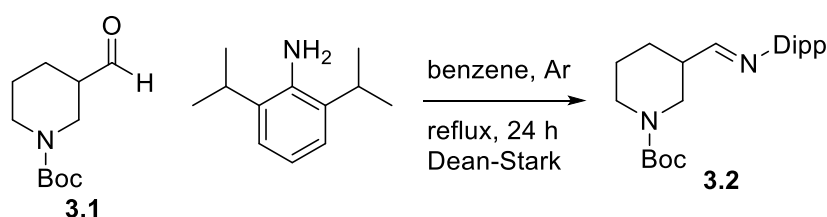
Figure 3. **a.** ^1H NMR spectrum (500 MHz, CDCl_3) of the monitoring of the reductive amination reaction of **3.1** and 2,6-diisopropylaniline. **b.** Extensions of relevant regions of the ^1H NMR spectrum monitoring.

Monitoring the reaction showed that even with a small excess, the aldehyde **3.1** is completely consumed after 3 hours, where there is still a lot of 2,6-diisopropylaniline in solution. The presence of the alcohol **III.15** confirmed that the aldehyde **3.1** was reduced during the reaction. The imine intermediate **3.2** is formed and slowly reduced to the desired amine **3.3**. As the reducing agent also reduced the aldehyde **3.1**, the imine **3.2** cannot be completely reduced. The reaction led to a mixture of the alcohol **III.15**, the 2,6-diisopropylaniline, the imine **3.2** and the targeted amine **3.3**. The

monitoring confirms that it is necessary to carry out the imine condensation and the reduction separately.

Imine condensation: synthesis of the imine **3.2**

The aldehyde **3.1** and 2,6-diisopropylaniline were allowed to react in dry methanol and under an argon atmosphere. The solution was dried over molecular sieves (3 Å) to remove the water produced from the condensation reaction. Slow conversion to the imine **3.2** was observed. It was found that carrying out the reaction in benzene using a Dean-Stark apparatus under reflux gave a better conversion (*Scheme 10*).



Scheme 10: Synthesis of **3.2** by imine condensation reaction of **3.1** with 2,6-diisopropylaniline.

The conversion was followed by ¹H NMR spectroscopy. Up to 90% conversion to the product **3.2** was obtained, with remaining trace of aniline (8%) and aldehyde **3.1** (2%). The ¹H NMR spectrum of the crude reaction mixture showed all the expected signals, with a signal (δ 7.61, d, 1H) found in the expected region for imine proton and matching integrations between the piperidine and the Dipp fragments (*Figure 4*).

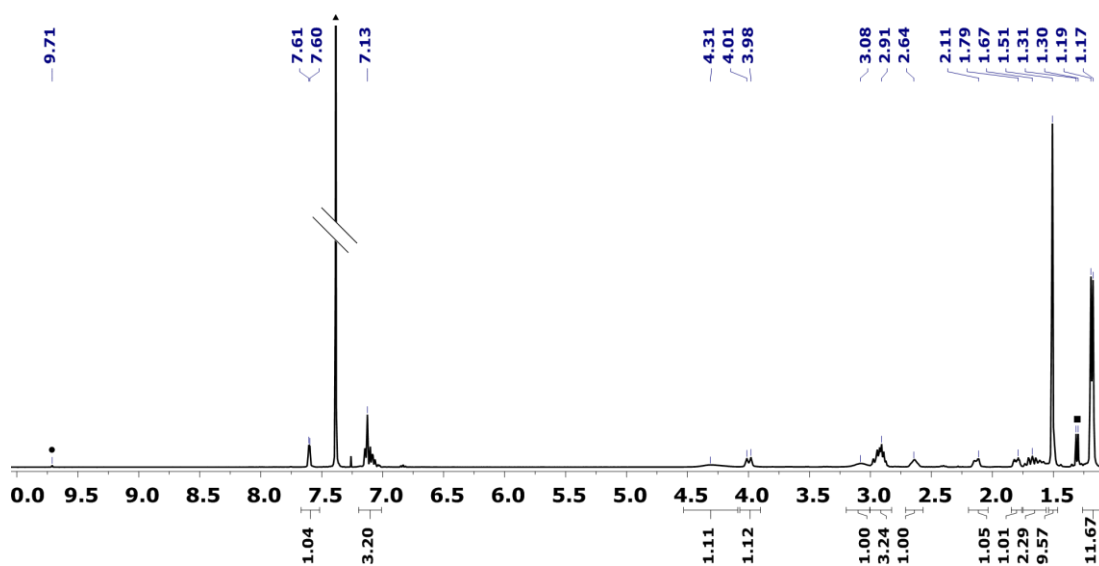
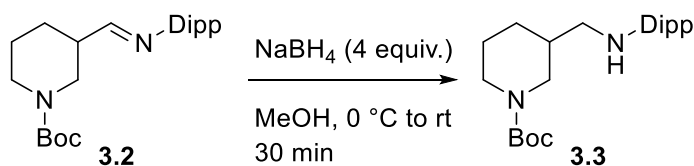


Figure 4: ^1H NMR spectrum (400 MHz, CDCl_3) of the crude of the reaction of **3.2** synthesis. ● Peak of remaining aldehyde **3.1**. ■ Peak of remaining 2,6-diisopropylaniline. ▲ Benzene peak.

Attempts to purify the imine **3.2** were unsuccessful. The product did not crystallise from hexane or pentane. Solvent extraction using ethyl acetate or diethyl ether were unsuccessful. Chromatographic column (hexane:ethyl acetate, 95:5) was also attempted, however decomposition to starting material **3.1** was observed by ^1H NMR spectroscopy. Due to the instability of the imine **3.2**, the reduction was carried out on the crude material.

Imine reduction: synthesis of the amine **3.3**

The crude imine **3.2** was treated with an excess of NaBH₄ in cold methanol (0 °C). Almost full conversion to the amine **3.3** was observed by ¹H NMR spectroscopy (Scheme 11).



Scheme 11: Synthesis of **3.3** by reduction of **3.2**.

The signal at δ 7.61, characteristic from the imine **3.2**, was not observed in the ¹H NMR spectrum. A new product was observed, the integration of its ¹H NMR resonance enabled the identification of amine **3.3** (Figure 5). Work-up of the crude reaction mixture afforded the amine **3.3** almost pure (> 95% purity). Solvent extraction or chromatographic column did not allow further purification of **3.3**, which is always contaminated with trace of 2,6-diisopropylaniline.

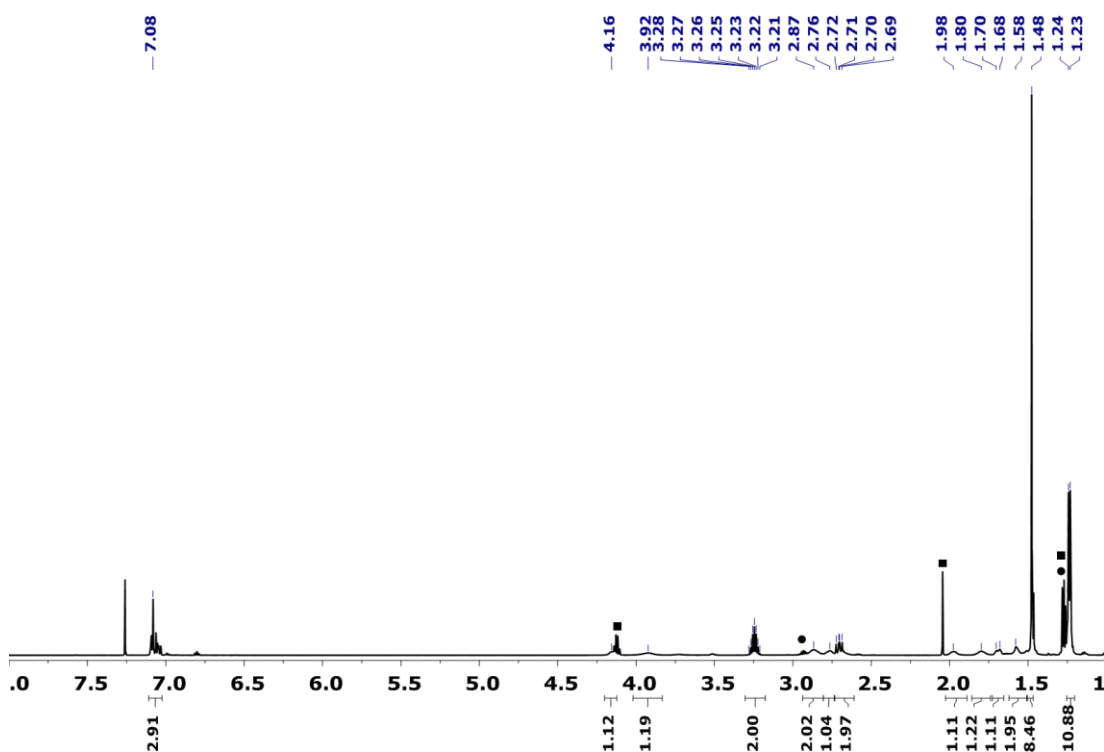
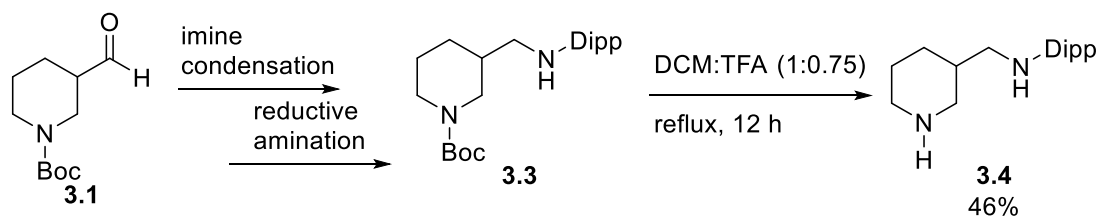


Figure 5: ^1H NMR spectrum (600 MHz, CDCl_3) of the crude reaction mixture of the synthesis of **3.3**. ■ Ethyl acetate. ● 2,6-diisopropylaniline.

Boc deprotection: synthesis of the ligand **3.4**

Trifluoroacetic acid (TFA), a common Boc-deprotecting agent was attempted with **3.3** in order to afford ligand **3.4**. The amine **3.3** was treated with a solution of DCM:TFA (1:0.75) and heated overnight under reflux (*Scheme 12*). Work-up followed by crystallisation from pentane afforded the deprotected ligand **3.4** as colourless crystals. The ligand **3.4** can be obtained in 46% yield over the three steps from **3.1**.



Scheme 12: Boc deprotection, synthesis of the ligand **3.4** from **3.1**.

The solid-state structure of **3.4** was obtained by X-ray analysis (*Figure 6*), confirming the deprotection of the piperidine N2 and the presence of the second amine N1. The N1–C13 bond (1.4669(12) Å) is in the typical range of carbon–nitrogen single bonds (1.47 Å)^[16] and slightly longer than the N1–C1 bond (1.4317(11) Å), which is due to the conjugation of N1 with the aromatic ring. The pyramidal geometry from N1 also attests to the absence of an imine.

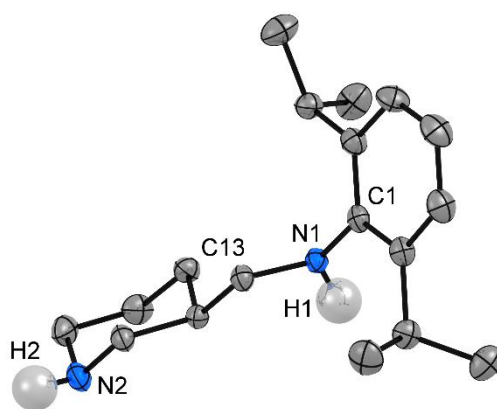


Figure 6: Molecular structure of **3.4** in the solid state. Ellipsoids are drawn at 50% probability; hydrogen atoms (except H1 and H2) are omitted for clarity. Selected bond distances [Å] for **3.4**: N1–C13 1.4669(12), N1–C1 1.4317(11).

The ¹H NMR spectrum of **3.4** is in accordance with the product with all the expected resonances (*Figure 7*). The signals from the piperidine fragment (δ 3.5-1.5) are less broad than that from the precursors **3.2** and **3.3**. This suggests a restricted rotation of the heterocycle due to the addition of the bulky Dipp substituent. The ¹H and ¹³C NMR resonances were fully assigned using ¹H-¹³C HMQC, HMBC and COSY NMR experiments.

The diamine ligand **3.4** can be isolated on gram scale and is stable in the solid state or in solution under air. Isolating **3.2** or **3.3** becomes unnecessary as working on the crude product for each step successfully affords **3.4**.

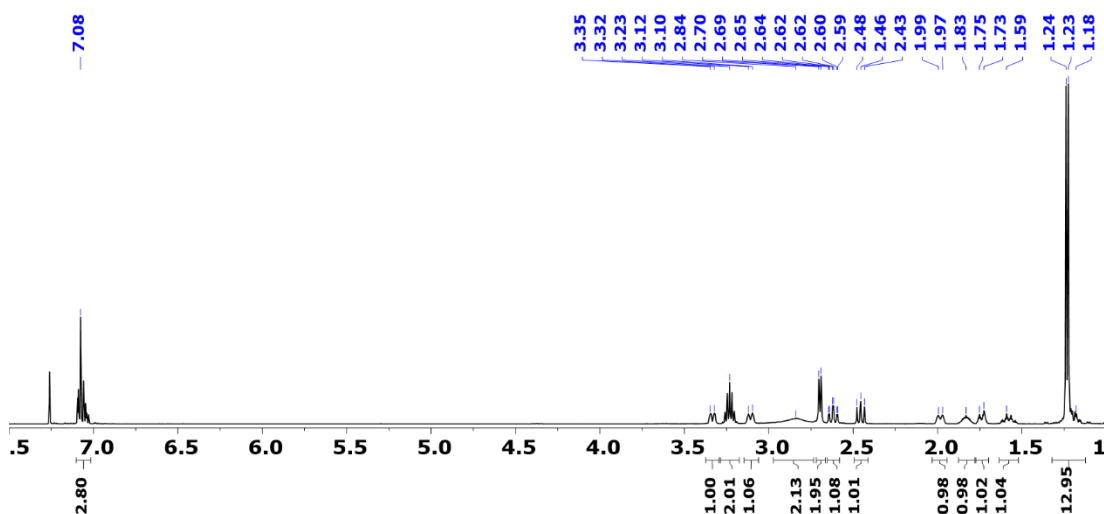
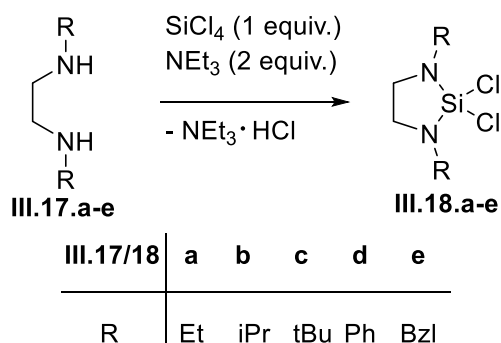


Figure 7: ^1H NMR spectrum (500 MHz, CDCl_3) of the isolated ligand **3.4**.

Synthesis of the dichlorosilane **3.5**

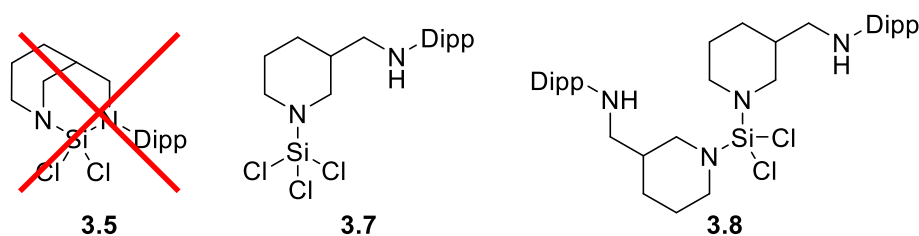
Triethylamine (NEt_3) and silicon tetrachloride (SiCl_4)

The synthesis of a series of N-heterocyclic dichlorosilanes **III.18.a-e** has been reported by treating the diamines **III.17.a-e** with SiCl_4 in the presence of a base, NEt_3 (Scheme 13).^[17] Reaction between the amine and the SiCl_4 , which forms HCl as a by-product, is under an equilibrium. The NEt_3 traps HCl and precipitates out as HNEt_3Cl , which favours the formation of the dichlorosilanes **III.18.a-e**.



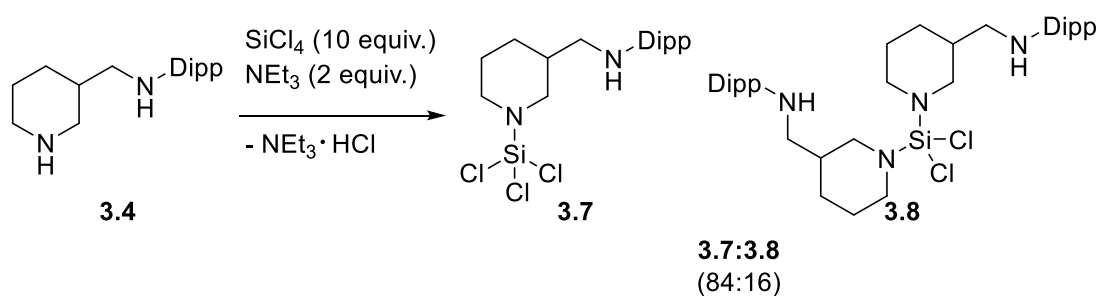
Scheme 13: Synthesis of N-heterocyclic dichlorosilanes **III.18.a-e** under basic condition.

This reported procedure was applied to the ligand **3.4**. ^1H NMR spectrum revealed the formation of two products. The ^{29}Si NMR spectrum showed a signal at $\delta -28.9$ for the main product and at $\delta -33.0$ for the minor one. An ^1H - ^{29}Si HMBC experiment showed that each silicon signal is coupling to four hydrogen atoms. The major ($\delta -28.9$) and minor ($\delta -33.0$) products were assigned as **3.7** and **3.8** respectively, by comparison with the ^{29}Si NMR signals of $\text{Cl}_3\text{SiN}^i\text{Pr}_2$ ($\delta -30.7$) and $\text{Cl}_2\text{Si}(\text{N}^i\text{Pr}_2)_2$ ($\delta -35.4$) (Scheme 14).^[18] Mass spectrometry confirmed the presence of **3.7** ($m/z = 406.1$) and **3.8** ($m/z = 644.4$), the desired product **3.5** was not observed. The ring strain which must be overcome for the ring closing seemed to be too high and a second substitution with a second ligand **3.8** seemed to be favoured. Product **3.7** and **3.8** could not be isolated from each other, they had similar solubilities and attempts to crystallise either were unsuccessful.



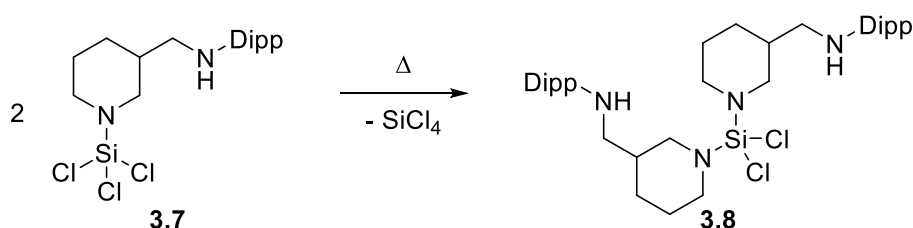
Scheme 14: Observed products from addition of NEt_3 and SiCl_4 to the ligand **3.4**.

The selective formation of **3.7** was of interest, as heating it could result in HCl elimination and ring closing, forming the desired dichlorosilane **3.5**. The procedure was modified and **3.4** was treated with a large excess of SiCl_4 (Scheme 15). The reaction resulted in the formation of a cleaner mixture **3.7**:**3.8** (84:16), but **3.7** could not be selectively formed.



Scheme 15: Attempt to selectively synthesise the silane **3.7**.

The crude product **3.7** was heated under vacuum. The white solid turned into an oil. However, heating **3.7** resulted in the formation of **3.8**, which was confirmed by ^1H and ^{29}Si NMR spectroscopy with the ^{29}Si signal at $\delta -33.0$ (Scheme 16). The ring closing step could not be achieved using this method.



Scheme 16: Heating **3.7** and formation of **3.8** by SiCl_4 elimination.

Lithiation of **3.4** and SiCl_4 addition

Study of lithiation of **3.4**

Another way to synthesise the dichlorosilane **3.5** would be the lithiation of ligand **3.4** followed by SiCl_4 addition. The lithiation of the ligand was studied beforehand. The diamine **3.4** was treated with two equivalents of $^n\text{BuLi}$ in diethyl ether at -78°C before letting the solution warm up to room temperature. The ^7Li NMR spectrum showed three new signals, each different from that of $^n\text{BuLi}$ ($\delta 1.23$ in THF- d_8) (Figure 8).

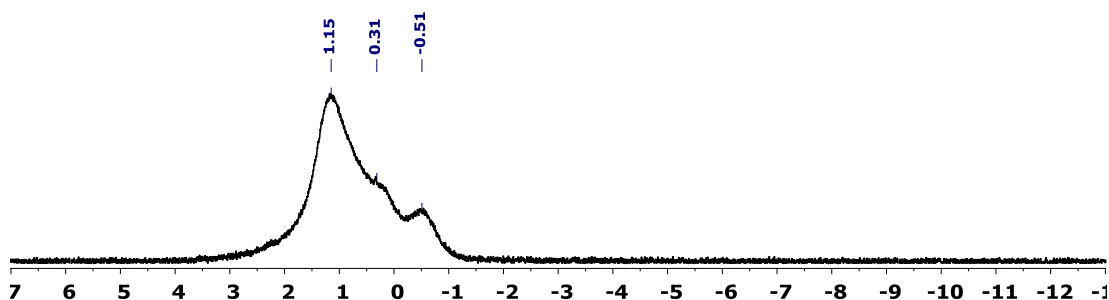
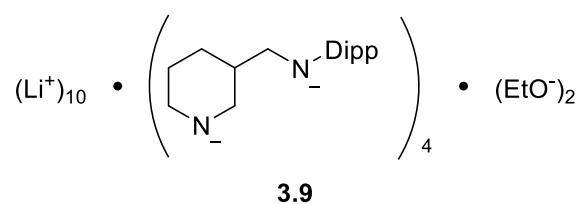


Figure 8: ${}^7\text{Li}$ NMR spectrum (500 MHz, THF- d_8) of reaction of **3.4** with $n\text{BuLi}$ (2 equiv.).

The multiple signals can be due to the tendency of organolithium compounds to form aggregates in solution. It could also be due to the partial lithiation of **3.4**. The pKa values of a typical amine is about 35. The two nitrogen atoms from **3.4** are neither conjugated nor close to each other, therefore the two pKa values can be considered as independent and their values are unlikely to be influenced by each other. $n\text{BuLi}$ is a strong base with pKa of 51.

To ensure that the double lithiation is occurring, **3.4** was treated with an excess of $n\text{BuLi}$ in Et_2O . The solid-state structure obtained by X-ray analysis revealed the complex **3.9** with doubly lithiated **3.4** and lithium ethoxide (Scheme 17 and Figure 9-10). The lithiated ligand crystallized as clusters composed of four ligands, two ethoxides and ten lithium atoms. Li1, Li2, Li3 and Li4 are tricoordinate with two nitrogen atoms and one oxygen atom from the ethoxide, Li5 is dicoordinate by two nitrogen atoms. This supports that the double lithiation of **3.4** is achieved and the excess of $n\text{BuLi}$ then reacts with the solvent.



Scheme 17: Formal representation of the complex **3.9**: $(\text{Li}^+)_{10} \cdot (\mathbf{3.4}^{2-})_4 \cdot (\text{EtO}^-)_2$.

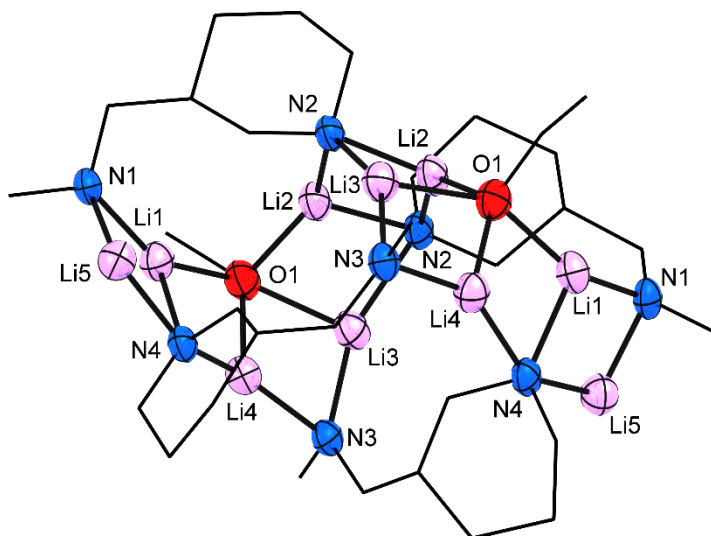


Figure 9: Molecular structure of **3.9** in the solid state. Ellipsoids are drawn at 50% probability; hydrogen atoms and diisopropylphenyl groups have been omitted for clarity.

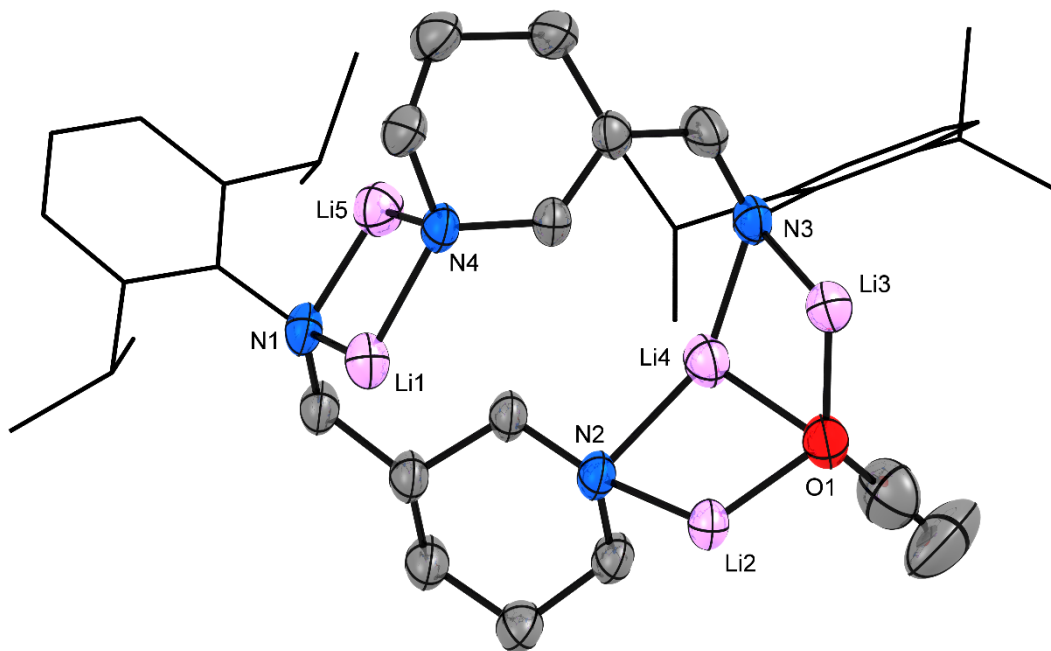
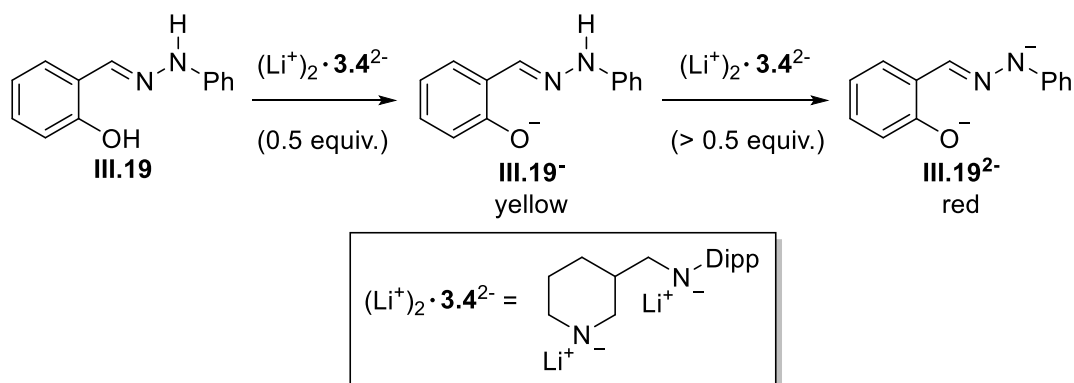


Figure 10: Molecular structure of **3.9** in the solid state. Ellipsoids are drawn at 50% probability; hydrogen atoms, two ligands, five lithium atoms and one ethoxide have been omitted for clarity.

Titration of the lithiated ligand 3.4

To confirm that the dilithiation is occurring with just two equivalents of ${}^n\text{BuLi}$, titration of the product was carried out. The ligand **3.4** was treated with two equivalents of ${}^n\text{BuLi}$ at $-78\text{ }^\circ\text{C}$. The reaction mixture was allowed to warm up to room temperature overnight, to give a yellow solution. The volatiles were removed under vacuum and the product extracted with hexane, before being dried.

The obtained solid was titrated with salicylaldehyde phenylhydrazone **III.19**, a titrating agent which has been used for titration of organometallic reagents such as Grignard and organolithium reagents.^[19] The addition of a base to **III.19** firstly forms the monoanion **III.19⁻** which has a yellow colour, the addition of more than an equivalent of a base forms the dianion **III.19²⁻**, which has a red colour. If **3.4** is dilithiated, half an equivalent should start forming the dianion **III.19²⁻**, and colour should change from yellow to orange (*Scheme 18*).

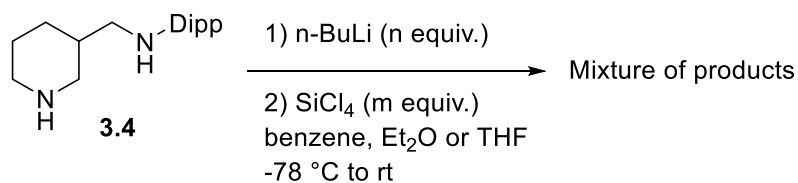


Scheme 18: Titration reaction of the lithiated **3.4** with **III.19**.

The addition of 0.8 equivalent of the lithiated **3.4** was necessary to see the colour change from yellow to orange. This shows that the lithiated product was a mixture of monolithiated and dilithiated ligand. An excess of ${}^n\text{BuLi}$ is necessary to carry out the double lithiation of **3.4**, however, it could also lead to lithium ethoxide formation. The addition of SiCl_4 to this mixture may undergo side reactions with the ethoxide.

Lithiation of 3.4, SiCl₄ addition: synthesis attempt of 3.5

The ligand **3.4** was treated with ⁿBuLi in order to synthesise the dilithiated intermediate **3.4**⁻², which was then treated with SiCl₄ (Scheme 19). Several conditions were screened to synthesise **3.5**. Changing the solvent (benzene, Et₂O or THF), the temperature or the time of lithiation, the number of equivalents of ⁿBuLi or SiCl₄ did not lead to the clean formation of **3.5** (Table 3). ¹H NMR spectrum of the attempts showed a mixture of **3.7**, **3.8** and other unidentified products. The ²⁹Si NMR spectrum showed the signal from **3.7** and **3.8** at δ -28.9 and -33.0 along with signals at very close chemical shift at δ -28.0, -28.4, -28.5 and -33.4. ¹H-²⁹Si HMBC experiment shows coupling between the silicon signals in the region at δ -28 and the aliphatic protons of the CH₃ from the Dipp fragment. This implies some activation of the Dipp ⁱPr CH groups. No further investigation was carried on the undesired products formed.



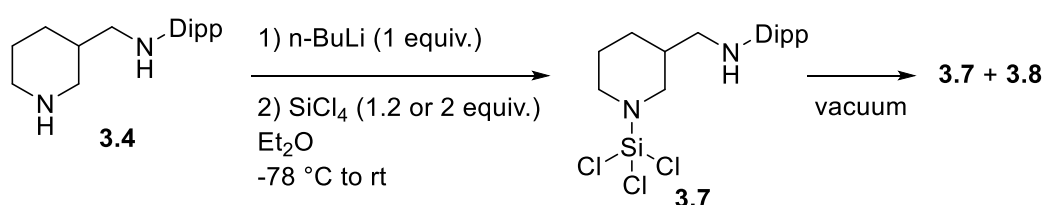
Scheme 19: Attempt of synthesis of **3.5** using ⁿBuLi.

Entry	Solvent	Equivalents of ⁿ BuLi	Temperature of lithiation (°C)	Time of lithiation (h)	Equivalents of SiCl ₄	Temperature of addition of SiCl ₄ (°C)
1	benzene	2	25	0.5	1	25
2	benzene	2	25	0.5	5	25
3 ^[a]	benzene	2	25	2.5	1.2	25
4 ^[a]	benzene	2	25	2	2	25
5	benzene	2.2	25	2	2.2	25
6	THF	2	-78	3	1	-78
7	Et ₂ O	2	25	0.5	1.2	-78

Table 3: Screened conditions of the attempts of synthesis of **3.7**. [a] Volatiles were removed after lithiation, the remaining solid was dissolved in benzene before SiCl₄ was added.

Stepwise lithiation: synthesis of **3.7**

As the double lithiation followed by addition of SiCl₄ did not afford a clean product, stepwise lithiation could be a possible route to **3.5**. The ligand **3.4** was treated with one equivalent of ⁿBuLi, followed by the addition of an excess of SiCl₄. This formed the product **3.7** almost cleanly (*Scheme 20*), as shown by ¹H and ²⁹Si NMR spectroscopy. However, attempts to purify the product always ended with contamination of **3.8**. Drying the product led to SiCl₄ elimination and substitution of a second ligand, forming **3.8**.



Scheme 20: Synthesis of **3.7** using ⁿBuLi procedure.

Conclusion and perspectives

A procedure for the gram-scale synthesis of a diamine ligand **3.4** has been successfully designed and carried out, however, the formation of the dichlorosilane **3.5** was not achieved. The procedure using the soft base NEt_3 gave the single substituted **3.7** or the double substituted **3.8**. Heating or lithiation of **3.7** did not lead to ring closing, but to the formation of **3.8**. The lithiation of the ligand is harder than expected. The use of strong bases in stoichiometric amount did not cleanly afford the dilithiated ligand. Treatment of lithiated products with SiCl_4 led to a mixture of **3.7**, **3.8** and silicon substitution on the Dipp group from the ligand. It is proposed that the ring strain seems to be too high to see any ring closing and formation of the dichlorosilane **3.5**.

Redesigning the ligand structure will be necessary to lower the structural constraint (*Figure 9*). Making the ligand with a slightly longer carbon chain could allow the ring-closed product using the same method. Another way to decrease the geometrical constraint would be to switch the position of the side chain on the piperidine to the *para* position.

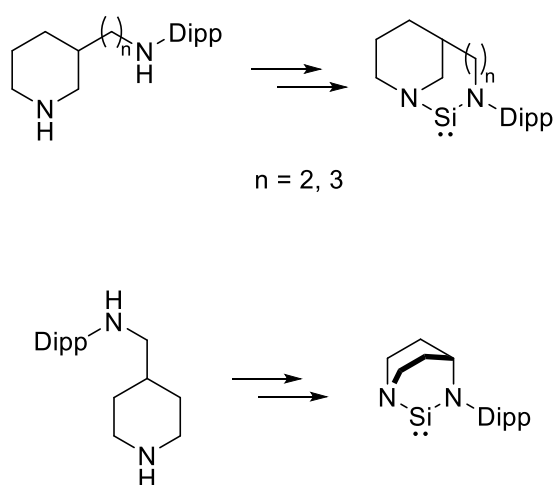


Figure 11: Suggested structures for new ligand and redesign of the targeted *N*-heterocyclic silylene with a bridged nitrogen atom.

The ligand **3.4** could be used on elements larger than silicon, such as a transition metal, which could fit in the pocket with a less strained geometry. The geometry on the nitrogen will still prevent its π -donating character and might give interesting properties, with a very labile nitrogen.

References

- [1] D. Martin, N. Lassauque, B. Donnadiou, G. Bertrand, *Angew. Chem. Int. Ed.* **2012**, *51*, 6172–6175.
- [2] L. Buchanan, *Chem. Soc. Rev.* **1974**, *3*, 41–63.
- [3] N. C. O. Nhc, D. G. Gusev, *Organometallics* **2009**, *28*, 6458–6461.
- [4] R. Dorta, E. D. Stevens, N. M. Scott, C. Costabile, L. Cavallo, C. D. Hoff, S. P. Nolan, *J. Am. Chem. Soc.* **2005**, *127*, 2485–2495.
- [5] R. Kelly, H. Clavier, S. Giudice, N. M. Scott, E. D. Stevens, J. Bordner, I. Samardjiev, C. D. Hoff, L. Cavallo, S. P. Nolan, *Organometallics* **2008**, *27*, 202–210.
- [6] U. S. D. Paul, U. Radius, *Organometallics* **2017**, *36*, 1398–1407.
- [7] O. Back, M. Henry-Ellinger, C. D. Martin, D. Martin, G. Bertrand, *Angew. Chem. Int. Ed.* **2013**, *52*, 2939–2943.
- [8] K. C. Mondal, S. Roy, B. Dittrich, D. M. Andrada, G. Frenking, H. W. Roesky, *Angew. Chem. Int. Ed.* **2016**, *55*, 3158–3161.
- [9] T. Kosai, S. Ishida, T. Iwamoto, *Angew. Chem. Int. Ed.* **2016**, *55*, 15554–15558.
- [10] M. Kira, S. Ishida, T. Iwamoto, C. Kabuto, *J. Am. Chem. Soc.* **1999**, *121*, 9722–9723.
- [11] M. Haaf, T. A. Schmedake, B. J. Paradise, R. West, *Can. J. Chem. Can. Chim.* **2000**, *78*, 1526–1533.
- [12] M. Hesse, U. Kligebl, *Angew. Chem. Int. Ed.* **1986**, *25*, 649–650.
- [13] H. Cui, C. Cui, *Dalt. Trans.* **2015**, *44*, 20326–20329.
- [14] D. G. Batt, *US2004067935A1*, **2004**.
- [15] A. F. Abdel-magid, K. G. Carson, B. D. Harris, C. A. Maryanoff, R. D. Shah, *J. Org. Chem.* **1996**, *61*, 3849–3862.
- [16] C. Bonds, *J. Phys. Chem* **1959**, *63*, 1346.
- [17] A. Sladek, *Z. Naturforsch.* **1994**, *49 b*, 1247–1255.
- [18] K. Sakamoto, S. Tsutsui, H. Sakurai, M. Kira, *Bull. Chem. Soc. Jpn.* **1997**, *70*, 253–260.
- [19] B. E. Love, E. G. Jones, N. Carolina, *J. Org. Chem.* **1999**, *64*, 3755–3756.

Chapter IV

Introduction to mixed group III-V compounds

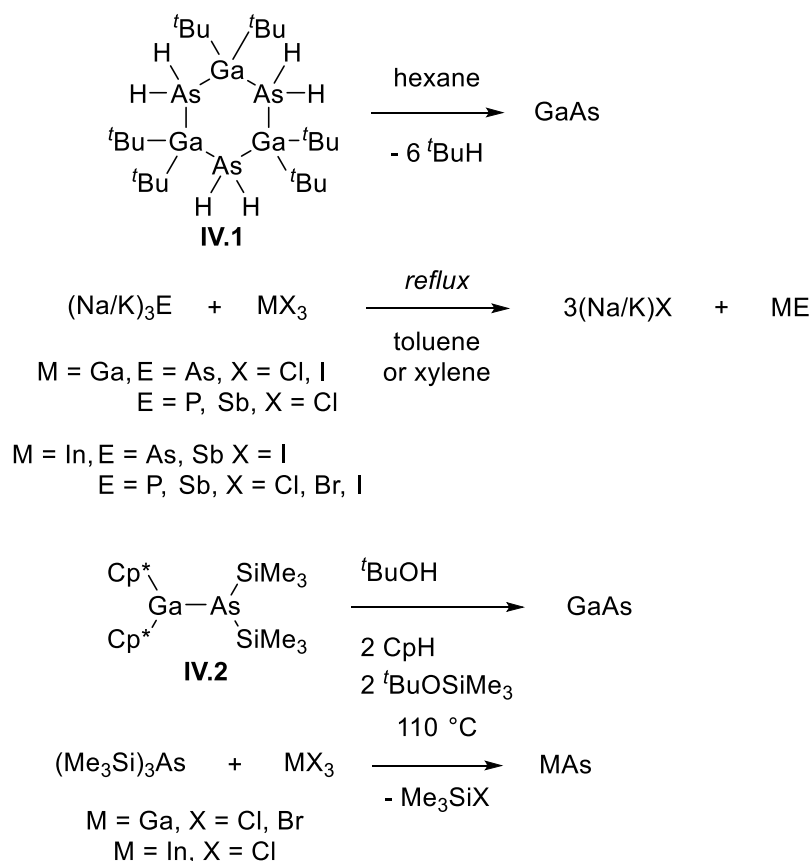
Chapter IV – Introduction to mixed group III-V compounds

Route to group III-V (13-15) semiconductors

Mixed group III-V compounds of heavier elements

The group III-V (13-15) semi-conductors are widely used in electronic devices such as photovoltaic solar cells. Gallium-arsenide (GaAs) is one of the most used semi-conductors (alongside silicon) in industry. The three common methods for the synthesis of semi-conductors are chemical vapor deposition (CVD), metal-organic chemical vapor deposition (MOCVD) and molecular beam epitaxy (MBE). These methods provide high purity material but involve high temperatures (eg. CVD of GaAs at 600-700 °C)^[1] and the use of toxic gas (AsH₃, PH₃ etc.).

Solution phase synthesis could be an alternative method to prepare semi-conductors and some group III-V semi-conductors have already been achieved using this route. A. Cowley and co-workers synthesized the gallium-arsenide six-membered ring **IV.1**, which successfully gives amorphous GaAs in solution (*Scheme 1*).^[2] Wells and Kher reported a series of group 13-15 nanoparticles (4-36 nm) by reacting sodium-potassium group 15 species ((Na/K)₃E, E = P, As, Sb) with trihalo-group 13 species (MX₃, M = Ga, In; X = Cl, Br, I) in refluxing toluene (*Scheme 1*).^[3] The gallium-arsenic precursor **IV.2** was also reported to afford GaAs by treatment with *tert*-butanol (*Scheme 1*).^[4] Simple Me₃SiX (X = Cl, Br) elimination from the reaction between (Me₃Si)₃As and GaX₃ (X = Cl, Br) or InCl₃ respectively gave GaAs and InAs (*Scheme 1*).^[5]



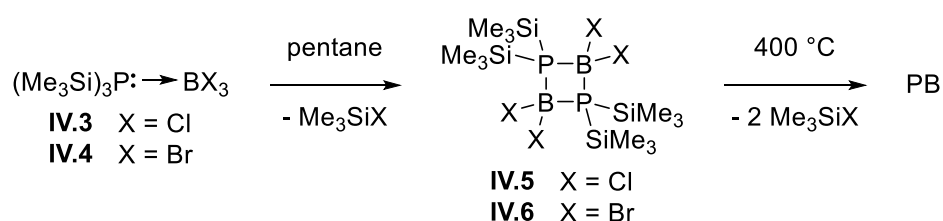
Scheme 1: Solution phase synthesis of the different group 13-15 semi-conductors.

Mixed group III-V compounds of lighter elements

Boron-nitride (BN) is the lightest analogue of the mixed group III-V compounds. BN is widely used in industry for lubricants or in ceramics for its high thermal resistance. More recently, boron-nitride nanomaterials have also been used in the field of nanoelectronics^[6] and optoelectronics.^[7] Boron-nitride is synthesized by the reaction between boron trioxide and boric acid with ammonia at high temperature, or by thermal decomposition of amine-borane adducts.^[8]

The semi-conductor properties of boron-nitride's heavier analogue, boron-phosphide (PB), have also been investigated for a long time.^[9] Boron-phosphide is an indirect band gap semi-conductor with a wide band gap of 2.1 eV,^[10] a high chemical inertness, a hardness similar to SiC^[11] and efficient heat conductor properties (400

$\text{W}\cdot\text{m}^{-1}\cdot\text{K}^{-1}$).^[12] Recent theoretical studies showed that monolayer boron-phosphide would be highly thermally stable (up to 1500 K) with a direct band gap of 1.833 eV, exhibit interesting optical absorptions in the visible light and near-infrared regions, and have redox potentials matching with the reduction and oxidation levels in water splitting.^[13] In spite of these promising properties, PB is not a commonly used material due to its challenging synthesis. The synthesis of boron-phosphide requires harsh synthetic conditions, involving high temperature thermal decomposition or reaction of boron and phosphorous precursors.^[14] In 2003, Qian *et al.* reported the synthesis of nanocrystalline boron-phosphide from the reaction between PCl_3 and NaBH_4 at 600 °C in an autoclave.^[15] Wells reported in 1996 spontaneous elimination of Me_3SiX in solution from phosphine-borane adducts **IV.3** and **IV.4** (Scheme 2),^[16] however, only the dimers **IV.5** and **IV.6** are formed and no further elimination occurs at room temperature. Thermolysis of the compounds **IV.3-6** were reported to give amorphous PB. Mild solution phase synthesis of boron-nitride and boron-phosphide has not been achieved to date.



Scheme 2: Synthesis of amorphous boron-phosphide by thermolysis.

Small-sized boron-phosphide molecules have been theoretically studied, with the analysis of the electronic structure and stability of B_nP_n clusters ($n = 2-4$).^[17] The most stable structures were determined for the dimer, trimer and tetramer (Figure 1). The dimer and trimer have the large singlet-triplet energy differences (2.52 and 2.17 eV

respectively), which attest to a relative stability of the clusters to reaction. The atomisation energy increases with the size of the clusters, which indicates that the formation of bigger clusters is a favourable process. The fragmentation study of these clusters showed surprising results, as only the trimer B_3P_3 is predicted to give the PB monomer through its fragmentation pathway. B_4P_4 is predicted to split into two dimers B_2P_2 , which then split into B_2 and $2P$.

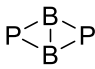
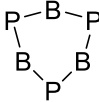
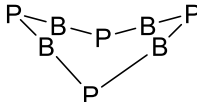
			
formula	B_2P_2	B_3P_3	B_4P_4
ground state	$^3B_{2g}$	1A_1	1A_1
symmetry	D_{2h}	D_{3h}	D_{2d}
atomisation energy (eV)	15.76	26.02	36.29

Figure 1: Predicted most stable structure of the different B_nP_n clusters ($n = 2-4$).

Decreasing the size of particles has shown that it can provide new properties and reactivities. Going from bulk material to nanoparticles, for example, can give new optical properties. By using Lewis-bases to limit the growing of particles, researchers even managed to isolate neutral base-stabilised low-coordinate main-group compounds, and again decreasing in size, new properties were discovered.

Base-stabilised low-coordinate main-group (E=E) compounds

Multiply-bonded species are not common below the second row (See Chap. I). The development of such compounds began with the synthesis of the disilene **I.2** (See Chap. I, Disilenes)^[18] and the diphosphene **IV.7** in 1981 (Figure 2).^[19] The emergence

of new ligands such as NHCs subsequently allowed the isolation of multiply-bonded low-coordinate main-group compounds, including base-stabilised homoatomic species featuring main-group elements in the formal oxidation state of zero.

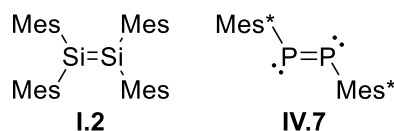
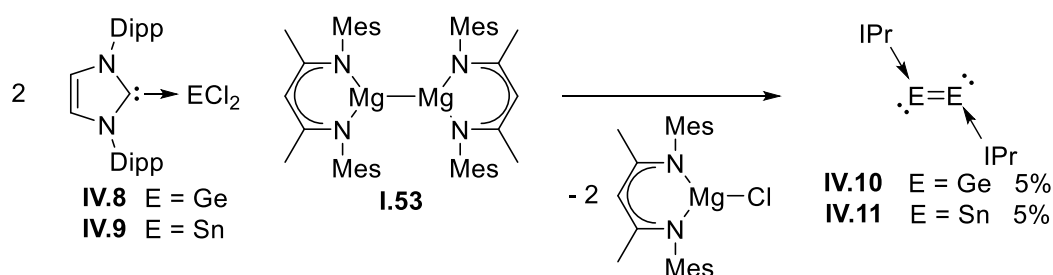


Figure 2: The first isolated multiply-bonded main-group compounds. Mes = 2,4,6-trimethylphenyl. Mes* = 2,4,6-tri-tert-butylphenyl.

Carbene-stabilised diatomic allotropes of main-group elements have been well explored for the past decade. These types of compounds have been isolated for several group 14 elements: silicon, germanium and tin. The disilicon(0) **I.75**, the digermanium(0) **IV.10** and the ditin(0) **IV.11** have been reported using the 1,3-bis(2,6-diisopropylphenyl)imidazol-2-ylidene (IPr).^[20–22] Compounds **IV.10** and **IV.11** have been achieved by reduction of their respective NHC adduct precursors **IV.8** and **IV.9** using the Jones Magnesium(I) reducing agent (*Scheme 3, See Chap. 1, Base-stabilised disilicon(0)*). The three (IPr)E=E(IPr) (E = Si, Ge, Sn) compounds have very similar structures, a *trans*-bent geometry with an E-E-C angle around 90° in each case (**I.75** 93.37(5)°, **IV.10** 89.87(8)° and **IV.11** 91.82(8)°), supporting the oxidation state of the centre atoms of zero, with one lone pair of electron located on each E atom. The E=E (E = Si, Ge, Sn) bond distances of each compounds are found in the range of their R₂E=ER₂ analogues, confirming the presence of a double bond.^[20–22] The carbene carbon signal gets more deshielded down the group ((IPr)E=E(IPr), ¹³C NMR: E = Si δ 196.3, E = Ge δ 203.3, E = Sn δ 210.3). This indicates that the C–E interaction becomes weaker when the molecular weight of E increases (free IPr ¹³C NMR: δ

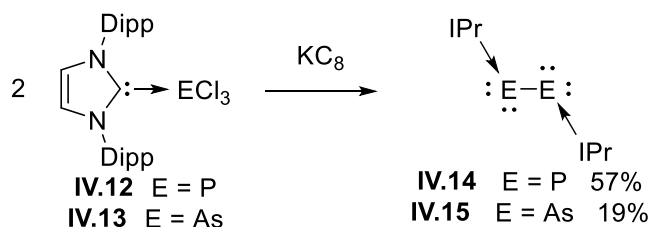
220.5).^[23] Related species with coordinated group 14 atom(s) in the formal oxidation state of zero have been isolated, like the carbodicarbene **I.87**, silylones **I.89** and **I.90** and the trisilicon(0) **I.104**, which are described in Chapter I (See *Chap. I, Base-Silicon(0) adducts*).



Scheme 3: Synthesis of the IPr-stabilised diatomic(0) group 14 compounds. Dipp = 2,6-diisopropylphenyl. Mes = 2,4,6-trimethylphenyl.

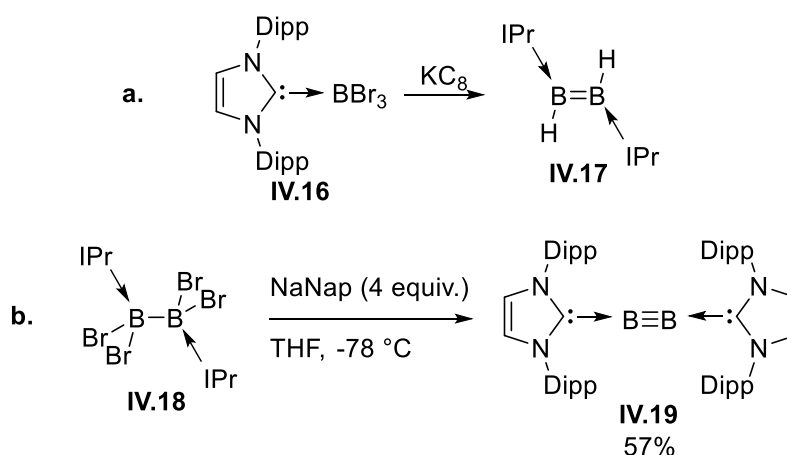
Group 15 diatomic(0) compounds have also been prepared. Robinson *et al.* reported the IPr-stabilised diphosphorus(0) **IV.14** and diarsenic(0) **IV.15** by reduction of their respective adduct precursors (IPr)ECl₃ **IV.12** and **IV.13** (E = P or As) with potassium graphite (KC₈) (*Scheme 4*).^[24,25] In these cases, the products also show a *trans*-bent structure, with a slightly larger C-E-E angle compared to that from group 14 analogues (**IV.14** 109.19(6)°, **IV.15** 101.11(5)°). However, the group 15 compounds **IV.14** and **IV.15** feature an E–E (E = P or As) single bond. The C_{Carbene}–E bond distance is intermediate between a C–E single and double bond lengths, indicating strong π-back donation from E (E = P or As) to the carbene ligand atoms. DFT calculations confirmed the E–E single bond, by showing one lone pair orbital (mainly p-character) with a π back-donation to the empty p orbital of the C_{Carbene} and a lone pair orbital (mainly s-character) located on each E atoms. Similar (L)E=E(L) compounds have been reported for silicon and phosphorus, where the ligands L are cyclic

alkylaminocarbenes (cAACs). No significant differences were observed between those compounds and the one featuring NHC as ligands.^[26,27]



Scheme 4: Synthesis of the IPr-stabilised diatomic(0) group 15 compounds.

In 2012, Braunschweig and co-workers isolated the first room temperature stable compound with a boron-boron triple bond.^[28] The diboryne **IV.19** was prepared by reduction of the NHC coordinated tetrabromodiborane **IV.18** using sodium naphthalenide (NaNap) at $-78\text{ }^\circ\text{C}$ (Scheme 5.b). Previous attempts carried out by Robinson *et al.* to reduce the adduct **IV.16** did not afford the diboryne **IV.19**, but the diborene **IV.17** instead (Scheme 5.a).^[29] Unlike the diatomic(0) group 14/15 analogues, the group 13 compound **IV.19** has a linear structure, with a $\text{B}\equiv\text{B}$ triple bond ($1.449(3)\text{ \AA}$) about 6% shorter than $\text{B}=\text{B}$ double bond.^[28] Computational study shows the HOMO and the HOMO-1 correspond to the $\text{B}\equiv\text{B}$ -centered π orbitals.



Scheme 5: a. Attempted synthesis of diboryne(0). b. Synthesis of the IPr-stabilised diboryne(0) **IV.17**.

Despite numerous reported examples of diatomic allotropes of groups 13, 14 and 15, mixed diatomic compounds have never been isolated. For instance, although isolated as bulk material (See Chap. IV., *Mixed group III-V compounds of lighter elements*), boron-nitride (NB) and boron-phosphide (PB) have not been isolated as a molecular unit. However, the chemistry of mixed group III-V (13-15) compounds has been investigated and multiply bonded mixed species R–E–B–R (E = N or P) have already been achieved and will be discussed in the following sections.

Aminoboranes and Phosphinoboranes

Phosphinoboranes and aminoboranes are isoelectronic to alkenes. Like alkenes, aminoboranes have a planar structure (Figure 3.b). However, unlike alkenes the B–N bond is polar (Figure 3.a). This polarisation gives to the pair of electrons involved in the B–N π bond some lone pair character, making aminoboranes undergo head-to-tail oligomerization. Steric protection was thus used to stabilise monomeric aminoboranes. Phosphinoboranes also undergo this head-to-tail reaction. The first characterised phosphinoboranes **IV.21** and **IV.22** revealed non-planar structures with

pyramidal configuration of the phosphorus atoms (*Figure 3.b*).^[30,31] Increasing the steric bulk favours a planar structure as well as a significant B–P bond shortening, evidencing some π overlap, as was observed in the phosphinoborane **IV.23**.^[32]

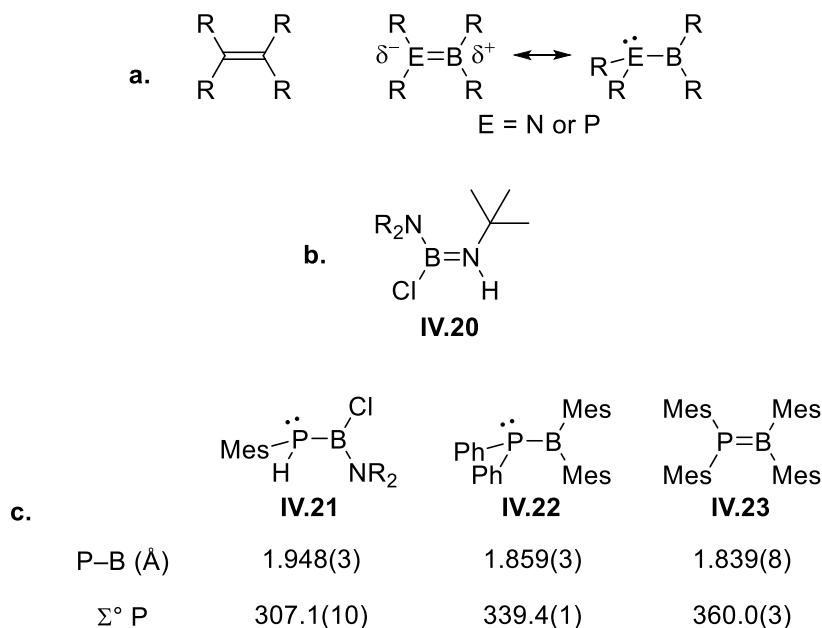


Figure 3: **a.** Comparison of alkenes, aminoboranes and phosphinoboranes. **b.** Example of aminoborane.^[33] **c.** The first reported phosphinoboranes. $\text{NR}_2 = 2,2,6,6$ -tetramethylpiperidine.

Several phosphinoboranes have been reported, with a large variety of substituents, typically using sterically bulky substituents for kinetic and thermodynamic stabilisation.^[34] The use of Lewis bases allows minimally substituted phosphinoboranes to be prepared, this will be discussed in Chapter V (*See Chap. V, Minimally substituted phosphinoboranes*).

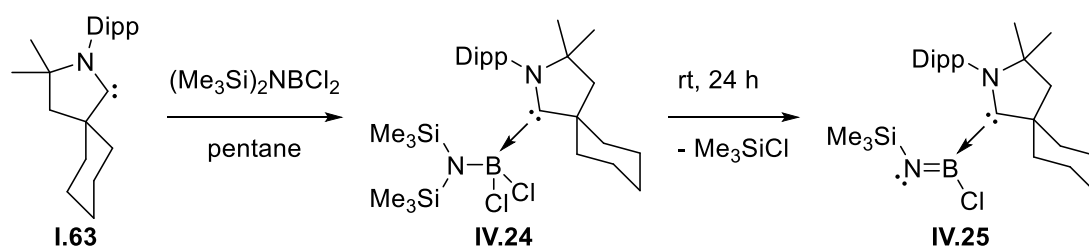
Iminoboranes

Iminoboranes (R–NB–R') are species isoelectronic to alkynes. They also have a linear structure (Figure 4). However, for the same reasons observed in aminoborane, the polarity of the N–B bond, which makes it weaker, induces differences in reactivity compared to alkynes. Iminoboranes are less stable and can undergo oligomerisation, they are also more reactive to addition across the multiple bond than alkynes. Similarly to iminoboranes, steric bulk is used to reach thermodynamically stable iminoboranes. Starting from 1979 with the work from Paetzold *et al.*,^[35] the synthesis and the reactivity of iminoboranes have been widely explored.^[36,37]



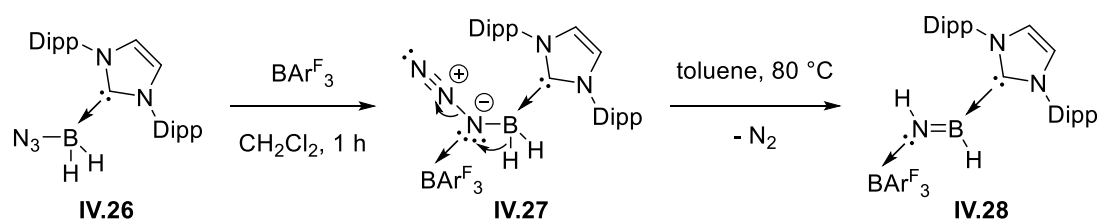
Figure 4: Comparison between alkynes and iminoboranes.

The use of Lewis bases such as NHCs or cAACs allowed the synthesis of iminoboranes with smaller substituents. Bertrand and co-workers reported that coordination of the cAAC **I.63** to the aminoborane (Me₃Si)₂NBCl₂ successfully formed the base-coordinate aminoborane **IV.24**, which undergo spontaneous Me₃SiCl elimination in solution to give the minimally substituted iminoborane **IV.25** (Scheme 6).^[38] Due to the coordination of the cAAC to the boron centre, the iminoborane **IV.25** does not have a linear structure. The B–N bond length in **IV.25** (1.300(3) Å) is slightly longer than the B–N bond distances observed for base-free iminoboranes (1.22–1.25 Å),^[36] due to the coordination of the cAAC ligand, which weakens the B–N bond by filling the empty p orbital of the boron atom.



Scheme 6: Synthesis of the minimally substituted iminoboranes **IV.25** by Me_3SiCl elimination.

In 2017, Rivard *et al.* reported the Lewis acid-base stabilised adduct of the parent iminoborane HBNH. Treatment of the NHC-borane adduct **IV.26** with the Lewis acid fluoroarylborane BAr^{F}_3 ($\text{Ar}^{\text{F}} = 3,5\text{-C}_6\text{H}_3(\text{CF}_3)_2$) gives the adduct **IV.27**, with coordinated BAr^{F}_3 to the azide moiety (Scheme 7). Heating **IV.27** promotes N_2 elimination along with a 1-2 hydride migration from the boron to the nitrogen atom, giving the parent iminoborane adduct **IV.28**. In this case as well, no linear structure is observed. The HBNH core of adduct **IV.28** has a *trans* geometry, due to the bulky Lewis acid and base ligands which are orienting the structure to minimise their intramolecular repulsion. The B–N bond distance of **IV.28** (1.364(2) Å) is slightly longer than the one observed for the base adduct **IV.25** (1.300(3) Å) due to the presence of the two ligands weakening the B–N bond. The presence of a hydridic (B–H) and an acidic (N–H) hydrogens suggest that dehydrogenation of **IV.28** could be favourable to give a diatomic allotrope of boron nitride through solution-phase route. Unfortunately, attempts to form boron nitride from **IV.28** were unsuccessful.



Scheme 7: Synthesis of the Lewis acid-base complex parent iminoborane **IV.28**.

Phosphaborenes

Phosphaborenes are compounds with P=B double bonds and are analogues of the mixed group 13-15 iminoboranes. Phosphaborenes are highly reactive and unstable to oligomerisation due to the polarisation of the P=B bond. Less stable than the phosphinoboranes, phosphaborenes remained elusive for a long time.

Although isoelectronic to alkynes and iminoboranes, calculations did not predict the parent phosphaborene HBPH to have a linear structure as in the case of alkynes or iminoboranes^[39] but a *cis*-planar structure, with an almost linear HBP fragment and a very narrow BPH angle of 94.5°, due to a hydrogen bridging the boron and the phosphorus atoms (*Figure 5*).^[40] The dimerization energy was calculated to be $-54 \text{ kcal mol}^{-1}$, which is in accordance with the tendency of phosphaborenes to dimerize to their diphosphaboretane (RPBR')₂ in the early attempts to isolate them.^[31,41]

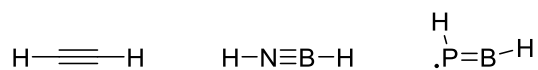
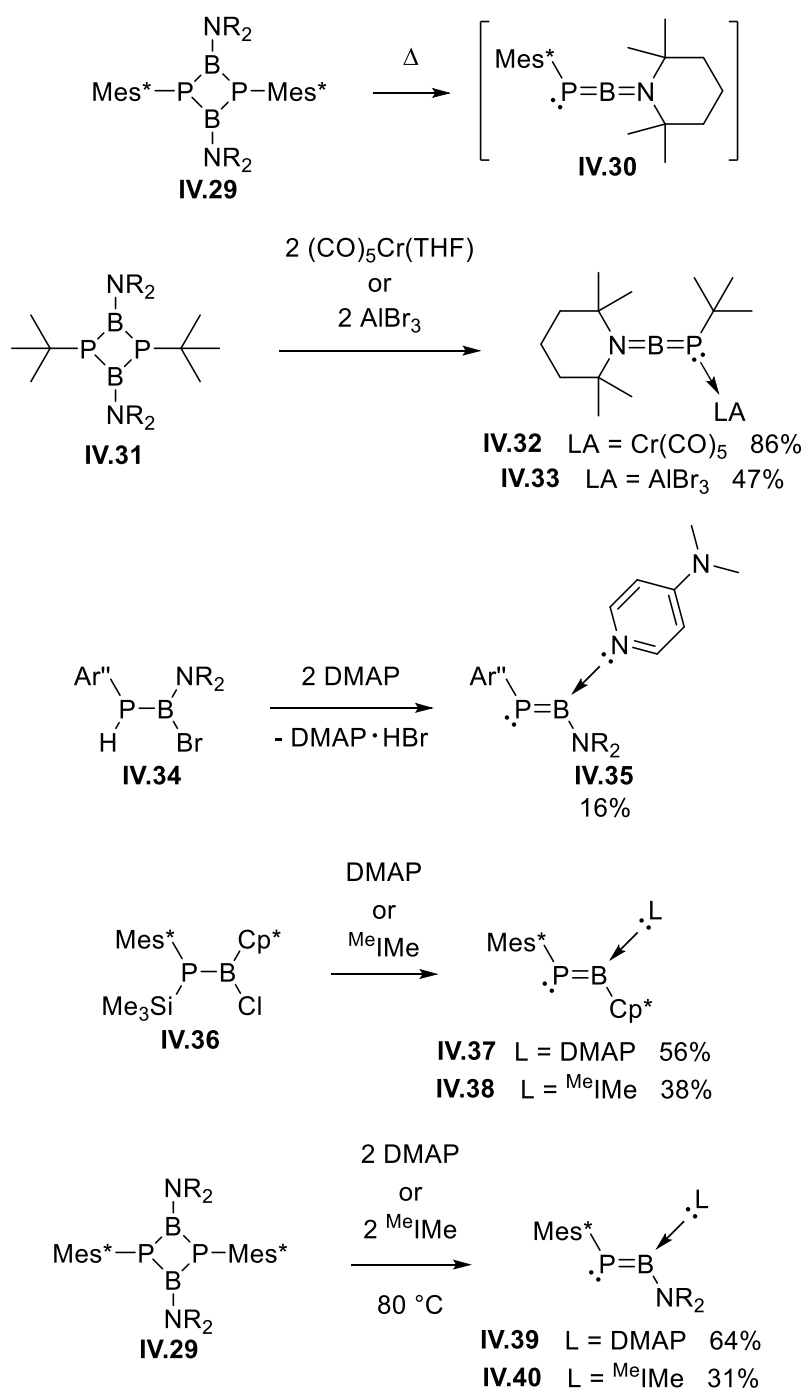


Figure 5: Comparison of the parent alkyne, iminoborane and phosphaborene.

In 1986 A. Cowley *et al.* observed by mass spectrometry the presence of monomeric phosphaborene **IV.30** by thermolysis of its dimer diphosphaboretanes **IV.29**, but they were unable to isolate them (*Scheme 8*).^[42] In 1990 and 2005, Nöth and co-workers

reported the respective Lewis acid-coordinated phosphaborenes **IV.32** and **IV.33** by ring opening of the diphosphaboretane **IV.31** using chromium pentacarbonyl $[\text{Cr}(\text{CO})_5(\text{THF})]$ or aluminium tribromide (AlBr_3) (*Scheme 8*).^[43,44] Power *et al.* reported in 2006 that treatment of the phosphinoborane **IV.34** with two equivalents of 4-dimethylaminopyridine (DMAP), eliminated HBr and successfully gave the phosphaborene **IV.35** (*Scheme 8*).^[45] Recently, our group (M. Cowley and Price) reported a series of base-stabilised phosphaborenes **IV.37-40** coordinated by DMAP and an NHC, using similar strategies employed for iminoboranes synthesis with the elimination of Me_3SiCl from phosphinoborane precursor **IV.36** or for previous phosphaborenes synthesis with the ring opening of the disphosphaboretane precursor **IV.29** (*Scheme 8*).^[46,47] Steric bulk from the substituents as well as electronic assistance from Lewis acid or base were necessary to isolate stable phosphaborenes.



Scheme 8: The phosphaborene **IV.30** observed by mass spectroscopy, and all the isolated phosphaborenes. $\text{Mes}^* = 2,4,6\text{-tri-}t\text{-butylphenyl}$. $\text{Ar}'' = \text{C}_6\text{H}_3\text{-}2,6(\text{C}_6\text{H}_2\text{-}2,4,6\text{-}i\text{Pr}_3)_2$. $\text{NR}_2 = 2,2,6,6\text{-tetramethylpiperidine}$. $\text{DMAP} = 4\text{-dimethylaminopyridine}$.

Compounds	IV.32	IV.33	IV.35	IV.37	IV.38	IV.39	IV.40
Substituent on B	NR ₂	NR ₂	NR ₂	Cp*	Cp*	NR ₂	NR ₂
Substituent on P	^t Bu	^t Bu	Ar'	Mes*	Mes*	Mes*	Mes*
Coordinated ligand	Cr(CO) ₅	AlBr ₃	DMAP	DMAP	^{Me} Ime	DMAP	^{Me} Ime
δ ³¹ P (ppm)	-45.3	-59.8	57.3	96.7	192.9	62.2	151.5
δ ¹¹ B (ppm)	62.9	68.4	41.2	52.4	48.5	42.4	44.1
P=B bond distance (Å)	1.743(5)	1.787(4)	1.8092(17)	1.795(3)	1.8067(15)	1.8211(16)	1.8309(16)
C-P-B angle (deg)	109.0(2)	110.6(2)	114.36(7)	106.12(13)	108.94(6)	108.39(7)	111.90(7)

Table 1: Comparison of the ³¹P and ¹¹B NMR chemical shift, P=B bond distance and C-P-B angle of the reported phosphaborenes.

The ¹¹B NMR signals are shifted upfield in the case of the Lewis base coordinated phosphaborenes (δ 41-53) compared to the Lewis acid coordinated phosphaborenes, which is in accordance with the shielding of the boron centre due to coordination of the Lewis base. The type of base (DMAP or the NHC ^{Me}Ime) or substituent on the boron atom do not significantly affect the ¹¹B NMR signal of the base stabilised phosphaborenes ($\Delta\delta < 5$ ppm).

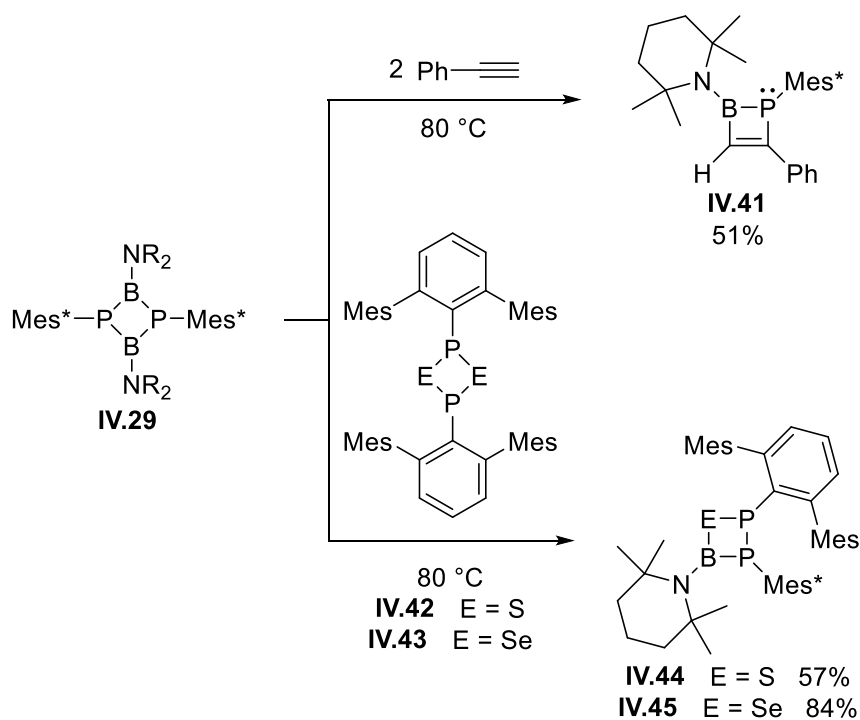
The ³¹P NMR signals from the Lewis acid coordinated phosphaborenes **IV.32** (δ -45.3) and **IV.33** (δ -59.8) are considerably upfield shifted compared to the Lewis base coordinated phosphaborenes **IV.35**, **IV.37-40** (δ 57-193). The ³¹P NMR signal is modified by its substituents and the type of base (DMAP or the NHC ^{Me}Ime) seems to strongly affect the ³¹P chemical shift, as evidenced by the difference between **IV.37** and **IV.38** ($\Delta\delta = 96.2$ ppm) and between **IV.39** and **IV.40** ($\Delta\delta = 89.3$ ppm).

The Lewis acid coordinated phosphaborenes **IV.32** and **IV.33** feature shorter P-B bond lengths than the Lewis base-coordinated phosphaborenes. This shortening is

most likely due to steric hindrance. The P=B bond of the Lewis base coordinated phosphaborenes **IV.35**, **IV.37-40** have similar length (1.79-1.84 Å), the bond distance differences between the different compounds are due to the size of the substituent and the ligand used.

All the C-P-B angles have nearly the same values (108-114°) and are narrow, but larger than the value predicted for the parent phosphaborene (94.5°) due to greater steric.

The reactivity of phosphaborenes has been recently explored. Even though no evidence of phosphaborene **IV.30** was observed in solution at temperatures up to 100 °C, heating the diphosphadiboretane **IV.29** at 80 °C in presence of phenylacetylene gave the [2+2] cycloaddition product **IV.41** (*Scheme 9*).^[47] In 2018, Paul J. Ragoona group and our group (M. Cowley, A. Price and I) reported the reaction between diphosphadichalcogenides **IV.42** or **IV.43** and the diphosphadiboretane **IV.29**, to give the four-membered ring PPBE **IV.44** and **IV.45** (E = S or Se) (*Scheme 9*).^[48]



Scheme 9: [2+2] cycloadditions reported on phosphaborene.

The chemistry of phosphaborenes has still not been fully explored. However, these compounds could be used in diverse domains. Phosphaborenes have an empty p orbital on the boron atom and a phosphorus-boron double bond with an accessible π orbital, making the phosphaborenes highly reactive and perhaps capable of small molecule activation. By observation of the reactivity between phosphaborenes and unsaturated compounds, phosphaborenes could be a way to introduce phosphorus and boron into extended π -systems. Finally, phosphaborenes can be seen as precursors to boron-phosphide. However, the substituents used in all the reported phosphaborenes are unreactive and just provide steric bulk following the approach to avoid oligomerisation. Modifying the substituents, for smaller or functionalizable moieties, would be necessary to reach a phosphaborene which could be a solution phase precursor to boron-phosphide. Base stabilised molecular boron-phosphide

could also be achieved through solution phase synthesis, giving mixed group III-V (13-15) analogues of the diatomic(0) compounds described above.

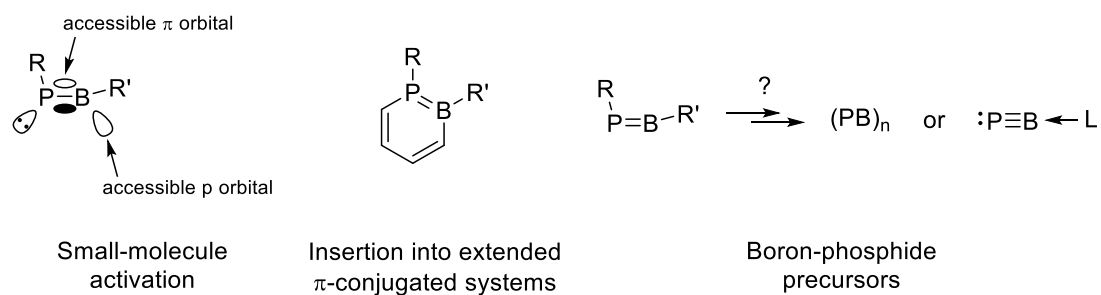


Figure 6: Interesting chemistry worth investigating on phosphaborenes.

References

- [1] A. Sammak, W. de Boer, A. van den Bogaard, L. K. Nanver, *ECS Trans.* **2010**, 28, 237–244.
- [2] A. H. Cowley, P. R. Harris, R. A. Jones, C. M. Nunn, *Organometallics* **1991**, 10, 652–656.
- [3] S. S. Kher, R. L. Wells, *Mater. Res. Soc. Symp. - Proc.* **1994**, 351, 293–298.
- [4] E. K. Byrne, L. Parkanyi, K. H. Theopold, *Science* **1988**, 241, 332–335.
- [5] R. L. Wells, C. G. Pitt, A. T. Mcphail, A. P. Purdy, S. Shafieezad, R. B. Hallock, *Chem. Mater.* **1989**, 1, 4–6.
- [6] T. Georgiou, R. Jalil, B. D. Belle, L. Britnell, R. V. Gorbachev, S. V. Morozov, Y. J. Kim, A. Gholinia, S. J. Haigh, O. Makarovsky, et al., *Nat. Nanotechnol.* **2013**, 8, 100–103.
- [7] P. Kumbhakar, A. K. Kole, C. S. Tiwary, S. Biswas, S. Vinod, J. Taha-Tijerina, U. Chatterjee, P. M. Ajayan, *Adv. Opt. Mater.* **2015**, 3, 828–835.
- [8] R. Haubner, M. Wilhelm, R. Weissenbacher, B. Lux, *Boron Nitrides — Properties, Synthesis and Applications*, **2002**.
- [9] B. Stone, D. Hill, *Phys. Rev. Lett.* **1960**, 4, 282–284.
- [10] J. Archer, R. Y. Koyama, E. E. Loebner, R. C. Lucas, *Phys. Rev. Lett.* **1964**, 12, 538–540.
- [11] T. Takenaka, M. Takigawa, K. Shohno, *Jpn. J. Appl. Phys.* **1976**, 15, 2235–2236.
- [12] Y. Kumashiro, T. Mitsuhashi, S. Okaya, F. Muta, T. Koshiro, Y. Takahashi, M. Mirabayashi, *J. Appl. Phys.* **1989**, 65, 2147–2148.
- [13] H. Shu, J. Guo, X. Niu, *J. Mater. Sci.* **2019**, 54, 2278–2288.
- [14] K. Woo, K. Lee, K. Kovnir, *Mater. Res. Express* **2016**, 3, DOI 10.1088/2053-1591/3/7/074003.
- [15] L. Chen, Y. Gu, L. Shi, J. Ma, Z. Yang, Y. Qian, *Chem. Lett.* **2003**, 32, 1188–1189.
- [16] M. S. Lube, R. L. Wells, P. S. White, *Inorg. Chem.* **1996**, 35, 5007–5014.
- [17] Q. U. Yuhui, W. Ma, X. Bian, H. Tang, W. Tian, *Int. J. Quantum Chem.* **2006**, 106, 960–967.
- [18] R. West, M. J. Fink, J. Michl, *Science* **1981**, 214, 1343–1344.
- [19] M. Yoshifuji, I. Shima, N. Inamoto, K. Hirotsu, T. Higuchi, *J. Am. Chem. Soc.* **1981**, 103, 4587–4589.

- [20] Y. Wang, Y. Xie, P. Wei, R. B. King, H. F. Schaefer, P. von R Schleyer, G. H. Robinson, *Science* **2008**, 321, 1069–1071.
- [21] A. Sidiropoulos, C. Jones, A. Stasch, S. Klein, G. Frenking, *Angew. Chem. Int. Ed.* **2009**, 48, 9701–9704.
- [22] K. C. Mondal, H. W. Roesky, M. C. Schwarzer, G. Frenking, B. Niepötter, H. Wolf, R. Herbst-Irmer, D. Stalke, *Angew. Chem. Int. Ed.* **2013**, 52, 2963–2967.
- [23] A. J. Arduengo, R. Krafczyk, R. Schmutzler, H. A. Craig, J. R. Goerlich, W. J. Marshall, M. Unverzagt, *Tetrahedron* **1999**, 55, 14523–14534.
- [24] Y. Wang, Y. Xie, P. Wei, R. B. King, H. F. Schaefer, P. V. R. Schleyer, G. H. Robinson, *J. Am. Chem. Soc.* **2008**, 130, 14970–14971.
- [25] M. Y. Abraham, Y. Wang, Y. Xie, P. Wei, H. F. Schaefer, P. V. R. Schleyer, G. H. Robinson, *Chem. Eur. J.* **2010**, 16, 432–435.
- [26] Y. Wang, G. H. Robinson, G. H. Robinson, *Dalt. Trans.* **2012**, 41, 337–345.
- [27] K. C. Mondal, P. P. Samuel, H. W. Roesky, R. R. Aysin, L. A. Leites, S. Neudeck, J. Lübben, B. Dittrich, N. Holzmann, M. Hermann, et al., *J. Am. Chem. Soc.* **2014**, 136, 8919–8922.
- [28] H. Braunschweig, R. D. Dewhurst, K. Hammond, J. Mies, K. Radacki, A. Vargas, *Science* **2012**, 336, 1420–1422.
- [29] Y. Wang, B. Quillian, P. Wei, C. S. Wannere, Y. Xie, R. B. King, H. F. Schaefer, P. V. R. Schleyer, G. H. Robinson, *J. Am. Chem. Soc.* **2007**, 129, 12412–12413.
- [30] X. Feng, M. M. Olmstead, P. P. Power, *Inorg. Chem.* **1986**, 25, 4615–4616.
- [31] A. M. Arif, A. H. Cowley, M. Pakulski, J. M. Power, *J. Chem. Soc. Chem. Commun.* **1986**, 889, 889–890.
- [32] D. C. Pestana, P. P. Power, *J. Am. Chem. Soc.* **1991**, 113, 8426–8437.
- [33] H. Nöth, S. Weber, *Zeitschrift für Naturforsch. - Sect. B J. Chem. Sci.* **1983**, 38, 1460–1465.
- [34] R. T. Paine, H. Nöth, *Chem. Rev.* **1995**, 95, 343–379.
- [35] P. Paetzold, A. Richter, T. Thijssen, S. Würtenberg, *Chem. Ber.* **1979**, 112, 3811–3827.
- [36] B. Bouckley, *Angew. Chem. Int. Ed.* **1988**, 27, 1603–1622.
- [37] J. C. Spirlet, J. R. Peterson, L. B. Asprey, *Advances in Inorganic Chemistry*, **1987**.
- [38] F. Dahcheh, D. Martin, D. W. Stephan, G. Bertrand, *Angew. Chem. Int. Ed.*

- 2014, 53, 13159–13163.
- [39] F. Zhang, P. Maksyutenko, R. I. Kaiser, A. M. Mebel, A. Gregušová, S. A. Perera, R. J. Bartlett, *J. Phys. Chem. A* **2010**, 114, 12148–12154.
- [40] J. D. Watts, L. C. Van Zant, *Chem. Phys. Lett.* **1996**, 251, 119–124.
- [41] H. Nöth, P. Kolle, G. Linti, G. L. Wood, C. K. Narula, *Chem. Ber.* **1988**, 121, 871–879.
- [42] A. M. Arif, J. E. Boggs, A. H. Cowley, J. G. Lee, M. Pakulski, J. M. Power, *J. Am. Chem. Soc.* **1986**, 108, 6083–6084.
- [43] G. Linti, H. Nöth, K. Polborn, R. T. Paine, *Angew. Chem. Int. Ed.* **1990**, 29, 682–684.
- [44] K. Knabel, T. M. Klapötke, H. Nöth, R. T. Paine, I. Schwab, *Eur. J. Inorg. Chem.* **2005**, 1099–1108.
- [45] E. Rivard, W. A. Merrill, J. C. Fettinger, P. P. Power, *Chem. Commun.* **2006**, 3800–3802.
- [46] A. N. Price, M. J. Cowley, *Chem. - A Eur. J.* **2016**, 22, 6248–6252.
- [47] A. N. Price, G. S. Nichol, M. J. Cowley, *Angew. Chem. Int. Ed.* **2017**, 56, 9953–9957.
- [48] C. M. E. Graham, C. R. P. Millet, A. N. Price, J. Valjus, M. J. Cowley, H. M. Tuononen, P. J. Ragoonna, *Chem. - A Eur. J.* **2018**, 24, 672–680.

Chapter V

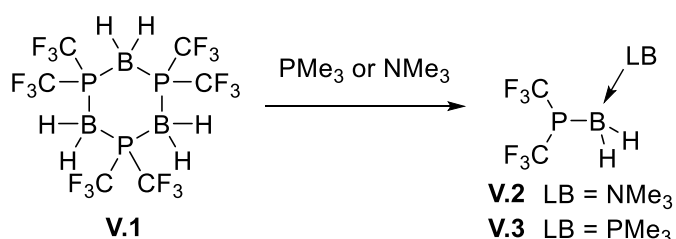
Functionalised Phosphaborenes

Chapter V – Functionalised Phosphaborenes

Introduction

Minimally substituted phosphinoboranes

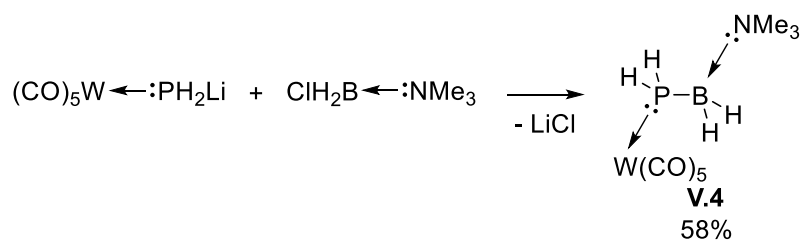
Although a wide range of phosphinoboranes have been reported (See Chap. IV, *Aminoboranes and Phosphinoboranes*),^[1] most of them required bulky substituents on the phosphorus or the boron centre to stabilise them. The use of coordinating Lewis bases allowed a reduction in size of the substituents of phosphinoboranes, by also providing electronic assistance as well as steric bulk. In 1978, A. Burg reported the isolation of two base-stabilised phosphinoboranes **V.2** and **V.3** by cleavage of the cyclic trimer $[(CF_3)_2PBH_2]_3$ **V.1** using trimethylamine (NMe_3) or trimethylphosphine (PMe_3) (Scheme 1).^[2] The phosphinoboranes **V.2** and **V.3** have small substituents on both phosphorus and boron atoms ($-CF_3$ and H respectively).



Scheme 1: Synthesis of minimally substituted phosphinoboranes **V.2** and **V.3** by cleavage of the trimer **V.1**.

The parent phosphinoborane (H_2PBH_2) was first isolated as a Lewis acid and base stabilised complex **V.4**. The reaction between the two adducts $(CO)_5W \leftarrow PH_2Li$ and $ClH_2B \leftarrow NMe_3$ gives the parent phosphinoborane stabilised by a Lewis base (NMe_3) and acid $(W(CO)_5)$ **V.4** (Scheme 2).^[3] The phosphinoborane **V.4**'s solid-state structure

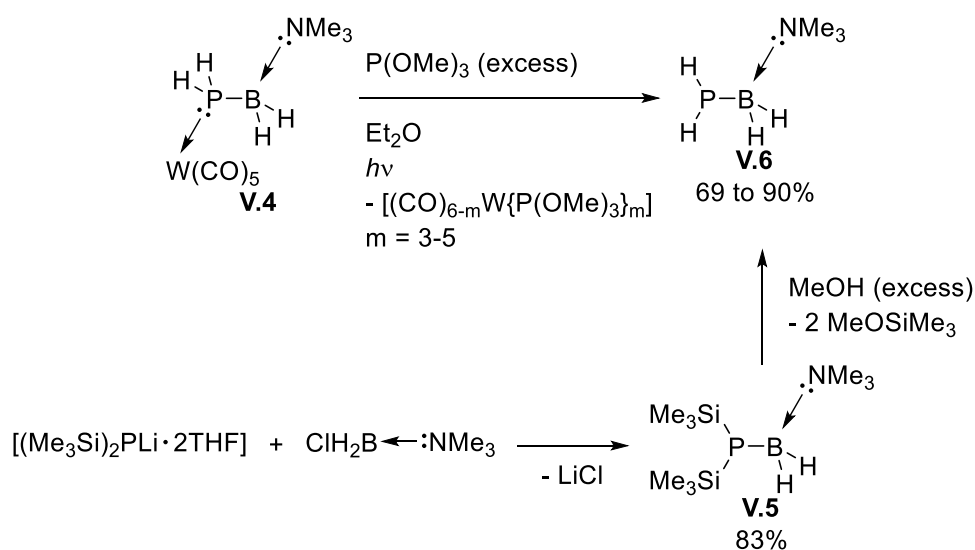
was confirmed by X-ray diffraction. The P–B bond distance (1.955(4) Å) is longer than in the calculated structure for the free parent phosphinoborane H₂PBH₂ (1.873 Å). This difference is due to the absence of π-bonding interactions in **V.4** compared to H₂PBH₂. Indeed, the lone pair of the phosphorus atom is donating to the tungsten atom, while the empty π-orbital of the boron is filled by the nitrogen lone pair. The ³¹P NMR signal of **V.4** (δ –184.2) comes in the range of the base free phosphinoboranes.^[1] The ¹¹B NMR signal of **V.4** (δ –7.6) is more shielded than the signal observed for the base free phosphinoboranes,^[1] which is consistent with the presence of a tetracoordinate boron atom.



Scheme 2: Synthesis of the Lewis acid and base stabilised parent phosphinoborane **V.4**.

A few years later, M. Scheer *et al.* reported base-stabilised minimally substituted phosphinoboranes, including the base-stabilised parent phosphinoborane **V.6**. The phosphinoborane **V.6** can be synthesized by removing the W(CO)₅ fragment from the complex **V.4**, using trimethylphosphite (P(OMe)₃) (Scheme 3).^[4] Compound **V.6** was also synthesized from the reaction between methanol and the phosphinoborane **V.5**, which was itself prepared by reaction between the lithiated phosphine [(Me₃Si)₂PLi•2THF] and the amino-borane adduct ClH₂B←NMe₃ (Scheme 3).^[5] The P–B bond length in **V.6** (1.976(2) Å) is slightly longer than in the complex **V.4** and considerably longer than the calculated values of the free parent phosphinoborane.

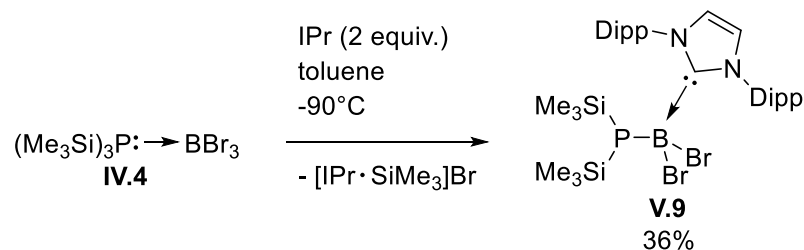
Again, this is due to the absence of a π -interaction in **V.6** due to the nitrogen lone pair donation of NMe_3 into the vacant p orbital from the boron centre. The ^{11}B NMR signals of **V.5** and **V.6** (δ -6.1 and -6.7) are close to those of complex **V.4** (δ -7.6). The ^{31}P NMR signal of base-stabilised parent phosphinoborane **V.6** (δ -215.5) is shifted considerably up field compared to the Lewis acid/base complex **V.4** (δ -184.2), which is consistent with the absence of the $\text{W}(\text{CO})_5$ fragment. Similarly, the phosphinoborane **V.5** has a ^{31}P NMR resonance of δ -251.4 , which is the most shielded resonance observed for free or base-coordinated phosphinoboranes. The base coordination to the boron centre and the strong σ -donating Me_3Si substituents explain this high-field ^{31}P NMR resonance.



Scheme 3: Synthesis of the base-stabilised minimally substituted phosphinoborane **V.5** and the base-stabilised parent phosphinoborane **V.6**.

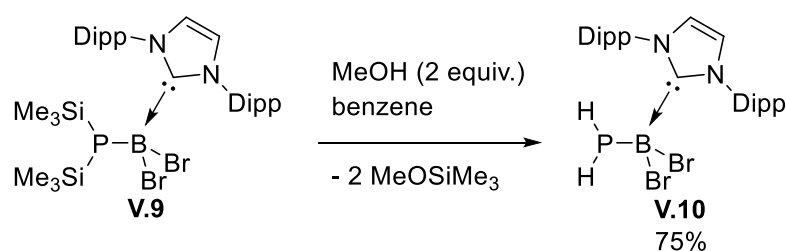
In 2018, M. Scheer and co-workers also reported the parent phosphinoborane stabilised by N-heterocyclic carbenes (NHC) **V.7** and **V.8**. This was achieved by depolymerization of poly(phosphinoboranes) using the respective NHC in boiling

resonance ($\delta -9.6$) was found in the high-field region corresponding to the four-coordinate boranes in base-coordinated phosphinoboranes.^[2–6]



Scheme 5: Synthesis of the phosphinoborane NHC adduct **V.9**.

$(\text{Me}_3\text{Si})_n\text{P}$ substituents can be converted to H_nP compounds by treatment with methanol.^[9–11] This has been already applied to phosphinoboranes for the synthesis of **V.6** (Scheme 3).^[5] A. Price obtained the NHC-stabilised 1-dihydro-2-dibromo-phosphinoborane **V.10** from **V.9** by reaction with methanol (Scheme 6).^[8]



Scheme 6: Synthesis of the NHC-stabilised 1-dihydro-2-dibromo-phosphinoborane **V.10**.

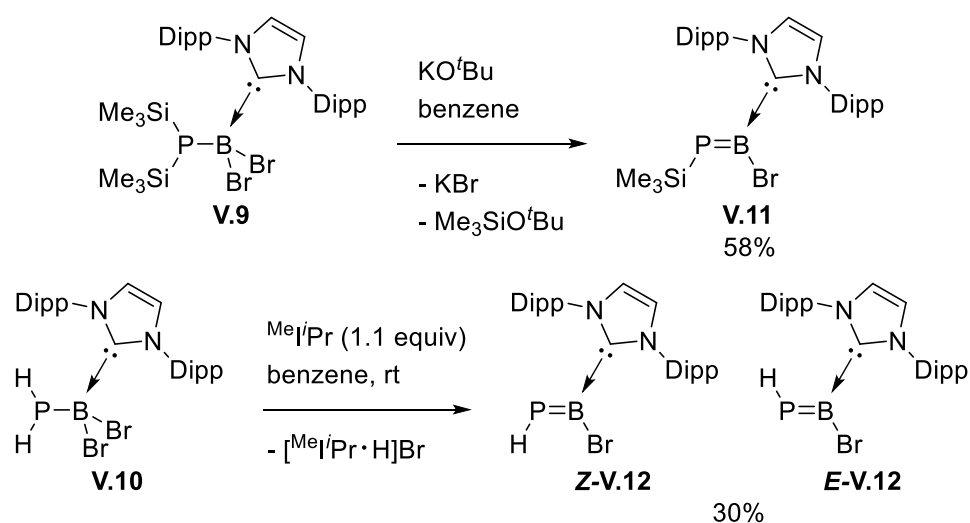
The key feature of the new phosphinoborane adducts **V.9** and **V.10** is the presence of reactive substituents, whilst the previous examples only featured either bulky substituents to provide steric effect around the P–B bond, or small but unreactive

substituents. The structure of both **V.9** and **V.10** are designed to favor further elimination Me_3SiBr or HBr to form base-stabilised phosphaborenes.

Minimally substituted phosphaborenes

Stepwise Me_3SiX ($\text{X} = \text{Br}, \text{Cl}$) elimination to reach unsaturated mixed group 13-15 compounds has been reported recently. Guy Bertrand *et al.* reported cyclic alkylaminocarbene (cAAC)-stabilised iminoborane **IV.25**, which formed from the cAAC adduct precursor **IV.24**, by spontaneous Me_3SiCl elimination in solution (See *Chap. IV, Iminoboranes*).^[12] In 2016, M. Cowley and A. Price reported the synthesis of base-stabilised phosphaborenes **IV.37** and **IV.38**, following similar preparation (See *Chap. IV, Phosphaborenes*).^[13]

A. Price achieved the synthesis of two minimally substituted phosphaborenes **V.11** and **V.12** by reacting **V.9** with KO^tBu and **V.10** with 1,3-diisopropyl-4,5-dimethylimidazol-2-ylidene ($^{\text{Me}}\text{I}^{\text{Pr}}$) respectively (*Scheme 7*), allowing the elimination of Me_3SiBr and HBr respectively.



Scheme 7: Synthesis of the minimally substituted phosphaborenes **V.11** and **V.12**.

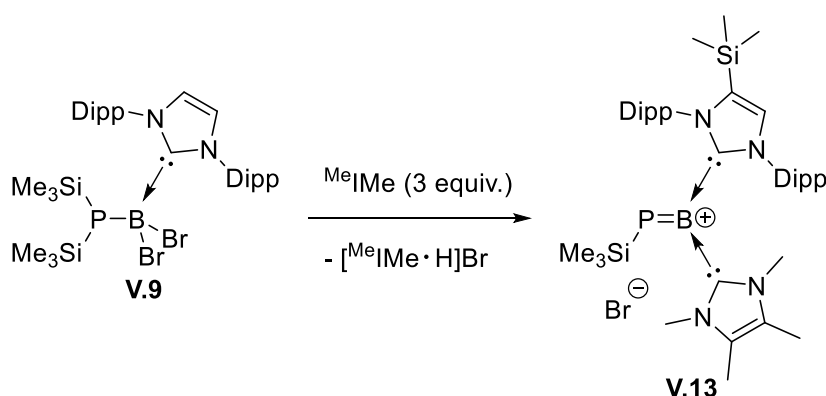
The ^{31}P and ^{11}B NMR chemical shifts of **V.11** (δ 72.0 and δ 42.3, respectively) are in the range of the previously reported base-coordinated phosphaborenes (See Chap. IV, *Phosphaborenes*).^[13–16] Similarly, the ^{31}P and ^{11}B NMR signals (δ 79.1, 51.7 and δ 44.1, 47.8 respectively) of **V.12** are also observed in the typical region of base-coordinated phosphaborenes.^[13–16] Interestingly, in the case of **V.12**, a mixture of two isomers is obtained, however, for **V.11** only the *Z*-isomer is observed. The reaction initially gives only the **E-V.12** isomer, which converts overtime to **Z-V12** until the ratio of the two species reaches 0,77:1. The observation of **E-V.12** is possibly due to the small size of the hydrogen substituent on the phosphorus compared to the Me_3Si for **V.11**, which allows to have a substituent on the same side of the ligand NHC. The P=B bonds in **V.11** (1.787(2) Å) and **V.12** (1.744(2) Å) are shorter than the previously reported base-coordinated phosphaborenes,^[13–16] due to the relatively small size of the substituents at both phosphorus and boron. The phosphaborene **V.12** is the smallest isolated phosphaborene.

Attempted synthesis of molecular boron-phosphide

Price attempted to reach base-stabilised molecular boron-phosphide. As trimethylsilylhalide eliminations are reported to occur at high temperature and to lead to boron phosphide (See Chap. IV, *Mixed group III-V compounds of lighter elements*),^[7] the phosphaborene **V.11** was heated at 200°C under vacuum, however only sublimation of **V.11** was observed.^[8]

When the phosphinoborane **V.9** was treated with an excess of NHC $^{\text{Me}}\text{IME}$, A. Price did not observe the formation of molecular boron-phosphide from further Me_3SiBr elimination. Instead the boron cation **V.13** was obtained as major product (Scheme 8). The product **V.13** showed that coordination of $^{\text{Me}}\text{IME}$ had occurred, but also that

C–H activation occurred on the backbone of the IPr ligand. Crystals of the cation **V.13** were isolated confirming the P=B multiple bond (1.807(3) Å), the B–C bond distances (1.589(4) and 1.591(4) Å) are similar to the phosphaborene **V.11** (1.586(3) Å), confirming coordination from the two NHCs. Unfortunately, **V.13** could not be isolated on a larger scale.

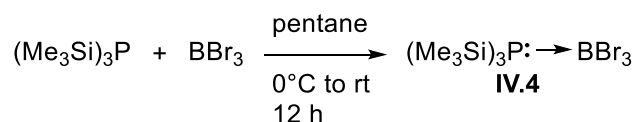


Scheme 8: Attempt of synthesis of molecular boron-phosphide, and generation of the boron cation **V.13**.

The C–H activation observed in the above reaction can be a problem to achieve molecular boron-phosphide. The backbone hydrogen atoms from IPr ligand are unstable to the harsh condition required to remove the last Me₃SiBr moieties. Changing the ligand from IPr to its saturated homologue the 1,3-bis(2,6-diisopropylphenyl)dihydroimidazole-2-ylidene (SIPr) could be a solution to avoid side reactions. The saturated backbone from SIPr, more stable to deprotonation, will prevent any C–H activation and may afford the clean formation of the boron cation homologue or base-stabilised molecular boron-phosphide.

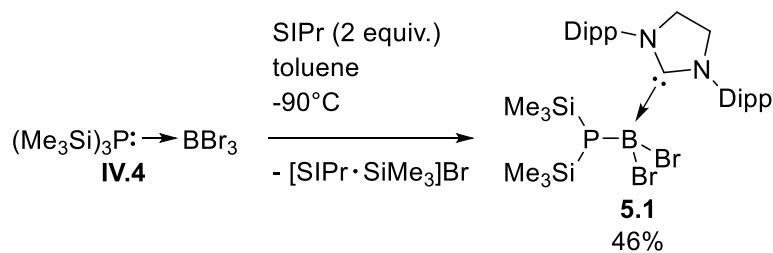
Synthesis of the SIPr coordinated 1-di(trimethylsilyl)-2-dibromo-phosphinoborane 5.1

The adduct $(\text{Me}_3\text{Si})_3\text{P}-\text{BBr}_3$ **IV.4** was synthesised using a slightly modified preparation from the reported procedure of White and co-workers (*Scheme 9*).^[7] Addition of a solution of $\text{P}(\text{SiMe}_3)_3$ in pentane to a solution of BBr_3 in pentane at low temperature ($0\text{ }^\circ\text{C}$) under inert atmosphere and absence of light afforded after 12 hours the adduct **IV.4** in quantitative yield.



Scheme 9: Synthesis of the phosphorus-boron adduct **IV.4**.

The phosphorus-boron adduct **IV.4** was treated with two equivalents of SIPr in toluene at $-90\text{ }^\circ\text{C}$ (*Scheme 10*). The solution turned orange overnight. The ^{31}P NMR spectrum revealed a singlet at $\delta -184.3$ and the ^{11}B NMR spectrum showed a sharp singlet at $\delta -9.8$. As expected, both signals are similar to the one from the IPr homologue **V.9** (^{31}P NMR $\delta -187.1$, ^{11}B NMR $\delta -9.6$). In this case as well, no boron-phosphorus coupling was observed in the NMR spectra. Analysis of the ^1H NMR spectrum confirmed the formation of the phosphinoborane SIPr adduct **5.1**: the Me_3Si resonance ($\delta 0.49$, d) integrates to 18, relative to the SIPr ligand proving the presence of two Me_3Si on the phosphorus centre (*Figure 1*). The trimethylsilylimidazolium salt is observed by ^1H NMR spectroscopy as a by-product from the reaction, which is in accordance with the Me_3SiBr elimination.



Scheme 10: Synthesis of the SIPr coordinated 1-di(trimethylsilyl)-2-dibromo-phosphinoborane **5.1**.

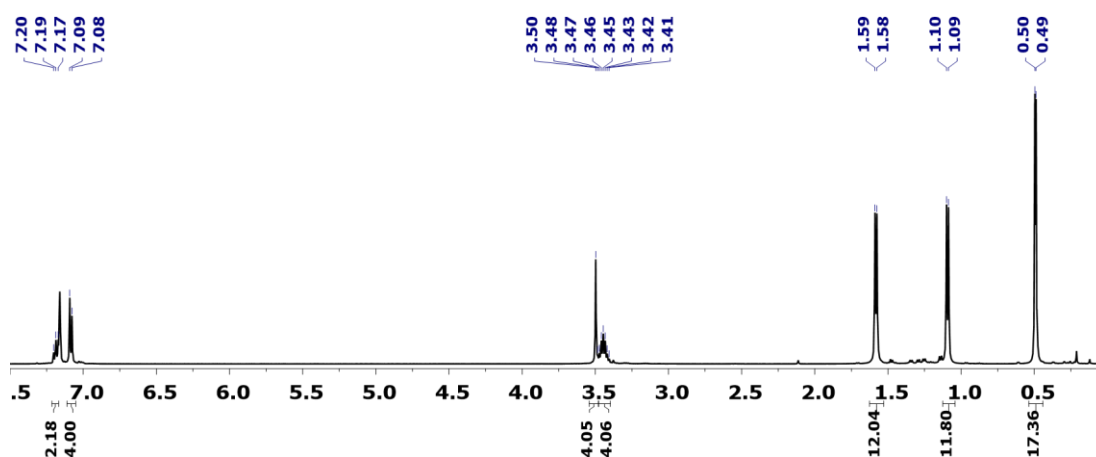


Figure 1: ^1H NMR (500 MHz, C_6D_6) of the SIPr coordinated 1-di(trimethylsilyl)-2-dibromo-phosphinoborane **5.1**.

The adduct **5.1** shows a remarkable difference in solubility compared to its unsaturated analogue **V.9**. Applying the purification procedure from **V.9** did not afford **5.1** as a pure product. Unlike **V.9**, the new phosphinoborane adduct **5.1** is soluble in hexane and could therefore not be washed with this solvent. It was found that extraction with pentane allowed the isolation of **5.1** as a tan powder in 46% yield.

SIPr coordination to the boron centre of **5.1** does not affect the ^{31}P chemical shift ($\delta = 184.3$), which comes in the range of previously reported base-free and base-coordinated phosphinoboranes.^[1,6] The ^{11}B NMR signal ($\delta = -9.8$) is in the range of the

previously reported base-coordinated phosphinoboranes,^[6] the high-field boron signal confirms the presence of a four-coordinate boron centre. ¹³C NMR spectroscopy also confirms the coordination from the NHC SIPr, with a carbene carbon significantly up-field compared to the free NHC (δ 180.3, $\Delta\delta$ –63.8). This shift was also observed in the case of **V.9** with similar value ($\Delta\delta$ –61.8).

The solid-state structure of **5.1** was confirmed by single crystal X-ray analysis (*Figure 2*). The P1–B1 bond length (1.995(4) Å) is typical for the phosphorus-boron single bonds. This value is also in the range of the previously reported base-coordinated phosphinoboranes (1.976(2)-1.993(2) Å).^[4–6] The boron centre has a tetrahedral geometry, confirming the coordination of the NHC. The B1–C1 bond length (1.655(5) Å) is longer than the previously reported NHC-stabilised phosphinoboranes (1.593(2)-1.599(3) Å).^[6] This small difference is likely due to the larger size of the bromine substituents compared to the hydrogen atoms in the reported NHC-stabilised phosphinoboranes. The phosphorus-silicon bonds (2.2689(13) and 2.2579(12) Å) in **5.1** are longer than the reported **V.5** [(Me₃Si)₂PBH₂(NMe₃)] (2.227(1) Å), due to the difference in steric bulk of the NHC ligand compared to the NMe₃.^[5] The length of the phosphorus-silicon bonds from **5.1** suggests further Me₃SiBr elimination to reach the SIPr-stabilised phosphaborene homologue to **V.11** would be favourable.

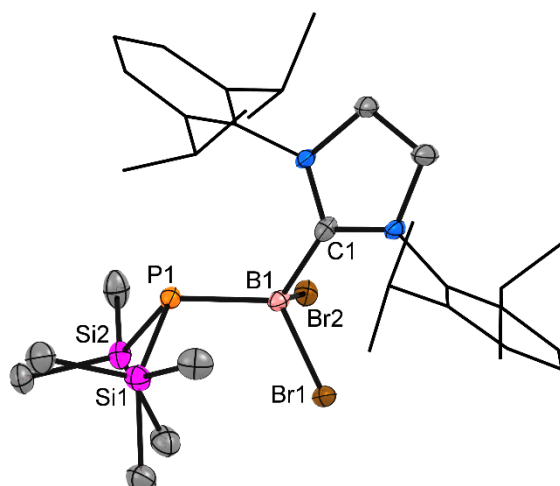
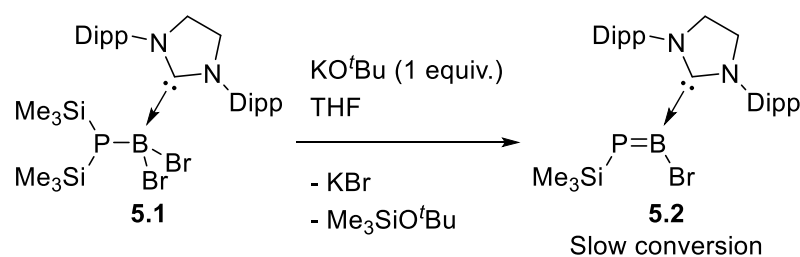


Figure 2: Molecular structure of **5.1** in the solid state. Ellipsoids are drawn at 50% probability; hydrogen atoms are omitted for clarity. Selected bond distances [Å] and angles [°] for **5.1**: P1–B1 1.995(4), Si1–P1 2.2689(13), Si2–P1 2.2579(12), B1–C1 1.655(5); Si1–P1–B1 109.06(11), Si2–P1–B1 107.85(11), Si2–P1–Si1 99.59(5), P1–B1–Br1 110.12(16), P1–B1–Br2 112.45(18), C1–B1–Br1 98.8(2), C1–B1–Br2 110.4(2), C1–B1–P1 117.3(2), Br1–B1–Br2 106.39(17).

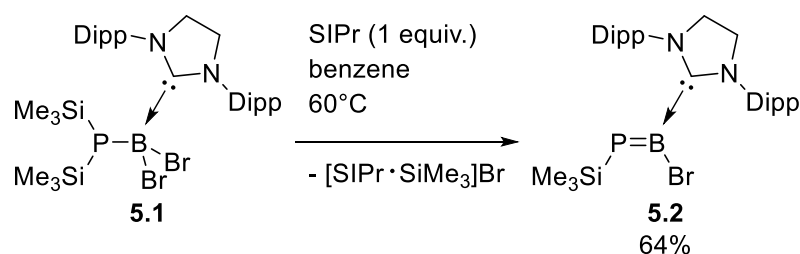
Synthesis of the SIPr coordinated 1-trimethylsilyl-2-bromophosphaborene **5.2**

Following the procedure used to synthesize **V.11**, the phosphinoborane adduct **5.1** was treated with one equivalent of KO^tBu in THF (*Scheme 11*). The reaction was monitored by ³¹P NMR spectroscopy. The ³¹P NMR spectrum showed a new singlet (δ 69.45, in THF-d₈), which is in a similar region of **V.11** (δ 72.0, in C₆D₆). After 12 hours only 44% of conversion to the product was observed by ³¹P NMR spectroscopy. Heating the reaction did not favor the formation of the product, but it induced formation of several side products (³¹P NMR δ 81.7(d), 42.7(d), –24.9, –146.9, –255.1 and –273.9). The formation of the phosphaborene **5.2** is very slow, as in the case of **V.11**, where four days were necessary to reach the full conversion to **V.11**. Consequently, other reagents were tried to find a more convenient protocol.



Scheme 11: Synthesis of the SIPr coordinated 1-trimethylsilyl-2-bromophosphaborene **5.2** using KO^tBu.

Treatment of **5.1** with an equivalent of SIPr under gentle heating in benzene resulted in full conversion after 16 hours (*Scheme 12*). The ³¹P NMR spectrum has a single signal at δ 77.8 (in C₆D₆), similar to **V.11** (δ 72.0). The ¹¹B NMR spectrum shows a broad singlet at δ 42.2, which is the same chemical shift as **V.11** (δ 42.3). The analysis of the integration of the different resonances from the ¹H NMR spectrum confirms the presence of a single trimethylsilyl group on the phosphorus, allowing to identify the NHC phosphaborene adduct **5.2** (*Figure 3*). The by-product from this reaction is again the trimethylsilylimidazolium salt, which is separated by filtration. The volatiles were removed *in vacuo*. Washing with pentane afforded the pure product **5.2** as a yellow solid in 64% yield.



Scheme 12: Synthesis of the SIPr coordinated 1-trimethylsilyl-2-bromophosphaborene **5.2** using SIPr.

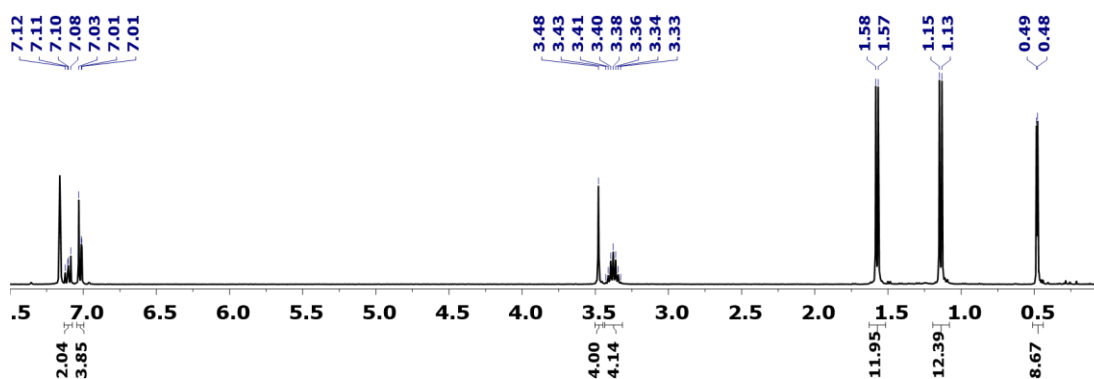


Figure 3: ^1H NMR (400 MHz, C_6D_6) of SIPr coordinated 1-trimethylsilyl-2-bromophosphaborene **5.2**.

In the case of **5.2** (and **V.12**) the ^{31}P NMR chemical shift (δ 77.8) is at much higher field than the previously reported NHC-stabilised phosphaborene **IV.38** and **IV.40** (δ 192.9 and 151.5).^[13,16] This large difference in chemical shift can be explained by the electronic donating property of the trimethylsilyl substituent, compared to the electron withdrawing aryl substituents in the case of **IV.38** and **IV.40**. The ^{11}B NMR chemical shift (δ 42.2) is in the typical region of the previously reported NHC-stabilised phosphaborenes.^[13,16] The ^{13}C NMR spectroscopy also confirms the coordination from the NHC SIPr, with a carbene carbon shifted significantly up-field compared to the free NHC (δ 180.9, $\Delta\delta$ -63.2). A similar upfield shift is also observed in the case of the ^{13}C NMR carbene carbon signal of **V.11** ($\Delta\delta$ -60).

Single crystal X-ray analysis confirmed the solid-state structure from **5.2** (Figure 4). The P=B bond distance in **5.2** (1.788(2) Å) is similar to the one in **V.11** (1.787(2) Å) and shorter than the previously reported base-coordinated phosphaborenes.^[13–16] This is a direct consequence of the smaller size of the substituent on both phosphorus and boron centre. The geometry of the boron is planar (sum of angles = 360.0(1)°). The B1–C1 bond (1.592(3) Å) is in the range of the dative carbene carbon-boron bond

of E=B(NHC) type compounds.^[13,16–22] The B1-P1-Si1 angle ($102.92(8)^\circ$) is slightly smaller than the previously reported base-stabilised phosphaborene ($106\text{--}115^\circ$),^[13–16] here again this can be correlated to steric effects. Only the Z-isomer was observed in the solid state for **5.2**, this is in accordance with the NMR spectra which feature a single set of signals. Overall the phosphaborene **5.2** has structural parameters and NMR chemical shifts very close to its unsaturated analogue **V.11**.

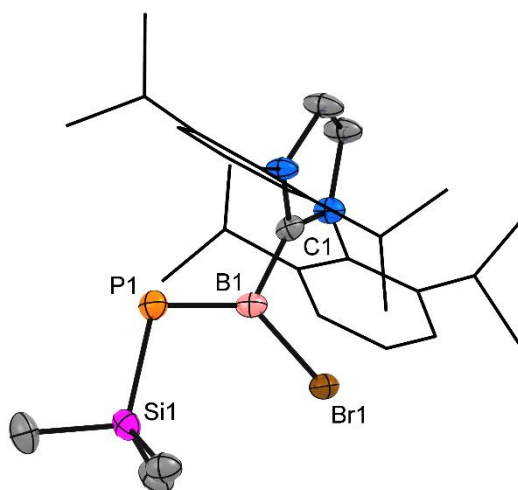
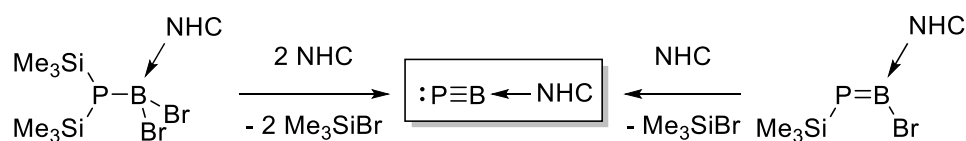


Figure 4: Molecular structure of **5.2** in the solid state. Ellipsoids are drawn at 50% probability; hydrogen atoms are omitted for clarity. Selected bond distances [\AA] and angles [$^\circ$] for **5.2**: P1–B1 1.788(2), Si1–P1 2.2394(9), B1–Br1 1.988(2), B1–C1 1.592(3); Si1–P1–B1 $102.92(8)$, P1–B1–Br1 $131.46(12)$, P1–B1–C1 $116.66(15)$, Br1–B1–C1 $111.80(15)$.

Attempted synthesis of NHC stabilised boron-phosphide

Successive Me_3SiBr elimination allowed the formation of the respective NHC phosphinoborane **5.1** and NHC phosphaborene **5.2** adducts. Several attempts were carried out to eliminate the last Me_3SiBr and reach NHC-coordinated boron-phosphide, an isoelectronic analogue to phosphalkynes.

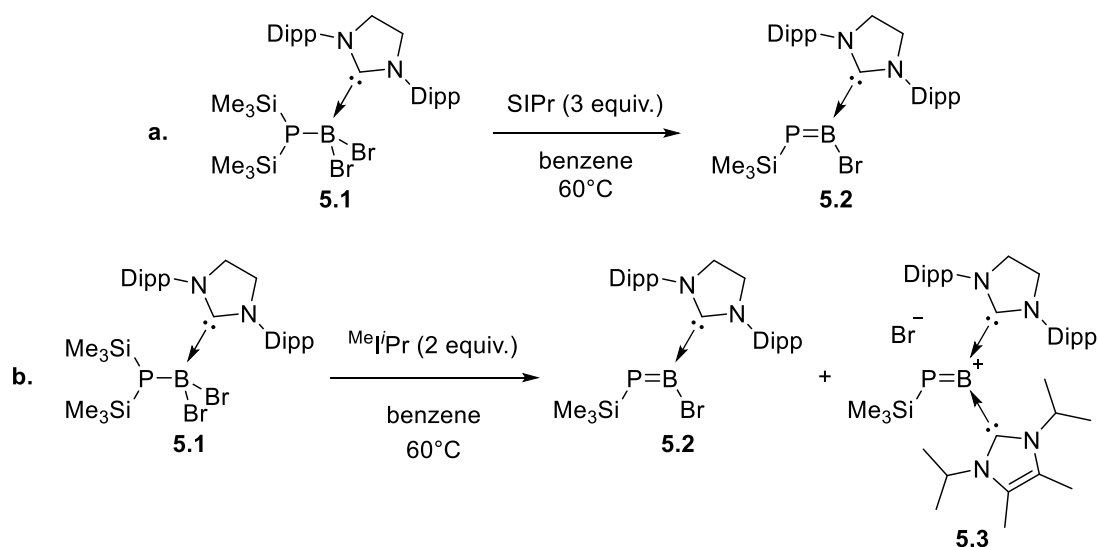


Scheme 13: Strategy of synthesis of NHC stabilised boron-phosphide.

Attempt from the SIPr phosphinoborane adduct 5.1

Treated with three equivalents of SIPr in benzene, the phosphinoborane **5.1** only gave the phosphaborene **5.2** (Scheme 14.a). Even after heating (60°C) for two days, ³¹P NMR spectroscopy only showed the signal at δ 77.8 from the phosphaborene. The ¹H NMR spectrum revealed the presence of the phosphaborene **5.2** along with unreacted SIPr.

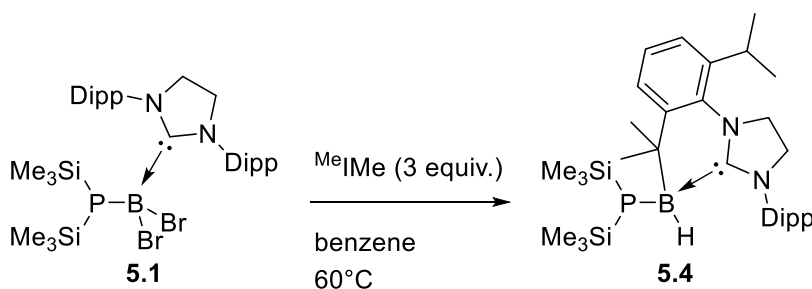
The adduct **5.1** was treated with three equivalents of a small NHC, ^{Me}I'Pr, in benzene at 60°C (Scheme 14.b). After one night, the ³¹P NMR spectrum showed once again the formation of the phosphaborene **5.2** as a major compound (> 90%). A trace product was observed at δ 150.5, which is in the region similar to the chemical shift observed for the boranylium cation **V.13** (δ 188). This signal can be assigned to the boranylium analogue **5.3**.



Scheme 14: **a.** Attempt of NHC boron-phosphide synthesis from **5.1** using SIPr. **b.** Attempt of NHC boron-phosphide synthesis from **5.1** using MeⁱPr.

The phosphinoborane **5.1** was reacted with two equivalents of another small NHC, MeⁱIme in benzene. Following the reaction by ³¹P NMR spectroscopy revealed slow conversion of **5.1** into the phosphaborene **5.2** at room temperature. When heated (60°C), two new signals were observed at δ 209.6 and –247.6 in the ³¹P NMR spectrum. Further heating formed a mixture of the unknown new product at δ –247.6 and the phosphaborene **5.2** (δ 77.8) in a 1:1 ratio. Heating for longer did not affect the ratio. This suggests that the two products are formed through two different reaction pathways. The ¹¹B NMR spectrum of the mixture showed the two main signals, the phosphaborene **5.2** (δ 42.2) and a sharp doublet corresponding to the new product at δ –20.5 (¹J_{BH} = 100.1 Hz), suggesting the presence of a four-coordinate boron. As the ³¹P NMR spectrum does not feature any coupling, the doublet in the ¹¹B NMR spectrum is most likely due to a coupling with a hydrogen atom. The ¹H NMR spectrum was highly complex, with a lot of signals in addition to those for phosphaborene **5.2**, and as such, no further information could be extracted from it.

Increasing the ratio of NHC ^{Me}Ime to phosphinoborane **5.1** (3:1) in benzene under heating (60°C), afforded the unknown compound at δ –247.6 as the major product (Scheme 15). The ³¹P and ¹¹B NMR spectra shows similar signals (δ –247.6 and –20.5(d) respectively). Analysis of the ¹H NMR resonances revealed the presence of two trimethylsilyl group on the phosphorus (δ 0.25 and 0.05) along with several signals in the region from the CH₃ of the Dipp group, suggesting an unusual, asymmetric structure of the ligand.



Scheme 15: Attempts of NHC boron-phosphide synthesis from **5.1** using ^{Me}Ime.

The reaction was scaled up under similar conditions to isolate this product. Filtration followed by hexane extraction separated the product from a purple solid, which is NMR silent and extremely air and moisture sensitive. Crystals suitable for X-ray analysis were obtained from a concentrated benzene solution and revealed the unexpected product **5.4** (Figure 5). The phosphorus still possesses two trimethylsilyl groups. The four-coordinate boron centre is confirmed and arises from a C–H bond activation of the isopropyl fragment from the SIPr ligand. Indeed, the boron centre is inserted between H1 and C22 and the carbene carbon C1 is still coordinated to it, with a dative C1–B1 bond distance in the typical range of boron-carbon adduct (1.596(2) Å).

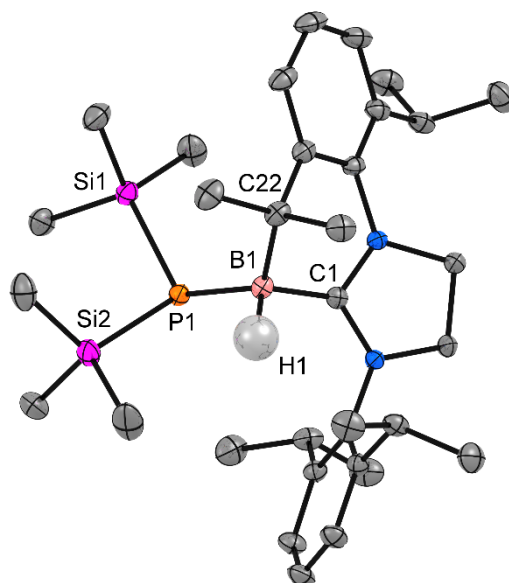
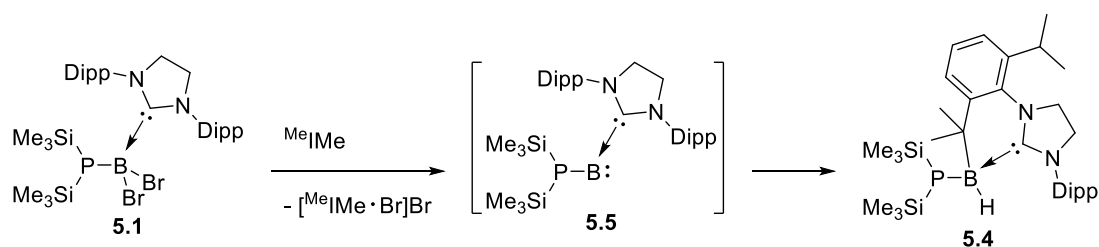


Figure 5: Molecular structure of **5.4** in the solid state. Ellipsoids are drawn at 50% probability; hydrogen atoms are omitted for clarity (except H1). Selected bond distances [\AA] for **5.4**: P1–B1 2.0103(18), B1–C1 1.596(2), B1–C22 1.636(3).

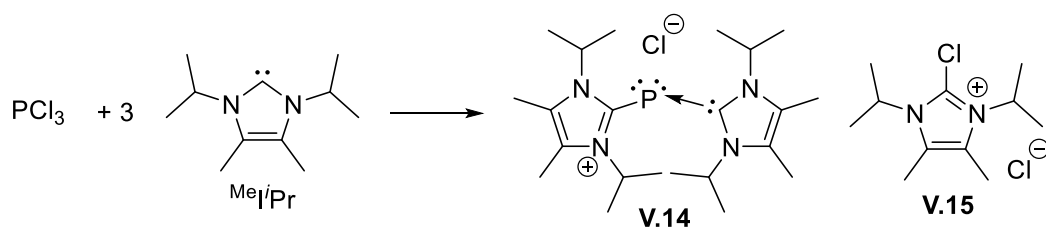
The solid-state structure of **5.4** is in accordance with the NMR data. The doublet in the ^{11}B NMR spectrum ($\delta -20.5$, $^1J_{\text{BH}} = 100.1$ Hz) is explained by the presence of the hydride on the four-coordinate boron centre. The very shielded phosphorus signal ($\delta -247.6$) can be explained by the substituents on the boron which are more electron donating compared to the bromine in the case of **5.1** and **5.2**, increasing the electron density on the phosphorus.

The structure of the C–H activated product with the two trimethylsilyl group on the phosphorus centre confirms that **5.4** is not formed from **5.2** but through a different reaction pathway. The formation of the product **5.4** can be explained by the following proposed mechanism (Scheme 16). A borylene intermediate **5.5** is formed by reduction of the boron centre of **5.1** by the NHC $^{\text{Me}}\text{IME}$. The borylene centre reacts with the ligand to give **5.4** by C–H activation of the isopropyl group.



Scheme 16: Proposed mechanism for the formation of the C–H activated product **5.4**.

C–H insertions have already been observed in several attempts of reduction of boron species, and were attributed to the formation of transient borylenes.^[23–25] Those borylenes are normally generated from reduction of boron halide precursors using alkali metal. Despite the absence of reported reduction of boron species by NHCs, reduction of PCl_3 has been achieved using NHC. Indeed, the reaction between PCl_3 and three equivalents of $^{\text{Me}}\text{iPr}$ was reported to give the phosphinidene **V.14** along with the 2,2-dichloro-1,3-diisopropyl-4,5-dimethylimidazole **V.15** (Scheme 17),^[26] suggesting that $^{\text{Me}}\text{iPr}$ may have reduced the boron centre of **5.1**. However, no evidence of the 2-bromo-1,3-diisopropyl-4,5-dimethylimidazolium bromide (bromine analogue of **V.15**) was observed by ^1H NMR spectroscopy.

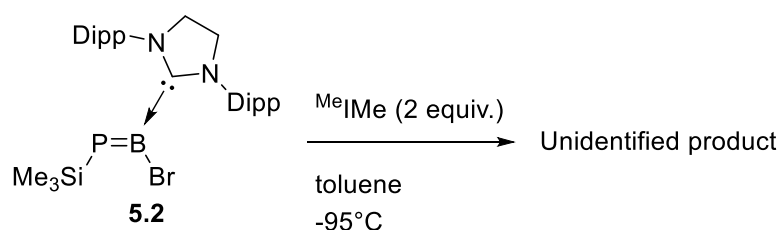


Scheme 17: Synthesis of the NHC stabilised phosphinidene **V.14** by reduction of PCl_3 with $^{\text{Me}}\text{iPr}$.

No further investigation was carried out on **5.4** as the compound was not of interest towards the formation of molecular boron-phosphide. Moreover, the product **5.4** represents a small part of the material recovered from the reaction. The purple solid, which is NMR silent, represents most of the material recovered from this reaction. A. Price observed a similar solid in the reaction between compound **V.9** and $^{\text{Me}}\text{Ime}$. In both cases, the purple solid did not show any signal in the ^1H , ^{11}B and ^{31}P NMR spectra. The solid does not crystalize from any solvent and slowly decomposes in solution even at low temperature under dry and inert atmosphere to a brown solid, which is also NMR silent. Mass spectrometry did not reveal the presence of NHC coordinate boron-phosphide or the imidazolium salt of any of the NHC (SIPr or $^{\text{Me}}\text{Ime}$). Attempts to characterize the purple solid were unsuccessful.

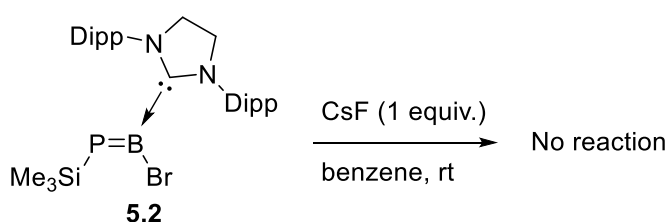
Attempt from the SIPr phosphaborene adduct **5.2**

The phosphaborene **5.2** was treated with two equivalents of the small NHC $^{\text{Me}}\text{Ime}$ at -95°C in toluene (*Scheme 18*). The reaction was kept at low temperature and monitored by ^{31}P NMR spectroscopy. In addition to the signal from the starting material, a signal at $\delta -148.8$ (d, $^1J_{\text{PH}} = 165.0$ Hz) slowly formed over 24 hours. No further study on the formed product was carried out as it clearly features a hydrogen atom on the phosphorus atom.



Scheme 18: Attempts of NHC boron-phosphide synthesis from **5.2** using $^{\text{Me}}\text{Ime}$.

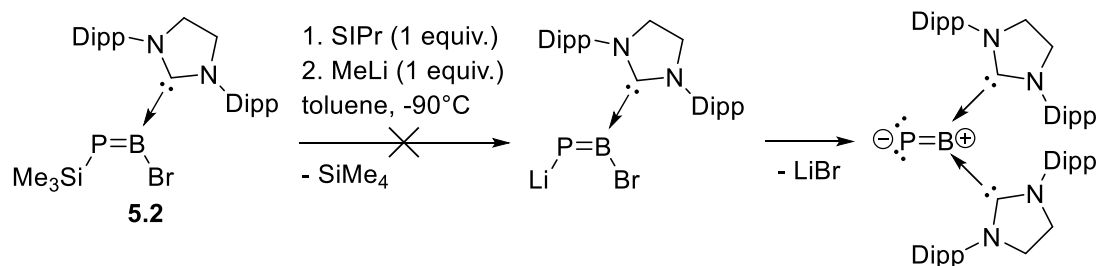
Compound **5.2** was allowed to react with cesium fluoride (CsF), a reagent known for silyl group deprotection by formation of a strong Si–F bond (*Scheme 19*). This reagent could promote Me₃SiBr elimination from **5.2**. After two days of reaction in benzene, ¹H, ¹¹B and ³¹P NMR spectroscopy showed no reaction had occurred.



Scheme 19: Reaction of phosphaborene **5.2** with cesium fluoride.

Phosphaborene **5.2** was treated with methyllithium (MeLi) in presence of NHC SIPr (*Scheme 20*). Reaction between P(SiMe₃)₃ and MeLi is known to form the lithiated phosphine LiP(SiMe₃)₂.^[27,28] The lithiation of the phosphaborene **5.2** could be followed by a favorable LiBr elimination. The presence of the SIPr may coordinate and trap the formed boron-phosphide.

However, no reaction was observed after six days. ³¹P NMR spectroscopy (δ 79.2, toluene) showed only the starting material, ¹¹B NMR spectroscopy showed starting material (δ 42.2, toluene) along with a small signal at (δ –16.8) and ¹H NMR spectroscopy showed the starting material. According to the NMR analysis no new phosphorus-boron species were formed and the phosphaborene **5.2** does not react with methyllithium.



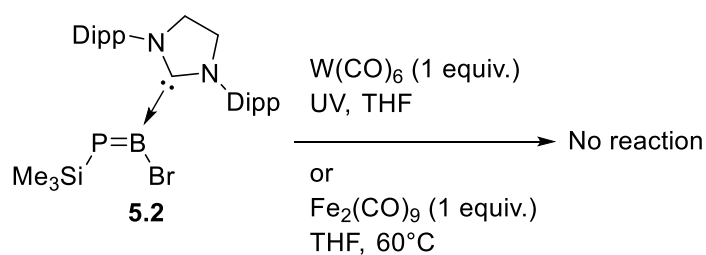
Scheme 20: Reaction of phosphaborene **5.2** with MeLi in presence of NHC SIPr.

Attempt of coordination from **5.2** to Lewis acid

Following the unsuccessful attempts to eliminate Me₃SiBr from **5.2**, the coordination of a Lewis acid was attempted. Coordination of the phosphorus centre to a Lewis acid could promote the elimination of Me₃SiBr as well as stabilising a boron-phosphide species as a push-pull complex with the Lewis base SIPr.

W(CO)₆ was irradiated (λ 420 nm) in THF for three hours before phosphaborene **5.2** in THF was added to it (*Scheme 21*). The mixture was irradiated further for 12 hours. The solution turned from yellow to red, however, the ¹¹B and ³¹P NMR spectra revealed only starting material. The ¹H NMR showed the starting material along with a small amount of imidazolium salt, with a characteristic signal from the imidazolium proton at δ 8.98, due to slow decomposition of the phosphaborene **5.2** in solution. No coordination of the phosphorus to the tungsten was observed.

The phosphaborene **5.2** was treated with diiron nonacarbonyl (Fe₂(CO)₉) in THF (*Scheme 21*). Even after one day at 60°C, the reaction only showed the starting material along with a small amount of the imidazolium salt. Here again no evidence of coordination was observed.



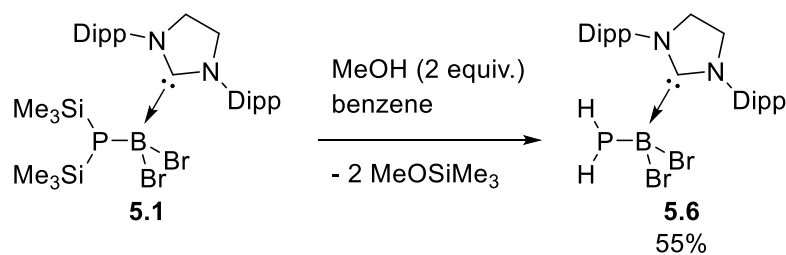
Scheme 21: Attempts of coordination from **5.2** to Lewis acid.

Functionalization of the phosphinoborane **5.1**

Synthesis of the 1-dihydro-2-dibromo-phosphinoborane **5.6**

Previous examples of conversion of $(\text{Me}_3\text{Si})_2\text{P}$ substituents to the parent H_2P compounds have been reported using methanol.^[9–11] A. Price also reported the successful conversion from the phosphinoborane **V.9** to the **V.10** using this preparation.^[8]

The phosphinoborane **5.1** was treated with two equivalents of methanol in benzene (*Scheme 22*). After only 15 minutes, full conversion of the starting material was observed by NMR spectroscopy, with a triplet in the ^{31}P NMR at $\delta -146.1$ ($^1J_{\text{PH}} = 199.6$ Hz). The ^1H NMR spectrum confirmed the presence of two hydrogen atoms on the phosphorus with a doublet at $\delta 2.48$ with the same coupling constant ($^1J_{\text{HP}} = 199.6$ Hz). Both NMR spectra allowed the identification of the SIPr coordinated 1-dihydro-2-dibromo-phosphinoborane **5.6**.



Scheme 22: Synthesis of the SIPr coordinate 1-dihydro-2-dibromo-phosphinoborane **5.6**.

Product **5.6** and **V.10** have very similar ^{11}B and ^{31}P NMR signals. The triplet in the ^{31}P NMR spectrum of **5.6** comes at $\delta -146.1$ ($^1J_{\text{PH}} = 199.6$ Hz), whilst **V.10** features a triplet at $\delta -145.1$ ($^1J_{\text{PH}} = 197.4$ Hz). The ^{11}B NMR spectrum of **5.6** shows a singlet at $\delta -10.8$ (**V.10**: ^{11}B NMR $\delta -11.1$). The ^1H NMR is fully assigned, the hydrogen-phosphorus coupling is also observed with the doublet at $\delta 2.48$ ($^1J_{\text{HP}} = 199.6$ Hz) (Figure 6 and 7).

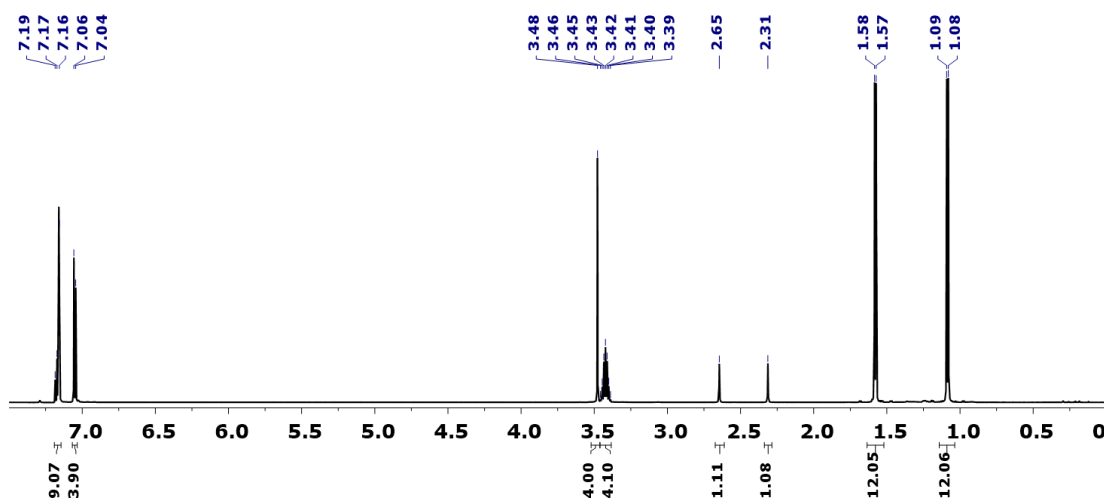


Figure 6: ^1H NMR spectrum (600 MHz, C_6D_6) of **5.6**.

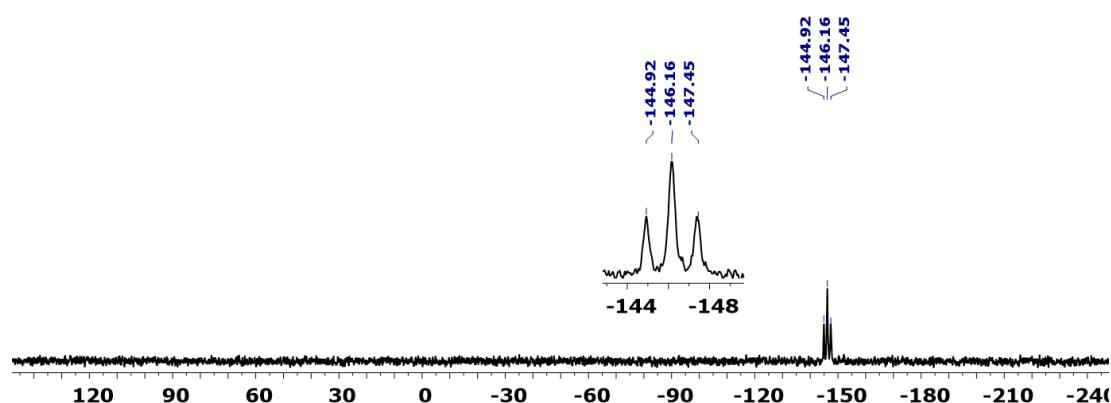


Figure 7: ^{31}P NMR spectrum (162 MHz, C_6D_6) of **5.6**.

The reaction was quick and the intermediate 1-hydrotrimethylsilyl-2-dibromophosphinoborane $[\text{H}(\text{Me}_3\text{Si})\text{PBr}_2]\text{SIPr}$ could not be observed. Simple filtration followed by washing with hexane afforded the adduct **5.6** as a white solid in 55% yield. Product **5.6** is stable in the solid state but slowly decomposes in solution. The instability of **5.6** in solution frustrated multiple attempts to obtain single crystals. However, X-ray quality crystals were obtained from slow evaporation of a benzene solution of **5.6** (Figure 8). Compound **5.6** co-crystallized along with its decomposition product, the imidazolium bromide salt, $[\text{SIPr}\cdot\text{H}]\text{Br}$. Significant disorder of the bromine and phosphorus positions was observed. It was not possible to place P–H bonds or hydrogen atoms either geometrically or by identifying peaks in a difference map. These missing H atoms (total of four per asymmetric unit, eight per unit cell) were included in the total chemical formula. Bond length and angles are not given for accuracy reasons.

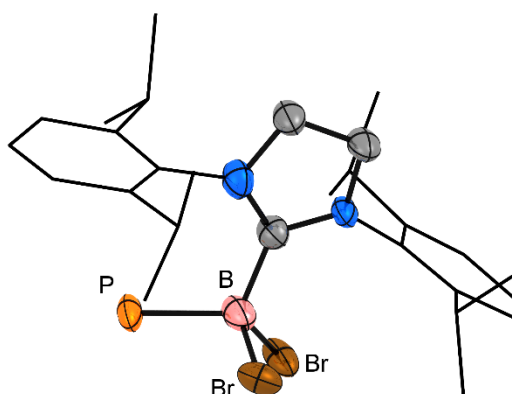
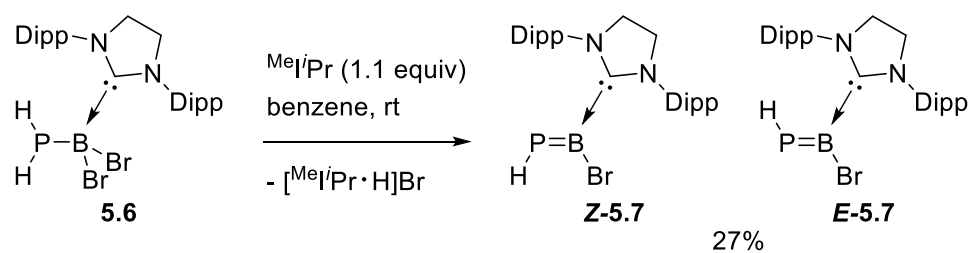


Figure 8: Molecular structure of **5.6** in the solid state. Ellipsoids are drawn at 50 % probability; hydrogen atoms are omitted for clarity. Co-crystallised C_6H_6 and $[SiPr-H]Br$ are not shown.

Synthesis of the 1-hydro-2-bromo-phosphaborene **5.7**

The presence of the imidazolium bromide salt, formed during the decomposition of **5.6**, suggests spontaneous HBr elimination from **5.6**. Treating **5.6** with the small NHC Me^iPr (1.1 equivalent) in benzene rapidly formed a white precipitate (Scheme 23). The ^{11}B NMR spectrum showed two new singlets at δ 44.4 and 47.6. The ^{31}P NMR spectrum revealed two new doublets at δ 90.5 ($^1J_{PH} = 141.1$ Hz) and 49.3 ($^1J_{PH} = 127.6$ Hz). These doublets suggested the effective elimination of HBr with the presence of a single hydrogen on the phosphorus, but also the presence of two different phosphorus-boron species. The chemical shift observed in the ^{11}B and ^{31}P NMR spectra is consistent with the formation of two phosphaborene species. With two sets of signals, the 1H NMR spectrum confirmed the presence of two different products as well as the presence of the phosphorus-hydrogen coupling from each product with similar coupling constant (δ 4.99, d, $^1J_{HP} = 141.1$ Hz and δ 4.29, d, $^1J_{HP} = 127.6$ Hz). Analysis of the relative integration of the 1H NMR spectrum allowed the identification of the two isomers **Z-5.7** and **E-5.7**.



Scheme 23: Synthesis of the 1-hydro-2-bromo-phosphaborene **5.7**.

Further NMR experiments were carried out to fully characterise the mixture of isomers. HMBC and HSQC allowed the full characterisation of both products. A ^1H NOESY experiment was necessary to assign the two isomers. The doublet at δ 4.29 from the H–P fragment showed a NOE correlation with the hydrogen atoms from the isopropyl fragment from the SIPr (δ 1.48 and 3.32) (Figure 9). This showed that the product with the signal at δ 4.29 has its hydrogen atom on the phosphorus closer to the SIPr, identifying it as **E-5.7**. By deduction, the other product was identified as **Z-5.7**.

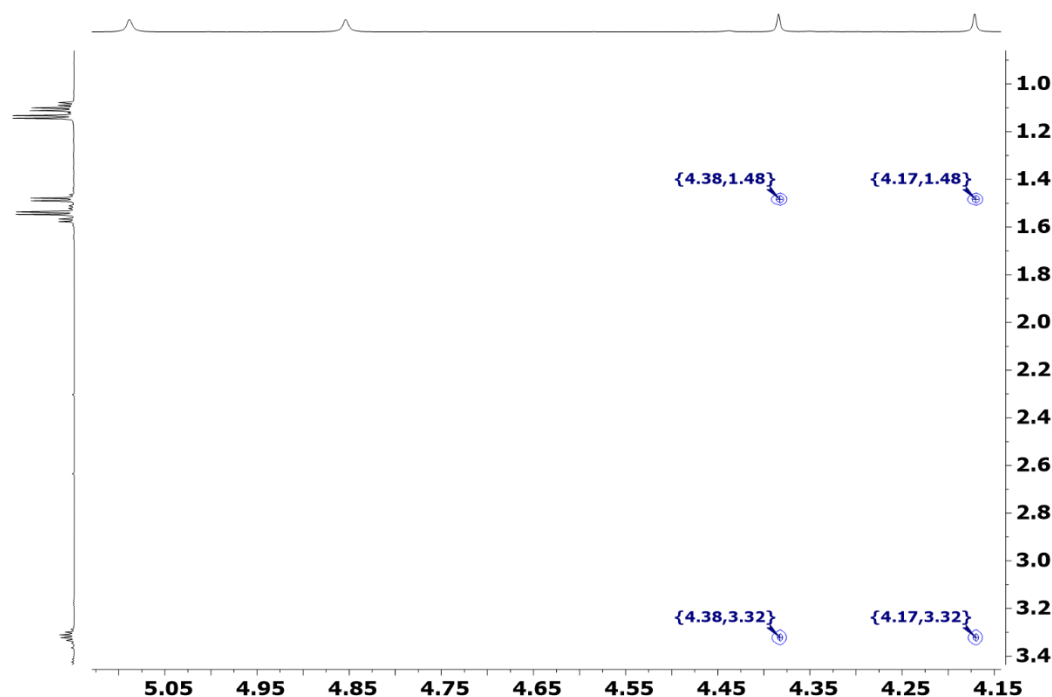


Figure 9: ^1H NOESY spectrum from **5.7** focused on the relevant region.

The phosphaborene **5.7** was isolated from the imidazolium bromide salt by fractional crystallisation as a yellow solid in 27% yield. In the case of **5.7** a ratio of *E* to *Z-5.7* is observed around 0.77:1 at 298K, which was always observed in this ratio.

The ^{31}P NMR resonances of *E-5.7* and *Z-5.7* (δ 49.3, d, $^1J_{\text{PH}} = 127.6$ Hz and δ 90.5, d, $^1J_{\text{PH}} = 141.1$ Hz) come in a region similar to the phosphaborenes **5.2**, **V.11** and **V.12**, much higher field than the NHC-stabilised phosphaborene with an aryl substituent.^[13,16] The multiplicity and the value of the coupling constant of the ^{31}P NMR signal, which is smaller compared to the one observed for **5.6** (199.6 Hz), are consistent with the formation of a P=B double bond and the presence of a single P–H substituent. The ^{11}B chemical shift of *E-5.7* and *Z-5.7* (δ 44.4 and 47.6) are similar to the previously reported NHC-stabilised phosphaborenes and **V.12**.^[13,16] The ^1H NMR has two set of signals corresponding to each isomer. The H–P=B signals come at δ 4–5, a similar region to compounds containing H–P=C or H–P=Si fragments.^[29,30]

Unlike the phosphaborene **5.2**, with the trimethylsilyl substituent, compound **5.7** shows two isomers. This is most likely due to steric effect, decreasing the size of the substituent from Me₃Si to H allows the formation of the *E* isomer in the case of **5.7**. A noticeable difference between **5.7** and **V.12** is observed in the formation of the different isomers. In the case of phosphaborene **V.12**, the *E* isomer (³¹P NMR δ 51.7, d, ¹J_{PH} = 129 Hz) is first obtained and converts over time to the *Z* isomer (³¹P NMR δ 79.1, d, ¹J_{PH} = 143 Hz) until the ratio of the two isomers reaches 0.77:1. In the case of **5.7**, both *E* and *Z* isomers are observed in the ratio 0.77:1, whether **5.7** is generated from **5.6** *in situ* or dissolved from solid material. This attests to a rapid interconversion between the two forms, evidenced by their equilibrium concentrations.

Variable temperature ¹H NMR experiment was carried out on the mixture of **5.7** to calculate the difference in energy between *E* and *Z* isomers. The ratio was recorded at different temperatures by ¹H NMR spectroscopy. It was possible to plot the equilibrium constant *K*_{eq} between *E* and *Z* as a function of the temperature (*Figure 10*). Linear regression and the use of the Van't Hoff equation ($\Delta G^\circ = -RT \ln K_{eq}$) allowed the calculation of the difference in energy between the two isomers. The *E* isomer was found to be 0.77 (+/- 0.24) kJ mol⁻¹ higher in energy than the *Z* isomer, which is close to the value obtained by computational study, carried by D. De Rosa (1.44 kJ mol⁻¹). **E-5.7** and **Z-5.7** are very close in energy, which is consistent with the observation of this equilibrium in solution.

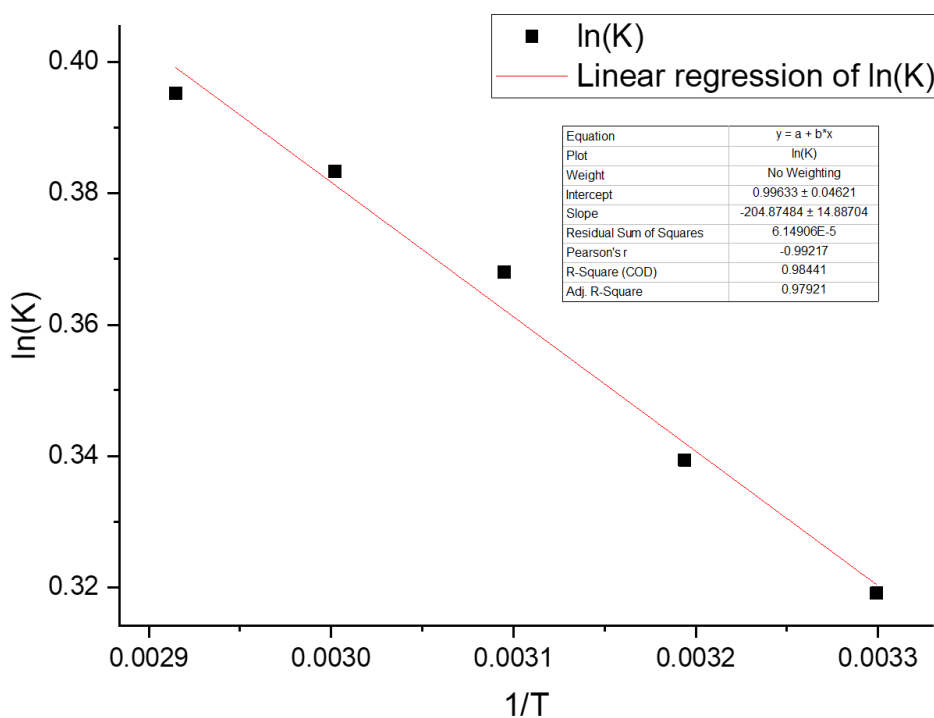


Figure 10: Plot of the equilibrium between *E* and *Z* isomers as $\ln(K) = f(1/T)$.

Crystals suitable for X-ray analysis were obtained from benzene. The solid-state structure from **5.7** revealed the expected compound (*Figure 11*). The phosphaborene **5.7** crystallises as a mixture of *E* and *Z* isomers, which leads to disorder of the Br and PH substituents at the boron centre. The P–H from the major isomer *E* was located in the Fourier difference map (*Figure 12*). The minor isomer *Z* was also observed; however, its structural parameters were not accurate. The small size of the substituents of **5.7** results in a shorter P=B bond distance (1.776(3) Å) compared to **5.2** (P=B 1.788(2) Å). This bond distance is close to its IPr analogue **V.12** (1.744(2) Å). The H1-P1-B1 angle is very narrow at 101.3(18)° for **5.7**. This value is narrower than the one found for **V.12** (H1-P1-B1 125.7(19)°). The bond angle H-P-B predicted for the parent phosphaborene HP=BH of 94.5° by Watts *et al.* is not observed,^[31] though this is predicted on the formation of a three-centre two-electron bond, with a shared hydrogen between the phosphorus and the boron atoms. The presence of the

NHC ligand disallows the observation of such a narrow H1-P1-B1 angle, by preventing the formation of the bridging hydrogen atom as it fills the vacant p orbital of the boron atom. The boron-carbene carbon bond B1-C1 (1.588(3) Å) is in the range of typical NHC coordinated boron compounds of E=B(NHC) type.^[13,16-22]

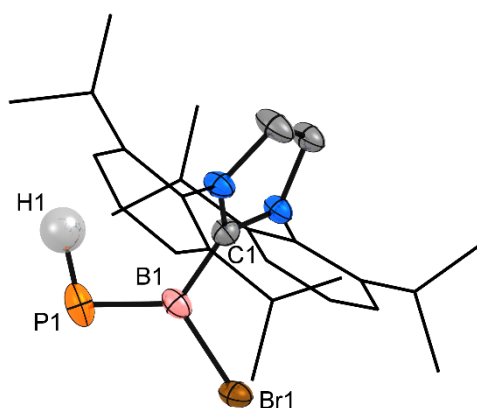


Figure 11: Molecular structure of **E-5.7** in the solid state. Ellipsoids are drawn at 50% probability; hydrogen (except H1) atoms are omitted for clarity. Selected bond distances [Å] and angles [°] for **5.7**: H1-P1 1.41(3), P1-B1 1.776(3), B1-Br1 1.982(2), B1-C1 1.588(3), H1-P1-B1 101.3(18), P1-B1-Br1 121.57(15), P1-B1-C1 125.28(19), Br1-B1-C1 113.04(16).

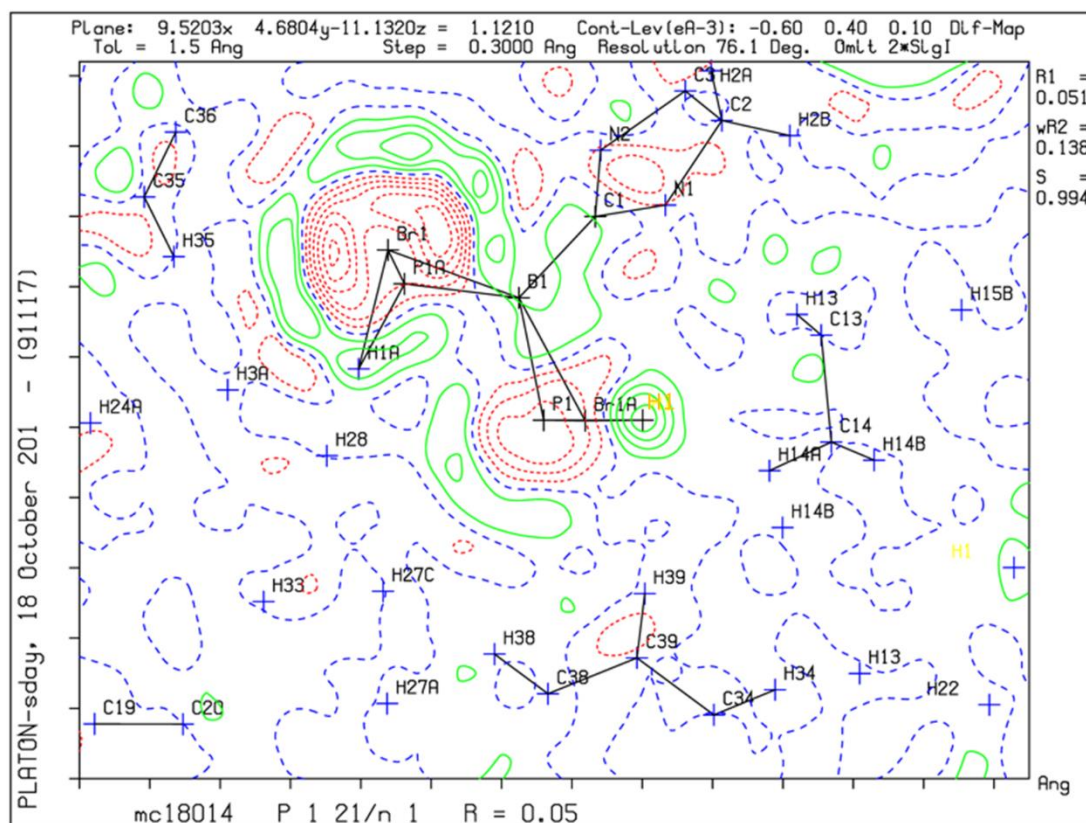
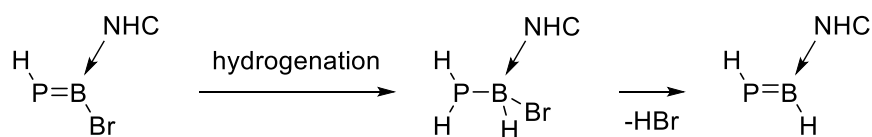


Figure 12: Fourier difference map of **E-5.7** (H1 labelled in yellow).

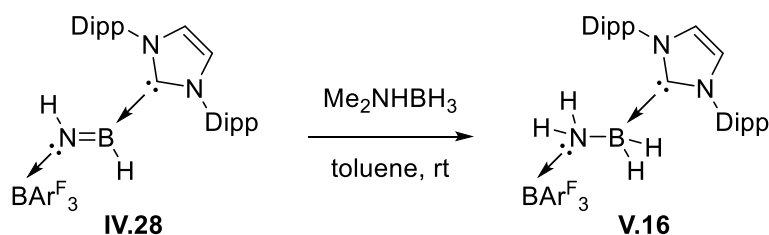
Synthesis of the 1-dihydro-2-bromohydro-phosphinoboranes **5.8** and **5.9**

Compounds **5.7** and **V.12** are the smallest of the phosphaborenes reported to date. A theoretical study has been carried out on the parent phosphaborene $\text{HP}=\text{BH}$,^[31] however, no experimental evidence of this compound has been observed. Hydrogenation of **5.7** or **V.12** followed by HBr elimination should allow the synthesis of the NHC-stabilised parent phosphaborene (*Scheme 24*).



Scheme 24: Strategy of synthesis to achieve the NHC-stabilised parent phosphaborene.

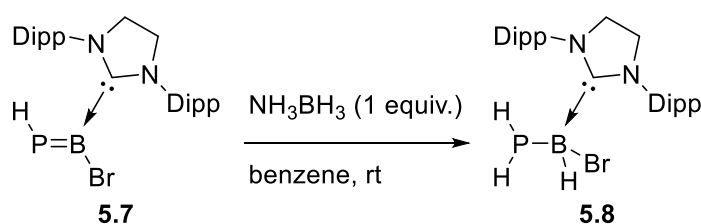
In 2017, E. Rivard *et al.* reported the hydrogenation of the iminoborane **IV.28** using dimethylamine borane complex (Me_2NHBH_3) to give the aminoborane **V.16** (Scheme 25).^[32]



Scheme 25: Reduction of the iminoborane **IV.28** using the dimethylamine borane complex.

Following this idea, phosphaborene **5.7** was allowed to react with one equivalent of ammonia borane adduct (NH_3BH_3) in benzene (Scheme 26). The solution slowly lost its yellow colour characteristic from phosphaborene species, to turn into a colourless solution, the full conversion was observed by ^1H NMR spectroscopy only after 24 hours. The ^{31}P NMR spectrum showed a new triplet at $\delta -183.6$ (t, $^1J_{\text{PH}} = 194$ Hz). The multiplicity of the new signal suggested the presence of two hydrogen on the phosphorus centre and the effective hydrogenation of the P=B double bond. The phosphorus signal is in the typical region of the base-free and base-coordinated phosphinoboranes.^[1,4–6] The ^{11}B NMR spectrum revealed a broad singlet at $\delta -19.7$.

The presence of a hydrogen on the boron centre was expected to split the boron signal into a doublet in the spectrum, however, the broad shape of the singlet can also explain it. The ^{11}B resonance is in the region similar to the reported base-stabilised phosphinoboranes.^[4–6]

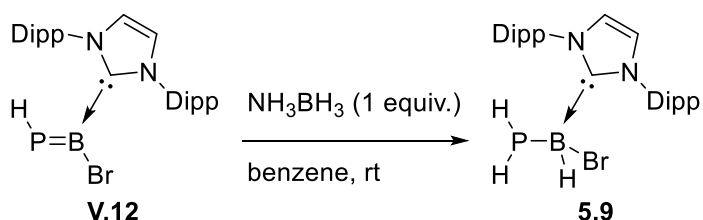


Scheme 26: Reaction of the phosphaborene **5.7** with NH_3BH_3 .

The ^1H NMR spectrum showed a set of signals corresponding to a new product. The hydrogen atoms on the phosphorus centre are inequivalent. A clear doublet of doublet of doublets is found at δ 1.96, with a large coupling constant ($^1J_{\text{HP}} = 195$ Hz) matching with the one observed in the phosphorus spectrum, and two smaller coupling constants (5.45 and 10.7 Hz). The values of the coupling constants are in the range of those observed in the phosphinoboranes $\text{RHPBH}_2(\text{NHC})$ ($\text{R} = \text{tBu}, \text{Ph}, \text{H}$, [$^3J_{\text{HH}} = 7\text{--}10$ Hz]).^[6] The ^1H NMR spectrum has evidence of a hydrogen atom coupling with the phosphorus atom and two non-equivalent hydrogens, which suggest the effective formation of the phosphinoborane **5.8**. A $^1\text{H}\text{--}^{31}\text{P}$ HMQC experiment was carried out and confirmed the coupling between the phosphorus and two non-equivalent hydrogen atoms at δ 1.34 (ddd, $^1J_{\text{HP}} = 195$ Hz, $^2J_{\text{HH}} = 10.7$ Hz, $^3J_{\text{HH}} = 10.7$ Hz) and 1.96 (ddd, $^1J_{\text{HP}} = 195$ Hz, $^2J_{\text{HH}} = 10.7$ Hz, $^3J_{\text{HH}} = 5.45$ Hz). The presence of the bulky SIPr ligand is most likely slowing down the rotation of the P–B bond making the two hydrogen atoms on the phosphorus centre inequivalent. Despite evidence of its presence, the hydrogen atom on the boron centre was not observed by ^1H NMR

spectroscopy. The ^1H , ^{31}P NMR spectra and the ^1H - ^{31}P HMQC experiment confirmed the successful formation of the phosphinoborane **5.8**.

Similarly, phosphaborene **V.12** was treated with one equivalent of ammonia borane adduct (NH_3BH_3) in benzene (Scheme 27). Here again, the solution turned from yellow to colourless, showing the consumption of the phosphaborene **V.12**. The ^{31}P NMR spectrum showed a new main triplet at $\delta -182.7$ (t, $^1J_{\text{PH}} = 192$ Hz), evidencing the presence of two hydrogen atoms on the phosphorus centre and effective hydrogenation of the $\text{P}=\text{B}$ double bond. The ^{31}P resonance is also in a region typical for phosphinoboranes.^[1,4-6] The ^{11}B NMR spectrum revealed a broad singlet at $\delta -19.7$, but again no splitting of the boron signal into a doublet was observed. The ^{11}B resonance is in the region similar to the reported base-stabilised phosphinoboranes.^[6]

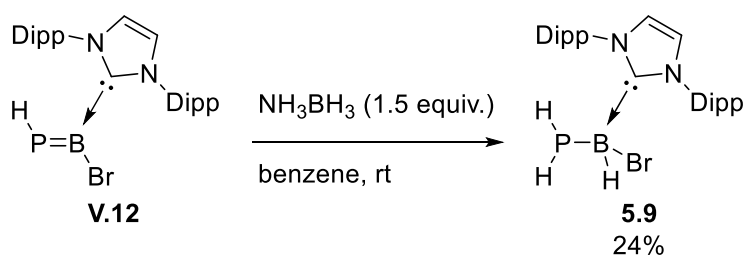


Scheme 27: Reaction of the phosphaborene **V.12** with NH_3BH_3 .

The ^1H NMR spectrum showed a set of signals corresponding to a new product, with two inequivalent $\text{P}-\text{H}$. A doublet of doublet of doublets is found at $\delta 2.07$, with a big coupling constant ($^1J_{\text{HP}} = 195$ Hz) matching with the one observed in the phosphorus spectrum, and two smaller coupling constants (5.65 and 10.8 Hz). The signal from the second hydrogen atom on the phosphorus centre is clearly observed as a doublet of doublet of doublets at $\delta 1.52$ (ddd, $^1J_{\text{HP}} = 192$ Hz, $^2J_{\text{HH}} = 10.55$ Hz, $^3J_{\text{HH}} = 10.55$ Hz).

A ^1H - ^{31}P HMQC experiment confirmed the coupling between the phosphorus and these two hydrogen atoms observed in the ^1H NMR spectrum. The IPr ligand, in this case again, is most likely slowing down the rotation of the P–B bond making the two hydrogen atoms on the phosphorus centre inequivalent. Despite evidence of its presence, the hydrogen on the boron centre could not be observed by ^1H NMR spectroscopy. The ^1H , ^{31}P NMR spectrum and the ^1H - ^{31}P HMQC experiment confirmed from the successful formation of the phosphinoborane **5.9**.

The preparation of phosphinoborane **5.9** was scaled up with an excess of NH_3BH_3 (1.5 equiv.) (*Scheme 28*). The reaction mixture was filtered when it turned colourless. The ^1H NMR spectrum showed the product. However, purification was necessary and was achieved by crystallisation from a concentrated solution of hexane:benzene (1:1). Pure **5.9** was obtained as a white solid in 24% yield. The ^1H , ^{11}B and ^{31}P NMR spectra showed the product previously observed. ^1H - ^{13}C HMBC and HSQC NMR experiments allowed full characterisation of **5.9**. The ^{13}C NMR spectrum confirmed the presence of the coordinated carbene carbon with a signal considerably shifted up field (δ 166.3, $\Delta\delta = -54.3$) compared to the free NHC. ^1H - ^{11}B HMQC experiment was carried out in an attempt to observe the hydrogen atom on the boron centre, but no coupling was observed in the 2D NMR spectrum. A proton decoupled ^{11}B NMR experiment showed a sharper signal (width = 254 Hz), confirming that the broadness previously observed (width = 427 Hz) is due to the presence of coupling to one or more hydrogen atoms.



Scheme 28: Optimised reaction of **V.12** with NH_3BH_3 .

The structure of **5.9** was confirmed by X-ray crystal analysis (*Figure 13*). The solid-state structure confirmed the presence of the hydrogen atom on the boron centre. The B1–H1 (1.21(3) Å) bond distance is in the range of typical boron-hydride bond.^[33] The P1–B1 bond length (1.940(3) Å) is also in the range of the previously reported base-coordinated phosphinoboranes.^[2–6] The B1–C1 bond length (1.605(4) Å) is longer than the previously reported NHC-stabilised phosphinoboranes (1.593(2)-1.599(3) Å),^[6] but shorter than the observed bond distance for **5.1** and **5.6** (1.655(5) and 1.629(12) respectively). The intermediate value of the B1–C1 bond in **5.9** is in accordance with the presence of a single bromine substituent on the boron atom. The previously reported phosphinoboranes have smaller values, with two hydrogen atoms, while compounds **5.1** and **5.6** have longer values, with two bromine atoms on the boron centre.

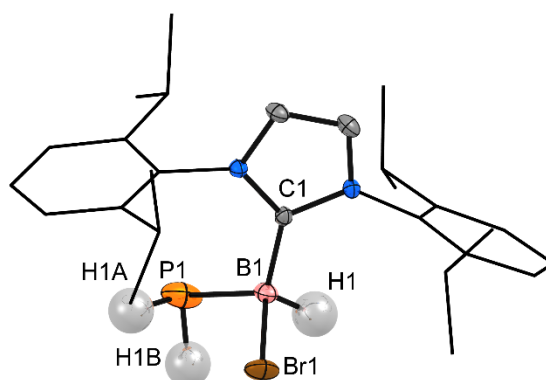
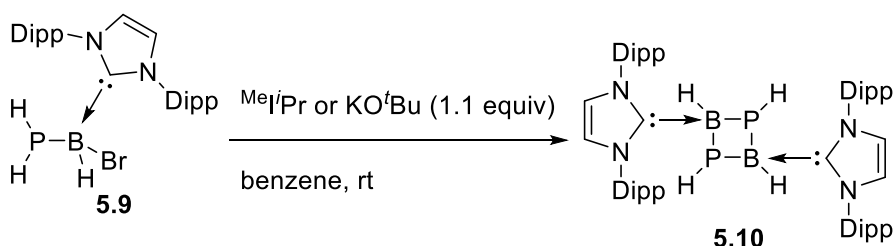


Figure 13: Molecular structure of **5.9** in the solid state. Ellipsoids are drawn at 50% probability; hydrogen (except H1, H1A and H1B) atoms are omitted for clarity. Selected bond distances [\AA] and angles [$^\circ$] for **5.9**: P1–B1 1.940(3), B1–C1 1.605(4), B1–H1 1.21(3), C1–B1–P1 116.89(19).

Attempted synthesis of the parent phosphaborene: synthesis of the parent diphosphadiboretane **5.10**

The phosphinoborane **5.9** was treated with the small NHC Me_iPr or KO^tBu , to form the NHC stabilised parent phosphaborene (*Scheme 29*). In both cases, the solution turned instantly to an orange colour, which is usually observed for the synthesis of phosphaborenes. However, NMR analysis did not show signals in accordance with the formation of a phosphaborene. Both reactions gave the same P-containing products, but cleaner for the one with NHC, which is discussed here.



Scheme 29: Reaction of phosphinoborane **5.9** with Me_iPr or KO^tBu .

The ^{31}P NMR spectrum showed resonances in the high-field region at $\delta -159.4$ (d, $^1J_{\text{PH}} = 146$ Hz) and $\delta -195.5$ (br d, $^1J_{\text{PH}} = 110$ Hz) as the major signals along with smaller signals at $\delta -134.3$ (d), $\delta -181.6$ (t), $\delta -198.7$ (d), $\delta -201.2$ (d) and $\delta -213.6$ (t), which disappeared over time. No signal was observed in the usual region of phosphaborenes (δ 40-200). The ^{11}B NMR spectrum showed only one main sharp signal at $\delta -29.7$ (d, $^1J_{\text{BH}} = 96$ Hz) along with two very small signals at $\delta -31.2$ (br) and $\delta -33.4$ (br, t), none of these signals are in the region of NHC-stabilised phosphaborenes (δ 40-50). The region for the ^{11}B NMR signal confirmed the coordination of the NHC and a tetracoordinate boron atom with an absence of a phosphorus-boron double bond. The ^{11}B resonance of this new product ($\delta -29.7$) is considerably shielded compared to its precursor ($\delta -19.7$), which can evidence the absence of the electron withdrawing bromine substituent on the boron atom.

The ^1H NMR spectrum showed several new signals from the ligand along with free NHCs (IPr and $^{\text{Me}}\text{IPr}$) and imidazolium salt for the reaction with $^{\text{Me}}\text{IPr}$ (Figure 14). Only one signal clearly showing coupling with phosphorus and boron was observed in the ^1H NMR spectrum, as a doublet of quartet of doublets at $\delta -0.95$ ($^1J_{\text{HP}} = 151$ Hz) with a coupling constant matching with that observed in the ^{31}P NMR spectrum ($\delta -159.4$ $^1J_{\text{PH}} = 146$ Hz), a coupling constant with the boron atom ($^2J_{\text{BH}} = 11$ Hz), which is in the range of 2J coupling constant observed for boron hydrides (B_nH_m)^[34] and a coupling constant with a hydrogen atom ($^nJ_{\text{HH}} = 13$ Hz). The signal at $\delta -0.95$ (dq_d) was assigned to a H–P and suggested the presence of a H–P=B–H type fragment. Due to the number of signals, integration of the ^1H NMR spectrum could not be relied upon.

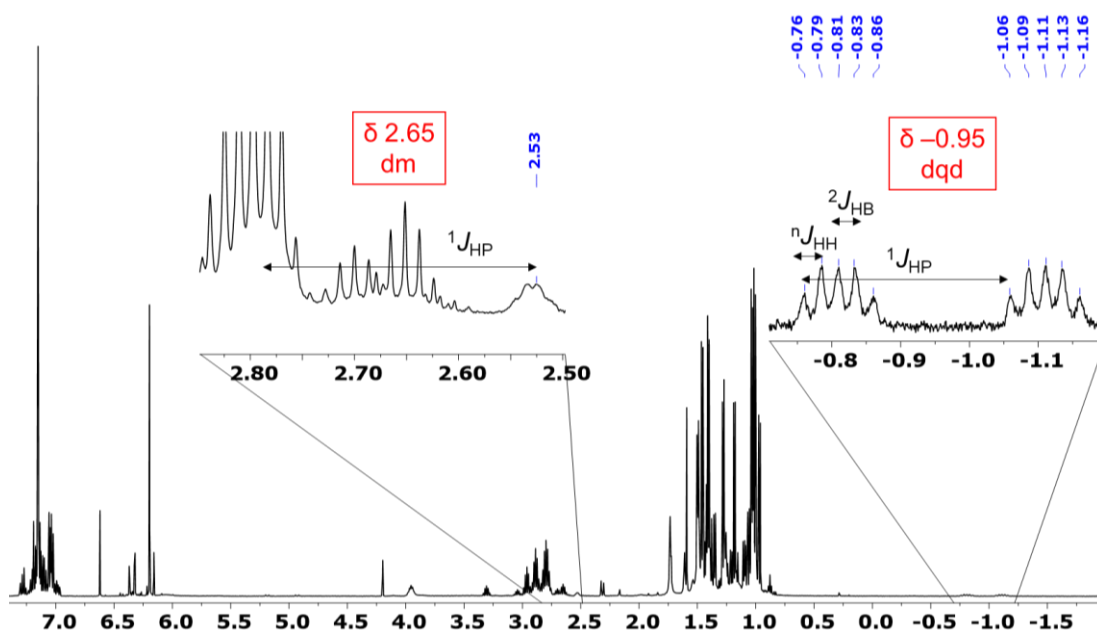


Figure 14: ^1H NMR spectrum (500 MHz, C_6D_6) of the reaction of **5.9** with $^{\text{Me}}i\text{Pr}$.

The ^{31}P and ^{11}B NMR spectra did not reveal the presence of any phosphaborene species. However, the formation of its dimer, the diphosphadiboretane **5.10** is possible considering the observed signals. The two main doublets in the ^{31}P NMR spectrum suggest the presence of a single hydrogen atom on each inequivalent phosphorus atom, moreover, the ^{31}P chemical shift ($\delta -159.4$ and -195.5) are in the range of the previously reported diphosphadiboretanes ($\delta 10$ to -163).^[1] The main ^{11}B NMR chemical shift ($\delta -29.7$) is significantly shifted up field compared to the reported base free diphosphadiboretanes ($\delta 30-90$), this difference is explained by the tetracoordinate boron with the NHC. The signal observed in the ^1H NMR spectrum at $\delta -0.95$ (dq) can also be due to the presence of a H–P–B–H fragment, without P=B double bond.

These observations by multinuclear NMR spectroscopy are in accordance with the proposed product **5.10**, however, the presence of two different signals in the ^{31}P NMR spectrum ($\delta -159.4$ and -195.5) cannot be explained, as the symmetrical structure of

5.10 would be expected to give a single doublet in the phosphorus spectrum. A ^1H - ^{31}P HMQC experiment was carried out confirming the coupling between the signal of the hydrogen atom at $\delta -0.95$ and the phosphorus at $\delta -159.4$ (Figure 15). The ^1H - ^{31}P HMQC NMR experiment also showed a coupling between the phosphorus signal at $\delta -195.5$ and a signal in the ^1H NMR spectrum at $\delta 2.65$ (Figure 15). The ^1H NMR signal at $\delta 2.65$ is a doublet of broad multiplets, but half of it overlaps with the signal from the Dipp moieties. The large coupling constant ($^1J_{\text{PH}} = 120$ Hz) was measured from the HMQC signal and is in accordance with the coupling constant observed in the ^{31}P NMR spectrum ($\delta -195.5$, br d, $^1J_{\text{PH}} = 110$ Hz). In each case the phosphorus atom is coupled with only one hydrogen atom, confirming the most likely structure **5.10**. Overall, the ^1H - ^{31}P HMQC NMR experiment allowed the identification of two inequivalent H–P fragments.

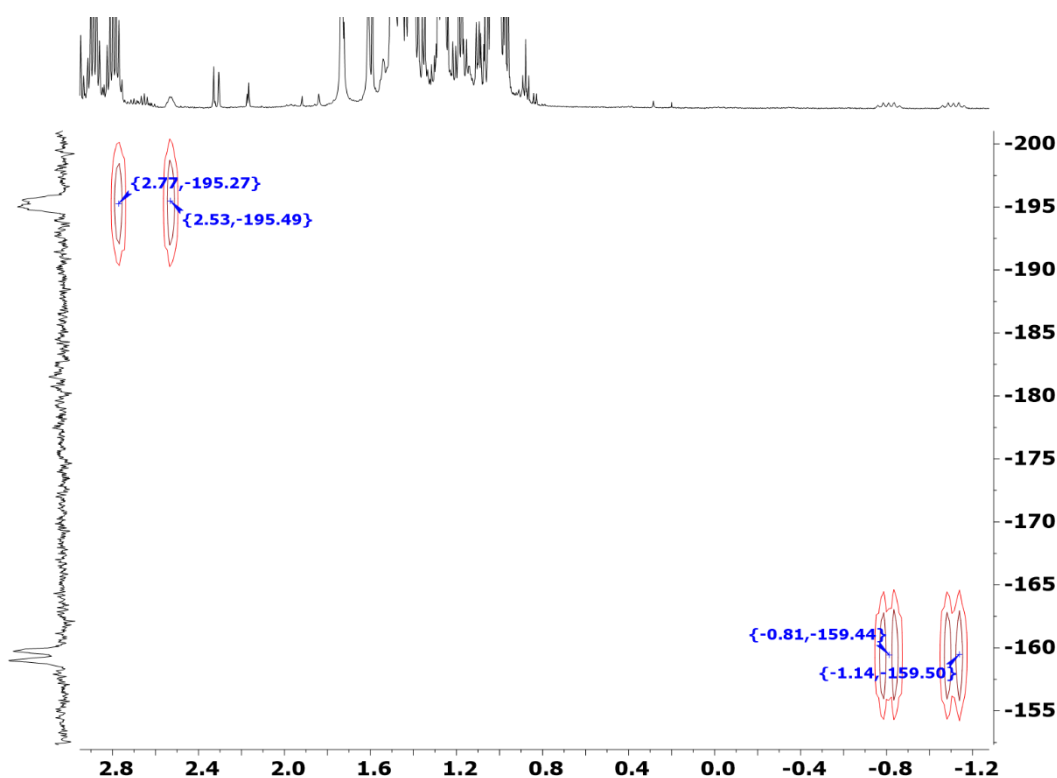


Figure 15: ^1H - ^{31}P HMQC NMR spectrum (500 MHz, 162 MHz, C_6D_6) of the reaction of **5.9** with $^{\text{Me}}\text{iPr}$.

A ^1H - ^{31}P HMBC NMR experiment was run and showed a long-range coupling between the ^{31}P NMR signal at δ -159.4 and the ^1H NMR signal at δ 2.65 , confirming that the two phosphorus atoms are part of the same molecule (Figure 16).

The B–H signal was located at δ 1.61 by a ^1H - ^{11}B HMQC NMR experiment, which revealed a coupling between the ^{11}B NMR signal at δ -29.7 and a ^1H NMR signal at δ 1.61 .

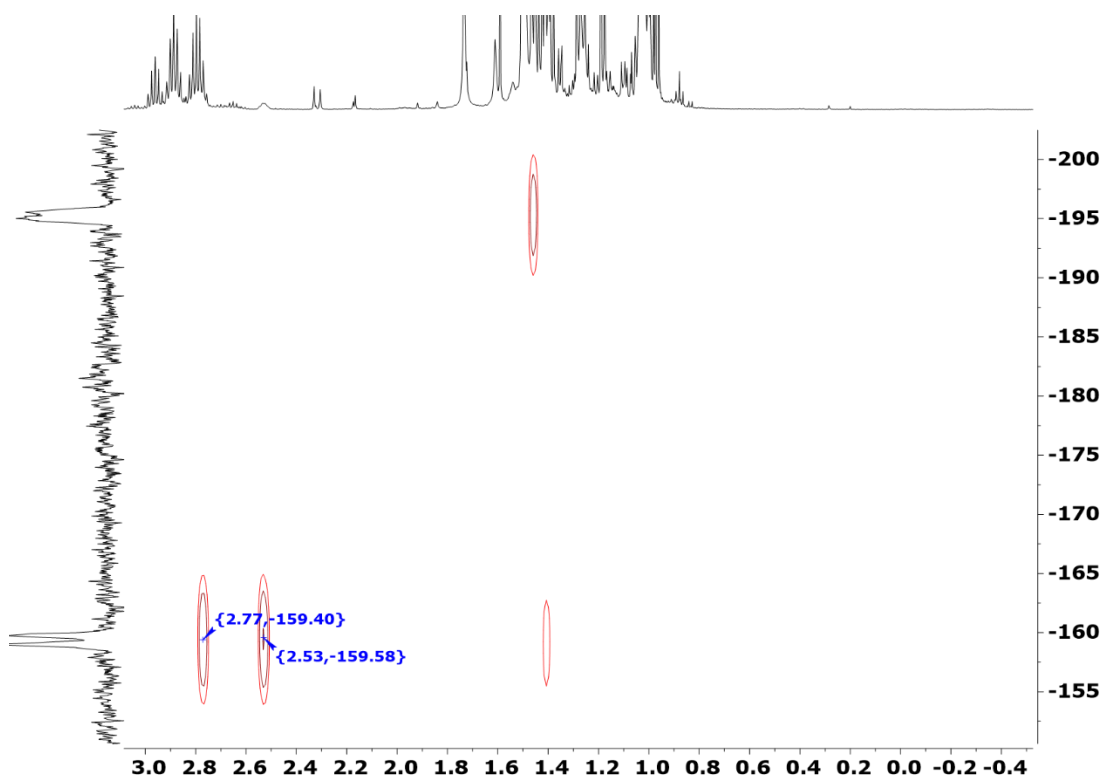


Figure 16: ^1H - ^{31}P HMBC NMR spectrum (500 MHz, 162 MHz, C_6D_6) of the reaction of **5.9** with $^{\text{Me}}i\text{Pr}$.

In summary, the different NMR analysis confirmed that the molecule contains two inequivalent phosphorus atoms, with a single hydrogen atom on each. This molecule also contains at least one tetracoordinate boron atom with a single hydrogen atom. The ^1H NMR signals for the ligand with new resonances also show the presence of

NHC (IPr) in an environment different from the starting material, free NHC and imidazolium salt. Together, this evidence suggests the effective formation of the parent diphosphadiboretane **5.10**. The asymmetry observed in the phosphorus and the hydrogen spectrum could possibly be due to a distortion of the four-membered ring. I propose the following asymmetric structure for **5.10**, which could explain the presence of two equivalent boron atoms, with two inequivalent phosphorus and hydrogen atoms (Figure 17). The two NHC ligands are on the same side, the ring is distorted as a butterfly conformation and one hydrogen substituent on the phosphorus is in an *endo* conformation, whilst the other one is in an *exo* conformation. The strained structure would provide a slow, if any, exchange of the hydrogen atoms between the *endo* and *exo* conformation and an asymmetry observable by ^{31}P and ^1H NMR spectroscopy.

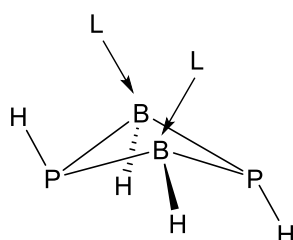


Figure 17: Proposed structure for product **5.10** ($L = \text{IPr}$).

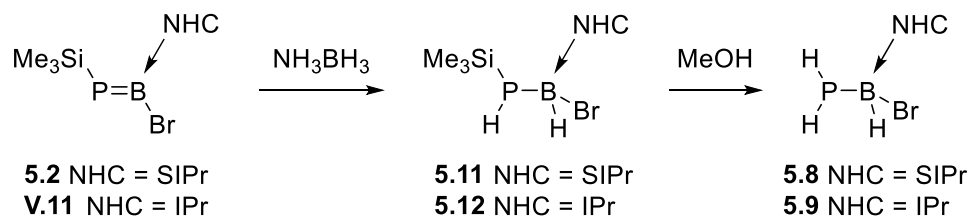
A variable temperature NMR experiment was run between room temperature and 70°C but no new product or disproportion of the product was observed by ^{31}P NMR spectroscopy. The product **5.10** showed thermal stability up to 70°C , where no change was observed by ^1H , ^{11}B and ^{31}P NMR spectroscopy.

Crystals were obtained; however, they were too small to be suitable for X-ray analysis. To date, the product has not been isolated.

Synthesis of the 1-hydrotrimethylsilyl-2-bromohydro-phosphinoboranes **5.11** and **5.12**

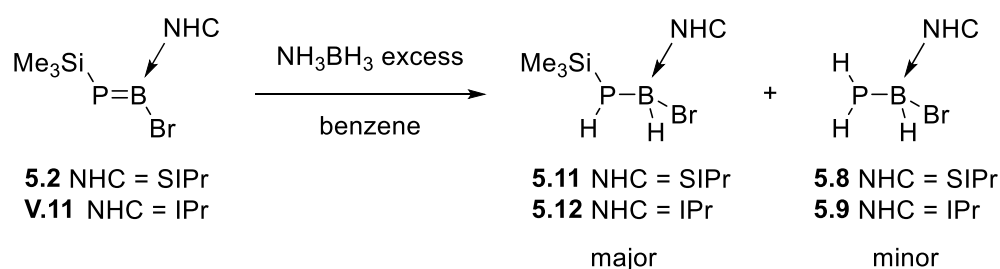
A different route to **5.10** or the SIPr equivalent would be to start from the phosphaborenes **5.2** or **V.11**. The advantage of this route would be to avoid the synthesis of **5.7** or **V.12**, which only gives a low yield.

Reacting the phosphaborenes **5.2** and **V.11** with the ammonia-borane (NH_3BH_3) gives the 1-hydrotrimethylsilyl-2-bromohydro-phosphinoboranes **5.11** and **5.12** respectively (*Scheme 30*). Reacting **5.11** and **5.12** with methanol allows the formation of **5.8** and **5.9** respectively. This route will provide a more convenient way to synthesise the necessary starting material to reach the NHC stabilised parent phosphaborene or diphosphadiboretane.



Scheme 30: New proposed route to the synthesis of **5.8** and **5.9**.

The phosphaborenes **5.2** and **V.11** were treated with an excess of NH_3BH_3 in benzene (*Scheme 31*). In both cases, NMR spectroscopic analysis showed the formation of the expected product **5.11** and **5.12**.



Scheme 31: Synthesis of the NHC-stabilised 1-hydrotrimethylsilyl-2-bromohydro-phosphinoboranes **5.11** and **5.12**.

The ^{31}P NMR spectrum from the reaction between **5.2** and NH_3BH_3 showed a new doublet at $\delta -196.2$ ($^1J_{\text{PH}} = 177$ Hz) as the major signal (Figure 18). The signal evidences the presence of a single hydrogen atom on the phosphorus centre and comes in the range of similar phosphinoboranes, confirming the formation of **5.11**. A small doublet at $\delta -233.5$ ($^1J_{\text{PH}} = 180$ Hz) and a small triplet at $\delta -214.1$ ($^1J_{\text{PH}} = 192$ Hz) are also observed but could not be assigned. Finally, the unexpected formation of **5.8** is observed in the ^{31}P NMR spectrum, with the triplet at $\delta -183.6$ ($^1J_{\text{PH}} = 195$ Hz). The ^{11}B NMR spectrum showed a broad singlet at $\delta -17.7$, which is in the range of the previously synthesised NHC coordinated phosphinoborane and was assigned to the product **5.11**. In addition to the main signal at $\delta -17.7$, smaller signals at $\delta 30.95$ and -20.8 , which cannot be assigned, are observed along with NH_3BH_3 ($\delta -33.9$).

The ^1H NMR spectrum showed the formation of one main product, the hydrogen atom on the phosphorus was not clearly identified. The different spectra evidenced the effective formation of the 1-hydrotrimethylsilyl-2-bromohydro-phosphinoborane **5.11**, along with the 1-dihydro-2-bromohydro-phosphinoborane **5.8**.

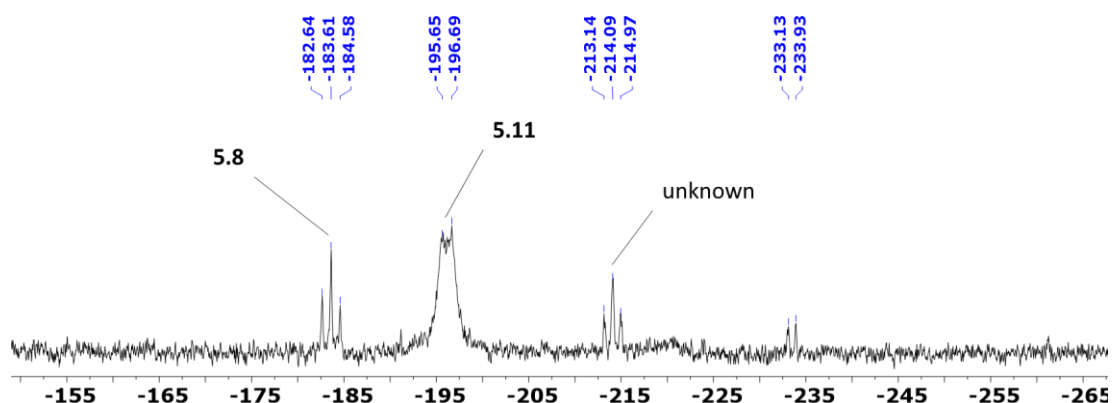


Figure 18: ^{31}P NMR spectrum (162 MHz, C_6D_6) of the reaction of phosphaborene **5.2** and NH_3BH_3 , focused on the relevant region.

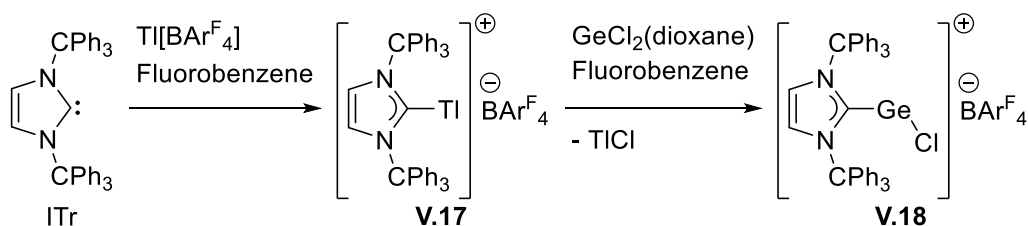
The reaction between **V.11** and NH_3BH_3 gave similar result (Scheme 31). The phosphinoborane **5.12** was observed as the main product in the ^{31}P NMR spectrum with a doublet at $\delta -194.0$ ($^1J_{\text{PH}} = 188$ Hz), along with two smaller unidentified signals at $\delta -213.1$ (t, $^1J_{\text{PH}} = 198$ Hz) and $\delta -234.1$ (d, $^1J_{\text{PH}} = 180$ Hz). Here again, the unexpected formation of **5.9** as a minor product occurred, evidenced by the triplet at $\delta -182.7$ ($^1J_{\text{PH}} = 192$ Hz). The ^{11}B NMR spectrum showed a singlet at $\delta -18.1$, which is in the typical region of the NHC coordinated phosphinoboranes and can be assigned to the product **5.12**, along with NH_3BH_3 . The ^1H NMR spectrum showed the formation of a new main product with all the expected signal, apart from the hydrogen atom on the phosphorus, which cannot be clearly identified due to the presence of many overlapping peaks. The NMR spectra evidenced the effective formation of the 1-hydrotrimethylsilyl-2-bromohydro-phosphinoborane **5.12** along with the 1-dihydro-2-bromohydro-phosphinoborane **5.9** as a minor product.

The unexpected formation of **5.8** and **5.9** as a minor product in the respective attempts to synthesise **5.11** and **5.12** suggested that treating the phosphaborene **5.2** or **V.11**

with a larger excess of NH_3BH_3 could form directly the phosphinoboranes **5.8** and **5.9** respectively, by abstracting the Me_3Si substituent on the phosphorus centre. No mechanistic study has been carried out to explain this substituent exchange on the phosphorus centre.

Attempted synthesis of a phosphinoborane with an extremely bulky NHC

In 2017, Eric Rivard and co-workers reported the facile synthesis of a new extremely bulky NHC, the 1,3-bis(trityl)imidazole-2-ylidene (ITr),^[35] along with the synthesis of low-valent inorganic cations **V.17** and **V.18** using this NHC (*Scheme 31*).

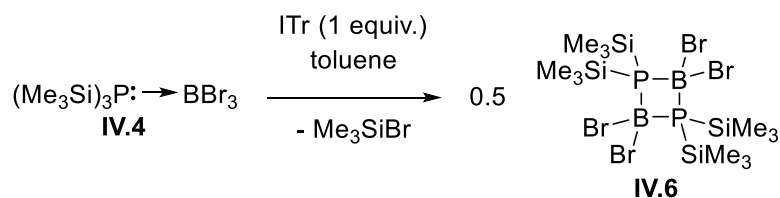


Scheme 31: Synthesis of low-valent inorganic complexes using ITr. $\text{BArF}_4 = \text{Tetrakis}(3,5\text{-bis}(\text{trifluoromethyl})\text{phenyl})\text{borate}$.

Using a bulkier NHC than the previously used IPr or SIPr could provide better shielding around the phosphorus-boron bond, allowing the possible stabilisation of molecular boron-phosphide, which cannot be achieved using common NHCs.

The phosphorus-boron adduct **IV.4** was treated with one equivalent of ITr in toluene (*Scheme 32*). The ^{31}P NMR spectrum showed one main species, represented by a septet at $\delta -98.0$ ($^1J_{\text{PB}} = 71$ Hz), while the ^{11}B NMR spectrum exhibited one main species represented by a triplet at $\delta -12.6$ ($^1J_{\text{BP}} = 72$ Hz). Analysis by NMR spectroscopy evidenced the formation of the reported dimer $[(\text{Me}_3\text{Si})_2\text{PBBR}_2]_2$ **IV.6**.^[7]

Interestingly the ^1H NMR spectrum revealed along with **IV.6** $[(\text{Me}_3\text{Si})_2\text{PBBBr}_2]_2$, only free Me_3SiBr and free ITr.



Scheme 32: Reaction between the phosphorus-boron adduct **IV.4** and ITr.

The bulky NHC ITr seems to promote catalytic elimination of Me_3SiBr . This is evidenced by the observation of free Me_3SiBr and free ITr along with the dimer **IV.6**. In spite of the interesting reactivity of ITr, the results showed unfortunately that ITr was too bulky to coordinate to the phosphinoborane or the phosphaborene and was just promoting the formation of the base free dimer $[(\text{Me}_3\text{Si})_2\text{PBBBr}_2]_2$ **IV.6**.

Conclusion and perspectives

A series of minimally substituted phosphinoboranes **5.1**, **5.4** and phosphaborenes **5.2**, **5.7** have been synthesized (*Figure 19*). These compounds are analogous to those synthesized by A. Price with IPr (**V.9-12**). The structural characteristics and reactivity were very close to their analogous IPr compounds. The *E/Z* equilibrium observed for the phosphaborene **5.7** has been experimentally and theoretically studied (*calculation carried out by D. De Rosa*), the results were concordant and showed a small difference in energy between the two isomers. This was in accordance with the equilibrium observed experimentally in solution.

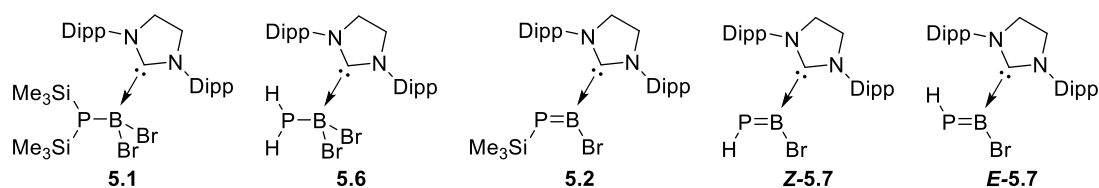


Figure 19: The isolated phosphinoboranes **5.1**, **5.6** and phosphaborenes **5.2** and **5.7**.

Attempts to coordinate Lewis acids to the phosphaborene **5.2** were unsuccessful. Changing the NHC from IPr to SIPr did not allow the synthesis of molecular boron-phosphide stabilised by the respective NHC. The phosphaborene **5.2** was not reactive to the different conditions tried to remove the last Me_3SiBr substituents from it. Attempts from the phosphinoborane **5.1** showed undesired C–H activated product (as with **5.4**). Changing the size of the ligand to bulkier NHC ITr did not afford coordination and gave catalytic elimination of Me_3SiBr from the phosphorus-boron adduct **IV.4**, promoting the formation of the dimer **IV.6** $[(\text{Me}_3\text{Si})_2\text{PBBr}_2]_2$ instead. These results suggest that base-stabilised boron-phosphide will not be achievable by simple Me_3SiBr elimination.

The reaction between the phosphaborenes **5.7** or **V.12** and NH_3BH_3 gave respectively the phosphinoboranes **5.8** and **5.9** (Figure 20). The phosphinoborane **5.9** was isolated and treatment with the NHC $^{\text{Me}}\text{IPr}$ or KO^tBu gave promising results, which evidenced the formation of the parent diphosphadiboretane **5.10**, however, **5.10** has not been isolated up to this date.

A different possible route to the NHC stabilised parent diphosphadiboretane **5.10** has been explored, with the successful hydrogenation of the phosphaborenes **5.2** and **V.11** using NH_3BH_3 , allowing formation of the phosphinoboranes **5.11** and **5.12**, observed by NMR spectroscopy.

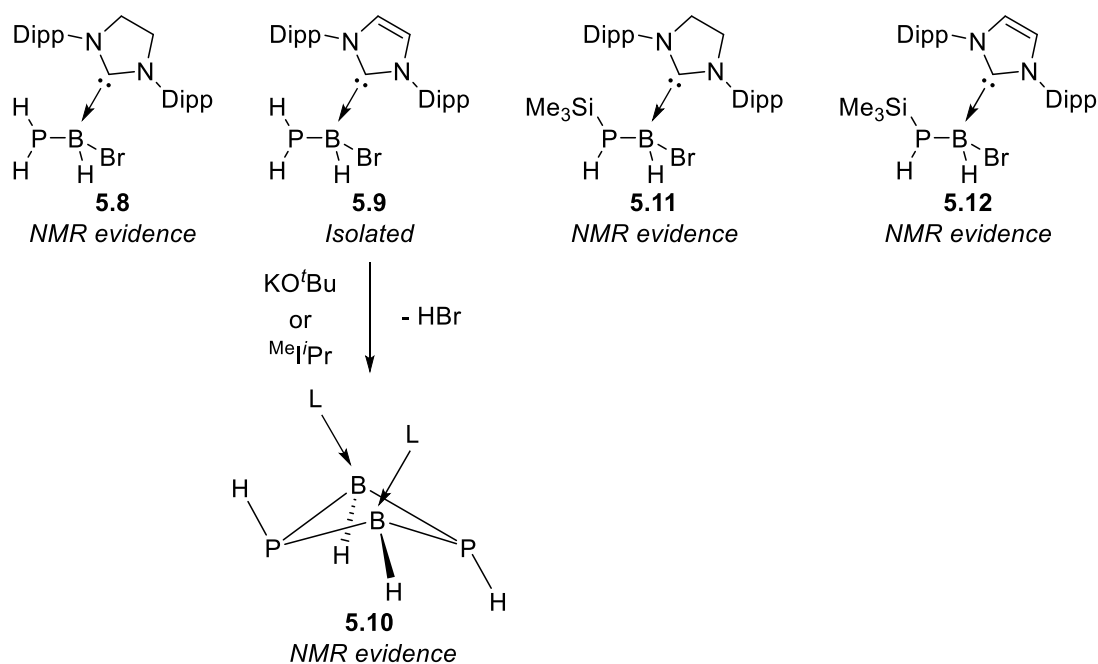


Figure 20: The isolated phosphinoborane **5.9**, the observed phosphinoboranes **5.8**, **5.11**, **5.12** and the observed parent diphosphadiboretane **5.10**.

Using **5.9** or **5.11**, isolation of **5.10** should be carried out, along with reactivity studies. Reduction of **5.10** could give interesting cluster of NHC stabilised boron-phosphide. Adding a Lewis base or Lewis acid could promote the ring opening and give the acid-base stabilised parent phosphaborene. Similar work could be carried out on the SIPr analogues **5.8** and **5.11**.

As the different routes explored with IPr, SIPr or ITr did not allow the successful synthesis of molecular boron-phosphide, redesigning the ligand could be a possibility, to provide stable molecular boron-phosphide. For example, bis-NHC ligand has shown abilities to stabilise the silylone **1.90** (See Chap. 1, *Silylone*). Using a bis-NHC ligand could provide an extra stabilisation to the borylene intermediate which has been shown to undergo C–H activation (like in the case of **5.4**). By preventing C–H activation, bis-NHC stabilised boron-phosphide could possibly be reached (Figure 21).

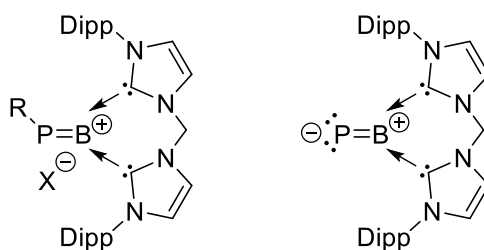


Figure 21: Proposed targets to reach molecular boron-phosphide using a bis-NHC ligand.

All attempts to synthesize base-stabilised boron-phosphide by elimination of Me_3SiBr or HBr from phosphinoboranes were unsuccessful, giving either phosphaborenes or other undesired products. The preparation of all the base-stabilised diatomic(0) compounds $(\text{L})\text{E}-\text{E}(\text{L})$ ($\text{E} = \text{B}, \text{P}, \text{As}, \text{Si}, \text{Ge}, \text{Sn}$) only involved reduction of halogenated base-adduct precursors (See Chap. IV, *Base-stabilised low-coordinate main-group (E=E) compounds*). A last possible route to reach molecular boron-phosphide could be to redesign the phosphorus-boron adduct used, in order to reach an NHC-stabilised phosphinoborane only substituted with halogen atoms (Figure 22). NHC-phosphorus adducts $\text{NHC} \rightarrow \text{PX}_3$ have only been achieved with halogen substituents on the phosphorus atom. The synthesis of a fully halogenated substituted phosphinoborane may allow coordination of NHC to both boron and phosphorus centres, creating a good candidate for reduction to reach molecular boron-phosphide or bigger clusters.

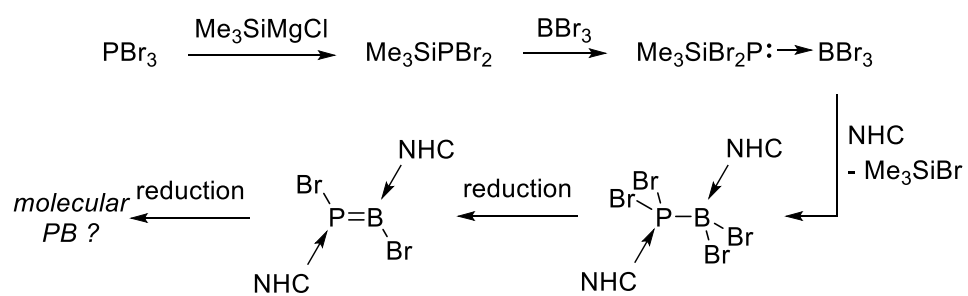


Figure 22: Proposed route to phosphinoborane and phosphaborene substituted with bromine atoms.

References

- [1] R. T. Paine, H. Nöth, *Chem. Rev.* **1995**, *95*, 343–379.
- [2] A. B. Burg, *Inorg. Chem.* **1978**, *17*, 593–599.
- [3] U. Vogel, P. Hoemensch, K. C. Schwan, A. Y. Timoshkin, M. Scheer, *Chem. - A Eur. J.* **2003**, *9*, 515–519.
- [4] K. C. Schwan, A. Y. Timoskin, M. Zabel, M. Scheer, *Chem. - A Eur. J.* **2006**, *12*, 4900–4908.
- [5] C. Marquardt, A. Adolf, A. Stauber, M. Bodensteiner, A. V. Virovets, A. Y. Timoshkin, M. Scheer, *Chem. - A Eur. J.* **2013**, *19*, 11887–11891.
- [6] C. Marquardt, O. Hegen, A. Vogel, A. Stauber, M. Bodensteiner, A. Y. Timoshkin, M. Scheer, *Chem. - A Eur. J.* **2018**, *24*, 360–363.
- [7] M. S. Lube, R. L. Wells, P. S. White, *Inorg. Chem.* **1996**, *35*, 5007–5014.
- [8] A. N. Price, *The Synthesis and Reactivity of Phosphorus-Boron Multiple Bonds*, University of Edinburgh, **2018**.
- [9] M. L. J. Hackney, A. D. Norman, *J. Chem. Soc., Chem. Commun.* **1986**, 850–851.
- [10] U. Vogel, M. Scheer, *Zeitschrift für Anorg. und Allg. Chemie* **2001**, *627*, 1593–1598.
- [11] U. Vogel, A. Y. Timoshkin, K. C. Schwan, M. Bodensteiner, M. Scheer, *J. Organomet. Chem.* **2006**, *691*, 4556–4564.
- [12] F. Dahcheh, D. Martin, D. W. Stephan, G. Bertrand, *Angew. Chem. Int. Ed.* **2014**, *53*, 13159–13163.
- [13] A. N. Price, M. J. Cowley, *Chem. - A Eur. J.* **2016**, *22*, 6248–6252.
- [14] E. Rivard, W. A. Merrill, J. C. Fettinger, P. P. Power, *Chem. Commun.* **2006**, 3800–3802.
- [15] E. Rivard, W. A. Merrill, J. C. Fettinger, R. Wolf, G. H. Spikes, P. P. Power, *Inorg. Chem.* **2007**, *46*, 2971–2978.
- [16] A. N. Price, G. S. Nichol, M. J. Cowley, *Angew. Chem. Int. Ed.* **2017**, *56*, 9953–9957.
- [17] Y. Wang, B. Quillian, P. Wei, C. S. Wannere, Y. Xie, R. B. King, H. F. Schaefer, P. V. R. Schleyer, G. H. Robinson, *J. Am. Chem. Soc.* **2007**, *129*, 12412–12413.
- [18] H. Braunschweig, R. D. Dewhurst, K. Hammond, J. Mies, K. Radacki, A. Vargas, *Science* **2012**, *336*, 1420–1422.

- [19] H. Braunschweig, W. C. Ewing, K. Geetharani, M. Schäfer, *Angew. Chem. Int. Ed.* **2015**, *54*, 1662–1665.
- [20] P. Bissinger, H. Braunschweig, A. Damme, C. Hörl, I. Krummenacher, T. Kupfer, *Angew. Chem. Int. Ed.* **2015**, *54*, 359–362.
- [21] H. Braunschweig, M. A. Celik, R. D. Dewhurst, K. Ferkinghoff, A. Hermann, J. O. C. Jimenez-Halla, T. Kramer, K. Radacki, R. Shang, E. Siedler, et al., *Chem. - A Eur. J.* **2016**, *22*, 11736–11744.
- [22] T. J. Hadlington, T. Szilvási, M. Driess, *Chem. Sci.* **2018**, *9*, 2595–2600.
- [23] W. J. Grigsby, P. P. Power, *J. Am. Chem. Soc.* **1996**, *118*, 7981–7988.
- [24] H. Braunschweig, T. Kupfer, K. Radacki, K. Wagner, A. Damme, P. Bissinger, R. D. Dewhurst, *J. Am. Chem. Soc.* **2011**, *133*, 19044–19047.
- [25] Y. Wang, G. H. Robinson, *Inorg. Chem.* **2011**, *50*, 12326–12327.
- [26] B. D. Ellis, C. A. Dyker, A. Decken, C. L. B. Macdonald, *Chem. Commun.* **2005**, 1965–1967.
- [27] J. Holz, A. Monsees, H. Jiao, J. You, I. V. Komarov, C. Fischer, K. Drauz, A. Börner, *J. Org. Chem.* **2003**, *68*, 1701–1707.
- [28] S. K. Gibbons, Z. Xu, R. P. Hughes, D. S. Glueck, A. L. Rheingold, *Organometallics* **2018**, *37*, 2159–2166.
- [29] K. Issleib, E. Leißring, M. Riemer, H. Oehme, *Zeitschrift für Chemie* **1983**, *23*, 99–100.
- [30] M. Driess, S. Block, M. Brym, M. T. Gamer, *Angew. Chem. Int. Ed.* **2006**, *45*, 2293–2296.
- [31] J. D. Watts, L. C. Van Zant, *Chem. Phys. Lett.* **1996**, *251*, 119–124.
- [32] A. K. Swarnakar, C. Hering-Junghans, M. J. Ferguson, R. McDonald, E. Rivard, *Chem. Sci.* **2017**, *8*, 2337–2343.
- [33] G. Glockler, *Trans. Faraday Soc.* **1963**, *59*, 1080–1085.
- [34] B. Wrackmeyer, *Z. Naturforsch.* **2004**, *59b*, 1192–1199.
- [35] M. M. D. Roy, P. A. Lummis, M. J. Ferguson, R. McDonald, E. Rivard, *Chem. - A Eur. J.* **2017**, *23*, 11249–11252.

Summary and Outlook

Summary and Outlook

In Chapter II, the reactivity of a silylene towards oxidative addition of main group halide compounds was studied. The products formed (**2.1**, **2.5**, **2.6**, **2.7**, **2.8** and **2.10**) have limited stability (*Figure 1*). This can be attributed to a lack of steric protection, or to the electronic properties of the N-heterocyclic silylene used. Heterocyclic silylenes with enhanced electronic properties could be the solution to approach reactivity comparable to N-heterocyclic carbenes.

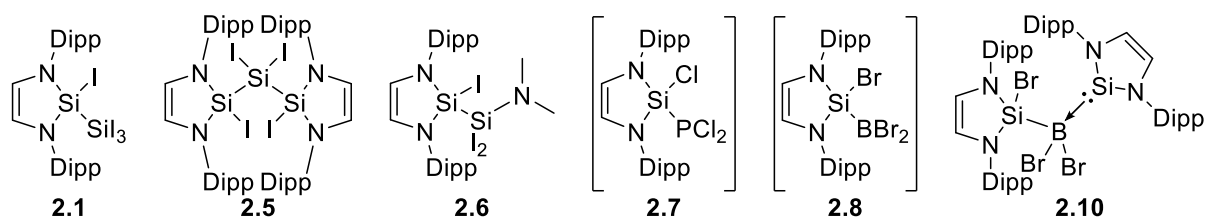


Figure 1: The synthesised species **2.1**, **2.5**, **2.6** and **2.10** and the transient compounds **2.7** and **2.8**.

Following this idea, in Chapter III the synthesis of an anti-Bredt silylene **3.6** was attempted (*Figure 2*). The diamine ligand precursor **3.4** has been successfully synthesised. Attempts of ring closing reactions between the ligand and silicon tetrachloride did not give the expected results (**3.5**), and silicon seems to be too small to fit in the pocket, possibly because the geometric constraint could be too high. However, the diamine ligand still has potential due to its cyclic structure and it would be interesting to study coordination to other main group elements or transition metals.

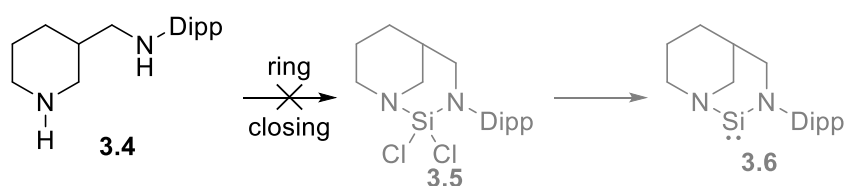


Figure 2: The synthesised diamine ligand **3.4** and the targeted product **3.5** and **3.6**.

A new series of phosphinoboranes (**5.1** and **5.6**) and phosphaborenes (**5.2** and **5.7**) has been synthesised (*Figure 3*). Hydrogenation of phosphaborenes back to the phosphinoboranes (**5.8**, **5.9**, **5.10** and **5.11**) is possible using NH_3BH_3 and further HBr elimination allowed the observation of the parent diphosphadiboretane **5.10** (*Figure 3*). All attempts to synthesise base-stabilised boron-phosphide were unsuccessful, coordination to Lewis acid, or further base-promoted elimination of Me_3SiBr did not work.

This leads to the conclusion that the approach used to molecular boron-phosphide must be rethought. Reduction of the precursor $\text{Br}_2\text{PBBr}_2(\text{IPr})$, or a complete change of ligand for a pincer ligand, could be a solution to reach base-stabilised boron phosphide.

The observed parent diphosphadiboretane **5.10** is a promising result. Isolating this compound is of interest as ring opening reactions using Lewis acid or bases could also lead to the parent base or acid-base-stabilised parent phosphaborene. Reduction reactions could also lead to molecular boron-phosphide or bigger phosphorus-boron clusters.

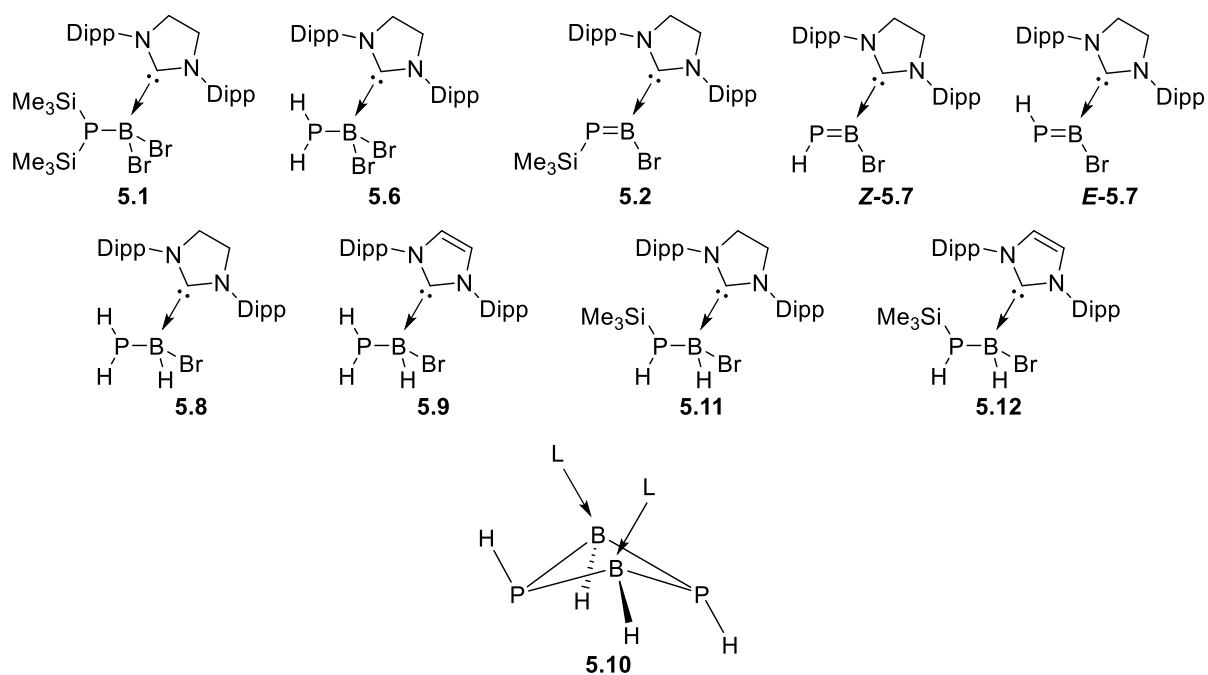


Figure 3: The isolated phosphinoboranes (**5.1**, **5.6** and **5.9**), the isolated phosphaborenes (**5.2** and **5.7**), the observed phosphinoboranes (**5.8**, **5.11** and **5.12**) and the observed base-stabilised parent diphosphadiboretane **5.10**. L = IPr.

Experimental Methods

Experimental Methods

General Information

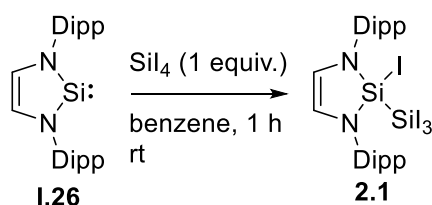
Unless stated otherwise, all manipulations were carried out under an argon atmosphere using standard Schlenk and/or glovebox techniques. Solvents were dried over Na/benzophenone and distilled under argon. C₆D₆ and THF-d₈ were dried over potassium then distilled under argon. NMR spectra were recorded on Bruker PRO 500 MHz (¹H 500.2 MHz, ¹¹B 160.5 MHz ¹³C 125.8 MHz, ³¹P 202.5 MHz, ²⁹Si 99.4 MHz), AVA 600 MHz (¹H 600.8 MHz, ¹³C 151.1 MHz), AVA 500 MHz (¹H 500.1 MHz, ¹³C 125.8 MHz) or AVA 400 MHz (¹H 400.1 MHz, ¹¹B 128.4 MHz ³¹P 162.0 MHz) spectrometers at 298K. ¹H and ¹³C spectra were referenced to residual signals in the solvent. ³¹P and ¹¹B NMR were referenced to external standards (phosphoric acid and trimethyl borate respectively). Background signals in ¹¹B NMR spectra arise to a significant degree from glass components of the cryoprobes used in our spectrometers; these cannot be mitigated through the use of quartz NMR tubes. UV/Vis spectra were acquired under argon in hexane or toluene using a Varian Cary® 50 UV-Vis Spectrophotometer. Melting points (mp) were determined on a Stuart Scientific SMP10 melting point apparatus in sealed capillary tubes under argon. Silylene **I.26**,^[1] 1,4-bis(trimethylsilyl)-1,4-diaza-2,5-cyclohexadiene **II.11**,^[2] IPr,^[3] MeⁱPr, MeIMe,^[4] SIPr,^[5] and ITr^[6] were prepared according literature methods.

Experimental Details for Chapter II

Reaction between silylene **1.26** and SiCl₄

Attempt 1: A solution of **1.26** (200 mg, 0.50 mmol, 1.0 equiv.) in hexane (10 mL) was added dropwise to a solution of SiCl₄ (62 μ L, 0.55 mmol, 1.1 equiv.) in hexane (10 mL) at room temperature. The solution was stirred for 12 hours at room temperature, filtrated and then all volatiles were removed under vacuum. ¹H and ²⁹Si NMR spectra showed only the starting material **1.26**.

Preparation of the disilane **2.1**

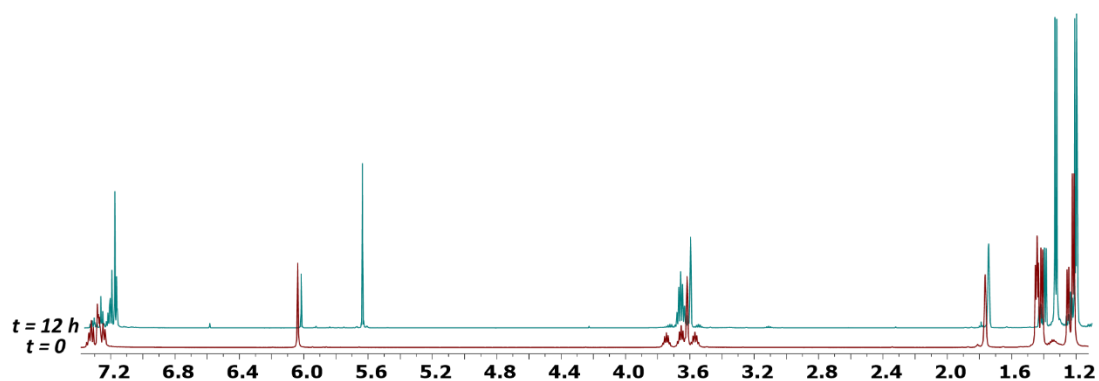


A solution of **1.26** (2.50 g, 6.20 mmol, 1.0 equiv.) in benzene (15 mL) was added to a solution of SiI₄ (3.60 g, 6.80 mmol, 1.1 equiv.) in benzene (15 mL). The resulting orange/red solution was stirred for one hour at room temperature. All volatiles were removed under vacuum. The obtained orange foam was washed with hexane, resulting in the precipitation of an orange solid. The solution was cooled down to –20°C overnight, filtered and the solid residue was dried *in vacuo*. The disilane **2.1** was obtained as a bright orange solid (3.29 g, 3.5 mmol, 57%). **Melting point** (argon sealed capillary) 157°C (dp). **Elemental analysis calculated** (%) for C₂₆H₃₆I₄N₂Si₂ (940.38): C 33.21, H 3.86, N 2.98; found: C 32.84, H 4.45, N 3.02%.

¹H NMR (500 MHz, C₆D₆, δ) 7.23-7.20 (m, 2H, Ar *para*-H), 7.18-7.14 (m, 4H, Ar *meta*-H), 5.74 (s, 2H, NCHCHN), 3.82 (sept, 2H, ³J_{HH} = 6.7 Hz, CH(CH₃)₂), 3.60 (sept, 2H, ³J_{HH} = 6.7 Hz, CH(CH₃)₂), 1.46 (d, 6H, ³J_{HH} = 6.7 Hz, CH(CH₃)₂), 1.44 (d, 6H, ³J_{HH} = 6.7 Hz, CH(CH₃)₂), 1.25 (d, 6H, ³J_{HH} = 6.7 Hz, CH(CH₃)₂), 1.19 (d, 6H, ³J_{HH} = 6.7 Hz, CH(CH₃)₂). **¹³C NMR (125 MHz, C₆D₆, δ)** 147.7 (s, 2C, Ar **C^{ortho}**), 147.1 (s, 2C, Ar **C^{ortho}**), 137.5 (s, 2C, Ar **C^{ipso}**), 128.2 (s, 2C, Ar **C^{para}**), 124.8 (s, 2C, Ar **C^{meta}**), 123.5 (s, 2C, Ar **C^{meta}**), 121.9 (s, 2C, NCHCHN), 29.8 (s, 2C, CH(CH₃)₂), 28.8 (s, 2C, CH(CH₃)₂), 26.4 (s, 2C, CH(CH₃)₂), 25.8 (s, 2C, CH(CH₃)₂), 24.1 (s, 2C, CH(CH₃)₂), 21.9 (s, 2C, CH(CH₃)₂). **²⁹Si NMR (99 MHz, C₆D₆, δ)** –74.5 (N-Si(I)-N, ¹J_{SiSi} = 201.3 Hz), –123.2 (Si-SiI₃, ¹J_{SiSi} = 201.3 Hz).

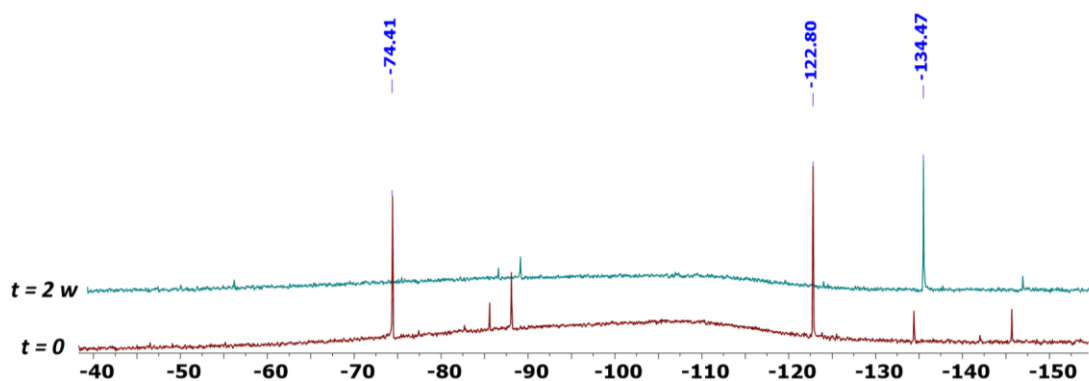
Monitoring of the stability of **2.1** in solution

A sample of pure **2.1** (5 to 10 mg) was dissolved in THF-d8 (1 mL) at room temperature. The decomposition of **2.1** in THF-d8 was monitored by ^1H NMR spectroscopy at room temperature.

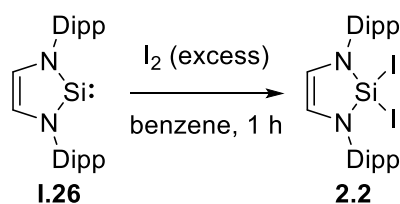


^1H NMR Spectrum (600 MHz, THF-d8) of the monitoring of the stability of **2.1** in polar solvent (THF-d8).

The silylene **1.26** (0.20 g, 0.50 mmol, 1.0 equiv.) and SiI_4 (0.29 g, 0.55 mmol, 1.1 equiv.) were dissolved in C_6D_6 (1 mL) at room temperature, to generate the disilane **2.1**. The decomposition of **2.1** in C_6D_6 was monitored by ^{29}Si NMR spectroscopy at room temperature.

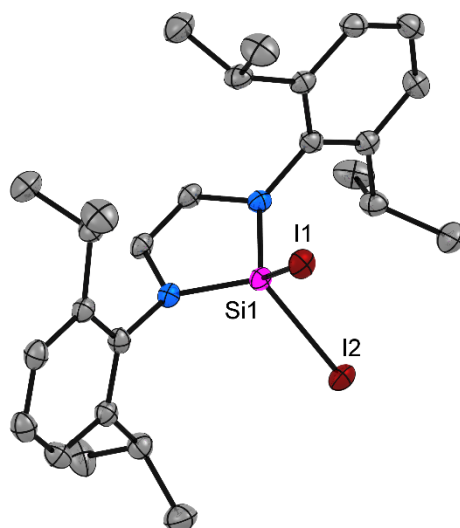


^{29}Si NMR (99 MHz, C_6D_6) of the monitoring of the stability of **2.1** in non-polar solvent (C_6D_6).

Preparation of the diiodosilane **2.2**

Silylene **1.26** (100 mg, 0.25 mmol, 1 equiv.) was dissolved in benzene (10 mL). Iodine (70.0 mg, 0.27 mmol, 1.1 equiv.) was added to the solution. The solution was stirred at room temperature for one hour. All volatiles were removed under vacuum. NMR showed full conversion, no isolated yield was calculated due to the instability of **2.2** in solid-state. **Mass Peak Analysis:** Calculated mass for **2.2** $C_{26}H_{36}I_2N_2Si$ for most abundant isotopes: 658.07318 Da; Observed mass peak: 658.07147 Da.

1H NMR (500 MHz, C_6D_6 , δ) 7.22-7.19 (m, 2H, Ar *para*-H), 7.16-7.14 (m, 4H, Ar *meta*-H), 5.77 (s, 2H, NCHCHN), 3.76 (sept, 4H, $^3J_{HH} = 6.8$ Hz, $CH(CH_3)_2$), 1.42 (d, 12H, $^3J_{HH} = 6.8$ Hz, $CH(CH_3)_2$), 1.17 (d, 12H, $^3J_{HH} = 6.8$ Hz, $CH(CH_3)_2$). **^{13}C NMR (125 MHz, C_6D_6 , δ)** 148.2 (s, 4C, Ar C^{ortho}), 135.4 (s, 2C, Ar C^{ipso}), 128.3 (s, 2C, Ar C^{para}), 124.4 (s, 4C, Ar C^{meta}), 121.1 (s, 2C, NCHCHN), 28.8 (s, 4C, $CH(CH_3)_2$), 26.1 (s, 4C, $CH(CH_3)_2$), 24.0 (s, 4C, $CH(CH_3)_2$). **^{29}Si NMR (99 MHz, C_6D_6 , δ)** -134.5.

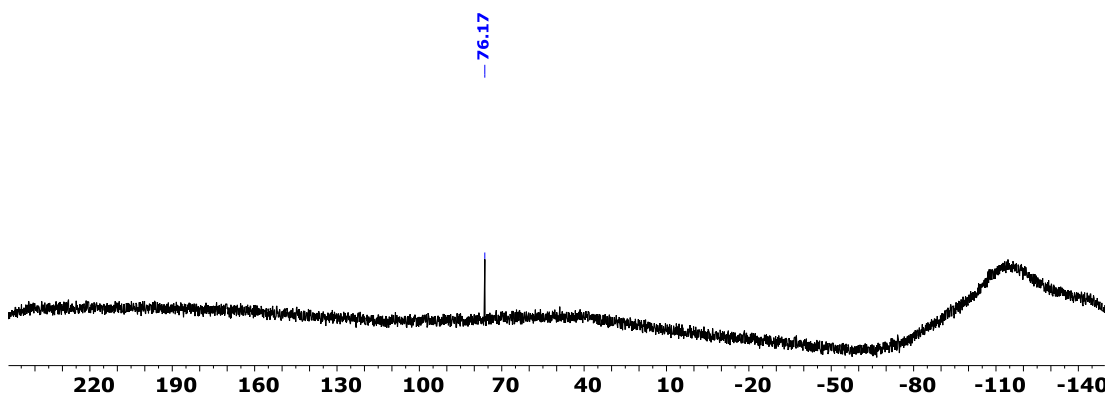


Molecular structure of **2.2** in the solid state. Ellipsoids are shown at 50% probability; hydrogen atoms are omitted for clarity. Selected bond distances [\AA] and angles [$^\circ$] for **2.2**: Si1–N1 1.712(2), Si1–N2 1.712(2), N1–Si1–N2 93.42(17).

Reduction of the disilane 2.1

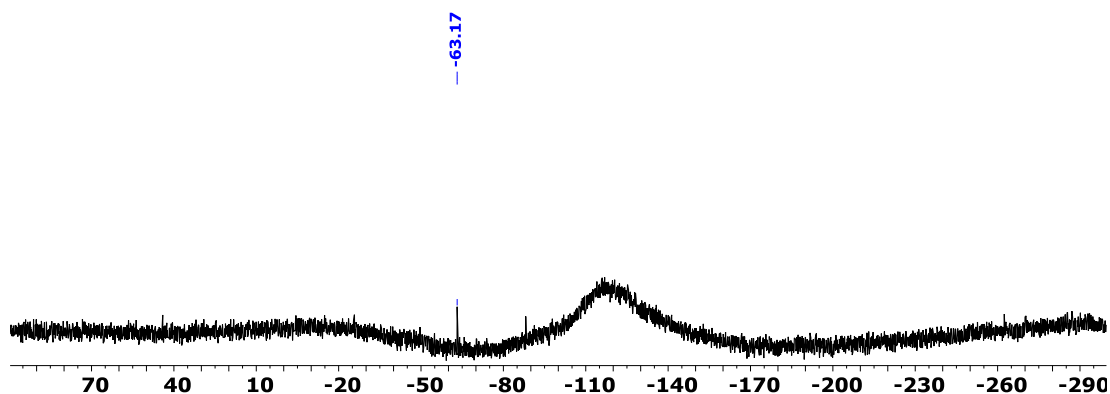
Attempt 1: Disilane **2.1** (200 mg, 0.21 mmol, 1.0 equiv.) and KC_8 (110 mg, 0.84 mmol, 4.0 equiv.) were dissolved in THF (10 mL) at room temperature. The mixture was stirred overnight and filtered. All volatiles were removed under vacuum. The ^{29}Si NMR spectrum (99 MHz, C_6D_6) showed no signal.

Attempt 2: Disilane **2.1** (1.00 g, 1.06 mmol, 1.0 equiv.) and KC_8 (0.57 g, 4.24 mmol, 4.0 equiv.) were dissolved in THF (30 mL) at room temperature. The mixture was stirred overnight and filtered. All volatiles were removed under vacuum. The ^{29}Si NMR spectrum (99 MHz, C_6D_6) showed a signal at δ 76.2, which corresponds to the silylene **I.26**.



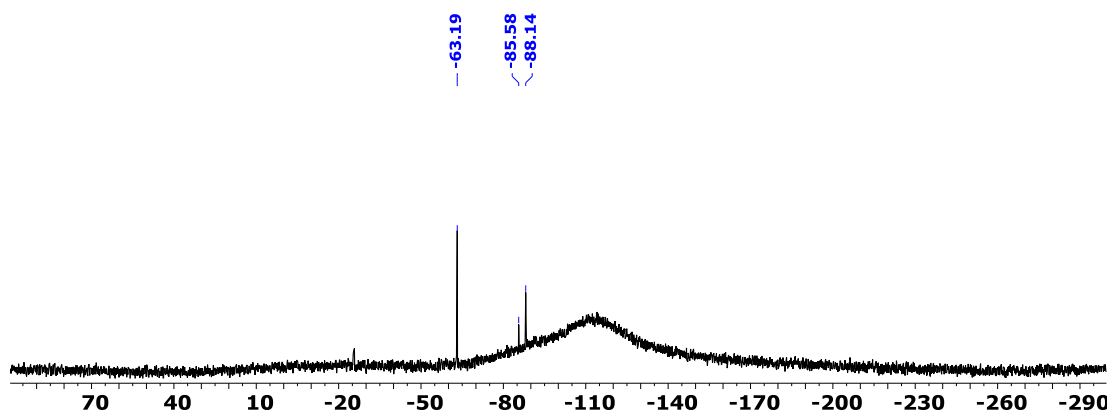
^{29}Si NMR (99 MHz, C_6D_6) of the reduction of **2.1** with KC_8 (4.0 equiv.) in THF.

Attempt 3: Disilane **2.1** (1.00 g, 1.06 mmol, 1.0 equiv.) and KC_8 (0.29 g, 2.17 mmol, 2.0 equiv.) were dissolved in THF (30 mL) at -70°C . The mixture was allowed to warm up to room temperature, stirred overnight and filtered. All volatiles were removed under vacuum. The ^{29}Si NMR spectrum (99 MHz, C_6D_6) showed a signal at δ -63.2.



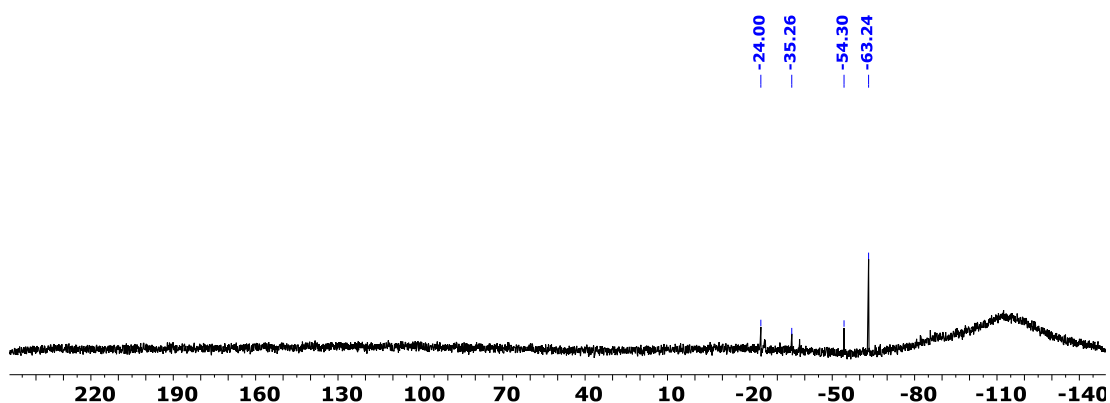
^{29}Si NMR (99 MHz, C_6D_6) of the reduction of **2.1** with KC_8 (2.0 equiv.) in THF at -70°C .

Attempt 4: Disilane **2.1** (0.30 g, 0.32 mmol, 1.0 equiv.) and KC_8 (0.09 g, 0.64 mmol, 2.0 equiv.) were dissolved in THF (10 mL) at room temperature. The mixture was stirred overnight and filtered. All volatiles were removed under vacuum. The ^{29}Si NMR spectrum (99 MHz, 298K, C_6D_6) showed signals at $\delta -63.2$, $\delta -85.6$ and $\delta -88.1$.



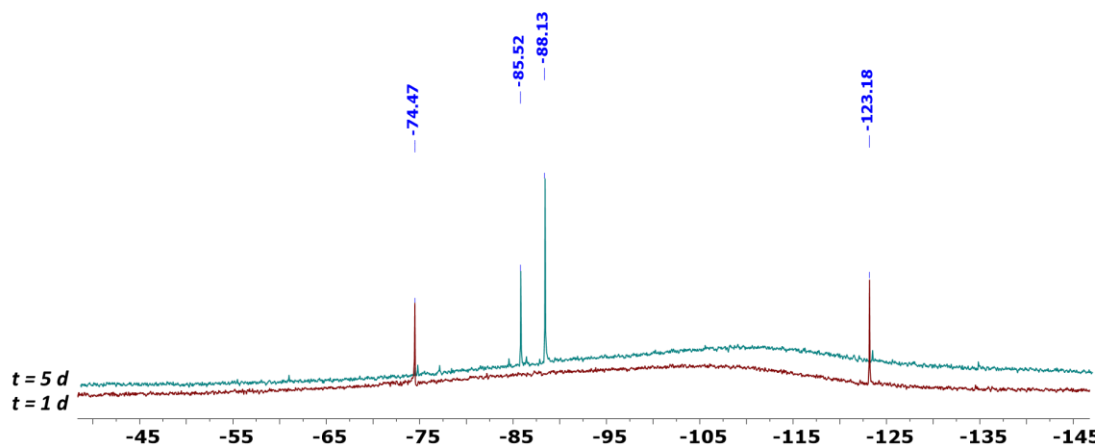
^{29}Si NMR (99 MHz, C_6D_6) of the reduction of **2.1** with KC_8 (2.0 equiv.) in THF at room temperature.

Attempt 5: A lithium naphthalenide solution in THF (1.6 mL, 0.64 mmol, $C = 0.4$ M, 2 equiv.) was added dropwise to a solution of disilane **2.1** (300 mg, 0.32 mmol, 1 equiv.) in THF (10 mL) at -80°C . The mixture was allowed to warm up to room temperature, stirred overnight and filtered. All volatiles were removed under vacuum. The ^{29}Si NMR spectrum (99 MHz, C_6D_6) showed unidentified signals at $\delta -24.0$, -35.3 , -54.3 , -63.2 .

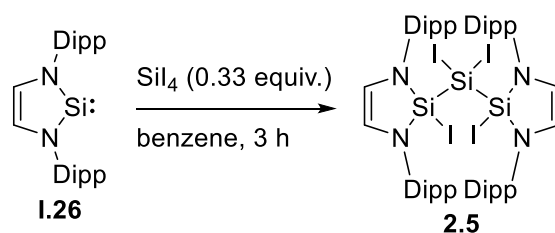


^{29}Si NMR (99 MHz, C_6D_6) of the reduction of **2.1** with LiNap (2.0 equiv.) in THF at -80°C .

Attempt 6: Disilane **2.1** (300 mg, 0.32 mmol, 1.0 equiv.) and KC_8 (170 mg, 1.28 mmol, 4.0 equiv.) were dissolved in benzene (10 mL) at room temperature. The solution was stirred and monitored by ^{29}Si NMR spectroscopy. After one day, only the starting material **2.1** was observed ($\delta -74.5, -123.2$). After five days, two signals at $\delta -85.6$ and $\delta -88.1$ were observed.



^{29}Si NMR (99 MHz, C_6D_6) of the monitoring of the reduction of **2.1** with KC_8 (4.0 equiv.) in benzene at room temperature.

Preparation of the trisilane **2.5**


SiI_4 (500 mg, 0.93 mmol, 1.0 equiv.) and **1.26** (1.13 g, 2.80 mmol, 3.0 equiv.) were dissolved in benzene (20 mL). The solution was stirred at room temperature for three hours. All volatiles were removed under vacuum. Crystals were grown from a pentane solution at -20°C overnight. The crystals were isolated by filtration and dried *in vacuo*, affording the trisilane **2.5** as a yellow solid (690 mg, 0.51 mmol, 55%). **Melting point** (argon sealed capillary) 126°C (dp). **Elemental analysis calculated** (%) for $\text{C}_{52}\text{H}_{72}\text{I}_4\text{N}_4\text{Si}_3$ (1345.05): C 46.43, H 5.40, N 4.17; found: C 43.10, H 5.55, N 4.10%.

^1H NMR (500 MHz, C_6D_6 , δ) 7.20-7.11 (m, 12H, Ar *meta*-H and *para*-H), 5.55 (d, 2H, $^3J_{\text{HH}} = 3.5$ Hz, NCHCHN), 5.49 (d, 2H, $^3J_{\text{HH}} = 3.5$ Hz, NCHCHN), 3.97 (sept, 2H, $^3J_{\text{HH}} = 6.8$ Hz, $\text{CH}(\text{CH}_3)_2$), 3.89 (sept, 2H, $^3J_{\text{HH}} = 6.7$ Hz, $\text{CH}(\text{CH}_3)_2$), 3.79 (sept, 2H, $^3J_{\text{HH}} = 6.8$ Hz, $\text{CH}(\text{CH}_3)_2$), 3.49 (sept, 2H, $^3J_{\text{HH}} = 6.7$ Hz, $\text{CH}(\text{CH}_3)_2$), 1.48 (d, 6H, $^3J_{\text{HH}} = 6.8$ Hz, $\text{CH}(\text{CH}_3)_2$), 1.45 (d, 12H, $^3J_{\text{HH}} = 6.7$ Hz, $\text{CH}(\text{CH}_3)_2$), 1.41 (d, 6H, $^3J_{\text{HH}} = 6.7$ Hz, $\text{CH}(\text{CH}_3)_2$), 1.17 (d, 6H, $^3J_{\text{HH}} = 6.7$ Hz, $\text{CH}(\text{CH}_3)_2$), 1.14 (d, 12H, $^3J_{\text{HH}} = 6.8$ Hz, $\text{CH}(\text{CH}_3)_2$), 1.12 (d, 12H, $^3J_{\text{HH}} = 6.8$ Hz, $\text{CH}(\text{CH}_3)_2$), 1.06 (d, 12H, $^3J_{\text{HH}} = 6.8$ Hz, $\text{CH}(\text{CH}_3)_2$). ^{13}C NMR (125 MHz, C_6D_6 , δ) 148.5 (s, 2C, Ar C^{ortho}), 147.9 (s, 4C, Ar C^{ortho}), 147.5 (s, 2C, Ar C^{ortho}), 140.3 (s, 2C, Ar C^{ipso}), 139.9 (s, 2C, Ar C^{ipso}), 128.2 (s, 4C, Ar C^{para}), 124.9 (s, 2C, Ar C^{meta}), 124.5 (s, 2C, Ar C^{meta}), 123.6 (s, 2C, Ar C^{meta}), 123.1 (s, 2C, Ar C^{meta}), 120.0 (s, 2C, NCHCHN), 119.5 (s, 2C, NCHCHN), 29.8 (s, 2C, $\text{CH}(\text{CH}_3)_2$), 29.0 (s, 2C, $\text{CH}(\text{CH}_3)_2$), 28.6 (s, 4C, $\text{CH}(\text{CH}_3)_2$), 26.4 (s, 2C, $\text{CH}(\text{CH}_3)_2$), 26.0 (s, 2C, $\text{CH}(\text{CH}_3)_2$), 25.7 (s, 2C, $\text{CH}(\text{CH}_3)_2$), 25.4 (s, 2C, $\text{CH}(\text{CH}_3)_2$), 24.8 (s, 2C, $\text{CH}(\text{CH}_3)_2$), 24.3 (s, 2C, $\text{CH}(\text{CH}_3)_2$), 24.1 (s, 2C, $\text{CH}(\text{CH}_3)_2$), 23.3 (s, 2C, $\text{CH}(\text{CH}_3)_2$). ^{29}Si NMR (99 MHz, C_6D_6 , δ) -85.5 (Si-Si(I₂)-Si), -88.1 (Si-Si(I₂)-Si).

 Reduction of **2.5** using KC_8

Trisilane **2.5** (100 mg, 0.07 mmol, 1.0 equiv.) and KC_8 (40.0 mg, 0.28 mmol, 4.0 equiv.) were dissolved in THF (10 mL) at -78°C . The mixture was allowed to warm up to room temperature, stirred overnight and filtered. All volatiles were removed

under vacuum. The ^1H NMR spectrum (600 MHz, C_6D_6) showed the silylene **I.26** as main product.

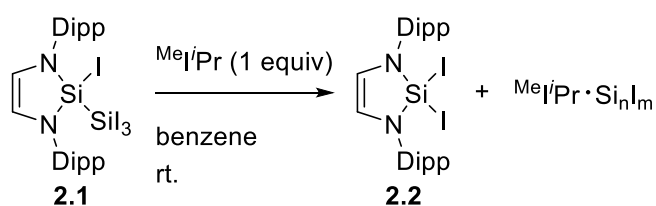
Reduction of **2.5** using organosilicon reagent

Attempt 1: Trisilane **2.5** (20 mg, 0.02 mmol, 1.0 equiv.) was dissolved in C_6D_6 (1 mL) in an NMR tube. 1,4-bis(trimethylsilyl)-1,4-diaza-2,5-cyclohexadiene **II.11** (14 mg, 0.06 mmol, 4.0 equiv.) was added to the solution. The ^1H NMR spectrum (600 MHz, C_6D_6) showed both starting material **2.5** and **II.11**. The solution was heated at 70°C for one hour. The ^1H NMR spectrum (600 MHz, C_6D_6) showed starting material **2.5** and **II.1** along with the silylene **I.26**.

Attempt 2: Trisilane **2.5** (20 mg, 0.02 mmol, 1.0 equiv.) was dissolved in C_6D_6 (1 mL) in an NMR tube. 1,4-bis(trimethylsilyl)-1,4-diaza-2,5-cyclohexadiene **II.11** (7 mg, 0.03 mmol, 2.0 equiv.) was added to the solution. The solution was heated at 40°C for one hour. The ^1H NMR spectrum (600 MHz, C_6D_6) showed starting material **2.5** and **II.1** along with the silylene **I.26**. The solution was heated for one hour more at 60°C . The ^1H NMR spectrum (600 MHz, C_6D_6) showed starting material **2.5** and **II.1** along with the silylene **I.26**.

Attempt 3: Trisilane **2.5** (20 mg, 0.02 mmol, 1.0 equiv.) was dissolved in C_6D_6 (1 mL) in an NMR tube. 1,4-bis(trimethylsilyl)-1,4-diaza-2,5-cyclohexadiene **II.11** (4 mg, 0.02 mmol, 1 equiv.) was added to the solution. The solution was heated at 40°C for one hour. The ^1H NMR spectrum (600 MHz, C_6D_6) showed starting material **2.5** and **II.1** along with the silylene **I.26**. The solution was heated for one hour more at 60°C . The ^1H NMR spectrum (600 MHz, C_6D_6) showed starting material **2.5** and **II.1** along with the silylene **I.26**.

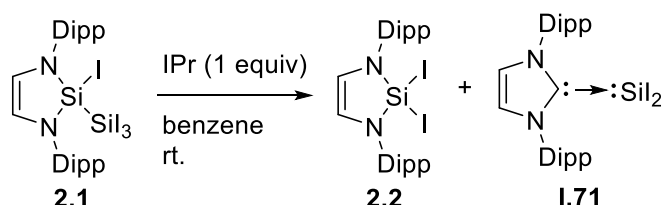
Reactions of the disilane **2.1** with coordinating-bases



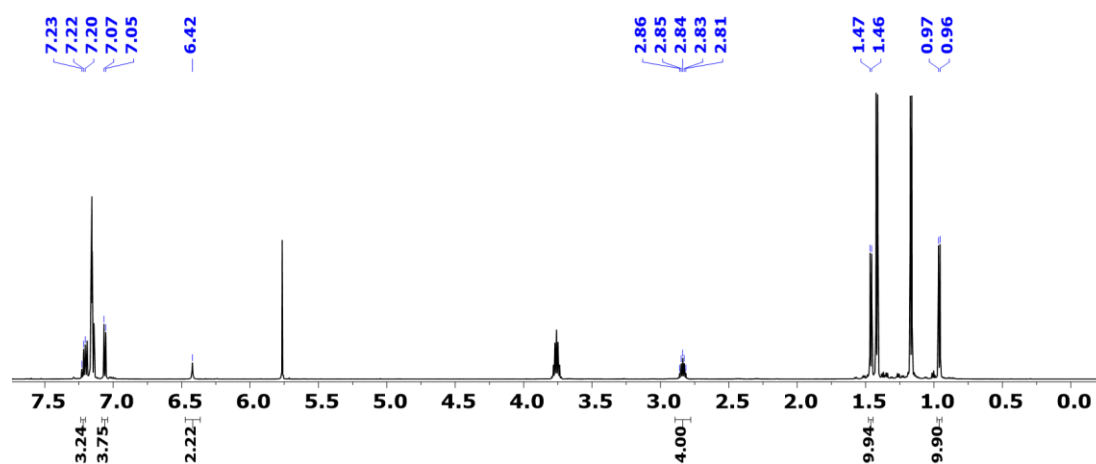
Attempt 1: A solution of disilane **2.1** (300 mg, 0.32 mmol, 1.0 equiv.) in benzene (5 mL), was slowly added to a solution of $\text{MeI}'\text{Pr}$ (60 mg, 0.32 mmol, 1.0 equiv.) in

Experimental Methods

benzene (5 mL) at room temperature. The solution was stirred overnight at room temperature. All volatiles were removed under vacuum. The ^1H NMR spectrum (600 MHz, C_6D_6) showed the product **2.2**.



Attempt 2: A solution of disilane **2.1** (300 mg, 0.32 mmol, 1.0 equiv.) in benzene (5 mL), was slowly added to a solution of IPr (120 mg, 0.32 mmol, 1.0 equiv.) in benzene (5 mL) at room temperature, without stirring. The solution was then stirred overnight at room temperature. The formed precipitate was separated by filtration and dried under vacuum. The soluble fraction was dried *in vacuo*. The ^1H NMR spectra (600 MHz, C_6D_6) of both fractions showed the product **2.2** along with the IPr-diiodosilylene adduct **1.71** (compared with literature).^[7]



^1H NMR spectrum (600 MHz, C_6D_6) of the reaction between **2.1** and IPr.

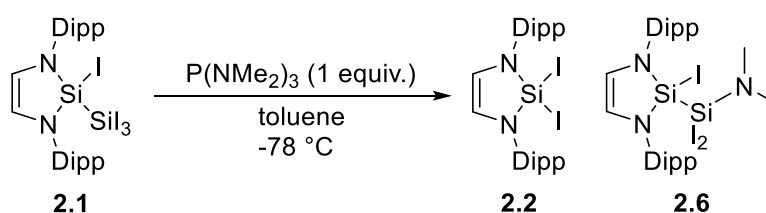
Attempt 3: Disilane **2.1** (50 mg, 0.05 mmol, 1.0 equiv.) was dissolved in C_6D_6 (1 mL) in an NMR tube. Triphenylphosphine (13 mg, 0.05 mmol, 1.0 equiv.) was added to the solution. The ^1H NMR spectrum (600 MHz, C_6D_6) showed that the disilane **2.1** was decomposing to **2.2** (17% conversion after a few minutes).

Attempt 4: Disilane **2.1** (50 mg, 0.05 mmol, 1.0 equiv.) was dissolved in C_6D_6 (1 mL) in an NMR tube. Tricyclohexylphosphine (14 mg, 0.05 mmol, 1 equiv.) was added to

the solution. The ^1H NMR spectrum (600 MHz, 298K, C_6D_6) showed that the disilane **2.1** was decomposing to **2.2** (50% conversion after 2 hours).

Attempt 5: A solution of disilane **2.1** (10 mg, 0.10 mmol, 1.0 equiv.) in toluene (20 mL) was added to a solution of tricyclohexylphosphine (28 mg, 0.10 mmol, 1.0 equiv.) in toluene (20 mL) at -78°C . The solution was allowed to warm up to room temperature overnight. All volatiles were removed *in vacuo*. The ^1H NMR spectrum (500 MHz, C_6D_6) showed the diiodosilane **2.2**.

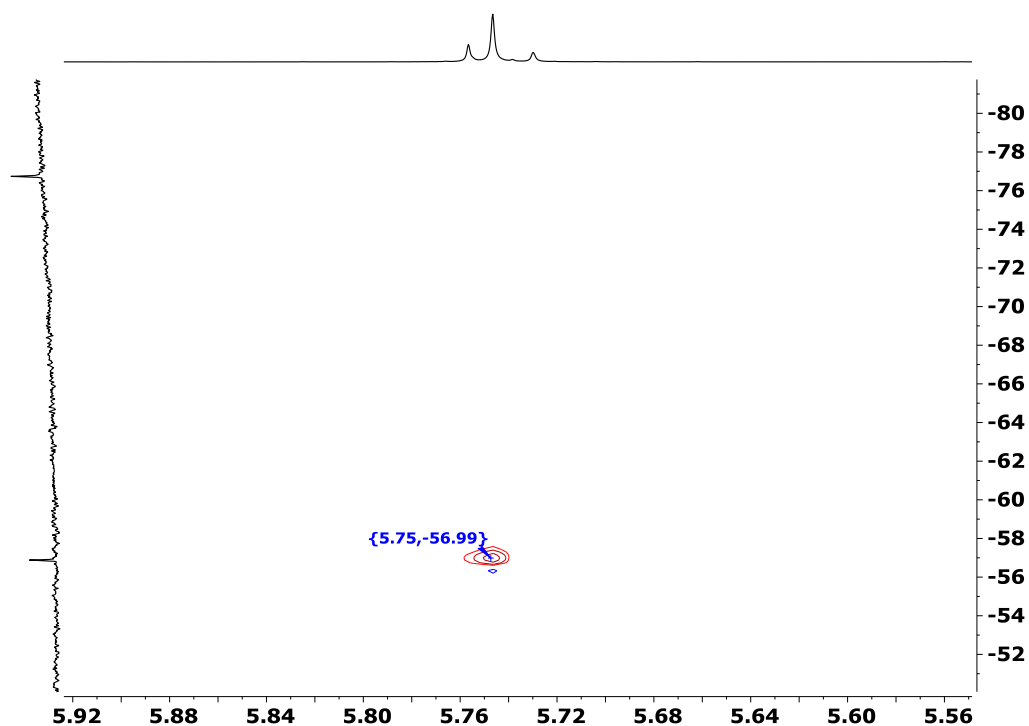
Generation of 2.6



NMR scale: Disilane **2.1** (50 mg, 0.05 mmol, 1.0 equiv.) was dissolved in C_6D_6 (1 mL) in an NMR tube. Tris(dimethylamino)phosphine (9 μL , 0.05 mmol, 1.0 equiv.) was added to the solution. The ^1H , ^{29}Si NMR spectra (600 MHz, C_6D_6) allowed identification of **2.6**.

Preparative scale: Disilane **2.1** (100 mg, 0.10 mmol, 1.0 equiv.) was dissolved in toluene (20 mL) at -78°C . Tris(dimethylamino)phosphine (18 μL , 0.10 mmol, 1.0 equiv.) was added to the solution using micro-syringe. The solution was allowed to warm up to room temperature overnight. Slow evaporation allowed the isolation of crystals suitable for X-ray analysis.

^1H NMR (500 MHz, C_6D_6 , δ) 7.23-7.12 (m, 6H, Ar *para*-H and Ar *meta*-H), 5.75 (s, 2H, NCHCHN), 3.96-3.68 (m, 4H, $\text{CH}(\text{CH}_3)_2$), 2.33 (s, 6H, $\text{N}(\text{CH}_3)_2$), 1.46 (d, 6H, $^3J_{\text{HH}} = 7.0$ Hz, $\text{CH}(\text{CH}_3)_2$), 1.42 (d, 6H, $^3J_{\text{HH}} = 6.8$ Hz, $\text{CH}(\text{CH}_3)_2$), 1.22-1.19 (m, 12H, $\text{CH}(\text{CH}_3)_2$). **^{29}Si NMR (99 MHz, C_6D_6 , δ)** -56.9 (N-Si-N), -76.7 (Si-Si-N(CH_3) $_2$).



^{29}Si - ^1H HMBC NMR spectrum (99 MHz - 500 MHz, C_6D_6) of **2.6**.

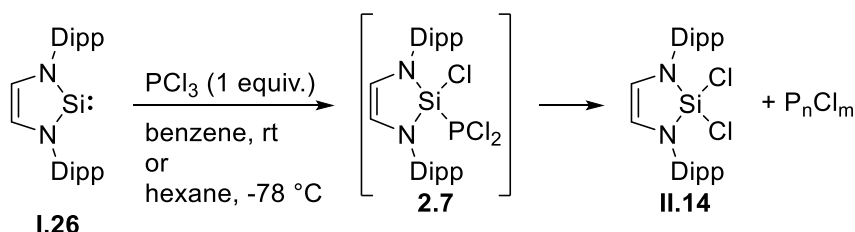
Reaction with organo-lithium reagents

Attempt 1: Disilane **2.1** (50 mg, 0.05 mmol, 1.0 equiv.) was added to a solution of mesityllithium (6 mg, 0.05 mmol, 1.0 equiv.) in toluene- d_8 (1 mL) at room temperature. The ^1H NMR spectrum (600 MHz, toluene- d_8) showed the starting material **2.1** along with a small amount of its decomposition product **2.2**.

Attempt 2: A solution of disilane **2.1** (9 mg, 0.01 mmol, 1.0 equiv.) in C_6D_6 (1 mL) is added to lithium diisopropylamide (1 mg, 0.01 mmol, 1.0 equiv.). The ^1H NMR spectrum (500 MHz, C_6D_6) showed the starting material **2.1** along with a small amount of its decomposition product **2.2**.

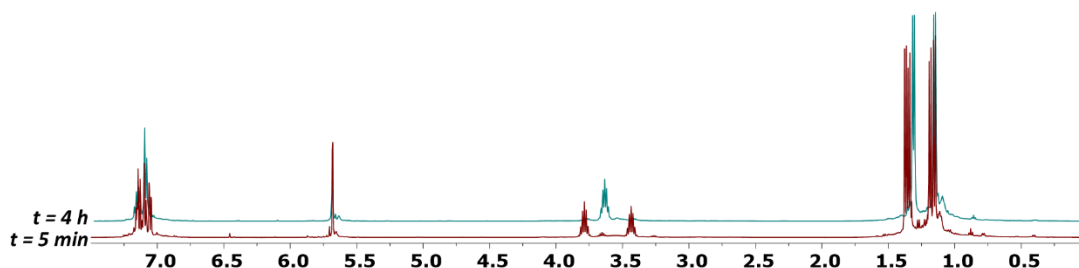
Oxidative addition of boron and phosphorus halide compounds on the N-heterocyclic silylene **I.26**

Reaction between **I.26** and PCl_3



Attempt 1: PCl_3 (5 μL , 0.05 mmol, 1.0 equiv.) was added using micro-syringe to a solution of silylene **I.26** (20 mg, 0.05 mmol, 1.0 equiv.) in C_6D_6 (1 mL). The ^1H NMR spectrum (500 MHz, C_6D_6) after few minutes showed the starting material **I.26** along with the proposed product **2.7**. The ^1H NMR spectrum (500 MHz, C_6D_6) after 12 hours showed the dichlorosilane **II.14**.

Monitoring of the reaction between **I.26 and PCl_3 :** PCl_3 (11 μL , 0.12 mmol, 1.0 equiv.) was added using micro-syringe to a solution of silylene **I.26** (50 mg, 0.12 mmol, 1.0 equiv.) in C_6D_6 (1 mL). The reaction is monitored by ^1H NMR spectroscopy (500 MHz, C_6D_6). The proposed product **2.7** was fully formed after 5 minutes but started decomposing into **II.14**. The complete degradation of the product occurred in less than four hours.



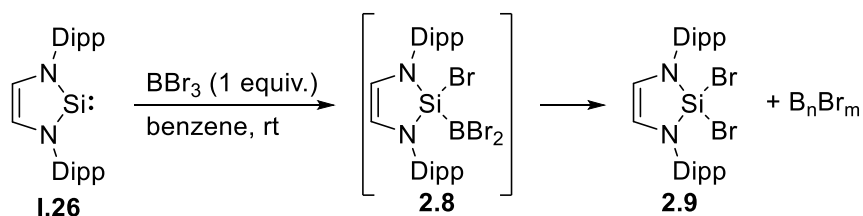
^1H NMR spectrum (500 MHz, C_6D_6) of the monitoring reaction between the silylene **I.26** and PCl_3 .

Attempt 2: PCl_3 (22 μL , 0.25 mmol, 1.0 equiv.) was added dropwise using micro-syringe to a solution of silylene **I.26** (100 mg, 0.25 mmol, 1.0 equiv.) in hexane (10

Experimental Methods

mL) at -78°C . The solution was stirred for 5 minutes and all volatiles removed *in vacuo*. The ^1H NMR spectrum (600 MHz, C_6D_6) showed the dichlorosilane **II.14**.

Reaction between **I.26** and BBr_3

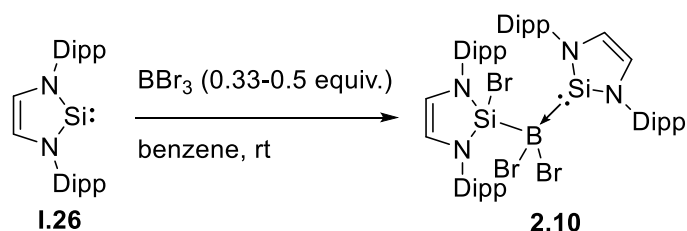


Attempt 1: BBr_3 (12 μL , 0.12 mmol, 1.0 equiv.) was added using micro-syringe to a solution of silylene **I.26** (50 mg, 0.12 mmol, 1.0 equiv.) in C_6D_6 (1 mL). The ^1H NMR spectrum (500 MHz, C_6D_6) showed the formation of the proposed product **2.8**. The ^1H NMR spectrum (600 MHz, C_6D_6) showed that **2.8** was slowly decomposing in solution into **2.9**.

Attempt 2: BBr_3 (24 μL , 0.25 mmol, 1.0 equiv.) was added using micro-syringe to a solution of silylene **I.26** (100 mg, 0.25 mmol, 1.0 equiv.) in benzene (10 mL) at room temperature. The solution was stirred for one hour. All volatiles were removed under vacuum. The residue was washed with hexane. The ^1H NMR spectrum (500 MHz, C_6D_6) showed no trace of the product **2.8**.

Attempt 3: BBr_3 (35 μL , 0.36 mmol, 3.0 equiv.) was added using micro-syringe to a solution of silylene **I.26** (50 mg, 0.12 mmol, 1 equiv.) in C_6D_6 (1 mL). The ^1H NMR spectrum (600 MHz, C_6D_6) and ^{11}B NMR spectrum (160.5 MHz, C_6D_6) taken after a few minutes showed the formation of the proposed product **2.8** along with its decomposition into **2.9** and B_2Br_4 .

Attempt 4: BBr_3 (12 μL , 0.12 mmol, 1.0 equiv.) was added using micro-syringe to a solution of silylene **I.26** (150 mg, 0.36 mmol, 3.0 equiv.) in C_6D_6 (1 mL). The ^1H NMR spectrum (500 MHz, C_6D_6) and ^{11}B NMR spectrum (160.5 MHz, C_6D_6) taken after a few minutes showed the product **2.10**.



Attempt 5: BBr_3 (121 μL , 1.24 mmol, 1.0 equiv.) was added using micro-syringe to a solution of silylene **1.26** (1.00 g, 2.47 mmol, 2.0 equiv.) in benzene (30 mL) at room temperature. The solution was stirred for 30 minutes. All volatiles were removed *in vacuo* and the residue was recrystallised from cold hexane.

Attempt 6: BBr_3 (56 μL , 0.58 mmol, 1.0 equiv.) was added using micro-syringe to a solution of silylene **1.26** (700 mg, 1.73 mmol, 3.0 equiv.) in benzene (30 mL) at room temperature. The solution was stirred for three hours. All volatiles were removed *in vacuo* and the residue was recrystallised from cold hexane. Suitable crystals for X-ray analysis were obtained from cold hexane (-20°C).

NMR of isolated crystals from 2.10: The signals from **2.10** come along with signals from the silylene **1.26** coming from the decomposition from **2.10** in solution.

^1H NMR (500 MHz, C_6D_6 , δ) 7.14-7.09 (m, 2H, Ar *para*-H), 7.04-7.01 (m, 4H, Ar *meta*-H), 5.75 (s, 2H, NCHCHN), 3.52 (sept, 4H, $^3J_{\text{HH}} = 6.9$ Hz, $\text{CH}(\text{CH}_3)_2$), 1.28 (d, 12H, $^3J_{\text{HH}} = 6.8$ Hz, $\text{CH}(\text{CH}_3)_2$), 1.12 (d, 12H, $^3J_{\text{HH}} = 6.8$ Hz, $\text{CH}(\text{CH}_3)_2$). **^{11}B NMR (160.5 MHz, C_6D_6 , δ)** -10.9 . **^{29}Si NMR (99 MHz, C_6D_6 , δ)** no signal observed.

Experimental Details for Chapter III

Preparation of the alcohol III.15

The boc-protected 3-(hydroxymethyl)piperidine **III.15** was prepared by a modified preparation from literature.^[8]

A solution of di-*tert*-butyl dicarbonate (47.3 g, 217 mmol, 1.0 equiv.) in 1,4-dioxane (60 mL) was added to a solution of 3-(hydroxymethyl)piperidine **III.11** (25.0 g, 217 mmol, 1.0 equiv.) and triethylamine (30.3 mL, 217 mmol, 1.0 equiv.) in 1,4-dioxane (500 mL). The solution was stirred at room temperature for 18.5 hours. The solution was concentrated until crystals started to crash out. The solution was stored at -20°C overnight. The formed crystals were isolated by filtration and washed with cold

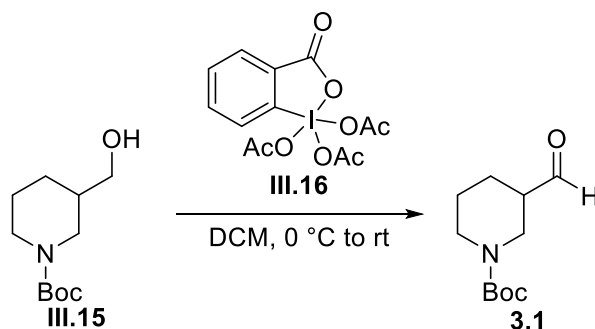
Experimental Methods

pentane (-20°C) affording **III.15** as a white off solid (36.42 g, 169 mmol, 78%). ^1H NMR spectrum (600 MHz, CDCl_3) was in accordance with the literature.^[8]

Swern oxidation of the alcohol **III.15**

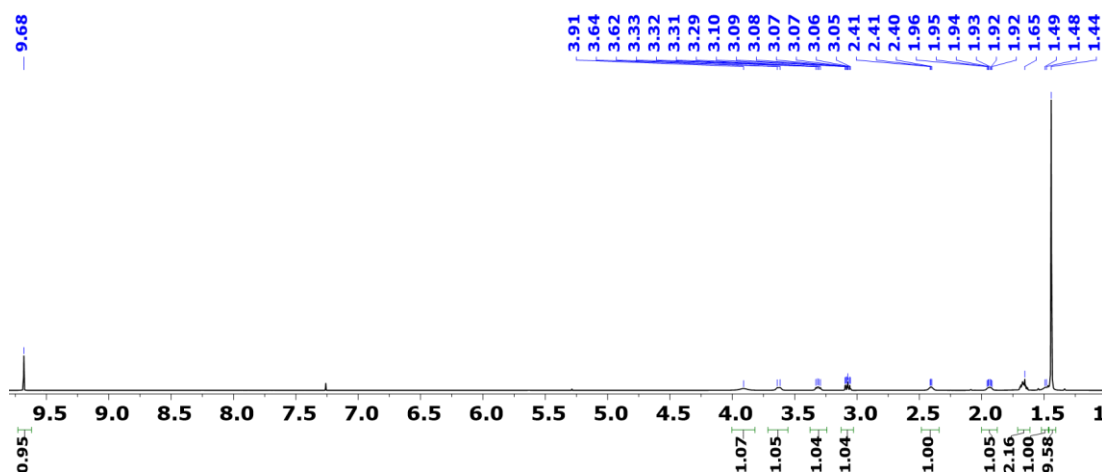
Oxalyl Chloride (1.65 mL, 19.0 mmol, 1.5 equiv.) was dissolved in DCM (20 mL) and cooled down to -78°C . DMSO (1.35 mL, 19.0 mmol, 1.5 equiv.) was added dropwise to the solution. The solution was stirred for 15 minutes at -78°C . A solution of **III.15** (2.7 g, 12.5 mmol, 1 equiv.) in DCM (5 mL) was added dropwise to the -78°C solution. The solution was warmed up to -20°C and stirred for 20 minutes. Triethylamine (5.24 mL, 37.6 mmol, 3.0 equiv.) was added to the solution. The solution was allowed to warm up to room temperature and stirred for one hour. DCM was added to the solution (50 mL). The solution was washed twice with water (2x30 mL). The isolated organic layer was dried with MgSO_4 and filtered. All volatiles were removed *in vacuo*. The residue was dissolved in THF and filtered through cotton wool. THF was removed *in vacuo*. The ^1H NMR spectrum (500 MHz, CDCl_3) showed the product **3.1** as a minor product.

Preparation of the aldehyde **3.1**



The preparation was carried out using distilled DCM, under Argon atmosphere. A cold solution (0°C) of Dess-Martin periodinane **III.16** (11.0 g, 26.0 mmol, 1.1 equiv.) in DCM (100 mL) was added to a solution of **III.15** (5.09 g, 23.6 mmol, 1.0 equiv.) in DCM (50 mL) at 0°C . The solution was allowed to warm up to room temperature and stirred for two hours. NaOH (C = 2 M, 140 mL) was added to the solution and the resulting mixture was stirred for 10 minutes. The organic layer was separated, dried with MgSO_4 and filtered. All volatiles were removed *in vacuo* affording pure **3.1** as a colourless oil (4.12 g, 19.3 mmol, 82%).

^1H NMR (600 MHz, CDCl_3 , δ) 9.68 (s, 1H, COH), 3.91 (br s, 1H, *piperidine-H*), 3.63 (d, 1H, $^3J_{\text{HH}} = 11.6$ Hz, *piperidine-H*), 3.31 (dd, 1H, $^3J_{\text{HH}} = 8.3$ Hz, $^3J_{\text{HH}} = 13.3$ Hz, *piperidine-H*), 3.07 (ddd, 1H, $^2J_{\text{HH}} = 3.3$ Hz, $^3J_{\text{HH}} = 9.3$ Hz, $^3J_{\text{HH}} = 13.0$ Hz, *piperidine-H*), 2.41 (br s, 1H, *piperidine-H*), 1.98-1.90 (m, 1H, *piperidine-H*), 1.71-1.62 (m, 2H, *piperidine-H*), 1.53-1.44 (m, 1H, *piperidine-H*), 1.44 (s, 9H, $\text{C}(\text{CH}_3)_3$).



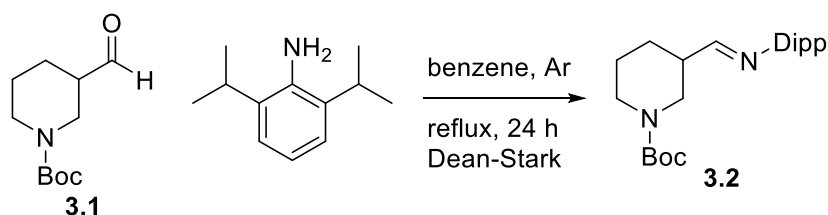
^1H NMR spectrum (600 MHz, CDCl_3) of the aldehyde **3.1**.

Attempt of one-pot synthesis of **3.3** from **3.1**

Attempt 1: 2,6-diisopropylaniline (415 mg, 2.34 mmol, 1.0 equiv.) and **3.1** (500 mg, 2.34 mmol, 1.0 equiv.) were dissolved in DCE (30 mL) at room temperature. $\text{NaHB}(\text{OAc})_3$ (700 mg, 3.28 mmol, 1.4 equiv.) was added to the solution. The solution was stirred at room temperature for 24 hours. The solution was quenched with aqueous saturated NaHCO_3 solution. The organic layer was separated, and the aqueous layer was extracted with EtOAc (3 x 30 mL). The combined organic layers were dried with MgSO_4 , filtered and dried under vacuum affording an oil. The ^1H NMR spectrum (400 MHz, CDCl_3) showed a mixture of 2,6-diisopropylaniline, alcohol **III.15**, the imine **3.2** and the amine **3.3**.

Monitoring of the reductive amination: 2,6-diisopropylaniline (1.21 g, 6.80 mmol, 1.0 equiv.) and **3.1** (1.60 g, 7.50 mmol, 1.1 equiv.) were dissolved in DCE (100 mL) at room temperature. $\text{NaHB}(\text{OAc})_3$ (2.02 g, 9.5 mmol, 1.4 equiv.) was added to the solution. The solution was stirred at room temperature for 48 hours and monitored by ^1H NMR spectroscopy (500-600 MHz, CDCl_3). The ^1H NMR monitoring showed a mixture of 2,6-diisopropylaniline, alcohol **III.15**, the imine **3.2** and the amine **3.3**.

Preparation of the imine 3.2



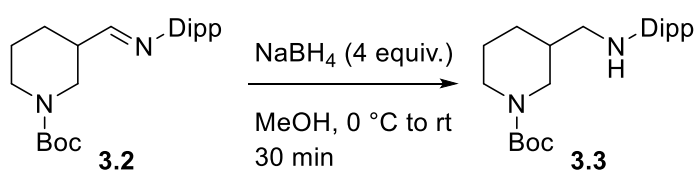
Attempt 1: 2,6-diisopropylaniline (80 mg, 0.43 mmol, 1.0 equiv.) and **3.1** (100 mg, 0.43 mmol, 1.0 equiv.) were dissolved in methanol-d₄ (1 mL) with molecular sieves (3 Å) at room temperature. The reaction was monitored by ¹H NMR spectroscopy (400-500-600 MHz, methanol-d₄). The ¹H NMR spectroscopy showed that the reaction led to a mixture of **3.2**:2,6-diisopropylaniline in a ratio 1:0.3.

Dean&Stark preparation of 3.2: 2,6-diisopropylaniline (4.27 g, 24.1 mmol, 1.0 equiv.) and **3.1** (5.16 g, 24.1 mmol, 1.0 equiv.) were dissolved in benzene (60 mL). The solution was refluxed under argon using a Dean&Stark apparatus for 20 hours. All volatiles were removed *in vacuo*. The ¹H NMR spectrum (400 MHz, CDCl₃) revealed a mixture of **3.2** (90%), 2,6-diisopropylaniline (8%), and **3.1** (2%). The crude material was used without further purification.

NMR signal of 3.2: The signal from **3.2** comes with residual signals of 2,6-diisopropylaniline and **3.1**.

¹H NMR (400 MHz, CDCl₃, δ) 7.61 (d, 1H, , ³J_{HH} = 3.8 Hz, N=CH), 7.16-7.05 (m, 3H, Ar *para*-H and Ar *meta*-H), 4.48-4.07 (br m, 1H, *piperidine*-H), 4.00 (br d, 1H, ³J_{HH} = 13.5 Hz, *piperidine*-H), 3.22-3.01 (br m, 1H, *piperidine*-H), 3.01-2.83 (m, 1H, *piperidine*-H and 2H, CH(CH₃)₂), 2.71-2.57 (br m, 1H, *piperidine*-H), 2.19-2.07 (br m, 1H, *piperidine*-H), 1.85-1.76 (br m, 1H, *piperidine*-H), 1.75-1.55 (br m, 2H, *piperidine*-H), 1.51 (s, 9H, C(CH₃)₃), 1.18 (d, 12H, ³J_{HH} = 6.9 Hz, CH(CH₃)₂).

Preparation of the amine 3.3

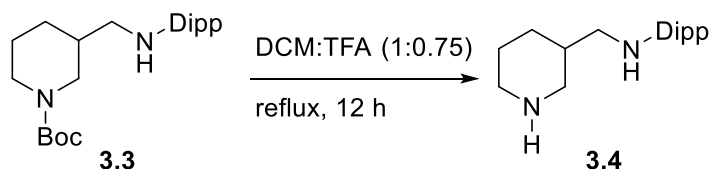


The reaction was carried out under air. NaBH₄ (3.65 g, 96.4 mmol, 4.0 equiv.) was slowly added to a cold solution of crude imine **3.2** in methanol (60 mL) at 0°C and stirred for 30 minutes. The reaction mixture was quenched with water (40 mL) and stirred for 20 minutes. EtOAc (60 mL) is added to the reaction mixture. The organic layer is separated and washed with brine (30 mL), dried with MgSO₄ and filtered. Removal of all volatiles *in vacuo* afforded the amine **3.3** with residual trace of **3.2** and 2,6-diisopropylaniline evidenced by ¹H NMR (500 MHz, 298K, CDCl₃). The crude material was used without further purification.

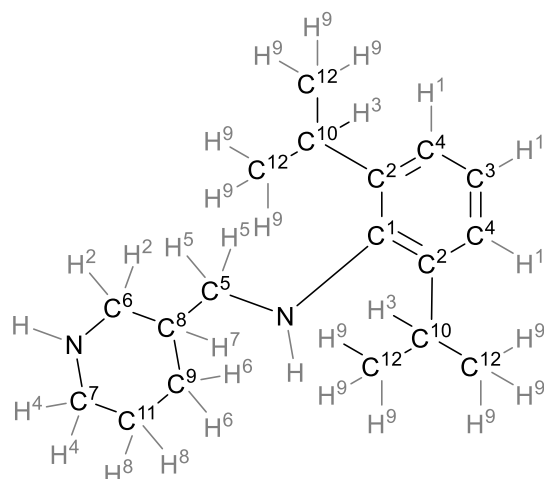
NMR signal of 3.3: The signal from **3.3** comes with residual signals of 2,6-diisopropylaniline and **3.2**.

¹H NMR (400 MHz, CDCl₃, δ) 7.11-7.02 (m, 3H, Ar *para*-H and Ar *meta*-H), 4.16 (m, 1H), 3.92 (m, 1H), 3.25 (sept, 2H, ³J_{HH} = 6.9 Hz, CH(CH₃)₂), 2.90-2.82 (m, 2H), 2.81-2.74 (m, 1H), 2.74-2.63 (m, 2H), 2.02-1.92 (m, 1H), 1.87-1.74 (m, 1H), 1.72-1.65 (m, 1H), 1.64-1.49 (m, 2H), 1.48 (s, 9H, C(CH₃)₃), 1.24 (d, 12H, ³J_{HH} = 6.8 Hz, CH(CH₃)₂).

Preparation of diamine 3.4



The reaction was carried out under air. The crude amine **3.3** was dissolved in a solution of DCM:TFA (4:3) and refluxed overnight. All volatiles were removed *in vacuo*. The residue was dissolved in an aqueous solution of NaOH (2M, 100 mL) and DCM (30 mL) and stirred for 10 minutes. The organic layer was separated, and the aqueous layer was extracted with DCM (4 x 30 mL) (Brine can be added to help separation). The combined organic layers were dried with MgSO₄ and filtered. All volatiles were removed *in vacuo*. Recrystallisation from cold pentane (−20°C) afforded the pure ligand **3.4** as colourless crystals (3.04 g, 11.1 mmol, 46% from **3.2**). **Melting point** (argon sealed capillary) 59°C. **Elemental analysis calculated** (%) for C₁₈H₃₀N₂ (274.45): C 78.77, H 11.02, N 10.21; found: C 78.67, H 10.89, N 10.09%.

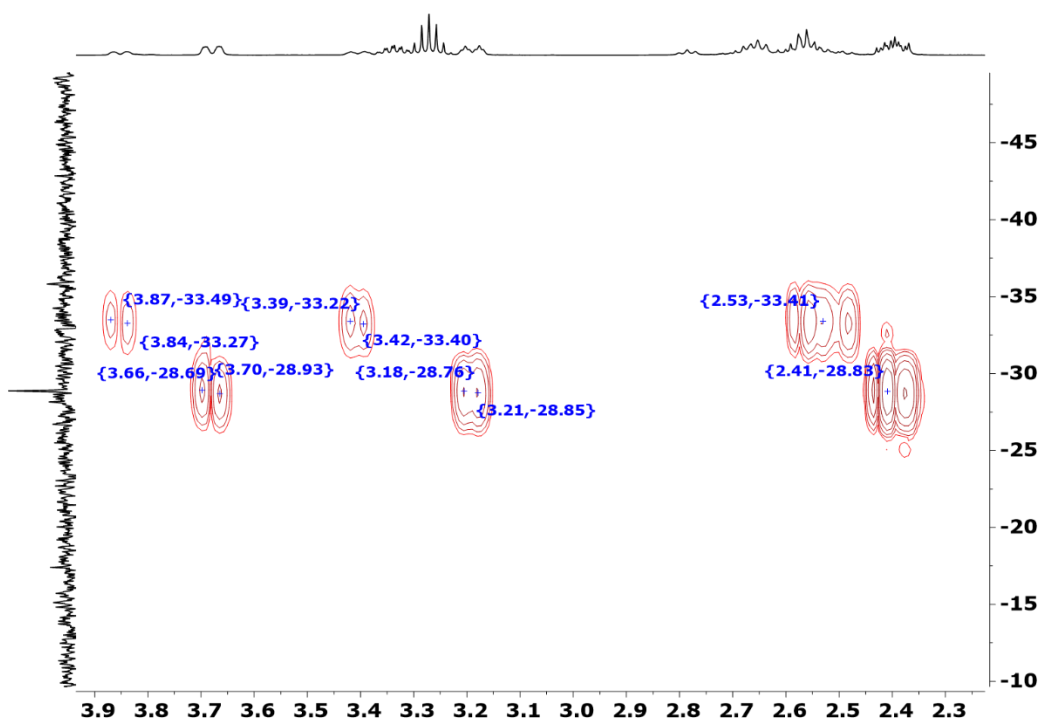


^1H NMR (500 MHz, CDCl_3 , δ) 7.10-7.02 (m, 3H, H^1), 3.33 (m, 1H, H^2), 3.23 (sept, 2H, $^3J_{\text{HH}} = 6.8$ Hz, H^3), 3.10 (m, 1H, H^4), 2.84 (br s, 2H, N-H), 2.70 (d, 2H, $^3J_{\text{HH}} = 6.6$ Hz, H^5), 2.62 (td, 1H, $^3J_{\text{HH}} = 12.0$ Hz, $^2J_{\text{HH}} = 3.0$ Hz, H^4), 2.46 (dd, 1H, $^3J_{\text{HH}} = 12.0$ Hz, $^3J_{\text{HH}} = 11.9$ Hz, H^2), 2.01-1.95 (m, 1H, H^6), 1.88-1.78 (m, 1H, H^7), 1.77-1.70 (m, 1H, H^8), 1.63-1.52 (m, 1H, H^8), 1.23 (d, 12H, 6.8 Hz, H^9), 1.26-1.14 (m, 1H, H^6). **^{13}C NMR (125 MHz, CDCl_3 , δ)** 143.4 (s, 1C, C^1), 142.7 (s, 2C, C^2), 123.9 (s, 1C, C^3), 123.5 (s, 2C, C^4), 56.2 (s, 1C, C^5), 50.6 (s, 1C, C^6), 46.8 (s, 1C, C^7), 38.5 (s, 1C, C^8), 29.5 (s, 1C, C^9), 27.6 (s, 2C, C^{10}), 25.9 (s, 1C, C^{11}), 24.3 (s, 4C, C^{12}).

Synthesis of the dichlorosilane 3.5

Triethylamine (NEt_3) and silicon tetrachloride (SiCl_4)

Attempt 1: A solution of **3.4** (300 mg, 1.10 mmol, 1.0 equiv.) and Et_3N (307 μL , 2.20 mmol, 2.0 equiv.) in pentane (10 mL) was added dropwise to a solution of SiCl_4 (126 μL , 1.1 mmol, 1.0 equiv.) in pentane (50 mL) at 0°C under vigorous stirring. After completion of the addition the reaction mixture was allowed to warm up to room temperature and refluxed for 12 hours. The solution was cooled down to room temperature and filtered. All volatiles were removed *in vacuo*. The ^{29}Si NMR spectrum (99 MHz, C_6D_6) showed two signals at $\delta -28.9$ (major compound **3.7**) and -33.0 (minor compound **3.8**).



^{29}Si - ^1H HMBC NMR spectrum (99 MHz – 500 MHz, C_6D_6) of the reaction between **3.4**, Et_3N and SiCl_4 .

Attempt 2: A solution of **3.4** (300 mg, 1.10 mmol, 1.0 equiv.) and Et_3N (303 μL , 2.2 mmol, 2.0 equiv.) in pentane (20 mL) was added dropwise to a solution of SiCl_4 (1.26 mL, 11.0 mmol, 10.0 equiv.) in pentane (50 mL) at 0°C under vigorous stirring. After completion of the addition the reaction mixture was allowed to warm up to room temperature and refluxed for 12 hours. All volatiles were removed *in vacuo*. Product was extracted with Et_2O . The ^1H NMR spectrum (600 MHz, C_6D_6) showed a mixture of **3.7**:**3.8** (84:16).

Heating the crude mixture of **3.7 and **3.8**:** A crude mixture of **3.7** and **3.8** was heated using the heat gun under vacuum. The white off solid turned into a yellow oil. The ^1H NMR spectrum (500 MHz, C_6D_6) showed a mixture of **3.7**:**3.8** (18:82). The ^{29}Si NMR spectrum (99 MHz, C_6D_6) showed two signals at δ -28.9 (minor compound **3.7**) and -33.0 (major compound **3.8**).

Lithiation of 3.4 and SiCl₄ addition

Study of lithiation of 3.4

Attempt 1: Ligand **3.4** (200 mg, 0.73 mmol, 1.0 equiv.) was dissolved in Et₂O (10 mL) and cooled down to -78°C. BuLi (580 µL, 1.46 mmol, C = 2.5 M in hexane, 2.0 equiv.) was added dropwise using syringe to the cold Et₂O solution. The solution was allowed to warm up to room temperature and all volatiles were removed *in vacuo*. The ⁷Li NMR spectrum (500 MHz, THF-d₈) showed three signals at δ 1.15, 0.31 and -0.51.

Attempt 2: Ligand **3.4** (200 mg, 0.73 mmol, 1.0 equiv.) was dissolved in Et₂O (10 mL) and cooled down to -78°C. BuLi (1.17 mL, 2.92 mmol, C = 2.5 M in hexane, 4.0 equiv.) was added dropwise using syringe to the cold Et₂O solution. The solution was allowed to warm up to room temperature and stirred overnight. The solution was concentrated and stored at -20°C, which allowed the formation of crystals of **3.9**.

Titration of the lithiated ligand 3.4: Ligand **3.4** (300 mg, 1.10 mmol, 1.0 equiv.) was dissolved in Et₂O (10 mL) and cooled down to -78°C. BuLi (880 µL, 2.2 mmol, C = 2.5 M in hexane, 2.0 equiv.) was added dropwise using syringe to the cold Et₂O solution. The solution was allowed to warm up to room temperature and stirred overnight. All volatiles were removed *in vacuo* and the residue was washed with hexane, affording off white solid.

This solid (163 mg, 0.57 mmol) was dissolved in THF (10 mL) and added dropwise to a solution of salicylaldehyde phenylhydrazone (80 mg, 0.38 mmol) in THF (10 mL). The solution turned yellow when the addition was started and turned from yellow to orange at 5.5 mL. An equivalence of 0.31 mmol (0.8 equiv.) was found.

Lithiation of 3.4, SiCl₄ addition: attempted synthesis of 3.5

Attempt 1 and 2: BuLi (73 µL, 0.36 mmol, C = 2.5 M in hexane, 2.0 equiv.) was added using a micro syringe to a solution of ligand **3.4** (50 mg, 0.18 mmol, 1.0 equiv.) in C₆D₆ (1 mL) at room temperature. After 30 minutes, SiCl₄ (21-103 µL, 0.18-0.90 mmol, 1.0-5.0 equiv.) was added slowly to the solution at room temperature.

Attempt 3 and 4: BuLi (880 µL, 2.2 mmol, C = 2.5 M in hexane, 2.0 equiv.) was added using a micro syringe to a solution of ligand **3.4** (300 mg, 1.1 mmol, 1.0 equiv.) in benzene (30-10 mL) at room temperature. After 2.5-2 hours all volatiles were removed under vacuum. The residue was dissolved in benzene (30-10 mL). SiCl₄ (151-252 µL,

1.32-2.2 mmol, 1.2-2.0 equiv.) was added to the solution at room temperature. The solution was stirred overnight, and all volatiles were removed *in vacuo*.

Attempt 5: BuLi (970 μL , 2.42 mmol, C = 2.5 M in hexane, 2.2 equiv.) was added using a micro syringe to a solution of ligand **3.4** (300 mg, 1.1 mmol, 1.0 equiv.) in benzene (10 mL) at room temperature. After 2 hours, SiCl_4 (277 μL , 2.42 mmol, 2.2 equiv.) was added dropwise to the solution at room temperature. The solution was stirred overnight, and all volatiles were removed *in vacuo*.

Attempt 6: BuLi (880 μL , 2.20 mmol, C = 2.5 M in hexane, 2.0 equiv.) was added using a micro syringe to a solution of ligand **3.4** (300 mg, 1.10 mmol, 1.0 equiv.) in THF (30 mL) at -78°C . After 3 hours, SiCl_4 (126 μL , 1.10 mmol, 1.0 equiv.) was added dropwise at -78°C . The solution was allowed to warm up to room temperature overnight. All volatiles were removed under vacuum and pentane was used to extract the product.

Attempt 7: BuLi (880 μL , 2.20 mmol, C = 2.5 M in hexane, 2.0 equiv.) was added using a micro syringe to a solution of ligand **3.4** (300 mg, 1.10 mmol, 1.0 equiv.) in Et_2O (30 mL) at room temperature and stirred for 30 minutes. The solution was cooled down to -78°C and SiCl_4 (151 μL , 1.32 mmol, 1.2 equiv.) was added dropwise. The solution was allowed to warm up to room temperature and stirred for two hours. All volatiles were removed under vacuum.

Every attempt was analysed by ^1H and ^{29}Si NMR spectroscopy (500 and 99 MHz, C_6D_6).

Stepwise lithiation: synthesis of 3.7

BuLi (440 μL , 1.10 mmol, C = 2.5 M in hexane, 1.0 equiv.) was added using micro syringe to a solution of ligand **3.4** (300 mg, 1.10 mmol, 1.0 equiv.) in Et_2O (30 mL) at room temperature and stirred for 30 minutes. The solution was cooled down to -78°C and SiCl_4 (151 μL , 1.32 mmol, 1.2 equiv.) was added dropwise. The solution was allowed to warm up to room temperature and stirred for two hours. All volatiles were removed under vacuum. The ^1H NMR spectrum (500 MHz, C_6D_6) showed a mixture of **3.7:3.8** in a ratio 88:12.

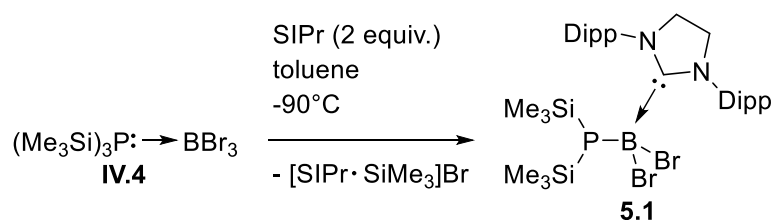
Experimental Details for Chapter V

Preparation of the (Me₃Si)₃PBBr₃ adduct IV.4

Compound **IV.4** was prepared from a slightly modified reported preparation.^[9]

A solution of P(SiMe₃)₃ (4.80 g, 19.2 mmol, 1.0 equiv.) in pentane (100 mL) was added to a solution of BBr₃ (1.85 mL, 19.2 mmol, 1.0 equiv.) in pentane (100 mL) at 0°C. The solution was allowed to warm up to room temperature and left overnight under vigorous stirring and in the dark. All volatiles were removed *in vacuo* affording **IV.4** as a white solid in an almost quantitative yield (9.00 g, 18 mmol, 94%).

Preparation of the SIPr coordinated 1-di(trimethylsilyl)-2-dibromophosphinoborane 5.1



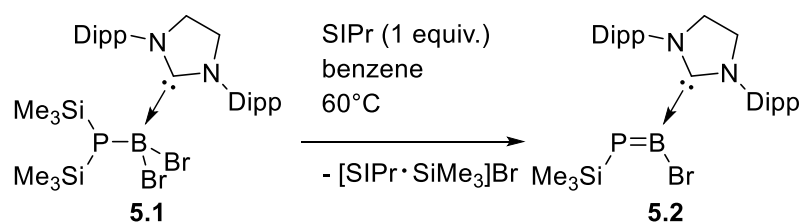
(Me₃Si)₃P→BBr₃ adduct (700 mg, 1.40 mmol, 1.0 equiv.) and SIPr (1.10 g, 2.80 mmol, 2.0 equiv.) were dissolved in toluene (60 mL) at -95°C. The solution was slowly warmed up overnight to room temperature under vigorous stirring. Solvent was removed under vacuum. The crude product was extracted with pentane (80 mL) and dried under vacuum, affording the product **5.1** as a tan powder (480 mg, 0.65 mmol, 46%). **Melting point** (argon sealed capillary) 195 °C (dp). **Elemental analysis calculated** (%) for C₃₃H₅₆BBr₂N₂PSi₂ (738.59): C 53.67, H 7.64, N 3.79; found: C 53.78, H 7.56, N 3.93%.

¹H NMR (500 MHz, C₆D₆, δ) 7.21-7.16 (m, 2H, Ar *para*-H), 7.11-7.05 (m, 4H, Ar *meta*-H), 3.50 (s, 4H, NCH₂CH₂N), 3.45 (sept, 4H, ³J_{HH} = 6.7 Hz, CH(CH₃)₂), 1.58 (d, 12H, ³J_{HH} = 6.5 Hz, CH(CH₃)₂), 1.09 (d, 12H, ³J_{HH} = 6.8 Hz, CH(CH₃)₂), 0.49 (d, 18H, ³J_{HP} = 4.0 Hz, Si(CH₃)₃). **¹³C NMR (125 MHz, C₆D₆, δ)** 180.3 (s, 1C, N-C-N), 145.9 (s, 4C, Ar C^{*ortho*}), 136.6 (s, 2C, Ar C^{*ipso*}), 129.7 (s, 2C, Ar C^{*para*}), 124.3 (s, 4C, Ar C^{*meta*}), 54.5 (s, 2C, NCH₂CH₂N), 29.2 (s, 4C, CH(CH₃)₂), 26.2 (s, 4C, CH(CH₃)₂), 23.8 (s, 4C, CH(CH₃)₂), 4.7 (d, 6C, ²J_{CP} = 10.6 Hz, Si(CH₃)₃). **¹¹B NMR (160 MHz, C₆D₆, δ)** -9.8 (br

s). ^{29}Si NMR (99 MHz, C_6D_6 , δ) 2.6 (d, $^1J_{\text{SiP}} = 21.8$ Hz, $\text{Si}(\text{CH}_3)_3$). ^{31}P NMR (202 MHz, C_6D_6 , δ) -184.3 (s).

Preparation of the SIPr coordinated 1-trimethylsilyl-2-bromophosphaborene **5.2**

Attempt 1: Phosphinoborane **5.1** (20 mg, 0.027 mmol, 1.0 equiv.) and KO^tBu (3 mg, 0.027 mmol, 1.0 equiv.) were dissolved in THF- d_8 (1 mL) at room temperature. After one day at room temperature, the ^{31}P NMR spectroscopy analysis (162 MHz, THF- d_8) showed slow conversion to **5.2**.



The phosphinoborane **5.1** (250 mg, 0.34 mmol, 1.0 equiv.) and SIPr (130 mg, 0.34 mmol, 1.0 equiv.) were dissolved in benzene (30 mL) at room temperature. The solution was heated at 60 °C overnight. The solution was cooled down to room temperature and filtered. All volatiles were removed under vacuum. The residue was washed with pentane (15 mL) and dried under vacuum. A second crop can be obtained from the pentane fraction by crystallisation at -20 °C. The product **5.2** was obtained as a yellow solid (0.13 g, 0.22 mmol, 64%). **Melting point** (argon sealed capillary) 199 °C (dp). **Elemental analysis calculated** (%) for $\text{C}_{30}\text{H}_{47}\text{BBrN}_2\text{PSi}$ (585.49): C 61.54, H 8.09, N 4.78; found: C 61.49, H 7.98, N 4.81%. **UV/vis (hexane):** $\lambda_{\text{max}} = 404$ nm, $\epsilon = 4192$ L mol $^{-1}$ cm $^{-1}$.

^1H NMR (400 MHz, C_6D_6 , δ) 7.13-7.07 (m, 2H, Ar *para*-H), 7.05-7.00 (m, 4H, Ar *meta*-H), 3.48 (s, 4H, $\text{NCH}_2\text{CH}_2\text{N}$), 3.38 (sept, 4H, $^3J_{\text{HH}} = 6.7$ Hz, $\text{CH}(\text{CH}_3)_2$), 1.57 (d, 12H, $^3J_{\text{HH}} = 6.7$ Hz, $\text{CH}(\text{CH}_3)_2$), 1.14 (d, 12H, $^3J_{\text{HH}} = 6.9$ Hz, $\text{CH}(\text{CH}_3)_2$), 0.48 (d, 9H, $^3J_{\text{HP}} = 3.2$ Hz, $\text{Si}(\text{CH}_3)_3$). **^{13}C NMR (125 MHz, C_6D_6 , δ)** 180.9 (s, 1C, N-C-N), 146.6 (s, 4C, Ar *C*^{ortho}), 134.4 (s, 2C, Ar *C*^{ipso}), 130.3 (s, 2C, Ar *C*^{para}), 124.9 (s, 4C, Ar *C*^{meta}), 52.9 (s, 2C, $\text{NCH}_2\text{CH}_2\text{N}$), 29.2 (s, 4C, $\text{CH}(\text{CH}_3)_2$), 26.3 (s, 4C, $\text{CH}(\text{CH}_3)_2$), 24.0 (s, 2C, $\text{CH}(\text{CH}_3)_2$), 23.9 (s, 2C, $\text{CH}(\text{CH}_3)_2$), 4.0 (d, 3C, $^2J_{\text{CP}} = 8.3$ Hz, $\text{Si}(\text{CH}_3)_3$). **^{11}B NMR (128 MHz, C_6D_6 , δ)** 42.2 (br s). **^{29}Si NMR (79 MHz, C_6D_6 , δ)** 3.7 (d, $^1J_{\text{SiP}} = 55.8$ Hz, $\text{Si}(\text{CH}_3)_3$). **^{31}P NMR (162 MHz, C_6D_6 , δ)** 77.8 (s).

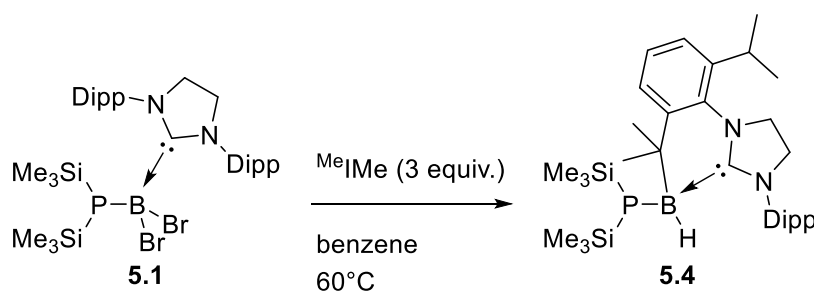
Attempted synthesis of NHC boron-phosphide adduct

Attempt from the SIPr coordinated phosphinoborane 5.1

Attempt 1: $^{\text{Me}}\text{IPr}$ (9.7 mg, 0.054 mmol, 2.0 equiv.) and **5.1** (20 mg, 0.027 mmol, 1.0 equiv.) were dissolved in C_6D_6 (1 mL) and heated at 60°C for 12 hours. The ^{31}P NMR spectrum (162 MHz, C_6D_6) showed a main signal at δ 77.8 (s) from **5.2** and a trace signal at δ 150.5 (s) assigned to **5.3**.

Attempt 2: SIPr (31.6 mg, 0.081 mmol, 3.0 equiv.) and **5.1** (20 mg, 0.027 mmol, 1.0 equiv.) were dissolved in C_6D_6 (1 mL) and heated at 60°C for two days. The ^1H NMR spectrum (500 MHz, C_6D_6) showed SIPr and **5.2**. The ^{31}P NMR spectrum (162 MHz, C_6D_6) showed a main signal at δ 77.8 (s) from **5.2**.

Attempt 3: $^{\text{Me}}\text{IME}$ (10.1 mg, 0.081 mmol, 3.0 equiv.) and **5.1** (20 mg, 0.027 mmol, 1.0 equiv.) were dissolved in C_6D_6 (1 mL) and heated at 60°C for 12 hours. The ^{31}P NMR spectrum (162 MHz, C_6D_6) showed a main signal at δ -247.6 (s) from **5.4** and two small signals at δ -146.7 (s) and -93.7 (s). The ^{11}B NMR (128 MHz, C_6D_6) showed a signal at δ -20.5 (d) from **5.4**.



Scaled up reaction and crystal isolation of 5.4: $^{\text{Me}}\text{IME}$ (126 mg, 1.02 mmol, 3.0 equiv.) and **5.1** (250 mg, 0.34 mmol, 1.0 equiv.) were dissolved in benzene (30 mL) and heated at 60°C . Followed by ^{31}P NMR spectroscopy, the conversion was completed after 2.5 hours. The solution was filtrated, and all volatiles were removed *in vacuo*. Suitable crystals of **5.4** for X-ray analysis were obtained from hexane at -20°C .

NMR signal of 5.4: The ^1H NMR spectrum could not be fully assigned as the signal from **5.4** comes along with signals from imidazolium salt.

^{11}B NMR (128 MHz, C_6D_6 , δ) -20.5 (d, $^1J_{\text{BH}} = 71$ Hz). ^{31}P NMR (162 MHz, C_6D_6 , δ) -247.6 (s).

Attempt from the SIPr coordinated phosphaborene 5.2

Attempt 1: A solution of ^{Me}I₂Me (55 mg, 0.44 mmol, 2.0 equiv.) in toluene (20 mL) was added to a solution of **5.2** (128 mg, 0.22 mmol, 1.0 equiv.) in toluene (20 mL) at –95°C. The reaction was allowed to warm up to room temperature overnight. The ³¹P NMR spectrum (162 MHz, C₆D₆) showed a main signal at δ –148.8 (d, ¹J_{PH} = 165.0 Hz) along with remaining trace of **5.2** (δ 77.8 (s)).

Attempt 2: CsF (4 mg, 0.026 mmol, 1.0 equiv.) and **5.2** (15 mg, 0.026 mmol, 1.0 equiv.) were dissolved in C₆D₆ at room temperature. After two days, ¹H, ¹¹B and ³¹P NMR analysis (500-128-162 MHz, C₆D₆) showed the starting material **5.2**.

Attempt 3: SIPr (10.2 mg, 0.026 mmol, 1.0 equiv.) and **5.2** were dissolved in toluene-d₈ (1 mL) and cooled down to –90°C. MeLi (17 μL, 0.026 mmol, C = 1.6 M in Et₂O, 1.0 equiv.) was added dropwise to the cold solution. After 6 days, ¹H, ¹¹B and ³¹P NMR spectroscopy analysis (400-128-162 MHz, toluene-d₈) showed the starting material **5.2**.

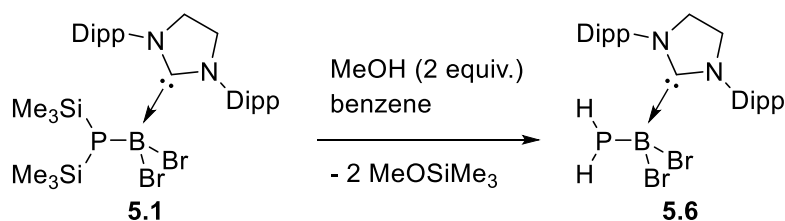
Attempted coordination of 5.2 to Lewis acid

Attempt 1: W(CO)₆ (9 mg, 0.026 mmol, 1.0 equiv.) was dissolved in THF-d₈ (1 mL) in a quartz NMR tube and irradiated (λ 420 nm) for three hours. Phosphaborene **5.2** (15 mg, 0.026 mmol, 1.0 equiv.) dissolved in THF-d₈ (1 mL) was added to the W(CO)₆-THF-d₈ solution. After 12 hours the ¹H and ³¹P NMR spectroscopy analysis (400-162 MHz, THF-d₈) showed the starting material **5.2** along with imidazolium salt.

Attempt 2: Fe₂(CO)₉ (9.5 mg, 0.026 mmol, 1.0 equiv.) and **5.2** (15 mg, 0.026 mmol, 1.0 equiv.) were dissolved in THF-d₈ (1 mL) and heated at 60°C for one day. The ¹H NMR spectrum (400 MHz, THF-d₈) showed the starting material **5.2** along with imidazolium salt.

Functionalization of the SIPr coordinated phosphinoborane 5.1

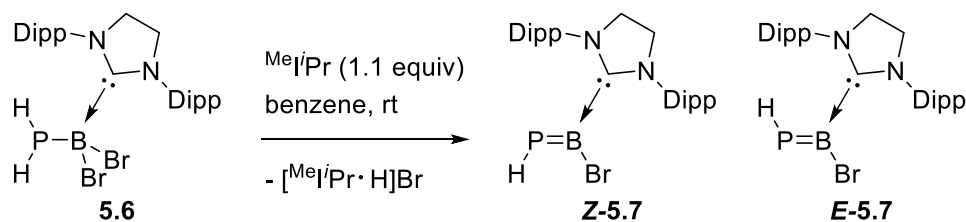
Preparation of the SIPr coordinated 1-dihydro-2-dibromo-phosphinoborane 5.6



The phosphinoborane **5.1** (300 mg, 0.41 mmol, 1.0 equiv.) was dissolved in benzene (20 mL). MeOH (33 μL , 0.81 mmol, 2.0 equiv.) was added dropwise, at room temperature, using micro syringe. The solution was stirred for 15 minutes. The solution was filtered, and all volatiles were removed under vacuum. The residue was washed with hexane (20 mL) affording the product **5.6** as a white solid (130 mg, 0.22 mmol, 55%). **Melting point** (argon sealed capillary) 238 $^\circ\text{C}$ (dp). **Elemental analysis calculated** (%) for $\text{C}_{27}\text{H}_{40}\text{BBr}_2\text{N}_2\text{P}$ (594.22): C 54.57, H 6.79, N 4.71; found: C 54.70, H 6.89, N 4.61%.

^1H NMR (600 MHz, C_6D_6 , δ) 7.19-7.14 (m, 2H, Ar *para*-H), 7.07-7.03 (m, 4H, Ar *meta*-H), 3.48 (s, 4H, $\text{NCH}_2\text{CH}_2\text{N}$), 3.42 (sept, 4H, $^3J_{\text{HH}} = 6.8$ Hz, $\text{CH}(\text{CH}_3)_2$), 2.48 (d, 2H, $^1J_{\text{HP}} = 199.6$ Hz, H_2P), 1.58 (d, 12H, $^3J_{\text{HH}} = 6.6$ Hz, $\text{CH}(\text{CH}_3)_2$), 1.08 (d, 12H, $^3J_{\text{HH}} = 6.9$ Hz, $\text{CH}(\text{CH}_3)_2$). **^{13}C NMR (151 MHz, C_6D_6 , δ)** 180.6 (s, 1C, N-C-N), 146.9 (s, 4C, Ar *C*^{ortho}), 135.2 (s, 2C, Ar *C*^{ipso}), 130.6 (s, 2C, Ar *C*^{para}), 125.2 (s, 4C, Ar *C*^{meta}), 53.8 (s, 2C, $\text{NCH}_2\text{CH}_2\text{N}$), 29.5 (s, 4C, $\text{CH}(\text{CH}_3)_2$), 26.4 (s, 4C, $\text{CH}(\text{CH}_3)_2$), 23.9 (s, 2C, $\text{CH}(\text{CH}_3)_2$), 23.8 (s, 2C, $\text{CH}(\text{CH}_3)_2$). **^{11}B NMR (128 MHz, C_6D_6 , δ)** -10.8 (s). **^{31}P NMR (162 MHz, C_6D_6 , δ)** -146.1 (t, $^1J_{\text{PH}} = 199.6$ Hz).

Preparation of the SIPr coordinated 1-hydro-2-bromo-phosphaborene 5.7



To a solution of phosphinoborane **5.6** (170 mg, 0.29 mmol, 1.0 equiv.) in benzene (10 mL) was added a solution of $\text{MeI}'\text{Pr}$ (60 mg, 0.32 mmol, 1.1 equiv.) in benzene (10 mL).

The solution was stirred for 15 min and filtrated. The product **5.7** was isolated by fractional crystallisation in benzene at room temperature as a yellow solid (40 mg, 0.08 mmol, 27%). In solution, a mixture of E and Z isomers in ratio 0.8:1 was observed by NMR spectroscopy. **Melting point** (argon sealed capillary) 172 °C (dp). **Elemental analysis calculated** (%) for C₂₇H₃₉BBrN₂P (513.31): C 63.18, H 7.66, N 5.46; found: C 63.28, H 7.53, N 5.45%. **UV/vis (toluene):** λ_{\max} = 401 nm, ϵ = 2907 L mol⁻¹ cm⁻¹

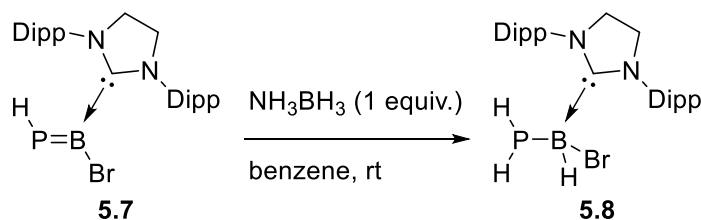
Z isomer

¹H NMR (500 MHz, C₆D₆, δ) 7.19-7.10 (m, 2H, Ar *para*-H), 7.06-7.02 (m, 4H, Ar *meta*-H), 4.99 (d, 1H, ¹J_{HP} = 141.1 Hz, HP), 3.50 (s, 4H, NCH₂CH₂N), 3.31 (sept, 4H, ³J_{HH} = 6.8 Hz, CH(CH₃)₂), 1.55 (d, 12H, ³J_{HH} = 6.7 Hz, CH(CH₃)₂), 1.14 (d, 12H, ³J_{HH} = 6.9 Hz, CH(CH₃)₂). **¹³C NMR (125 MHz, C₆D₆, δ)** 182.5 (s, 1C, N-C-N), 146.5 (s, 4C, Ar C^{ortho}), 134.5 (s, 2C, Ar C^{ipso}), 130.3 (s, 2C, Ar C^{para}), 125.0 (s, 4C, Ar C^{meta}), 53.1 (s, 2C, NCH₂CH₂N), 29.3 (s, 4C, CH(CH₃)₂), 26.3 (s, 4C, CH(CH₃)₂), 23.9 (s, 2C, CH(CH₃)₂), 23.8 (s, 2C, CH(CH₃)₂). **¹¹B NMR (128 MHz, C₆D₆, δ)** 44.4 (s). **³¹P NMR (162 MHz, C₆D₆, δ)** 90.5 (d, ¹J_{PH} = 141.1 Hz).

E isomer

¹H NMR (500 MHz, C₆D₆, δ) 7.19-7.10 (m, 2H, Ar *para*-H), 7.02-6.98 (m, 4H, Ar *meta*-H), 4.29 (d, 1H, ¹J_{HP} = 127.6 Hz, HP), 3.51 (s, 4H, NCH₂CH₂N), 3.32 (sept, 4H, ³J_{HH} = 6.8 Hz, CH(CH₃)₂), 1.49 (d, 12H, ³J_{HH} = 6.9 Hz, CH(CH₃)₂), 1.11 (d, 12H, ³J_{HH} = 6.9 Hz, CH(CH₃)₂). **¹³C NMR (125 MHz, C₆D₆, δ)** 181.4 (s, 1C, N-C-N), 146.6 (s, 4C, Ar C^{ortho}), 133.9 (s, 2C, Ar C^{ipso}), 130.4 (s, 2C, Ar C^{para}), 125.0 (s, 4C, Ar C^{meta}), 52.9 (s, 2C, NCH₂CH₂N), 29.3 (s, 4C, CH(CH₃)₂), 26.5 (s, 4C, CH(CH₃)₂), 23.7 (s, 4C, CH(CH₃)₂). **¹¹B NMR (128 MHz, C₆D₆, δ)** 47.6 (s). **³¹P NMR (162 MHz, C₆D₆, δ)** 49.3 (d, ¹J_{PH} = 127.6 Hz).

Generation of the SIPr coordinated 1-dihydro-2-bromohydrophosphinoborane **5.8**



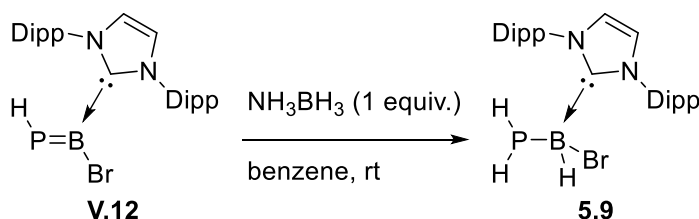
NMR scale: Phosphaborene **5.7** (10 mg, 0.01 mmol, 1.0 equiv.) and NH₃BH₃ (0.3 mg, 0.01 mmol, 1.0 equiv.) were dissolved in C₆D₆ (1 mL). Almost full conversion to **5.8**

Experimental Methods

was observed by NMR spectroscopy after two hours, with remaining trace signals of **5.7**.

¹H NMR (500 MHz, C₆D₆, δ) 7.21-7.15 (m, 2H, Ar *para*-H), 7.09-7.01 (m, 4H, Ar *meta*-H), 3.55-3.27 (m, 8H, NCH₂CH₂N and CH(CH₃)₂), 1.96 (ddd, 1H, ¹J_{HP} = 195 Hz, ²J_{HH} = 10.7 Hz, ³J_{HH} = 5.45 Hz, HP), 1.58 (d, 6H, ³J_{HH} = 6.6 Hz, CH(CH₃)₂), 1.48 (d, 6H, ³J_{HH} = 6.8 Hz, CH(CH₃)₂), 1.34 (ddd, 1H, ¹J_{HP} = 195 Hz, ²J_{HH} = 10.7 Hz, ³J_{HH} = 10.7 Hz, HP), 1.12-1.07 (m, 12H, CH(CH₃)₂). **¹¹B NMR (128 MHz, C₆D₆, δ)** -19.7 (s). **³¹P NMR (162 MHz, C₆D₆, δ)** -183.6 (t, ¹J_{PH} = 194 Hz).

Preparation of the IPr coordinated 1-dihydro-2-bromohydrophosphinoborane **5.9**



NMR scale: Phosphaborene **V.12** (10 mg, 0.01 mmol, 1.0 equiv.) and NH₃BH₃ (0.3 mg, 0.01 mmol, 1.0 equiv.) were dissolved in C₆D₆ (1 mL). Almost full conversion to **5.9** was observed by NMR spectroscopy after two hours, with remaining trace signals of **V.12**.

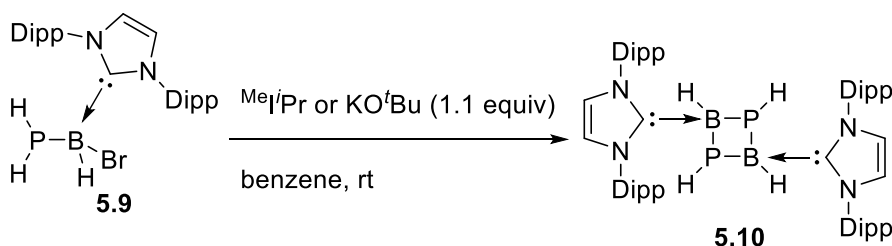
Preparative scale: Phosphaborene **V.12** (174 mg, 0.34 mmol, 1.0 equiv.) and NH₃BH₃ (15.5 mg, 0.50 mmol, 1.5 equiv.) were dissolved in benzene (20 mL) at room temperature. The solution was stirred for two hours, going from yellow to colourless. The solution was filtered, dried *in vacuo*. Crystallisation from a benzene:hexane (1:1) solution at -20°C afforded **5.9** as colourless crystals (42 mg, 0.08 mmol, 24%).

Elemental analysis calculated (%) for C₂₇H₃₉BBrN₂P (513.31): C 63.18, H 7.66, N 5.46; found: C 63.09, H 7.53, N 5.58%.

¹H NMR (500 MHz, C₆D₆, δ) 7.24-7.19 (m, 2H, Ar *para*-H), 7.12-7.06 (m, 4H, Ar *meta*-H), 6.40 (s, 2H, NCHCHN), 2.97 (sept, 2H, ³J_{HH} = 6.9 Hz, CH(CH₃)₂), 2.78 (sept, 2H, ³J_{HH} = 6.8 Hz, CH(CH₃)₂), 2.07 (ddd, 1H, ¹J_{HP} = 195 Hz, ²J_{HH} = 10.8 Hz, ³J_{HH} = 5.65 Hz, HP), 1.52 (ddd, 1H, ¹J_{HP} = 192 Hz, ²J_{HH} = 10.55 Hz, ³J_{HH} = 10.55 Hz, HP), 1.50 (d, 6H, ³J_{HH} = 6.75 Hz, CH(CH₃)₂), 1.42 (d, 6H, ³J_{HH} = 6.75 Hz, CH(CH₃)₂), 0.99 (d, 6H, ³J_{HH} = 6.85 Hz, CH(CH₃)₂), 0.98 (d, 6H, ³J_{HH} = 6.85 Hz, CH(CH₃)₂). **¹³C NMR (125 MHz, C₆D₆, δ)** 166.3 (s, 1C, N-C-N), 146.2 (s, 2C, Ar C^{ortho}), 146.0 (s, 2C, Ar C^{ortho}),

133.8 (s, 2C, Ar \mathbf{C}^{ipso}), 131.1 (s, 2C, Ar \mathbf{C}^{para}), 124.5 (s, 2C, Ar \mathbf{C}^{meta}), 124.4 (s, 2C, Ar \mathbf{C}^{meta}), 123.6 (s, 2C, NCHCHN), 29.4 (s, 1C, $\mathbf{CH}(\mathbf{CH}_3)_2$), 29.3 (s, 1C, $\mathbf{CH}(\mathbf{CH}_3)_2$), 29.2 (s, 2C, $\mathbf{CH}(\mathbf{CH}_3)_2$), 26.2 (s, 2C, $\mathbf{CH}(\mathbf{CH}_3)_2$), 25.8 (s, 2C, $\mathbf{CH}(\mathbf{CH}_3)_2$), 23.1 (s, 1C, $\mathbf{CH}(\mathbf{CH}_3)_2$), 23.0 (s, 1C, $\mathbf{CH}(\mathbf{CH}_3)_2$), 22.9 (s, 2C, $\mathbf{CH}(\mathbf{CH}_3)_2$). $^{11}\mathbf{B}$ NMR (128 MHz, $\mathbf{C}_6\mathbf{D}_6$, δ) -19.6 (s). $^{31}\mathbf{P}$ NMR (162 MHz, $\mathbf{C}_6\mathbf{D}_6$, δ) -182.7 (t, $^1J_{\text{PH}} = 191.6$ Hz).

Generation of the parent diphosphadiboretane 5.10



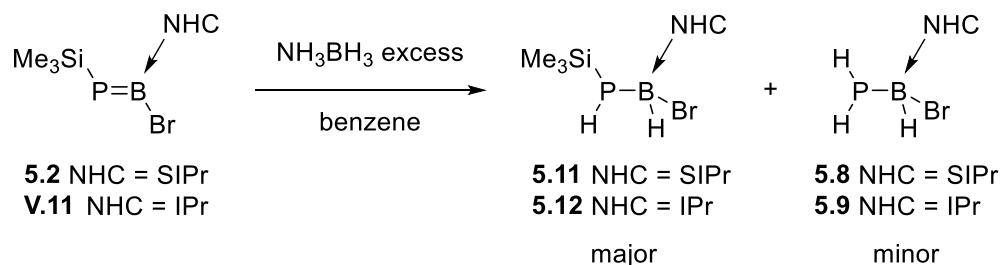
Attempt 1: The phosphinoborane **5.9** (10 mg, 0.019 mmol, 1.0 equiv.) was dissolved in $\mathbf{C}_6\mathbf{D}_6$ (1 mL) and added to KO^tBu (2.4 mg, 0.021 mmol, 1.1 equiv.) at room temperature. After one hour, the ^1H , ^{11}B and ^{31}P NMR spectroscopy analysis (500-128-162 MHz, $\mathbf{C}_6\mathbf{D}_6$, δ) showed the product **5.10**.

Attempt 2: The phosphinoborane **5.9** (10 mg, 0.019 mmol, 1.0 equiv.) was dissolved in $\mathbf{C}_6\mathbf{D}_6$ (1 mL) and added to MeI^tPr (4 mg, 0.021 mmol, 1.1 equiv.) at room temperature. After one hour, the ^1H , ^{11}B and ^{31}P NMR spectroscopy analysis (500-128-162 MHz, $\mathbf{C}_6\mathbf{D}_6$) showed the product **5.10**. The solution was heated between room temperature and 70°C for a variable temperature NMR experiment. No new product was observed by ^{31}P NMR spectroscopy and **5.10** was thermal stable up to 70°C with no degradation observed during the experiment.

The signals from **5.10** come along with unidentified products and could not be fully assigned.

$^{11}\mathbf{B}$ NMR (128 MHz, $\mathbf{C}_6\mathbf{D}_6$, δ) -29.7 (d, 2B, $^1J_{\text{BH}} = 96$ Hz). $^{31}\mathbf{P}$ NMR (162 MHz, $\mathbf{C}_6\mathbf{D}_6$, δ) -159.4 (d, 1P, $^1J_{\text{PH}} = 146$ Hz), -195.5 (br d, 1P, $^1J_{\text{PH}} = 110$ Hz).

Generation of the SIPr coordinated 1-hydrotrimethylsilyl-2-bromohydro-phosfinoborane 5.11



Phosphaborene **5.2** (10 mg, 0.019 mmol, 1.0 equiv.) was dissolved in C_6D_6 (1 mL) and added to NH_3BH_3 (0.6 mg, 0.019 mmol, 1.0 equiv.) at room temperature. After one hour, ^1H , ^{11}B and ^{31}P NMR spectroscopy analysis (500-128-162 MHz, C_6D_6) showed the formation of the phosphinoborane **5.11** along with the phosphinoborane **5.8**. An excess of NH_3BH_3 (5 mg) was added to the solution. The ^1H and ^{31}P NMR spectroscopy analysis (500-162 MHz, C_6D_6) showed formation of more **5.8**.

The NMR signals from **5.11** comes with trace signals of unidentified side product and **5.8**. Due to the number of small signals, **HP** and **HB** could not assigned.

^1H NMR (500 MHz, C_6D_6 , δ) 7.20-7.16 (m, 2H, Ar *para*-H), 7.09-7.05 (m, 4H, Ar *meta*-H), 3.54-3.32 (m, 8H, $\text{NCH}_2\text{CH}_2\text{N}$ and $\text{CH}(\text{CH}_3)_2$), 1.62 (d, 6H, $^3J_{\text{HH}} = 6.50$ Hz, $\text{CH}(\text{CH}_3)_2$), 1.54 (d, 6H, $^3J_{\text{HH}} = 6.60$ Hz, $\text{CH}(\text{CH}_3)_2$), 1.12-1.09 (m, 12H, $\text{CH}(\text{CH}_3)_2$), 0.27 (d, 9H, $^3J_{\text{HP}} = 3.65$ Hz, $\text{Si}(\text{CH}_3)_3$). **^{11}B NMR (128 MHz, C_6D_6 , δ)** -17.7 (s). **^{31}P NMR (162 MHz, C_6D_6 , δ)** -196.2 (d, 1P, $^1J_{\text{PH}} = 177$ Hz).

Generation of the IPr coordinated 1-hydrotrimethylsilyl-2-bromohydro-phosfinoborane 5.12

Phosphaborene **V.11** (10 mg, 0.017 mmol, 1.0 equiv.) was dissolved in C_6D_6 (1 mL) and added to NH_3BH_3 (0.6 mg, 0.017 mmol, 1.0 equiv.) at room temperature. After one hour, ^1H , ^{11}B and ^{31}P NMR spectroscopy analysis (500-128-162 MHz, C_6D_6) showed the formation of the phosphinoborane **5.12** along with the phosphinoborane **5.9**. An excess of NH_3BH_3 (5 mg) was added to the solution. The ^1H and ^{31}P NMR spectroscopy analysis (500-162 MHz, C_6D_6) showed formation of more **5.9**.

The NMR signals from **5.12** comes with trace signals of unidentified side product and **5.9**. Due to the number of small signals, **HP** and **HB** could not assigned.

¹H NMR (500 MHz, C₆D₆, δ) 7.22-7.18 (m, 2H, Ar *para*-H), 7.12-7.07 (m, 4H, Ar *meta*-H), 6.37 (s, 2H, NCHCHN), 3.01-2.92 (m, 2H, CH(CH₃)₂), 2.84 (sept, 2H, ³J_{HH} = 6.90 Hz, CH(CH₃)₂), 1.53 (d, 6H, ³J_{HH} = 6.80 Hz, CH(CH₃)₂), 1.47 (d, 6H, ³J_{HH} = 6.80 Hz, CH(CH₃)₂), 1.01-0.96 (m, 12H, CH(CH₃)₂), 0.31 (d, 9H, ³J_{HP} = 4.04 Hz, Si(CH₃)₃). **¹¹B NMR (128 MHz, C₆D₆, δ)** -18.1 (s). **³¹P NMR (162 MHz, C₆D₆, δ)** -194.0 (d, 1P, ¹J_{PH} = 188 Hz).

Reaction between IV.4 and ITr

Phosphorous-boron adduct **IV.4** (15 mg, 0.030 mmol, 1.0 equiv.) and ITr (16.6 mg, 0.030 mmol, 1.0 equiv.) were dissolved in toluene-d₈ (1 mL) at room temperature. The ¹H, ¹¹B and ³¹P NMR spectroscopy analysis (500-128-162 MHz, C₆D₆) showed ITr along with the formation of the reported dimer **IV.6**.

X-Ray Crystallography Details

Information related to the collection and solving of the X-ray structures mentioned in the thesis for each compound can be found in electronic appendix **A**.

NMR and UV-Vis Data

The raw data NMR and UV-Vis for each compound as reported or discussed in the thesis can be found in electronic appendix **B**.

DFT-Calculations

DFT-Calculations were carried out by D. De Rosa.

Geometry optimizations and harmonic frequency calculations were performed using the Gaussian16 program package^[10] employing the M06-2X density functional^[11] in combination with the 6-311G(d,p) basis set.^[12] Stationary points were characterized as minima by eigenvalue analysis of the computed Hessians. Single-point calculations were conducted on the optimized geometries using the M06-2X functional in combination with the 6-311G(d,p) basis set. The SMD polarizable continuum model^[13] was employed to account for solvent effects (Benzene), SMD-M06-2X/6-311G(2d,2p). The wave functions used for bonding analysis were obtained

Experimental Methods

at the M06-2X/6-311G(d,p) level of theory. Unscaled zero-point vibrational, thermal and entropic corrections were obtained from computed Hessian matrices computed at the M06-2X/6-311G(d,p) level using standard procedures as implemented in Gaussian16 to obtain free energy values at standard conditions ($T = 298.15$ K, $p = 1$ atm).

The DFT-calculations can be found in electronic appendix **C**.

Origin Calculation

Calculations of the difference in energy between the two E and **Z-5.7** from experimental measurements can be found in electronic appendix **D**.

References

- [1] P. Zark, A. Schäfer, A. Mitra, D. Haase, W. Saak, R. West, T. Müller, *J. Organomet. Chem.* **2010**, *695*, 398–408.
- [2] R. A. Sulzbach, A. F. M. Iqbal, *Angew. Chem. Int. Ed.* **1971**, *10*, 127.
- [3] P. Tang, W. Wang, T. Ritter, *J. Am. Chem. Soc.* **2011**, *133*, SI.
- [4] N. Kuhn, T. Kratz, *Synthesis (Stuttg.)* **1993**, 561.
- [5] A. C. Filippou, O. Chernov, G. Schnakenburg, *Chem. - A Eur. J.* **2011**, *17*, 13574–13583.
- [6] M. M. D. Roy, P. A. Lummis, M. J. Ferguson, R. McDonald, E. Rivard, *Chem. - A Eur. J.* **2017**, *23*, 11249–11252.
- [7] A. C. Filippou, Y. N. Lebedev, O. Chernov, M. Straßmann, G. Schnakenburg, *Angew. Chem. Int. Ed.* **2013**, *52*, 6974–6978.
- [8] D. G. Batt, *US2004067935A1*, **2004**.
- [9] M. S. Lube, R. L. Wells, P. S. White, *Inorg. Chem.* **1996**, *35*, 5007–5014.
- [10] M. J. Frisch, G. W. Trucks, H. B. Schlegel, G. E. Scuseria, M. A. Robb, J. R. Cheeseman, G. Scalmani, V. Barone, G. A. Petersson, H. Nakatsuji, X. Li, M. Caricato, A. V. Marenich, J. Bloino, B. G. Janesko, R. Gomperts, B. Mennucci, H. P. Hratchian, J. V. Ortiz, A. F. Izmaylov, J. L. Sonnenberg, D. Williams-Young, F. Ding, F. Lipparini, F. Egidi, J. Goings, B. Peng, A. Petrone, T. Henderson, D. Ranasinghe, V. G. Zakrzewski, J. Gao, N. Rega, G. Zheng, W. Liang, M. Hada, M. Ehara, K. Toyota, R. Fukuda, J. Hasegawa, M. Ishida, T. Nakajima, Y. Honda, O. Kitao, H. Nakai, T. Vreven, K. Throssell, J. A. Montgomery, Jr., J. E. Peralta, F. Ogliaro, M. J. Bearpark, J. J. Heyd, E. N. Brothers, K. N. Kudin, V. N. Staroverov, T. A. Keith, R. Kobayashi, J. Normand, K. Raghavachari, A. P. Rendell, J. C. Burant, S. S. Iyengar, J. Tomasi, M. Cossi, J. M. Millam, M. Klene, C. Adamo, R. Cammi, J. W. Ochterski, R. L. Martin, K. Morokuma, O. Farkas, J. B. Foresman, and D. J. Fox, Gaussian, Inc., Wallingford CT. *Gaussian 16*; **2016**.
- [11] Y. Zhao, D. G. Truhlar, *Theor. Chem. Acc.* **2008**, *120*, 215–241.
- [12] R. Krishnan, J. S. Binkley, R. Seeger, J. A. Pople, *J. Chem. Phys.* **1980**, *72*, 650–654.
- [13] A. V Marenich, C. J. Cramer, D. G. Truhlar, *J. Phys. Chem. B* **2009**, *113*, 6378.